Università degli Studi di Ferrara

DOTTORATO DI RICERCA IN SCIENZE DELLA TERRA

CICLO XXX

COORDINATORE Prof. Massimo Coltorti

Innovative Approaches for the Evaluation of Coastal Risk on Sandy Mediterranean Beaches

Settore Scientifico Disciplinare GEO-04

Dottorando

Dott. Enrico Duo

(firma)

Tutore

Prof. Paolo Ciavola

(firma)

Co-tutori

Prof. Clara Armaroli

(firma)

Prof. Arthur C. Trembanis

(firma)

Anni 2014/2017

Università degli Studi di Ferrara

DOTTORATO DI RICERCA IN SCIENZE DELLA TERRA

CICLO XXX

COORDINATORE Prof. Massimo Coltorti

Innovative Approaches for the Evaluation of Coastal Risk on Sandy Mediterranean Beaches

Settore Scientifico Disciplinare GEO-04

Dottorando

Dott. Enrico Duo

(firma)

Tutore

Prof. Paolo Ciavola

(firma)

Co-tutori

Prof. Clara Armaroli

(firma)

Prof. Arthur C. Trembanis

(firma)

Anni 2014/2017

He started to walk towards it. People jostled him on their way to platforms nine and ten. Harry walked more quickly. He was going to smash right into that ticket box and then he'd be in trouble - leaning forward on his trolley he broke into a heavy run - the barrier was coming nearer and nearer - he wouldn't be able to stop - the trolley was out of control - he was a foot away - he closed his eyes ready for the crash -

It didn't come... he kept on running... he opened his eyes.

A scarlet steam engine was waiting next to a platform packed with people. A sign overhead said *Hogwarts Express, 11 o'clock*. Harry looked behind him and saw a wrought-iron archway where the ticket box had been, with the words *Platform Nine and Three-Quarters* on it. He had done it.

Harry Potter and the Philosopher's Stone
J.K. Rowling

Acknowledgments

I'd like to thank Prof. Paolo Ciavola for all the support, psychological and financial, during these years. If I am here, at this very important point of my academic career, it is largely because of his persistence. I want to thank him, especially, for his ability of being a team leader, rather than being a boss.
I am very grateful to Prof. Clara Armaroli, that showed me how to get rid of my engineering prejudices to evolve in what I call a "Coastal EnGeomorphologist". Then, I'd like to thank Prof. Arthur C. Trembanis (University of Delaware) and Prof. José A. Jiménez (Universitat Politècnica de Catalunya) because they gave me the opportunity to work with them and their teams, sharing their knowledge. I am grateful to Dr. Ap Van Dongeren (Deltares, Delft, The Netherlands) and Prof. Tom Spencer (University of Cambridge, Cambridge, United Kingdom) for their very useful reviews of this thesis. A great thank goes to Dr. Andrea Ninfo, which landed in Ferrara last year and immediately began to share everything he knows about photogrammetric reconstruction and other interesting stuff. His contribution to part of this work is invaluable. I am most grateful to my co-authors, colleagues and friends. It was an honour to collaborate, trying to improve the human's knowledge in the wide field of coastal risk. I'd like to thank Luisa Perini (Servizio Geologico Sismico e dei Suoli della Regione Emilia-Romagna, Bologna, Italy) for her special contribution to this work. She provided data for the risk assessments, valuable suggestions and comments. A special thank to Francesco Droghetti and Paolo Chiarelli, the technicians of my department that can literally fix everything.
I really want to thank my team: Edoardo Grottoli, Silvia Cilli and Tomás Fernández-Montblanc. It is simply wonderful how much fun we have at work, in the office and on the field. Guys, thank you for your support!
I'd like to thank all the people of the EU FP7 RISC-KIT (GA603458) project, the RISC-KIDs. Very awesome people, led by a very awesome Dutch guy. Ap (yes, that guy! ☺) will always be a guide for me, since we met for the first time in Delft in 2013, for my first abroad experience. Actually, all the RISC-KIDs taught me a lot of what I know now, especially about team work and sharing. At the end of the project we were more than colleagues, we were friends, kept together by work deadlines and beers.
I am very grateful to my sister and her family. A special thought goes to my mum and dad, that are passing a difficult moment. Have faith, everything will get better! I want to thank all my friends, especially Tommaso and the "Engineers". A surprise of these last 3 years is the Itinera Agility Dog club, that I'd like to thank as it showed me how amazing is the dogs' world. I cannot name all of them, they are too many, especially including their owners! ☺
From my heart, I thank Marc Sanuy. Part of the work of this thesis would not be even conceivable, without him. Besides that, rather than a colleague, I consider him a real friend. One of those that you are lucky to meet few times in life. They are rare. We shared a lot. He initiated me to the wonderful world of bikers, while he got caught by my passion for dogs. And yes, we'll keep on seeing each other. Because we are very good at working and having fun...
Finally, my best love and gratitude are for Marcella, my very patient life mate that helps me finding the beauty even where it's not supposed to be. Thanks, because I am still listening to the cicadas... ♥ Then, I know it's weird, but I cannot avoid it, I thank our dogs, Brunilde and Spugna, which makes every single day not boring at all... 🐾🐾

Summary

The increase in frequency and intensity of extreme coastal storms and the continuous exponential development of the coasts of the world are threatening coastal communities, exposing them to higher levels of risk. Notwithstanding the future projections are affected by large uncertainty, coastal managers, as recommended by the United Nations and the European Union, need to properly evaluate coastal risk in order to propose adequate risk reduction plans for the current and future climate change scenarios. This should be done while considering all the components that influence risk: hazard, vulnerability and exposure. The involvement of local stakeholders and the adoption of multi-disciplinary approaches, that include social-based ones, are becoming very frequent in coastal risk studies, supporting the idea that the same should be done at the management level, to properly address coastal risk issues.

The work of this PhD thesis aimed at applying innovative approaches for the evaluation of coastal risk, at different scales, on Mediterranean sandy beaches. The approaches were applied for diverse aspects that help at properly understanding and analyzing coastal risk. The innovations are related to fieldwork methodologies, numerical applications and coastal risk assessment. Part of the work was done in the framework of the EU FP7 RISC-KIT project, that aimed at providing tools in support of coastal managers, in order to increase the resilience of coastal communities. The approaches were implemented at locations along the Emilia-Romagna (Italy) and Catalunya (Spain) coasts.

The first part of this PhD thesis focuses on fieldwork activities. Post-storm and seasonal surveys were implemented based on up-to-date low-cost drones and photogrammetric techniques for post-processing. The approach allowed to collect local-scale high-resolution data (i) for the analysis of the effects of an extreme storm that hit the Emilia-Romagna coast in February 2015, focusing on the beach of Lido degli Estensi (Comacchio, Italy); (ii) to analyze the seasonal behaviour of a beach in Porto Garibaldi (Comacchio, Italy), where artificial sandy dunes are used as temporary protection during the storm season. The outcomes were used, in the first case, to integrate the regional post-storm assessment implemented by the regional authorities, including qualitative information collected involving the local community. This allowed to highlight some limitations of the regional protocol and proposing solutions, such as the integration of the tested local approach into the regional one. In the second case, the methodological approach provided high-accuracy topographic data used to detect significant changes of the beach due to the influence of coastal storms and winds.

Numerical models were used to analyze the propagation of errors due to the use of synthetic time-series of waves in a process-based chain of models (i.e. XBeach and LISFLOOD-FP) used to simulate erosion and flooding hazards. The models were applied at the beaches of Lido degli Estensi-Spina (Italy) and Tordera Delta (Spain) and results were analyzed with a Bayesian-based approach. Outcomes evidenced how the used of synthetic input can produce significant errors in the hazard assessment, if compared with the use of real time-series. These errors can have a significant influence on integrated risk assessments and thus, numerical studies should be considered on the basis of their limitations and supported by uncertainty analysis.

Focusing on integrated coastal risk assessments, in the last part of this PhD thesis two studies are presented, respectively at the local and regional levels. The assessments were implemented by applying the definition of risk as the product of the probability of the hazard and its consequences and using the RISC-KIT tools: the Coastal Risk

Assessment Framework (CRAF) Phase 1 for the identification of critical areas (hotspots) at the regional level and the Bayesian-based Hotspot tool for testing local measures for disaster reduction, in the current and future scenarios. The CRAF Phase 1 was validated on the Emilia-Romagna coast, confirming that it is able to detect well-known hotspots. The Hotspot tool provided useful insights on the tested measures. Notably, soft-measures (i.e. artificial temporary protections, nourishments and managed retreat) were found to be very effective at the two analyzed case study sites, Lido degli Estensi-Spina (Italy) and Tordera Delta (Spain). The applications confirmed that the RISC-KIT approach for regional and local scale assessments is valuable for coastal managers, in order to propose adequate and acceptable solutions for risk reduction.

An interesting aspect of this PhD work is that the majority of the tools applications were done including local people and managers in the process. In particular, the post-storm drone-based survey was supported by qualitative information collected through interviews to local stakeholders. The implementation of the RISC-KIT CRAF tool was done in collaboration with coastal managers that provided data and comments during the whole study. The measures tested with the RISC-KIT Hotspot tool were selected on the basis of stakeholders' interviews and the outcomes of the study were used as a basis for a participatory evaluation process where stakeholders were asked to select risk reduction strategies. A further consideration is that large parts of the integrated risk assessments were supported by a strong collaboration between physical scientists and social ones. This confirms that a multi-disciplinary approach is a key aspect in order to properly understand and reduce coastal risk.

Finally, coastal managers should be aware of all the aspects analyzed in this PhD thesis that can affect risk assessments, from the fieldwork to the deskwork. Moreover, they should be able to properly address risk by interacting with physical and social scientists, as well as with local communities, if they want to provide effective and acceptable risk reduction strategies.

Riassunto

Le coste del mondo sono minacciate dall'incremento, in termini di frequenza ed intensità, delle mareggiate e dello sviluppo costiero. Di conseguenza, le comunità costiere sono esposte a livelli di rischio sempre più elevati. Le Nazioni Unite e l'Unione Europea richiedono ai manager costieri di valutare il rischio, legato agli eventi estremi, sulle coste in modo da proporre piani adeguati per la riduzione dello stesso, sia per lo scenario attuale, sia per quello futuro, considerando i possibili effetti del cambiamento climatico, nonostante le proiezioni future siano caratterizzate da incertezze non trascurabili. Le valutazioni di rischio devono essere basate considerando pericolosità, vulnerabilità ed esposizione. Inoltre, queste analisi dovrebbero essere fatte adottando approcci multi-disciplinari e coinvolgendo i portatori di interesse.

Il lavoro svolto durante il progetto di Dottorato, oggetto di questa tesi, si è svolto applicando, a diverse scale spaziali, approcci innovativi per la valutazione del rischio su spiagge sabbiose del Mediterraneo. Gli approcci sono stati applicati in diversi campi relativi all'analisi e riduzione rischio costiero, dalle misure sul campo, all'utilizzo di modelli numerici, fino alle valutazioni integrate del rischio. Parte del lavoro si è svolto nell'ambito del progetto europeo RISC-KIT, il cui obiettivo è stato quello di fornire ai manager costieri strumenti utili alla riduzione del rischio ed all'incremento della resilienza delle comunità costiere. Gli approcci sono stati applicati in diverse località costiere, in Emilia-Romagna (Italia) e Catalogna (Spagna).

La prima parte di questa tesi di Dottorato riguarda aspetti di misure sul campo. Sono stati utilizzati moderni droni a basso-costo e tecniche di fotogrammetria per rilievi post-evento e stagionali. L'approccio ha permesso di ricavare a scala locale dati ad alta risoluzione (i) per l'analisi degli effetti dell'evento estremo che ha colpito la località di Lido degli Estensi (Comacchio, Italia) sulla costa Emiliano-Romagnola nel Febbraio 2015 e (ii) per analizzare l'evoluzione stagionale di una spiaggia a Porto Garibaldi (Comacchio, Italia), dove vengono costruite dune artificiali in sabbia durante la stagione invernale, come protezione dagli eventi estremi. Nel primo caso, i risultati hanno permesso di integrare i rilievi post-evento fatti, a livello regionale, dalle autorità regionali, includendo informazioni qualitative ottenute coinvolgendo la comunità locale. Questo ha permesso l'identificazione delle limitazioni della metodologia regionale e conseguentemente sono state proposte soluzioni migliorative, come l'integrazione dell'approccio locale testato durante lo studio nel protocollo regionale. Nel secondo caso, l'approccio metodologico scrupoloso ha fornito dati topografici estremamente accurati, utili all'analisi delle variazioni significative della spiaggia, dovute alle mareggiate e ai venti.

Sono stati utilizzati modelli numerici per analizzare la propagazione degli errori dovuti all'utilizzo di mareggiate sintetiche in input ad una catena di modelli (i.e. XBeach and LISFLOOD-FP) per la simulazione di erosione ed inondazione costiere. I modelli sono stati applicati alle località costiere di Lido degli Estensi-Spina (Italia) e Tordera Delta (Spagna) ed i risultati sono stati analizzati con un approccio Bayesiano. I risultati hanno evidenziato come l'uso di input sintetici produca errori significativi nella valutazione dei pericoli di erosione ed inondazione, se confrontato con l'uso di serie temporali reali. Gli errori propagati possono avere effetti importanti sulle successive caratterizzazioni del rischio. Pertanto, gli studi che si basano su modellazioni numerici devo essere considerati sulla base delle loro limitazioni e dovrebbero sempre essere accompagnati da valutazioni di incertezza.

Nell'ambito degli studi integrati di rischio costiero, nell'ultima parte di questa tesi sono presentati due studi, uno a livello regionale, l'altro a livello locale. Le valutazioni sono state fatte assumendo la definizione di rischio come prodotto della probabilità del pericolo per le sue conseguenze (o impatti). Sono stati applicati gli strumenti forniti da RISC-KIT, la prima fase (Phase 1) del Coastal Risk Assessment Framework (CRAF) per l'identificazione delle aree critiche (hotspot) a livello regionale e l'Hotspot tool, un approccio Bayesiano per l'analisi dell'efficacia di misure di riduzione del rischio, per gli scenari attuale e futuro. Il CRAF Phase 1 è stato validato per la costa dell'Emilia-Romagna e si è dimostrato efficace nell'identificare aree ben note, ai manager regionali, per essere critiche in termini di erosione ed inondazione. L'Hotspot tool ha fornito informazioni utili alla caratterizzazione dell'efficacia delle misure. In particolare, le misure "soft", come l'utilizzo di argini temporanei in sabbia e ripascimenti, o il ritiro strategico, sono risultate le misure più efficaci in entrambi i casi studio analizzati, Lido degli Estensi-Spina (Italia) e Tordera Delta (Spagna). Le applicazioni hanno dimostrato che l'approccio di RISC-KIT è utile ai manager costieri per analisi di rischio a scala regionale e locale e, conseguentemente, per la preparazione di piani adeguati di riduzione del rischio.

Un aspetto interessante di questo progetto di Dottorato riguarda il coinvolgimento dei portatori di interesse e dei manager costieri nella maggior parte delle analisi svolte. In particolare, il rilievo post-evento è stato guidato ed integrato da informazioni qualitative raccolte tramite interviste ad alcuni portatori di interesse locali. Lo strumento di RISCKIT per l analisi del rischio a livello regionale, il CRAF, è stato utilizzato in collaborazione con i manager costieri che hanno fornito preziosi dati e commenti durante tutto lo svolgimento dello studio. Le misure di riduzione del rischio analizzate tramite l'Hotspot tool sono state selezionate sulla base di interviste. I risultati delle analisi, invece, sono stati utilizzati come base per il processo di valutazione partecipativo, in cui ai portatori di interesse è stato richiesto di valutare strategie di riduzione del rischio. Una considerazione aggiuntiva riguarda la forte collaborazione tra rappresentanti delle scienze naturali e sociali, di estrema importanza per l'appropriata valutazione integrata del rischio costiero, a diverse scale spaziali. Questo conferma che l'approccio multi-disciplinare è un aspetto chiave per comprendere e ridurre il rischio costiero.

Infine, i manager costieri dovrebbero essere capaci di comprendere tutti gli aspetti considerati in questa tesi e che influenzano le valutazioni di rischio, dalle misure sul campo al lavoro alla scrivania. Inoltre, dovrebbero interagire maggiormente con i ricercatori che lavorano sulle coste, sia dal punto di vista fisico, sia sociale, e con i portatori di interesse, in modo da fornire strategie per la riduzione del rischio che siano efficaci e condivisibili.

Table of contents

List of figures

List of tables

1 GENERAL INTRODUCTION

This introductory chapter aims at giving a picture of the recent definitions and approaches used in coastal risk research, with a strong emphasis on the importance of implementing multi-disciplinary studies. Then, part of the text focuses on the recent EU FP7 RISC-KIT project (GA 603458). Next, a brief introduction of the Mediterranean sandy coasts of Emilia-Romagna and Catalunya follows. Innovative approaches for coastal risk assessment were applied at these locations. Finally, the rationale and structure of this PhD thesis are given.

1.1 Defining coastal risk

The concept of risk for natural disasters is a relatively modern notion that developed through the second half of the twentieth century as result of worldwide, multi-disciplinary scientific and political efforts. Pioneering investigations of causes, damages and possible measures against natural extremes were implemented after major damaging events, such as, for example, the work of the Waverley Committee (Waverley, 1954) following the 1953 North Sea storm surge that severely damaged the English and Dutch coasts. A first overview of the scientific progress in the broad field of natural hazards achieved in the following two decades can be found in Burton et al. (1978) that, although subjected to some limitations (Hewitt, 1980), represented the basis for future hazard and risk studies, as it included earliest insights on the importance of social aspects and management.

In the past, earthquakes, river floods or other natural disasters were seen as the consequences of god's will (Gaillard and Texier, 2010). Actually, even nowadays religion is sometimes used to explain the occurrence of natural extreme events, such as after Hurricane Katrina in the United States, in 2005 (Steinberg, 2006). Recently, however, the scientific community, supported by the political effort of supra-national and intergovernmental organizations, provided science- and social-based concepts in order to understand why natural disasters occur and how human beings can deal with them.

Risk, in its more general and recent definition (Poljanšek et al., 2017), is considered as the interaction of hazard, exposure and vulnerability components. The hazard component is the event causing the loss (i.e. loss of lives; damage to properties, infrastructures, ecosystems, etc.) and represents the very natural aspect of risk. The exposure is determined by the elements (i.e. people, buildings, infrastructure, ecosystems, etc.) that are directly or indirectly threatened by the event. The vulnerability defines how the elements, directly or indirectly exposed to the event, are vulnerable/susceptible to the hazard and it is also related to their capacity to cope with and to adapt to the adverse conditions. Exposure and vulnerability are generally related to the human component of risk, being, especially the second one, affected by local culture and beliefs, social and economic contexts, etc. These three components are extremely variable, in space and time, and their understanding is necessary in order to understand risk.

It follows that risk is a relative concept. Simplifying, extremely severe events (very high hazard) happening in unpopulated natural areas (null exposure) do not cause consequences to human assets, thus do not generate risk. On the other hand, minor events (low hazard) happening in highly populated areas (high exposure) can have very important consequences, potentially generating high levels of risk. Additionally, the characteristics of the populated and built environment (e.g. whether people are mainly

rich or poor, young or old, well-educated or not; buildings and infrastructures are designed to cope with extreme natural events or not, etc.) affect the vulnerability component and, thus, the possible consequences of an event. This is the reason why a very severe earthquake happening today in Japan, where these type of events are expected, people are aware of the seismic risk and buildings are well designed to survive to major events, is likely not to cause significant damages while, less intense events, such as the medium magnitude earthquake in L'Aquila (Italy) in 2009, caused disproportionate consequences (Alexander, 2010). Likewise, this is why cyclones in Bangladesh nowadays are less destructive than they were in the past (from about 300,000 deaths in 1970 to around 4,000 in 2007; Tatham et al., 2009), thanks to disaster prevention and preparedness actions that decreased the vulnerability of the population. Hurricane Katrina in 2005 mainly killed the black poor and elderly people in New Orleans (Cutter et al., 2006), emphasizing the importance of education and preparedness.

A large part of the coasts of the world is threatened by storm events, whatever the geographical location and oceanographic setting. Clearly the magnitude of the hazard can change. Waves and storm surges can generate local hazards for the coastal elements (i.e. people, buildings, infrastructures, ecosystems, etc.), such as flooding or erosion. Coastal risk can be therefore considered, following the general definition of risk, as the interaction between hazard, exposure and vulnerability components on the coasts. However, a more practical definition, useful for the implementation of coastal risk assessments, is that risk can be quantified as the product between the probability of a hazard and its impacts (Viavattene et al., 2015). This last component is the result of the interaction between the exposure and vulnerability of the elements affected by given hazards. Impacts are therefore defined as the consequences generated by an hazardous event in the form of direct and indirect losses (Viavattene et al., 2015). This approach allows for a very detailed definition of diverse direct and indirect consequences that can be used to understand and quantify the potential overall impacts of multiple hazards on the society. This, indeed, is a very important aspect as risk assessments should account for the whole range of economic and social costs (Kreibich et al., 2014). However, there is still some confusion in the literature about the use of the term impact as some studies consider, as example, the erosion of the dune or the inundation of the back-barrier as storm impacts. In those cases the term is used in its more general meaning, to define an effect (e.g. on the beach morphology).

A practical implementation of this definition of risk (i.e. hazard · consequences) is the Source-Pathway-Receptor-Consequences (SPRC) concept (Samuels et al., 2008), which has been adapted to coastal risk studies (e.g. Narayan et al., 2014; Zanuttigh et al., 2014; Oumeraci et al., 2015). The source of the hazard is the event itself (i.e. the coastal storm) which propagates from deep water to the shoreline where pathways generate different hazards (i.e. overwash, flooding, erosion, etc.). The receptors are the elements exposed to the hazards (i.e. a seafront boulevard endangered by erosion; a flooded building; an ecosystem threatened by salt intrusion; etc.) that can generate short- and long-term damages, consequences. This approach is the basis for detailed coastal risk assessment at regional and local scales.

It is worth mentioning that assessing coastal risk, as other risks, is subjected to a large range of uncertainties on the quantification of hazard and consequences (i.e. social, economic, environmental, etc.), mainly driven by lack of knowledge or experience. Also, the way people and decision-makers perceive the risk affects how they understand it, and cope with it.

1.2 Dealing with coastal risk today

The increase in frequency and intensity of extreme coastal storms and the continuous exponential development of the coasts are acknowledged not only by the scientific community (e.g. Brown et al., 2013; Neumann et al., 2015) but also by the United Nations (IPCC, 2012, 2013), although the future projections are subjected to considerable uncertainty. As a result, coastal communities are exposed to increasing levels of risk. Above all, the 2017 hurricane season on the US east coast and the Gulf of Mexico was one of the hardest in records with four major events (namely Harvey, Irma, Jose and Maria) occurring within a few weeks (preliminary analyses on these events can be found at https://www.usgs.gov/hurricanes). European coasts also experienced very recent and rare events, such as Xynthia in France in 2010 (Kolen et al., 2013) or Ophelia in Ireland and the United Kingdom in October 2017, just to cite a few. Supra-national administrations and intergovernmental organizations are stressing the need for properly addressing risk, at all levels, by encouraging national authorities to implement risk assessments and management plans (e.g. the UNISDR Sendai Framework for disaster risk reduction 2015-30 or, more specific on floods, the EU Floods Directive 2007/60/EC). Therefore, coastal managers need to properly address coastal risk acting at the different phases of the disaster management cycle (i.e. being, in order after the impact of the extreme event: response, recovery, prevention and preparedness; see the following sections). With regard to the prevention phase, coastal risk needs to be properly evaluated in order to propose adequate risk reduction plans, for the short and long-term, including climate change projections of hazard and exposure components. Moreover, this should be done including the local communities in the decision process.

However, the work of coastal managers needs a strong support from the research community that can, and should, provide them with up-to-date, flexible and easy-to-understand (and apply) concepts, models and solutions for risk assessment and reduction. Besides, researchers need to adopt more integrated, multi-disciplinary scientific approaches as risk is the result of a complex interaction, characterized by iterative feedbacks between nature and human assets. The latter, in particular, show a strong variability in space and time and vulnerability and exposure assessments are subjected to uncertainty at various temporal and spatial scales (Figueiredo and Martina, 2016; Nguyen et al., 2016). In terms of socio-economic aspects, it can be very complex to evaluate that interaction without the support of experts in this field. Thus, the traditional approaches for risk assessment, that mainly considered the hazard component along with simplified input in terms of exposure of the vulnerable assets (e.g. land use maps), are insufficient to properly characterize the possible consequences of extreme events and/or climate change.

The human sciences can provide valuable input that physical scientists can adapt and implement to improve risk assessments. Further to the cooperation with economists, mainly aiming at properly assessing the economic direct and indirect consequences of hazards (e.g. Kunz et al., 2013), other inter-disciplinary collaborations are needed. Currently, multi-disciplinary studies are more and more often reported in the literature as effective at achieving research objectives in the field of coastal hazard and risk assessments. Indeed, historical analyses were recently adopted in support of traditional coastal research approaches for identifying and reconstructing past events aiming at better probabilistic representation of extremes (Baart et al., 2011). In the recent multi-disciplinary study of Chaumillon et al. (2017), past-event reconstruction (i.e. through historical documents and sedimentary records) was applied, in particular, for long-term (i.e. millennial-scale) analysis of storm patterns and variability. Historical maps and archaeological remains were analyzed by Fernández-Montblanc et al. (2018) in order to

reconstruct past coastal landscapes (i.e. palaeo-bathymetry and shoreline position) and, therefore, to assess past and recent rates of shoreline change. Historical investigations can also help at renewing the local "historical memory" of risk that strongly affects the perception of risk among the coastal communities by increasing a "false sense of security" (Garnier et al., 2017). Regarding these aspects, sociologists and anthropologists can be helpful in understanding the local social and cultural risk perception while supporting coastal managers and scientists to properly involve the local communities in the participatory assessment process, also contributing at proposing acceptable risk reduction plans (Becu et al., 2017; Gray et al., 2017; Martinez et al., 2017).

It follows that physical and natural scientists need to slightly change the traditional way of "doing science" by providing more accessible, easily understandable information and open their mind to diverse and more "social science" approaches. In the case of coastal sciences, in particular, a simplification and standardization of methodological approaches is currently in process. A first formal attempt to drive the interest of the international coastal research community on the topic can be found in Van Koningsveld et al. (2005), who was the first one to propose the famous Frame of Reference approach, lately applied in the MICORE project for the development of Storm Impact Indicators (SIIs)(Ciavola et al., 2011a, 2011b). This work, based on the outcomes of the EU CoastView project (Davidson et al., 2007), highlighted the need to define simplified, physically-based indicators of the state of the coast to be used in a common framework, shared by scientists and managers, for coastal management purposes. Since then, coastal research has evolved, especially in terms of field monitoring (e.g. Turner et al., 2016), modelling (e.g. Roelvink and Reniers, 2012) and risk assessment approaches (e.g. Narayan et al., 2014). Moreover, while some recent studies are still investigating the complex coastal physical interactions (e.g. Odigie and Warrick, 2017) or recalibrating models of coastal processes (e.g. Passarella et al., 2017), scientific reviews are trying to define simplified common frameworks for hazard and risk assessment (e.g. Carapuço et al., 2016; Nguyen et al., 2016; Ciavola and Coco, 2017; Ferreira et al., 2017), and climate change impacts (e.g. Ranasinghe, 2016). These reviews are likely to speed up the homogenization process and to facilitate multi-disciplinary future assessments at different temporal and spatial scales.

1.3 The EU FP7 RISC-KIT project

The EU FP7 Resilience-Increasing Strategies for Coast - toolKIT (RISC-KIT; GA 603458) (Van Dongeren et al., 2017; www.risckit.eu) collected the legacy of past EU projects, such as MICORE and ConHaz (Ciavola et al., 2011a, 2011b), as well as THESEUS (Zanuttigh, 2014). In fact, they contributed at reaching a better understanding and awareness of coastal risk issues at the European level, building the basis for a shared scientific platform where researchers and coastal managers could easily interact with the aim of reducing risk on European coasts. Indeed, the RISC-KIT project aimed at designing and test tools in support of coastal risk management in order to increase its capacity to properly assess coastal risk and provide effective and acceptable solutions for disaster risk reduction, increasing the resilience of coastal communities by acting at diverse phases of the disaster management cycle (i.e. response, prevention and preparedness, excluding recovery; Van Dongeren et al., 2017; Figure 1.1). The work of the project was based on the definition of risk as the product of the probability of a hazard and its impacts (for more details see Viavattene et al., 2015). On the basis of this assumption, the project created a storm impact database (Ciavola et al., 2017), a risk reduction web-guide (Stelljes et al., 2017), a conceptual framework for regional risk assessment (Viavattene et al., 2017), integrated numerical tools for early

warning and scenario (i.e. climate change and risk reduction measures) evaluation at the local scale (Jäger et al., 2017), further supported by a guided participatory process to assess the proposed measures (Barquet and Cumiskey, 2017). Every tool was thought to be inclusive in terms of stakeholders' involvements and strongly multi-disciplinary by including historical and socio-economical concepts (Barquet and Cumiskey, 2017; Cumiskey et al., 2017; Garnier et al., 2017; Martinez et al., 2017). For the first time, physical, economics, social and historical scientists worked together, shared ideas, concepts and aims to achieve a better understanding of the meaning of coastal risk and learn how to properly address it at the regional and local scale, in support to coastal managers.

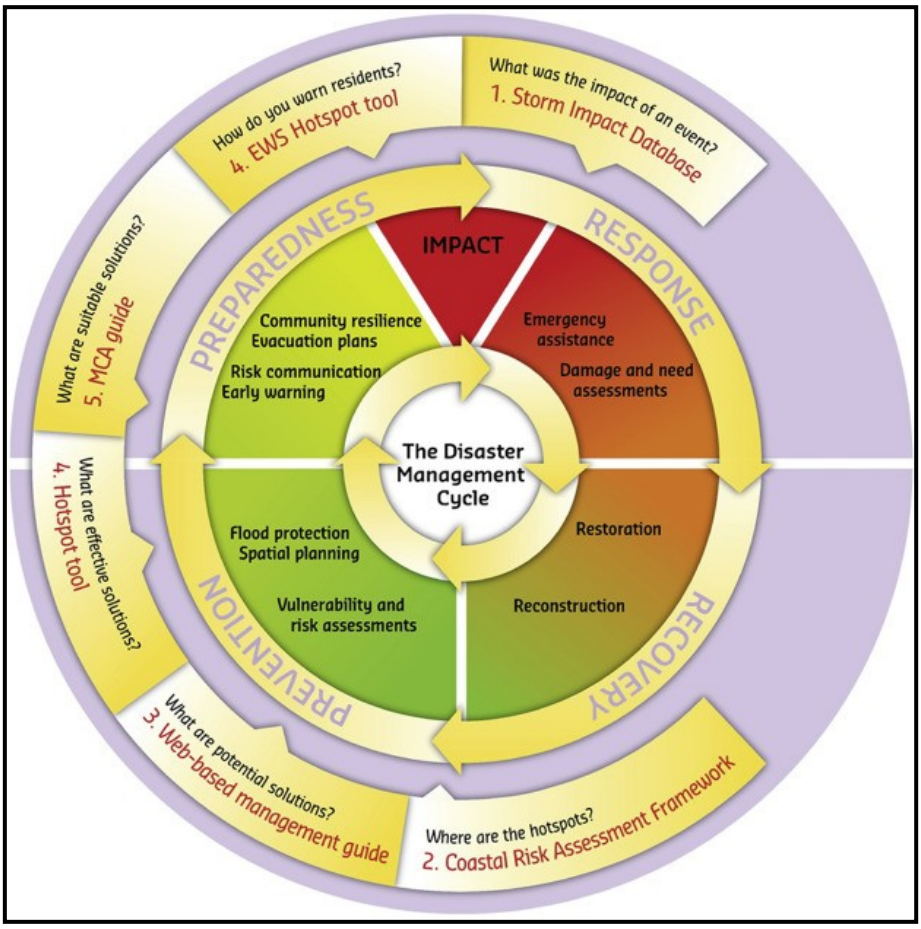

Figure 1.1 The disaster management cycle and the position of the RISC-KIT tools (Source: Van Dongeren et al., 2017).

The project successfully tested the tools in several case study sites along the EU coasts, representative of different coastal settings. More important, it highlighted how multi-disciplinary approaches can increase the quality of the assessments and the acceptance of the proposed strategies. For example, historical research was able to detect past events with characteristics similar to recent ones for most of the selected study cases, demonstrating that the perception of exceptionality of a storm is affected by the memory of the coastal community. That is the case of La Faute-sur-Mer in France, where the first report of coastal storm damages dates back to 1882, or the case of Porto Garibaldi in Italy, that in 1927 was hit by a coastal event comparable to the one recently observed in February 2015 (Garnier et al., 2017). Another example of multiple science interaction

is related to the collaboration with social scientists, which contribution was found to be invaluable when dealing with local stakeholders, in particular to interpret the outcomes of the interviews performed locally, used to understand the local context and select local measures for disaster reduction (Martinez et al., 2017), to evaluate the degree of effectiveness of the local implementation of measures (Cumiskey et al., 2017) and to moderate the participatory process for the evaluation of risk reduction strategies (Barquet and Cumiskey, 2017). All these aspects were found to be crucial in order to adapt strategies at the local level that could be accepted by the coastal community, taking into account the local contexts and competing interests.

From a practical point of view, at each case study regional domain, the regional tool for risk assessment was applied to select the local critical areas (hotspots). At the identified hotspots, after a desk-top research (including the historical research) aiming at understanding the general (regional and local) context in terms of coastal risk and risk reduction strategies, local stakeholders were interviewed in order to assess the risk awareness of the population and to select a set of measures that could easily be accepted by the coastal community. Then, the measures were tested with the tool for local risk assessment (that can also be used for local early warning), able to quantify their effectiveness for risk reduction in the current and future (climate change) scenarios. The effectiveness at the local level was also investigated including considerations on the socio-economic context. Later, the measures (and their effectiveness) were discussed during the participatory process, where stakeholders were asked to interact through a guided procedure in order to select acceptable measures to be applied as an integrated local strategy for risk reduction.

The project outcomes confirmed how multi-disciplinary approaches and stakeholders' involvement are therefore necessary, if scientists want their knowledge to be transmitted and understood by the public, from the coastal manager to the local communities.

1.4 Notes on the coasts of Emilia-Romagna and Catalunya

The Mediterranean sea is the theatre of less intense events, when compared with the hurricanes that hit the US coasts, such as Hurricane Sandy in New York in 2012 (Kunz et al., 2013), or the extreme events that impacted the coast of Northern Europe, such as the already mentioned Xynthia or the Southern North Sea storm in 2013 (Spencer et al., 2015). However, severe or extreme storms are frequent and their impacts can produce disproportionate consequences to coastal communities, especially when the coasts are intensively exploited and, at the same time, the effort of coastal managers is insufficient to guarantee an effective risk management strategy.

This is, for example, the case of the Emilia-Romagna region, in Italy, whose long coast faces the Northern Adriatic and is often threatened by high storm surges and waves, such as the recent event of February 2015 (Perini et al., 2015a) that caused significant impacts to numerous locations. Or the case of Catalunya (Jiménez et al., 2012), where erosion and flooding affect several economic sectors, tourism *in primis*. However, in both cases the risk is not only related to the single extreme occurrence (i.e. the short term), but also to the inherent problems that affect their sandy beaches, such as structural erosion or subsidence that have long term causes and effects. In both cases the human pressure is high. In both cases, the coast is the place of conflict of interests, private and public. In both cases, the coastal managers are aware of the issues related to coastal risk, current and future. In both cases, local researchers are very active in investigating their beaches. And, finally, in both cases, critical areas were chosen as case study sites in the framework of the EU FP7 RISC-KIT project which partially

supported the work of this PhD thesis. Notably, specific information on the two regional coastal domains and their critical areas can be found in the following chapters.

1.5 About this PhD thesis

This PhD thesis is the product of a three year journey through coastal risk. It collects input from many people and places that helped the author to understand how physical, social and economic aspects interact to generate risk in coastal areas and how it can be reduced, or at least how people can adapt to it.

The author had the opportunity to work with innovative, multi-disciplinary approaches for field data collection, numerical modelling and coastal management. These three aspects were found to be essentially linked. Indeed, nowadays coastal managers are more and more relying upon models for, as example, issuing alerts and designing risk reduction plans. However, models simply remain a fascinating numerical exercise when not supported (qualitatively and/or quantitatively) by field measurements that show how real world looks like. Besides, coastal managers that have enough resources (actually, very rarely) are aware that proper coastal monitoring programs are needed. Thus, they support long term measuring activities.

Thus, in this collection of articles in press or under review in scientific journals, and of manuscripts in preparation, the reader will find interesting applications of drone-based surveys (Chapters 2 and 3), numerical applications for the investigation of the propagation of uncertainties (Chapter 4) and for regional (Chapter 5) and local (Chapter 6) coastal risk assessments, implemented by integrating socio-economic aspects. Statistical concepts are included, especially by applying Bayesian Network approaches to evaluate the interconnections between variables (Chapter 4) and analyze large amount of simulations in an integrated manner (Chapter 6). The inclusion of stakeholders in the evaluation process represented a key aspect for many applications: regional coastal managers provided data and constructive comments on the risk assessment applications (Chapters 5 and 6) while, local stakeholders provided valuable specific information, as example, to better organize fieldwork, especially when implemented in a post-emergency situation, or to identify lacks in the emergency preparedness and response phases (Chapter 2). The applications mainly focused on the Emilia-Romagna (Italy) sedimentary coast and some of its critical locations. Some studies (Chapters 4 and 6) also included a comparative analysis with the Tordera Delta, a sandy deltaic coast in Catalunya (Spain). Both areas are characterized by high levels of exploitation (i.e. mainly tourism) prone to the impact of coastal storms that have different origin and evolution, according to the local oceanographic setting. While the majority of the applications aim at improving and supporting the prevention phase of the disaster risk cycle, for some of them, their potential implementation in support of preparedness and response phases are also highlighted.

This PhD thesis contributes to improve the traditional approaches for risk evaluation, with a strong interest in transferring scientific findings to coastal managers. Whereas risk assessments belong to the prevention phase of the disaster management cycle (see Figure 1.1), some aspects of this work are affected by, or affect, other phases, such as the preparedness and the response ones. Indeed, this path through coastal risk begins with two applications of coastal drone-based surveys, the first for local post-storm assessment (i.e. damage assessment, response phase; Figure 1.1) in support of a large scale (i.e. regional) response protocol, the second for the analysis of the seasonal behaviour of a sedimentary beach with artificial dune protections (in support of protection measure assessments, prevention phase; Figure 1.1); then it proceeds to an investigation of the limitation of specific simplifications in modelling and their effects

on the results (therefore, on the hazard and risk assessments, prevention phase; Figure 1.1); and finally, it leads to the application of two innovative tools in support of coastal managers, for risk assessment (in support of risk management plans design , prevention phase; Figure 1.1) at the regional and local level, respectively. All topics, contribute to improve the preparedness phase (see Figure 1.1) either by increasing the level of knowledge and awareness (and thus the resilience) of the coastal community or, in the case of the local scale risk assessment, providing tools that can be adapted for operational purposes. The main coastal risks considered are linked to flooding and erosion.

As anticipated, each chapter is adapted from papers in press, in review, or in preparation. All contributions were the product of strong international collaboration between the PhD candidate, the research team he belongs to (the COSTUF team of the Department of Physics and Earth Sciences of the University of Ferrara, Ferrara, Italy) and EU and US institutes. In all cases the PhD candidate played a prominent role either by doing field surveys, analyzing and interpreting the outcomes and writing large parts of the papers. In particular:

- Chapter 2: this piece of work is the product of a collaboration between the COSTUF team and the CSHEL team of the School of Marine Science and Policy of the University of Delaware (Newark, DE, US). The PhD candidate contributed to the field data (i.e. qualitative and quantitative) collection, data analysis, interpretation and manuscript preparation. The original manuscript was accepted for review in Natural Hazard and Earth System Sciences as:

  Trembanis, A. C., Duo, E., Dohner, S., Grottoli, E., and Ciavola, P.: Quick Response Assessment of the Impact of an Extreme Storm Combining Aerial Drone and RTK GPS, Nat. Hazards Earth Syst. Sci. Discuss., in review, doi:10.5194/nhess-2017-337, 2017.

  The chapter represents a restructured and revised version of the manuscript and addresses the main issues highlighted by the anonymous reviewers (see interactive discussion at https://www.nat-hazards-earth-syst-sci-discuss.net/nhess-2017-337/). However, it does not represent the version that will be resubmitted in case the manuscript will be accepted. That version will be prepared in agreement with all the co-authors. Given the major changes applied, the authors' order and the title will change as follows:

  Duo, E., Trembanis A. C., Dohner, S., Grottoli, E. and Ciavola, P.: Integrating Regional Protocols for Post-Event Assessments with Local GPS and UAV-based Quick Response Surveys: a Pilot Case from the Emilia-Romagna (Italy) Coast.

- Chapter 3: this work is the product of a pilot drone-based surveying campaign that was held between October 2016 and April 2017 at the beach of Porto Garibaldi (Comacchio, Italy) and implemented by the COSTUF team, supported by Dr. A. Ninfo (Dep. of Physics and Earth Science of the University of Ferrara, Ferrara, Italy). The aim of the program was to design and test a procedure for drone beach monitoring in a location that is historically impacted by extreme events and where local stakeholders regularly implement soft risk reduction measures, such as temporary artificial dunes as protection against coastal storm impacts for beach concessions. Given the lack of significant coastal storm events on the area during the monitored period, only the preliminary results of the study are shown and discussed. The PhD candidate contributed to the field surveys,

implemented the photogrammetric reconstruction, analyzed and interpreted the results and wrote the present chapter. Indeed, this chapter represents a first draft of a manuscript that will be updated as soon as more interesting results will be available. At the moment of the submission of this PhD thesis, the research team was again operative since October 2017, waiting for the "Big One" storm to occur for testing the procedure.

- Chapter 4: this piece of work is the product of a collaboration between E. Duo and M. Sanuy , PhD student at the Laboratori d'Enginyeria Marítima (LIM) of the Universitat Politècnica de Catalunya (Barcelona, Spain). This study was also funded by the Grant Programme for Young Researchers of the University of Ferrara through the "5 per mille assegnato all'Università di Ferrara - dichiarazione dei redditi dell'anno 2013". The PhD candidate owns the idea of the study and implemented it at the Italian site, contributed to the analysis, interpretation and manuscript preparation. This chapter represents the most recent version of the manuscript that is in preparation for the submission to the Elsevier journal Coastal Engineering. The manuscript will be submitted in the next weeks as:

  Duo, E., Sanuy, M., Jiménez, J.A. and Ciavola, P.: Synthetic Storms: Uncertainties and Limitations of their Application in Coastal Hazard Modelling.

- Chapter 5: this analysis was developed in the framework of the EU FP7 RISC-KIT Project (GA 603458) as application and validation of the Coastal Risk Assessment Framework on the Emilia-Romagna coast. The PhD candidate contributed to the implementation of the hazard assessment, data analysis, interpretation and manuscript preparation. This chapter is in press for Coastal Engineering, as research paper contribution to the RISC-KIT Special Issue:

  Armaroli, C. and Duo, E.: Validation of the coastal storm risk assessment framework along the Emilia-Romagna coast, Coast. Eng., in press, doi:10.1016/j.coastaleng.2017.08.014, 2017.

- Chapter 6: the analyses presented were developed in the framework of the EU FP7 RISC-KIT Project (GA 603458) as application of the RISCKIT Hotspot tool for local scale coastal risk assessment and scenarios testing. The work was the product of a collaboration between E. Duo and M. Sanuy , PhD student at the Laboratori d'Enginyeria Marítima (LIM) of the Universitat Politècnica de Catalunya (Barcelona, Spain). The PhD candidate implemented the study at the Italian site, contributed to the analysis, interpretation and manuscript preparation. The original manuscript was accepted with "Major revision with further review by Editor and Referees" for the publication in Natural Hazard and Earth System Sciences as:

  Sanuy, M., Duo, E., Jäger, W. S., Ciavola, P., and Jiménez, J. A.: Linking source with consequences of coastal storm impacts for climate change and risk reduction scenarios for Mediterranean sandy beaches, Nat. Hazards Earth Syst. Sci. Discuss., in review,doi:10.5194/nhess-2017-345, 2017.

  The chapter represents a revised version of the original manuscript and addresses the main issues that were highlighted by the anonymous reviewers

(see interactive discussion at https://www.nat-hazards-earth-syst-sci-discuss.net/nhess-2017-345/). However, it does not represent the version that will be resubmitted. That version will be prepared in the next weeks in agreement with all the co-authors.

A final conclusive chapter (Chapter 7) will summarize the findings of each chapter and will give an integrated view of the lessons learned and opportunities for improvements.

This PhD thesis was reviewed by two external referees between 1 December 2017 and 8 January 2018. The referees were Dr. Ap Van Dongeren (Deltares, Delft, The Netherlands) and Prof. Tom Spencer (University of Cambridge, Cambridge, United Kingdom). This version of the thesis addresses all their comments and suggestions.

The thesis, is addressed to students, researchers, and professionals, that will find useful insights especially on drone, numerical and Bayesian applications; and, finally, to coastal managers, that will find up-to-date approaches dealing with post-storm monitoring, coastal risk assessments, climate change scenario and disaster risk reduction (DRR) measures evaluation.

2 INTEGRATING REGIONAL PROTOCOLS FOR POST-EVENT ASSESSMENTS WITH LOCAL GPS AND UAV-BASED QUICK RESPONSE SURVEYS: A PILOT CASE FROM THE EMILIA-ROMAGNA (ITALY) COAST

2.1 Introduction

Coastal flooding and erosion caused by extreme storm events shape coastlines, impact coastal infrastructure, and present hazards to coastal inhabitants that can thus suffer their consequences. The most damaging events consist of a combination of extreme wave heights, storm surge, wind direction, and tidal stage, that interact with the morphology of the beach and adjacent infrastructures generating direct and indirect impacts (Van Dongeren et al., 2017; Viavattene et al., 2017). With expectations of increasing storm intensities and occurrence (Bason et al., 2007), coastal communities are in need of accurate field data to inform management and policy decisions (Casella et al., 2016). To ensure appropriate plans are enacted, precise and high-resolution field measurements are required to understand storm effects on the community and to provide input for numerical modelling for future impact prediction purposes (Lee et al., 1998; Stone et al., 2004; Nicholls et al., 2007). Besides, the inclusion of local stakeholders in the assessment process is essential to better understand the local point of view and properly address risk reduction plans (Martinez et al., 2017).

Coastal managers are requested to adopt plans and protocols for risk management, ranging from prevention, preparedness, response and recovery phases of the risk cycle. Indeed, the importance of protocols and standard approaches for risk management is recognized at the European level (Poljanšek et al., 2017). The role of post-event assessments (response) are of vital importance to properly address coastal risk management. The forecasting and early warnings (preparedness) can support the assessments and help at coordinating the response tasks on the field. Consequently, the results of the assessments can be used to improve hazard and risk maps, and enhance risk reduction plans (prevention). In this context the Emilia-Romagna Region already adopted effective protocols for coastal risk management and, of particular interest for this work, regarding early warning and post-storm hazard and risk assessments (Ligorio et al., 2012; Perini et al., 2015b, 2016).

Capturing the physical signature of a storm event requires a rapid quantitative mapping response to assess the impacts to the coastline after the storm, before either natural or human induced recovery processes take place (Morton et al., 1993; Bush et al., 1999; Morton, 2002). Notably, in order to properly quantify these impacts, it is also desirable to collect pre-storm elevation data. In recent years, autonomous platform methodologies for coastal mapping and extreme event impact assessment were proposed and tested, beyond the traditional GPS, LIDAR, and satellite remote sensing techniques, such as the use of unmanned vehicles for mapping the emerged beach (Mancini et al., 2013; Casella et al., 2016; Turner et al., 2016) and the submerged area (Trembanis et al., 2013).

The classic stadia rod and level beach surveying technique, while still functional, has been replaced by time and cost efficient Real-Time Kinematic Geographical Positions Systems (RTK GPS) for ground-based surveys (Morton et al., 1993; Theuerkauf and Rodriguez, 2012). RTK GPS is the preferred method for any data collection requiring highly accurate (few centimeter) positioning measurements and is utilized in the coastal environment for temporal and spatial monitoring of many coastal morphologic features (Larson and Kraus, 1994; Benedet et al., 2007; Hansen and Barnard, 2010; Theuerkauf and Rodriguez, 2012). With RTK GPS surveys, questions arise regarding the accuracy

of beach morphology representation due to insufficient resolution when traditional profile spacings of more than 100 meters are used (Swales, 2002; Bernstein et al., 2003; Pietro et al., 2008; Theuerkauf and Rodriguez, 2012). Terrestrial laser scanners or total stations improve point density but require more time and physical effort as RTK GPS, particularly when surveying large areas (Saye et al., 2005; Theuerkauf and Rodriguez, 2012; Lee et al., 2013). Improvements in remote sensing technology have increased point density through airborne lasers (LiDAR) and satellite imagery but the high costs of operations and infrequent surveys render these options impractical for local scales and rapid or frequent repeated surveys (Stockdon et al., 2002; Young and Ashford, 2006; Anderson and Gaston, 2013). A recent LiDAR application was proposed by Phillips et al. (2017) by fixing a laser system on a building to continuously monitor beach profiles. The system was able to provide interesting results for beach recovery analysis and showed a great potential for other investigations. However, the measurements are performed on a single location, in the cross-shore direction.

Recent improvements in autonomous technology have made Unmanned Aerial Vehicles (UAV) a useful emerging tool in the survey world which accommodates local scales, rapid and frequent surveys, and can be economically feasible with accurate results for monitoring hydro-morphological changes in the coastal zone (Berni et al., 2009; Westoby et al., 2012; Casella et al., 2016; James et al., 2017).

Focusing on the social dimension of the problem, it was demonstrated that the inclusion of local people in the processes of coastal risk assessment and preparation of reduction plans, can improve the quality of the outcomes and can have a positive feedback on the population, increasing its risk awareness and preparedness (Pescaroli and Magni, 2015; Becu et al., 2017; Gray et al., 2017; Martinez et al., 2017). In this sense, performing interviews of local people in the immediate aftermath of a coastal extreme event can provide important information on the local evolution of the storm, and, even more importantly, on the effectiveness of the implemented emergency preparedness and response phases (Martinez et al., 2017).

Here, a pilot case study of a quick response protocol for local post-storm assessment, utilizing a combination of traditional on-ground RTK GPS surveys together with aerial imagery gathered by an Unmanned Aerial Vehicle (UAV or drone) for digital photogrammetric reconstruction further supported by qualitative data collection (i.e. interviews of local stakeholders), is presented. This combination of technologies allows for a rapid and more holistic coverage of the field site. The presented results of the pilot test demonstrate that the approach can provide high-resolution data for capturing storm impacts. Furthermore, this integrated approach can provide detailed insights that can be applied at the local, as well as at regional and national levels, for coastal management purposes. The evidences also show that the local protocol could be integrated in the regional protocol for post-storm assessment, creating a very effective coordinated protocol.

2.2 Case Study

2.2.1 Regional settings and study site

Regional settings

A stretch (~7 km) of the coastal area of the Ferrara province (Emilia-Romagna region), on the Italian side of the Northern Adriatic Sea (Figure 2.1A,B), was surveyed starting in the waning period of an extreme storm event (hereafter called the Saint Agatha storm, see Section 2.2.3) that occurred on 5-7 February 2015. The survey continued for a week

following the passage of the storm. The coastal landscape in Emilia-Romagna is generally comprised of low-lying sandy beaches with limited topographically elevated areas usually in the form of either relict beach ridges or artificial embankments (Armaroli et al., 2012). The shore is comprised of alternating spaces of natural areas with native dunes and intermixed with more prevalent urbanized areas with tourist facilities and coastal protection structures (i.e. groins and breakwaters). Through continued development and urbanization over the last 60 years as a result of grants to commercial beach concession operators, most of the shore is now occupied by tourist facilities, residential buildings, and bathing structures often replacing the ancient coastal dune ridges (Sytnik and Stecchi, 2015). Since the end of World War II, a sediment deficit has affected the littoral budget as a result of a decrease in sediment transport towards the shore by local rivers, mainly because of the human interventions on the rivers and their basins (Preciso et al., 2012) and the reforestation of the Apennines (Billi and Rinaldi, 1997). The exposure to coastal flooding is high, especially in the Ferrara and Ravenna provinces, where some elevations are below Mean Sea Level (MSL)(Perini et al., 2010a), and several defence structures (groins, breakwaters, etc.) have been built along the coast in the hope that beach retreat would cease (Armaroli et al., 2012). This problem has been exacerbated over the last few decades by land subsidence, which has been caused mostly by groundwater and gas extraction activities (Teatini et al., 2005; Taramelli et al., 2015).

The wave climate for the region is characterized by low wave energy (mean $H_s \approx 0.4$ m, $T_p \approx 4$ s) with a semidiurnal micro-tidal regime (neap tidal range = 0.30 m; spring tidal range = 0.8 m). Storm waves with 1-year return period range up to 3.3 m (Armaroli et al., 2009) and storm surges with a 2-year return period are up to 0.6 m (Masina and Ciavola, 2011). These storm events can occur, particularly in the fall and winter months (October-March), which comprises the storm season. Storms are mainly characterized by ENE waves associated with Bora (NE) winds or by SE waves if caused by Scirocco winds. Storm surge events predominantly occur during SE winds, which also coincide with the main SE–NW orientation of the Adriatic Sea. Bora storm waves are generally higher and steep, whereas Scirocco waves are smaller but with a longer wave period. This is because the latter are generated over a longer fetch by winds of lower intensity (Harley et al., 2016).

Several methods for storm characterization have been developed and implemented in recent years for the Mediterranean coast. Mendoza et al. (2011) proposed a five-class intensity scale, defining a storm as an event in which the significant wave height exceeds 1.5 m for at least 6 hours (Mendoza and Jiménez, 2006). Moving to a more local perspective, Armaroli et al. (2012) adopted the same physical definition of storm events for the northern Adriatic. Two storms are considered separated when the significant wave height decreases below the 1.5 m threshold for 3 or more consecutive hours. As a resulting of the combined analysis of the events and their impacts, that study classified a storm as “potentially damaging” when it exceeds the critical wave and total water level (TWL = surge + tide) threshold which are: $H_s >= 2$ m and TWL >= 0.7 m for urbanized beaches; $H_s >= 3.3$ m and TWL >= 0.85 m for natural beaches. The Saint Agatha storm was identified utilizing the nearest offshore buoy and tide gauge (Figure 2.1C and Figure 2.2) records of waves and water levels, and following the Armaroli et al. (2012) storm definition.

Case study site and target area

The case study site is the portion of coast between Porto Garibaldi and Lido di Spina and is characterized by highly developed, low-lying sandy beaches, with commercial concessions (i.e. properties located on public beach areas, granted to privates for

commercial/tourism activities) directly facing the sea. The width of the beach ranges from ~20 m to ~150 m. The predominant sediment transport is directed northward. The southern jetty of the canal harbour (Porto Canale) in Porto Garibaldi traps this sediment, resulting in widening of the beach of Lido degli Estensi and depleting the Porto Garibaldi beach. Erosion appears again in the southern part of Lido di Spina (Nordstrom et al., 2015), as it can be seen in Figure 2.1D. The southernmost concession at Lido di Spina defines the southern boundary of the case study. In the whole area, the concessions can be affected by coastal storm impacts during extreme events (Nordstrom et al., 2015). The pilot case study presents areas that are well known at the regional level as coastal risk prone area (Perini et al., 2016; Armaroli and Duo, 2017). The target area of the analysis of this pilot study, is the southernmost portion of the beach at Lido degli Estensi (Figure 2.1E) in the municipality of Comacchio, east of Ferrara and north of Ravenna.

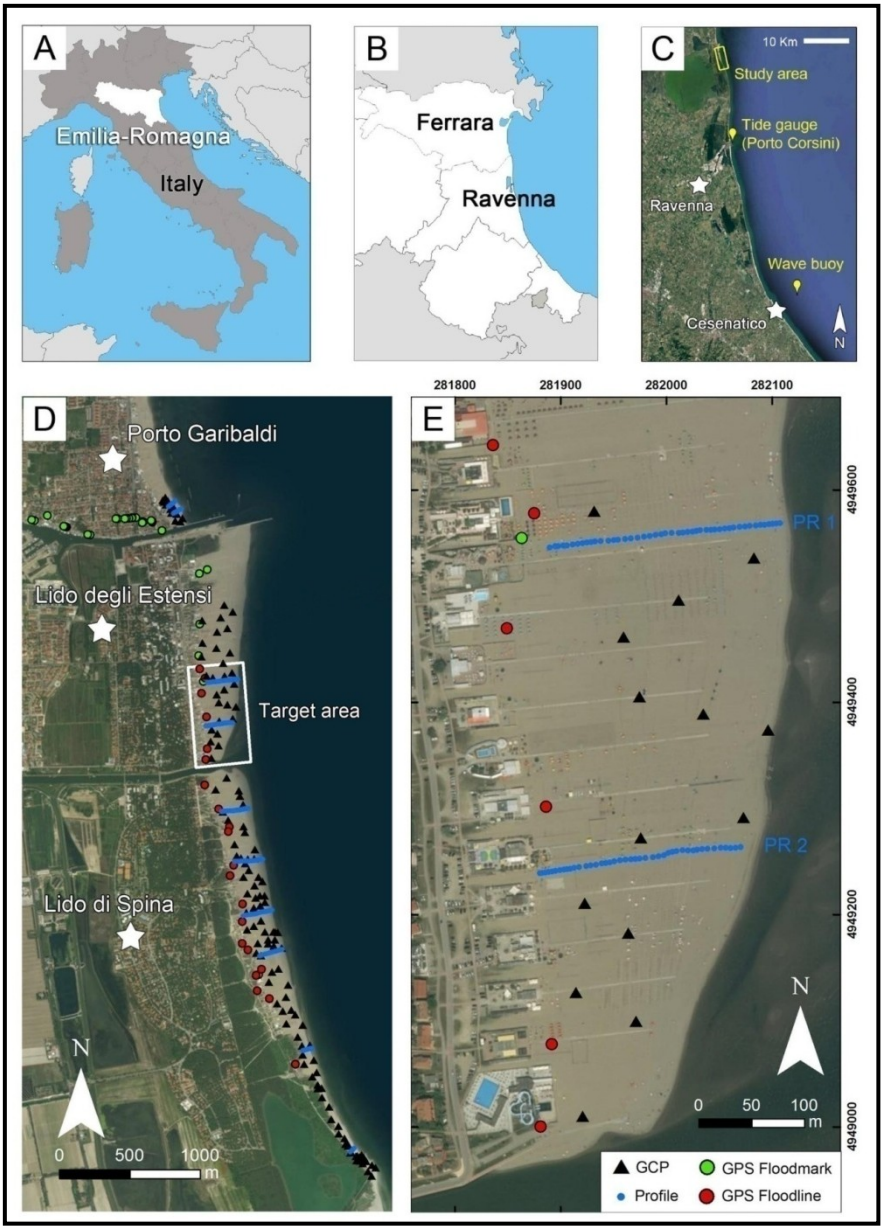

Figure 2.1 Field study site locations: A) Emilia-Romagna region; B) Coastal regional domain; C) Locations of the nearest tide gauge and wave buoy; D) Pilot case study site; E) Target area for data comparison.

2.2.2 Coastal alerts and monitoring in Emilia-Romagna

The Emilia-Romagna Region (RER) developed a protocol for coastal storm alert and monitoring, in the framework of a wider system for hydro-geological risk alert, and several agencies and regional services are involved in the process (Ligorio et al., 2012). The daily forecasting of waves, surge and coastal impacts, provided by the Servizio IdroMeteoClima of the Agenzia Regionale per la Prevenzione, l'Ambiente e l'Energia (ARPAE-SIMC), are evaluated, along with the weather forecast, by the regional geological service (Servizio Geologico Sismico e dei Suoli, SGSS), the Centro Funzionale of ARPAE (ARPAE-CF), the regional Servizio Difesa del Suolo della Costa e Bonifica (SDSCB), the technical services (Servizi Tecnici di Bacino, STB), the inter-regional agency of the Po river (Agenzia Interregionale Fiume Po, AIPO) and the Civil Protection.

The forecasting of coastal hazards and impacts is provided through the regional Early Warning System (EWS), developed in the framework of the EU FP7 MICORE project (www.micore.eu), with the objective to predict the imminent arrival of a storm as a tool to be used by Civil Protection agencies and local communities (Ciavola et al., 2011b; Harley et al., 2012, 2016; Jiménez et al., 2017b). The Emilia-Romagna EWS is operational and is run by ARPAE-SIMC and the University of Ferrara (UNIFE) by executing a daily sequence of connected numerical models (COSMO, SWAN, ROMS, and XBeach), comprised of 22 cross-shore profiles, with the final output transformed into a format suitable for decision-makers and end-users (Harley et al., 2012). The EWS tool is based on Storm Impact Indicators (SIIs) (Ciavola et al., 2011b), focusing on the magnitude of water ingression and the type of exposed assets, which are described as natural or urbanized beaches (Harley et al., 2016). The daily outputs are published online at http://geo.regione.emilia-romagna.it/schede/ews/.

From 2017, the RER activated an online portal (https://allertameteo.regione.emilia-romagna.it/) where the alerts are published in a GIS-based interface. In case of forecasted over-threshold events, or unexpected ones, the alert is issued to the Civil Protection that forwards it to the local technical services and municipalities, and the monitoring phase begins and updates are issued on the basis of observations (i.e. waves, water levels, wind, rains, etc.) and forecasting updates. If necessary, the emergency response is activated and implemented by the Civil Protection.

The SGSS is in charge of data collection and elaboration for coastal risk management purposes (Perini et al., 2015b; Armaroli and Duo, 2017). During and after a coastal event the geological service collects all available information from forecasting, observations, online pictures, webcam movies and news. After significant coastal events, the STBs are activated and implement on the ground surveys, documenting local impacts and measuring the water ingression. The SGSS also survey (with DGPS techniques) 18 beach profiles in 13 locations along the coast, belonging to the regional beach monitoring network (Rete di Monitoraggio dei Profili di Spiaggia, REMPS). After an important event, the Civil Protection fly over the impacted areas taking oblique aerial pictures. However, this is not a regular procedure and is occasionally implemented. All the information are elaborated and archived by the SGSS in the public GIS-based coastal information system (Sistema Informativo del Mare e della Costa, SIC; http://ambiente.regione.emilia-romagna.it/geologia/temi/costa/sistema-informativo-del-mare-e-della-costa-sic), in the in_Risk and in_Storm platforms (Perini et al., 2015b).

The Emilia-Romagna Region (RER) can actually be considered acting at the state-of-the-art in coastal alert and monitoring at the EU level (Perini et al., 2015b), as also

publicly declared in a press release by the European Commission on the 26 September 2014 (http://europa.eu/rapid/press-release_IP-14-1046_en.htm).

2.2.3 Storm event

During the period February 5-7 2015, an extreme storm hit the Emilia-Romagna coast and the whole of the northern Adriatic Sea, causing flooding of extensive portions of urban and natural areas. The storm occurred in the context of extreme regional weather conditions, which included heavy snow in the Apennines and rain in the alluvial plain of the Emilia-Romagna region (ARPA E-R SIMC, 2015; Perini et al., 2015a, 2015b). As anticipated, the storm was named by the colloquial name of the Saint Agatha storm as it began the day of the celebration of Saint Agatha in Italy. The storm started at night and lasted for more than two days (51 hrs), making it one of the longest duration storms in the record of the local wave buoy offshore of Cesenatico (Figure 2.1C), deployed in May 2007. The maximum water level (surge + tide) of 1.20 m was measured at 23:40 GMT on 5 February (Figure 2.2). The non-tidal residual time-serie was assessed on the basis of the tidal predictions (calculated for Porto Corsini using data for the period 2007-2015 with t_tide; Pawlowicz et al., 2002) and showed a peak of 1.27 m in the morning of 6 February (Figure 2.2). The skew surge for the tidal cycle that included the peak of the total water level was calculated and resulted in 0.92 m. The maximum significant wave height (4.6 m) was recorded in the morning of 6 February (Figure 2.2). The wave direction was consistently from the ENE sector for the entire event duration. The recorded water level was provided by the tide gauge of ISPRA (Istituto Superiore per la Protezione e la Ricerca Ambientale) located in Porto Corsini, Ravenna (Figure 2.1C). Wave data was recorded by the ARPA-ER (Agenzia Regionale per la Prevenzione e l'Ambiente dell'Emilia-Romagna) offshore wave buoy located at 10 m depth, 5.5 km offshore from the town of Cesenatico (Figure 2.1C).

According to the Mediterranean storm classification of Mendoza et al. (2011), the Saint Agatha storm is assigned the severity class IV ("Severe"). The storm severity was amplified by the combination of high waves, high water level and intense rainfall that created combined problems to the local river discharge (Perini et al., 2015a, 2015b). Furthermore, according to the classification of Armaroli et al. (2012), the Saint Agatha storm was expected to have a strong impact on the coast, exceeding the combined wave and water level hazard thresholds over a wide area (Figure 2.2).

Perini et al. (2015b) reported that the event was forecasted by the regional forecasting chain and the EWS. An alert of Level 1 (out of 3 levels, from 1 to 3) was issued at regional level already on the 4 of February. The day after it was increased up to Level 2. The regional protocol allowed to monitor the evolution of the event with the support of measuring stations (i.e. weather, waves, water levels), webcams, waves and surge forecasts and the EWS alerts (updated every day). The monitoring of the damages started on the 6 of February: while the STBs were visiting the impacted locations from the ground, the Civil Protection implemented a first helicopter flight, providing oblique aerial pictures used to map impacts. Two other flights were performed on the 8 and the 10 of February, in order to complete the survey. In that period, the SGSS collected online material such as pictures, movies and news. All the information were archived in the regional database, although the material is not yet visible online. However, information on the storm and its impacts are available at the RISC-KIT Storm Impact Database (http://risckit.cloudapp.net/risckit/#/) (Ciavola et al., 2017).

The whole dataset was used to evaluate the impacts along the coast and the observed ingression line (elaborated from aerial pictures and local measurements, where available) was compared with the risk maps produced for the Floods Directive

(2007/60/EC) (Perini et al., 2016). On the basis of this analysis, Perini et al. (2015b) showed that the inundation extension was similar to the inundation scenario defined by an event with a representative return period of 100 years. In specific locations, however, the inundation exceeded the 100 year scenario limit, or, on the contrary, resulted more similar to the 10 year flooding scenario.

Severe damage to several concession properties and urban areas was recorded along the coast (Perini et al., 2015a, 2015b). While in the Ferrara province the impacts were mainly confined to the exposed beach, causing significant damage to the concessions (urbanized beaches), to the dune systems (natural areas) and smaller harbours (e.g. flooding of the Porto Canale in Porto Garibaldi), in the Ravenna province several coastal towns experienced extensive flooding of residential areas (e.g. Lido di Dante, Classe and Savio, where a flood water depth of 2 m was recorded, Perini et al., 2015b).

As part of the quick response effort, the research team was able to visit several locations, in the Ferrara and Ravenna provinces, in the two weeks immediately following the event, with a focus on directly observing and quantifying the effects of the event, where rapid post-storm intervention did not occur. In this chapter, the analysis of the survey is presented for the case study and Lido degli Estensi in the Comacchio municipality (i.e. the target area in Figure 2.1E) is shown.

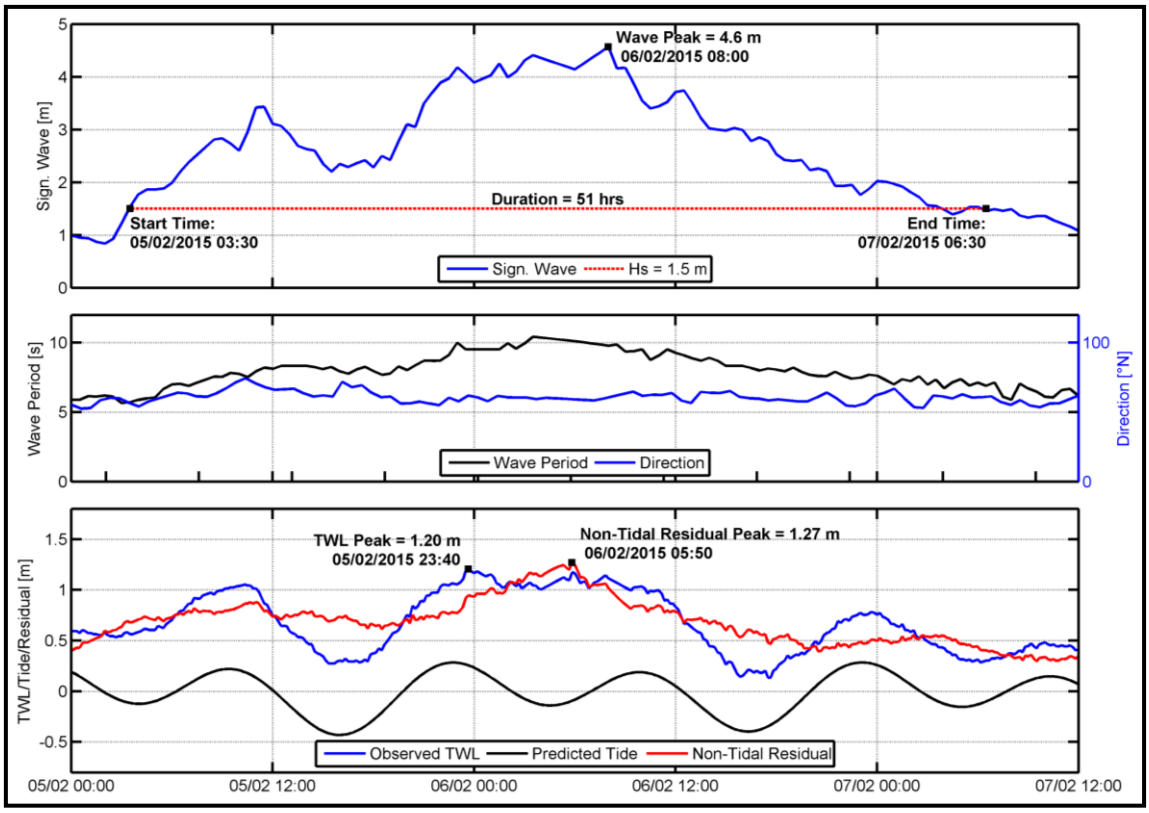

Figure 2.2 Saint Agatha storm hydrodynamic data including significant wave height (m), wave period (s), direction of waves (nautical degrees), total water level (m), predicted tide (m) and non-tidal residual (m). The start and end time of the storm is referenced to the local storm threshold condition of H_s = 1.5 m and referenced to GMT.

2.3 Methods

2.3.1 Quick Response Protocol

It was developed, and it is presented here, a coordinated Quick Response Protocol (QRP) for a quick storm impact assessment at local level to be implemented by Quick Response Team (QRT) by integrating EWS (Early Warning System) input, RTK GPS and drone survey techniques, along with quantitative observation and collection of data through interviews with local stakeholders and damage annotation. In the framework of the risk management cycle, the QRP is shown in Figure 2.3. The available regional EWS is able to provide early information on the specific coastal areas within the regional domain that are likely to be impacted by an approaching storm. In this case study, the EWS has been operational for several years and is utilized by the RER and results made available to the general community (see Section 2.2.2). Thus, the QRT is able to know in advance where the quick response will most likely be needed and prepare in advance personnel scheduling and survey equipment. The pre-storm survey, mainly topo-bathymetric survey through both RTK GPS and UAV techniques, should be performed whenever possible, given enough time and resources. However, it is most critically necessary (i) in case studies where important morphological changes take place over short time-scales and/or (ii) when other sources of information are not available on the pre-storm condition in the likely impacted area. The regional forecasting system (see Section 2.2.2) can provide further guidance to the QRT by indicating when storm conditions have subsided sufficiently to allow survey activities on the ground and in the air.

The QRP for storm local impact assessment included a sequence of steps to acquire both qualitative and quantitative measurements of the storm in the aftermath of the event. The critical tasks of the quick response strategy during the days immediately following the storm included the following activities:

- Conduct interviews of citizens, shopkeepers, restaurant owners, and other local stakeholders;
- Annotate the visible damage to coastal defences, buildings, infrastructures;
- Take pictures of the horizontal flood limits and vertical flood marks;
- Measure the vertical elevation of flood marks on buildings and defence structures;
- Map the horizontal flood limit by means of RTK GPS;
- Survey of the beach by means of RTK GPS (profiles) and aerial drone flights.

The survey tasks focused on the emerged part of the beach as the drone system was not capable to acquire reliable information on the submerged area. In general, for micro-tidal environments, the GPS technique can be used to survey the intertidal area of the cross-shore profiles. The information could be used in comparison with the pre-storm dataset, when covering the same area. However, the information would not be useful to perform 2D analysis. Some possible improvements of this and other aspects are given in Section 2.6.

The QRP steps provided data to allow for an integrated analysis of the storm impacts. The need to conduct rapid field survey activities in this study required the contribution of several people: at least 2 to 3 skilled operators were necessary to accomplish all the tasks in the field, every day. Depending on the alongshore extension and width of the coast that needs to be covered, the implementation of the protocol could last from a few days to a few weeks. In this study, 7 days were sufficient to complete the

aforementioned tasks along a total beach length of almost 7 km for the case study site (Figure 2.1D), resulting in the integrated assessment rate of 1km per day. In total, 10 profiles and more than 40 flood limits and flood marks were surveyed with RTK GPS technique and 6km of beach were surveyed with the drone and a further 50-60 GCPs (Ground Control Points) were surveyed on the ground with RTK GPS for use in the drone data processing, error analysis and data comparison.

The data processing and analysis of the acquired information is further described in the next sections, specifically focusing on the target area (Figure 2.1E). The integrated information will help to understand the overall effect of the storm in the surveyed area. The scientific aim of the QRP is to provide useful input to coastal managers for hazard and risk assessment purposes (Figure 2.3), integrating the post-storm information collected at the regional level.

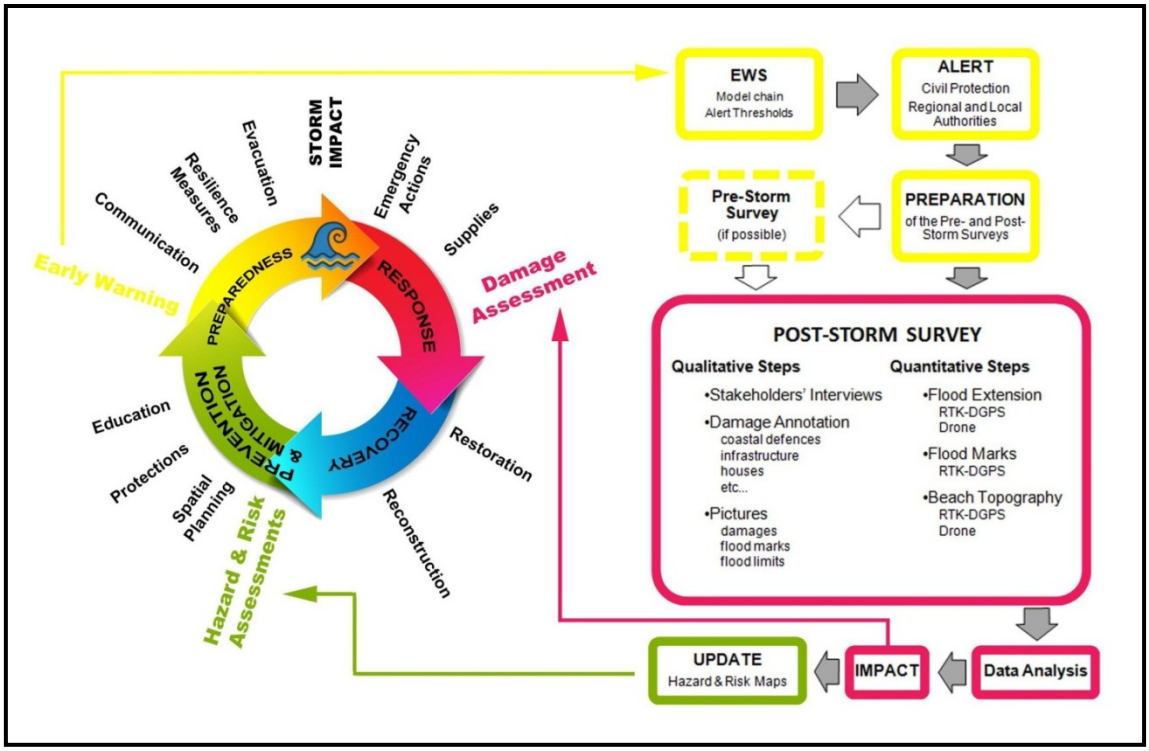

Figure 2.3 The Quick Response Protocol (QRP) in the framework of the Disaster Management Cycle.

2.3.2 Pre-storm conditions

The pre-storm conditions of the subaerial beach and backshore were assumed to be represented by the available LIDAR-derived DTM from October 2014. The dataset was used as reference for the morphological variations of the emerged beach due to the storm impact, as no major events occurred in the period before the survey and the Saint Agatha event.

2.3.3 Stakeholder interviews

Local stakeholders (SH) were interviewed by the QRT on the morning of the 7 of February 2015. The interviews were mainly based on informal questions on the recent experience, focusing on the timing of the evolution of the flood event; what the people were doing before, during and after the event; if they were alerted and prepared. They

were also requested to give an interpretation of the causes of the impacts of the event. Ten SHs were interviewed in Porto Garibaldi (Figure 2.1D), the town in the north of Lido degli Estensi. The group included mainly owners of commercial or touristic services (e.g. concessions, restaurants, shops and others), a resident, a fisherman and a fireman. Notably, in this work, the interviews were mainly used to understand which local areas were mostly impacted, in order to better organize the field activities, and to understand the timing of the storm impact evolution.

2.3.4 Ground GPS survey

Field measurements relative to flood limits, flood marks, and beach profiles were undertaken using a RTK GPS (Trimble R6). All measurements were referenced to WGS84 UTM33N coordinates and the national geoid Italgeo99 for elevation. The flood limit denotes the maximum water progression on the plan view, evidenced by the presence of objects and debris moved inland by the water during the storm. It was associated with a GPS location (see Figure 2.4A). These type of points are hereafter called "GPS Floodlines". A flood mark denotes the maximum water depth at a specific location where the water level was clearly visible, for example, walls, buildings, trees or dunes (e.g. Figure 2.4B). These points, hereafter called "GPS Floodmarks", were associated with a GPS location and a water depth measured, e.g., with a simple meter (see Figure 2.4B). Cross-shore beach profiles were also surveyed in order to have a comparison (i.e. *a posteriori*) with the post-storm Digital Elevation Model (DEM) generated from the drone photogrammetric analysis. Ten cross-shore profiles were measured throughout the surveyed area highlighted in Figure 2.1D. The measurements were done on the terrain and thus excluding variation in the elevation due to debris, wood or others. The profiles belonging to the case study target area are two (Profile 1 and Profile 2 in Figure 2.1E). These profiles were then used to provide a validation/quantification of error (i.e. RMSE) of the drone processed data.

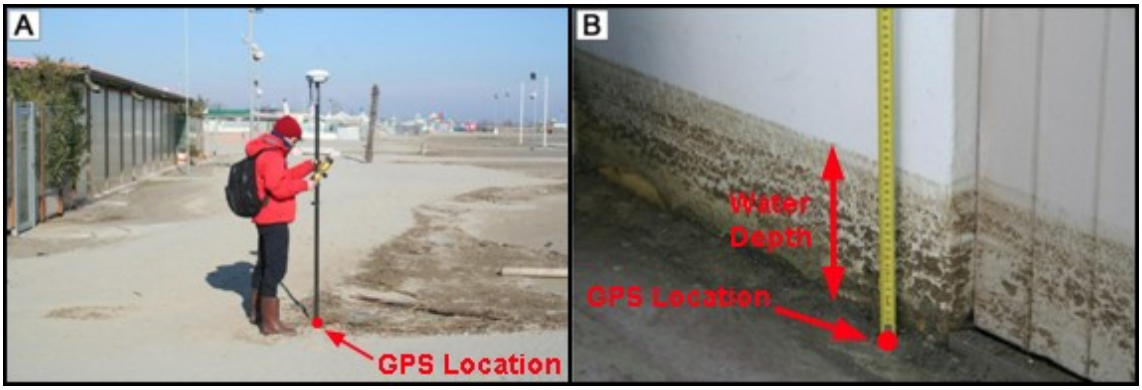

Figure 2.4 Examples of "GPS Floodline" (A) and "GPS Floodmark" (B) measurements.

2.3.5 UAV survey and Ground Control Points

A commercial off-the-shelf unmanned aerial vehicle (UAV), the DJI Phantom Vision 2+, was used to conduct the aerial remote sensing imagery capture. Photos were collected from elevations between 40-60 m at speeds of 4 m/s with manual flight controls used to fly in a lawn-mower pattern (e.g. boustrophedon flight pattern) back and forth across the beach with 65-75% overlap between images resulting in more than five photos per common point within the survey domain. Manual flights were performed as, at the time of the survey , the team did not have at its disposal automatic

flight tools and software. This approach influenced the results (as expected) and this aspect will be emphasized and discussed in the following sections. The drone camera utilized a fixed focal length, constant exposure, and timed image capture every five seconds. Fourteen Ground Control Points (GCPs) were measured using a RTK GPS (Trimble R6) for use in support of the photogrammetric process. A commercially available photogrammetric software package, specifically Pix4D, was used to stitch the collected UAV photos into one continuous mosaic by matching points within overlapping photos utilizing structure-from-motion (SfM) algorithms. The application of drone based SfM photogrammetry for coastal morphology assessment has been demonstrated recently by the studies of Casella et al. (2014, 2016), Dohner et al. (2016), Turner et al. (2016) and Scarelli et al. (2017). Drone photo post-processing followed the step-wise process illustrated in Figure 2.5, whereby photos are matched using embedded GPS metadata from the UAV then GCPs are added to the mosaic to constrain error with the more accurate RTK GPS positioning for horizontal and vertical control. Orthophoto mosaics are then reduced to dense points clouds with elevation values calculated from the stitched mosaic. Digital Elevation Models (DEMs) and mesh models are created from the dense point cloud. The dense cloud was not cleaned during the process, meaning that the points representing debris, wood or other objects were not removed and affected the drone products. This limitation, presented in other published works such as Casella et al. (2014), will be stressed and discussed in the following sections and specific remedies will be proposed in Section 2.6. The DEM and orthomosaic were then exported for use in comparison to the RTK GPS survey (see Section 2.4). The drone based survey approach allowed to quickly survey an area of 0.25 km^2 within a 10-minute flight resulting in a ground sampling distance of 2.5 cm/pixel.

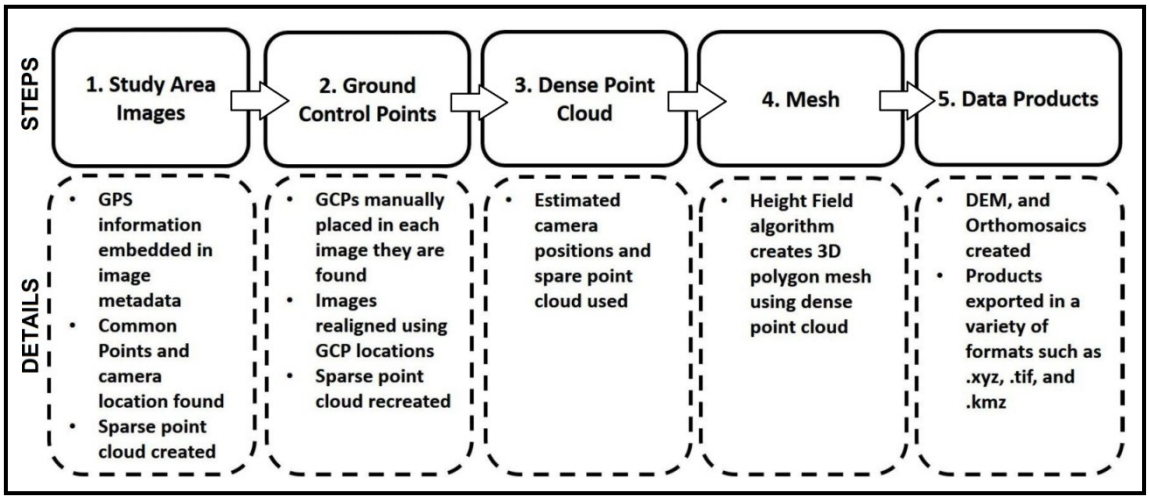

Figure 2.5 Sequence of processing steps used in the photogrammetric process of UAV images. Main details of each step are given in the dashed boxes.

2.4 Results

With the goal of demonstrating the reliability of an integrated local assessment of the storm impacts, implemented following the QRP, the results are presented in the following. First, a summary of the interviews is given. Then, the results of the extensive on-ground survey effort during the week following the storm are presented for the target area (Figure 2.1E) of the pilot case study (Figure 2.1D). The results are presented in sequential sections showing comparisons between the on-the-ground (RTK-GPS) and aerial drone survey results.

2.4.1 Summary of the interviews

Most of the SHs reported that on the evening of the 5 of February (Thursday) the water level inside the Porto Canale of Porto Garibaldi (Figure 2.1D) was approaching the level of the embankments (~1.8 m above MSL) due to the combined effect of the canal discharge and the sea conditions. At that moment, the emerged beaches were already impacted by high water levels and waves. The overflow of the canal started between 1 and 2am and continued till 4am, mainly because of the oscillations of the water surface due to the action of waves that propagated inside the canal. On Friday, early morning, the situation was still critical, it improved only at lunch time, when the sea conditions began to subside. Some of them claimed that they did not remember a similar event in the last 30, 50 and 60 years.

For the local people in Porto Garibaldi it was already clear on the 5 February 2015, that a strong coastal event was approaching their towns. However, several SHs claimed that no clear local alert to the population was given and none of the interviewed knew about the regional EWS. Basically, local know-how and experiences were their only instruments to understand what was happening and prepare themselves (e.g. posing sand bags). They also reported that the Civil Protection arrived at the location on the 6 of February (Friday), at lunch time, bringing sand bags and assistance.

2.4.2 Topographic profiles and Digital Elevation Model surface

An indication of the quality of the DEM produced from the analysis of the drone images is given comparing it with the RTK GPS cross-section points (see Figure 2.1E). The comparison is shown in Figure 2.6 for both profiles. For both datasets the assumed (i.e. *a priori*) vertical uncertainty is shown, namely ±15 cm for drone derived data and ±5 cm for RTK GPS data, illustrated by the shaded outlines. It is important to note that elevation outliers were deleted from the drone derived data extracted for Profile 1 and 2 when they were visually determined to be clearly not representative of the terrain surface. However, it was not possible to correct in a similar way the variations induced by debris or other small objects that affected the comparison. A smoothing (i.e. moving average) of the profiles was also applied to both drone and RTK GPS derived data. The Root Mean Square Errors (RMSEs) of the vertical elevation between the ground measured (RTK GPS) and remote sensing (drone) data were 14 cm and 12 cm for Profiles 1 and 2, respectively. Note that Profile 2, with an RMSE of 12 cm, is located in the central portion of the survey area, where more precision was expected due to greater image overlap and GCP control, while Profile 1, with an RMSE of 14 cm, is closer to the edge of the domain where the drone DEM is expected to be less accurate. Since the drone data comes from a commercial off-the-shelf unit and thus relies on RTK GPS ground control points for positioning accuracy, the drone surveys are therefore not wholly independent of the GPS system. Nevertheless, the drone surveys provided a useful and efficient extension of the RTK GPS ground surveys.

This target study aimed to give an indication of precision and reliability of the resulting drone-derived DEM which was corrected using the available RTK GPS ground control points. The drone data, while overestimating the elevation in the higher portion of the Profile 1, with the strongest difference in the order of 25-30 cm, converged with the RTK GPS profile in the lower portion of Profile 1 near the swash zone. For Profile 2, most of the morphological features were captured, including the storm berm (with a vertical error on the berm top of ~15 cm). The slopes of the emerged foreshore are comparable for both profiles: for Profile 1 the slope calculated was 0.016 for the drone derived profile, while it resulted 0.014 for the RTK GPS profile. The same slopes

calculated for Profile 2 resulted 0.021 and 0.018, respectively. This profile convergence is implemented in further morphological change analysis as shown in Section 2.4.4.

Thus, the foreshore slope, berm shape, and berm crest locations are well captured by the drone DEM in Figure 2.6. The largest disagreement between the drone and RTK GPS profiles occurs landward of the berm in the back portion of the beach (around 30 cm for Profile 1 and 20 cm for Profile 2). A combination of factors contributed to this difference including lower sampling resolution of the RTK GPS compared to the drone, the manual flight that does not allow for a full control on flight altitude and images overlap, and the inclusion of non-terrain elevations such as wood and debris in the DEM (see Sections 2.5 and 2.6 for the discussion of these limitations and proposed remedies, respectively).

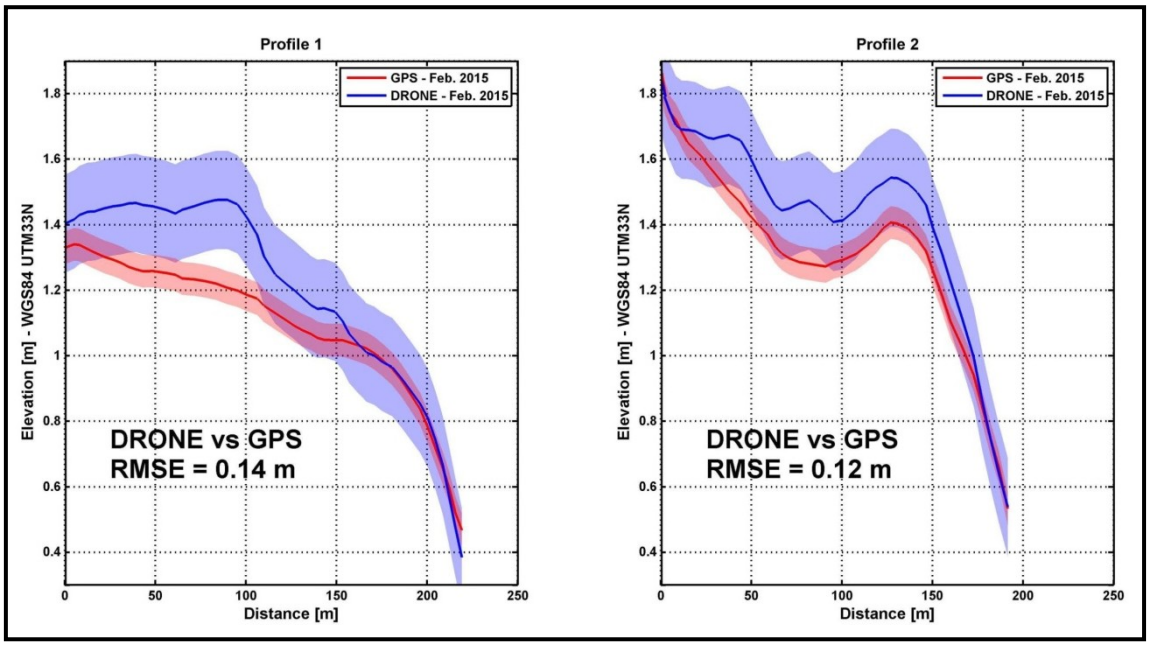

Figure 2.6 Comparisons between the February 2015 post-storm observed GPS profile survey and post-storm drone DEM for Profiles 1 and 2. The error bands, defined *a priori* (±15 cm for drone and ±5 cm for GPS) for visualization purposes, are shown. The RMSE calculated *a posteriori* between the GPS and drone-derived data are reported.

2.4.3 Coastal flooding

In Figure 2.7, the results obtained for the flood extension from the drone derived data are shown in comparison with the GPS observed Floodline and Floodmarks. The drone orthomosaic was analyzed to extract the floodline by observing the debris line that was deposited inland (i.e. "Drone Floodline" in Figure 2.7). In order to also take into account visible areas in the drone orthomosaic that were reached by the water through small paths but that are not included in the main flooded area, several spot areas, hereby and in Figure 2.7 called "Drone Secondary Flood" areas, were defined. Notably, the high-resolution of the orthomosaic enabled to extract a really detailed continuous flood extension, if compared to the GPS survey.

An agreement is seen between the "Drone Floodline" and the RTK GPS derived flood line ("GPS Floodline"). As both depend on the observation of objects and debris moved inland during the storm that remained visible during both the GPS survey and in the

drone orthomosaic, the comparison can be considered as validation of the drone orthomosaic for remote sensing of storm floodlines. The flooding was mainly limited to the subaerial beach in front of the concessions (Figure 2.7). Some of the concessions, however, experienced secondary flooding where the limit of the flood reached the border of the concessions and the water found a path to flow into the properties (Figure 2.7A, B, C, D). A water depth of 30 cm was measured in the location of the flood mark (Figure 2.7A).

2.4.4 Erosion and sedimentation patterns

The erosion and sedimentation patterns are shown in Figure 2.8. The drone derived patterns (Figure 2.8A1, B1 and C1) were obtained from the comparison between the DTM of October 2014 and the post-event DEM generated by the drone. The results are only presented for the area limited by the GCPs. Notably, as the drone derived DEM included non-terrain objects and buildings, the analysis of the morphological features only focused on the emerged beach. The inclusion of non-beach features in the drone derived DEM, mainly because of the presence of different sized debris, affected the non-uniformity of the drone derived pattern.

The morphological features are recognizable in the drone orthomosaic (Figure 2.8A). From the drone results (Figure 2.8A1) a formation of a storm berm is clearly visible running alongshore with a varying width of 20 to 50 m. The vertical deposit is interrupted by erosion scour channels due to some return flows (Figure 2.8A1). Seaward the depositional area (i.e. the storm berm) a negative variation pattern highlights the erosion of the ordinary berm, which emphasizes just in front of the scour channels (Figure 2.8A1). Thus, the berm vertically grew and moved landward during the storm as result of sediment transport in the breaker zone (Figure 2.8A1). At the same time, a small portion of deposit in the intertidal area probably corresponds to the development of a low tide terrace, just at the edge of the analyzed domain. However the domain does not include the lower intertidal area. Therefore it is not possible to evaluate the morphological variation of the lower limit of the foreshore. A general lowering landward of the storm berm can be noted (Figure 2.8A1), which actually corresponds to the area where the differences between the RTK GPS profiles and the drone derived one were higher (see Section 2.4.2 and Figure 2.6). Thus, the highlighted erosion can be subjected to error. Focusing on the selected frames (Figure 2.8B, B1, C, C1), visible scour channels are highlighted, that possibly developed from the footpaths which provided the fastest preferential way for the water to flow back to sea during the storm. This highlights the UAV's ability to map finer resolution features such as scour channels.

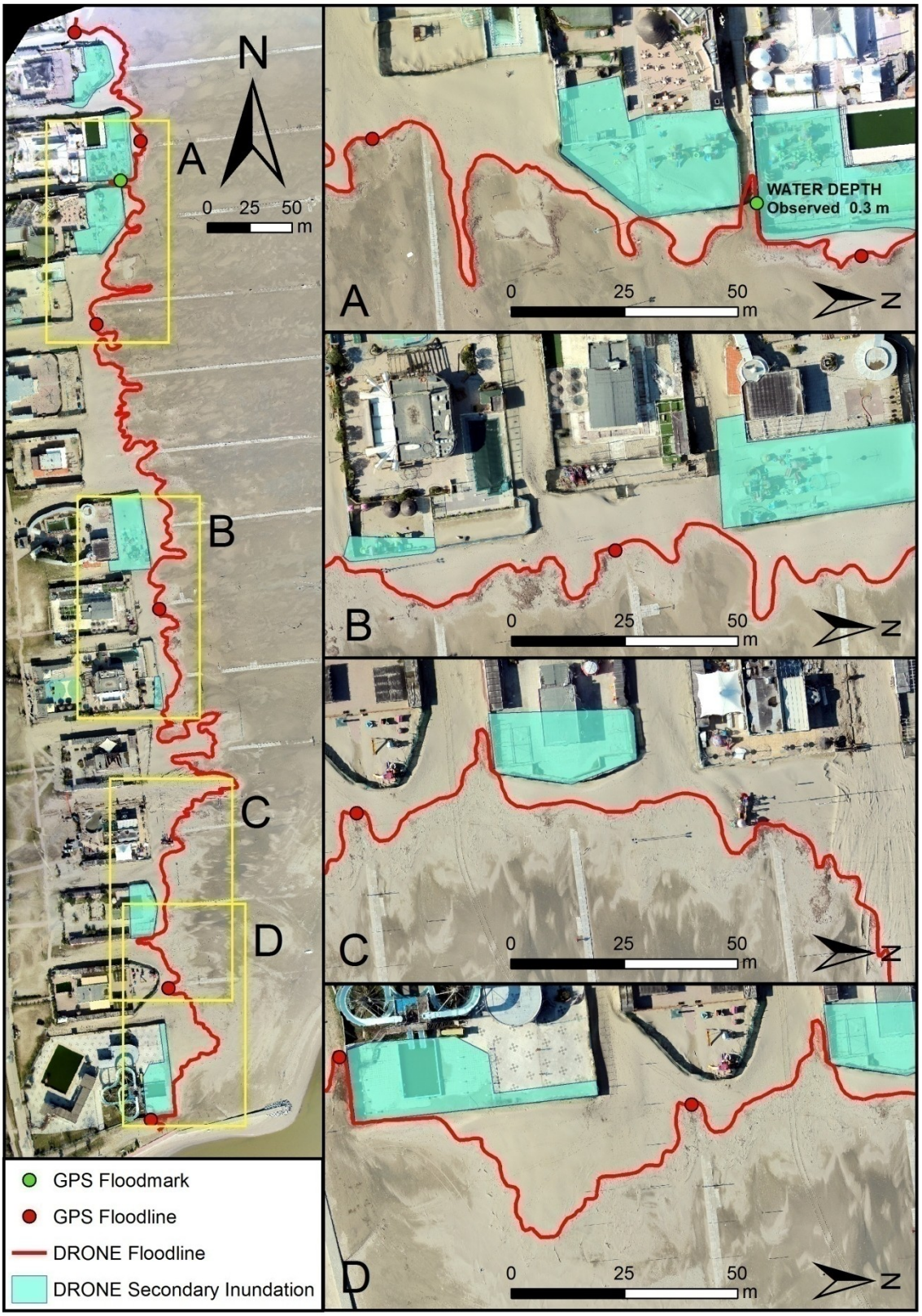

Figure 2.7 Observed "GPS Floodline" and "GPS Floodmark" (green and red circles), drone (red solid line and light-blue polygons) flood extension comparisons: the box on the left shows an overview of the target area while on the right (A, B, C and D) some spot-focuses are given.

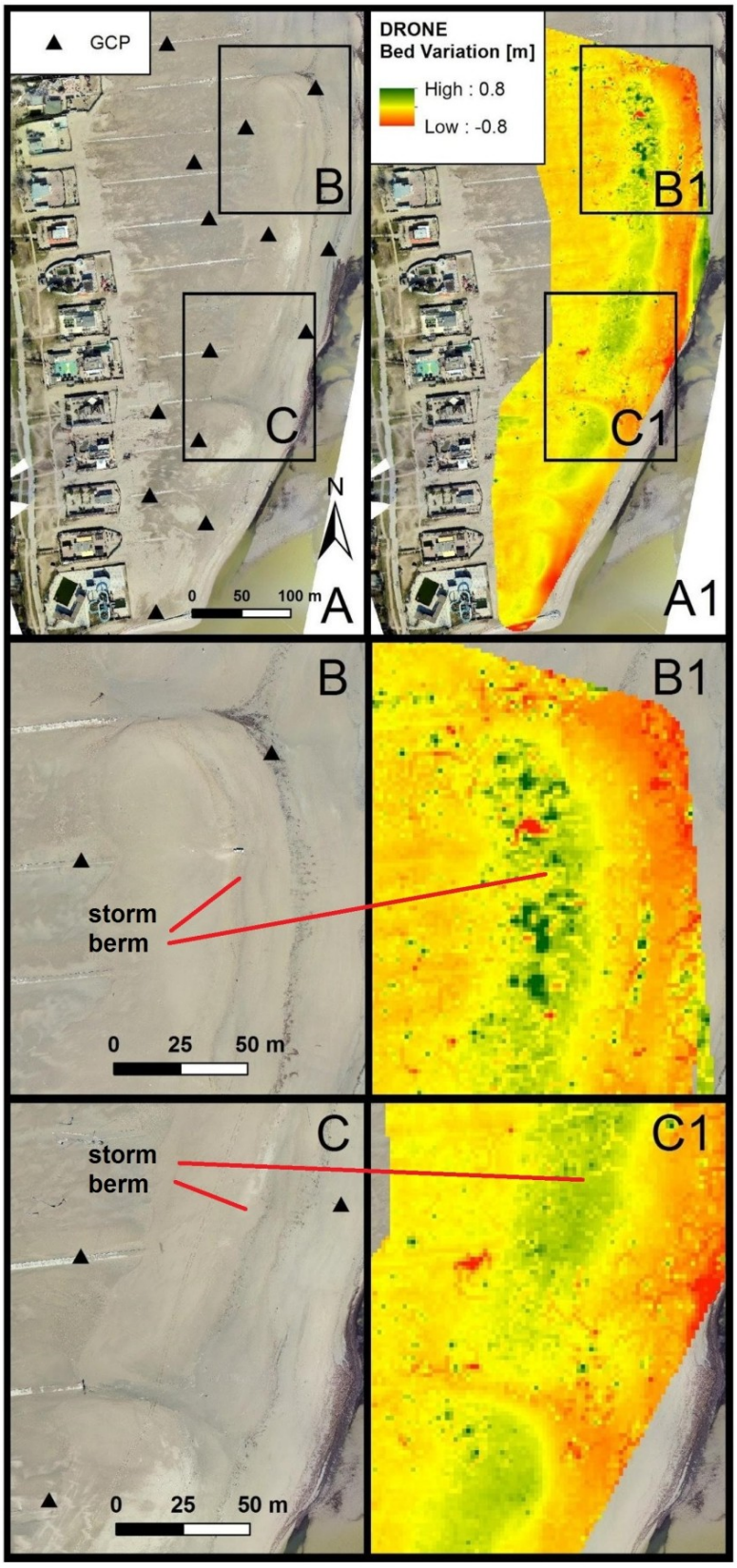

Figure 2.8 Morphological variations: (A) the drone orthomosaic of the target area, where morphological features are visible along with the position of the GCPs; (A1) the difference between the post-event drone-derived DEM and the pre-storm Lidar-derived DEM. In B, B1 and C, C1 enlargements of the main features are given. The morphological variations are only shown for the area surrounded by the GCPs.

2.5 Discussion

In this section the results are discussed, along with their limitations, with focus on the summary of the local interviews and the comparisons between GPS and drone derived data. A focus on the integration of the regional assessment with the local information is given.

The interviews to local SH were useful at giving a picture of what happened during the night between the 5 and the 6 of February 2015. The evolution of the event described by people was consistent with the observations. Actually, the interviews were focusing on the impacts in Porto Garibaldi mainly due to the overflow of the canal harbour. However, the interviewed were able to give indications on the impacted areas in the surroundings (i.e. Lido degli Estensi and Spina) and thus helping the research team at better organizing the field activities. An interesting aspect that was highlighted was that the population did not receive specific alerts. However, coastal managers reported that several alerts were issued before the event to municipalities and Civil Protection agencies (Perini et al., 2015b). The fact that the Civil Protection reached the location only on 6 of February (Friday), after the peak of the event, supports the hypothesis that, even if the alert was issued from the regional to the municipality level, there was a communication problem between the managers, the people in charge of responding to the emergency and the local population. This was also indirectly confirmed by the interviewed fireman which claimed that they were not even prepared to act on coastal locations. It also appeared that the population of the area was not aware of the online EWS that they could have monitored. These aspects support the idea that more effort should be spent improving the preparedness and response of the Civil Protection and the awareness of the local population, especially by improving the communication channels and spreading the risk knowledge. These aspects were also reported by Martinez et al. (2017), with regard to the same event and the same locations, in the wider framework of the aims of the EU FP7 RISC-KIT Project (GA 603458; www.risckit.eu)(Van Dongeren et al., 2017). Pescaroli and Magni (2015) also highlighted the importance of this aspects on the basis of the analysis of interviews to local people in Cesenatico (Figure 2.1C). The limitations of the interviews here presented are mainly related to the lack of a standardized methodology, as the questions were mainly informal, and the limited number of people involved. It is demonstrated that a standard approach (e.g. using prepared questionnaire) can produce more reliable information that can be statistically analyzed, if the number of interviewed is large enough. Several examples of methodological approaches for stakeholder interviews and the analysis of their outcomes exist in the literature, for diverse purposes (Pescaroli and Magni, 2015; Becu et al., 2017; Gray et al., 2017; Martinez et al., 2017), that could be adapted to be applied during a post-storm assessment.

The variability in vertical accuracy seen in the drone derived-data was mainly related to the flight parameters (manual flight, variable altitude and timed image capture), the number and type of GCPs used to constrain the SfM equations used in processing workflow. A recent study by James et al. (2017) provides practical suggestions for photogrammetric considerations (i.e. modifications to drone flight characteristics) and control considerations (i.e. the number and spacing of GCPs) that echo the operational findings from our study, namely that overall DEM improvement is achieved through increased numbers of overlapping imagery (that can be controlled, for example, with automated flights) and greater number of distributed GCPs. Of note with regards to our DEM analysis, non-terrain objects (i.e. human structures and debris) were not removed from the point cloud during processing and remained in the resulting DEM as was seen also in a similar storm response study by Casella et al. (2014). Thus, objects such as

wood, litter and buildings, locally affected the represented surface and, consequently, the comparison with the post-storm RTK GPS observations, which only represented the terrain surface. Notably, the profile comparisons showed disturbances that can be due to these aspects. Also, the drone derived DEM should be considered valid in the area limited by the GCPs. The RMSEs of 14 cm and 12 cm vertically, that were calculated between the drone processed DEM from photogrammetric processing using GCPs and the RTK GPS data (Figure 2.6), are similar for both analyzed profiles and comparable with the LiDAR derived data uncertainty. In comparison with error estimates of drone products reported by recent studies, the resulting RMSE values of the drone DEM compared to the traditional RTK GPS profile surveys are comparable (Casella et al., 2014, 2016; Dohner et al., 2016) or higher (Turner et al., 2016; James et al., 2017; Scarelli et al., 2017). This is attributed to manual flights, inappropriate GCP selections which were unidentifiable due to image resolution at the survey altitude and the variations induced by the presence of debris and others (see Section 2.6 for proposed improvements). However, the resulting drone DEM was still able to well capture morphological features.

The drone derived orthomosaic offered a very easy and quick way to assess the flood extension of the event. The general agreement with the RTK GPS on the ground observations confirmed the close geopositioning of the images and provided a validation of the assessed flood extension. Notably, the opportunity to observe the flood extension from the drone data made it possible to define a really detailed and continuous floodline. In order to obtain the same results with a GPS survey, the operator should increase the point sampling (or even use a continuous sampling method). This implies prolonging the field activities on the beach. Also, the drone point of view is essential to have a complete view of the flood line evolution while, from the GPS point of view, the random distribution and spreading of the debris can mislead the operator.

The morphological patterns derived from the drone data gave an opportunity to assess the morphological response of the beach at a very detailed resolution. The results showed the erosion of the ordinary berm and the formation of a storm berm. The scouring channels highlighted in Figure 2.8 were probably triggered by the presence of concrete pathways of local activities that concentrated and accelerated the return water flux during the storm. In order to reduce the formation of these scouring channels and the consequent worsening of beach erosion, a reasonable choice would be to remove, or at least retreat landward, the pathways during the winter season (Nordstrom et al., 2015). The level of detail of the outcomes suggests that it is possible to use drone-derived DEMs to calculate volume variations, as already confirmed by the literature on the topic (e.g. Turner et al., 2016).

When compared with the post-storm regional assessment reported in Perini et al. (2015b), the proposed survey approach for local assessments can produce very detailed and accurate data. Indeed, the flood ingression extracted from the dataset of Perini et al. (2015b) is not as accurate and detailed as the information that can be capture with drones flying at ~50 m height. Notably, the regional analysis of the flood ingression was not implemented in this case study because the Civil Protection flight was performed too late, when the markers of the limit of the inundation were not anymore identifiable from the helicopter (Armaroli C., personal communication). Thus, a direct comparison between the two observed flood extension was not possible. However, the comparison of the regional flood maps (T10 and T100; Perini et al., 2016) with the "Drone Floodline" is shown in Figure 2.9, for the target area. In this location, the inundation extension was lower than the extension calculated for the 10 year return period event (T10). This is in contrast with the evidences of Perini et al. (2015b) at regional level and for the two reported examples of Lido di Savio and Cesenatico (see Section 2.2.3) that

showed more similarity with the 100 year (T100) scenario. This difference can be due to the fact that the regional maps are calculated with a static approach, not based on process-based formulas or models, applying a constant total water level at the shoreline and propagating the inundation with a modified bathtub-based approach (more details in Perini et al., 2016). Thus, site specific processes are not taken into account, probably leading to the differences highlighted above. Regarding the morphological analysis, the variations captured from drones can be used to calculate more accurate volume changes, at local level, than those that can be calculated on representative beach profiles along the coast. The regional approach indeed only focus on a limited number of beach profiles along the coast. Moreover, the regional protocol does not include any attempt to involve local people with interviews or other methods as the STBs, activated after the event, mainly collect qualitative information through direct observations and pictures (see Section 2.2.2).

In this sense, the QRP can be very helpful at integrating and completing the regional protocol for post-storm assessment. As the regional authorities do not have sufficient manpower and instruments to perform such local detailed assessments along the whole coast, it is advisable to integrate local protocols (such as the QRP) in the regional one. The proposed approach can be performed at local level by academic and private survey teams (such as the QRT) that can be activated as STBs are (see Section 2.2.2), after the coastal event. The regional assessment, indeed, would benefit of the inclusion of more local, qualitative and quantitative information. By properly organizing the tasks assignments at different locations on the coast (i.e. the most impacted areas), it will be possible to activate a quick, coordinated protocol in the immediate aftermath of an event acting at regional and local level. This will provide more holistic data coverage, filling gaps and increasing the details and reliability of the assessments.

Figure 2.9 Comparisons between the observed "DRONE Floodline" and the flood scenarios (T10 and T100) computed by Perini et al. (2016).

2.6 Suggestions for possible improvements

Through the initial rapid response field collection effort the research team determined specific methodologies to ensure quality data following a major storm event. With respect to remote sensing drone survey, the placement and quantity of GCPs, plays a critical role in the resulting DEM and its uncertainty. In order to obtain high quality data, the following guidelines are suggested for flight planning and GCP distribution:

- Perform drone flight surveys at the same altitude and image overlap. This is easily done with any autopilot and mission planning application available for phones and tablets;
- Survey a significantly larger domain (~10% buffer) than needed for data collection. Survey domain edge photos are often removed due to low overlap between images and data is lost;
- Distribute GCPs throughout the survey domain and near boundaries to prevent skewing within the DEM;
- GCPs should be flat, large, and uniquely shaped or marked in such a manner as to be confidently identified from aerial images;
- On the ground, photos of GCP locations should be taken to have the idea of exactly where the RTK GPS point were taken on the target object and within the context of the survey domain;
- Remove outlier and/or non-terrestrial points from the dense point cloud such as storm debris, people, and vehicles for surface calculations.

As anticipated in the list, the GCPs should be easily detectable. This depends on both the quality of the images (that depends on the camera system, the type and altitude of the flight) and of the type of GPSs. An example of GCPs used during the survey can be found in Figure 2.10 with images of good (A, B) and poor (C, D) quality ones.

The photogrammetric process can also be improved, as example, by spending more effort in cleaning the point cloud, thus minimizing the effect of debris and others on the final products. However, the primary source of uncertainty is still related to the quality of the images and the flight that are affected by the camera system and the field application (e.g. manual vs automated flight), respectively.

As anticipated in the Section 2.3.1 the post-storm survey did not include the submerged area. In order to extend the protocol to this part of the beach, other innovative approaches should be adopted, such as near-shore low-cost autonomous surface systems (e.g. Hampson et al., 2011). However, it is beyond the aim of this work to include these aspects in the protocol.

Qualitative observations and interviews are also important and should be performed as soon as possible and as detailed as possible during the implementation of the QRP. It is important to adopt standard approaches for stakeholder involvement and interview a large number of people in order to allow statistical analysis of qualitative information.

Thus, the larger is the number of people involved for the post-event survey, the fastest can be the collection of data as the team can be divided in thematic groups. Planning the activities is crucial for the good performance of the team. This can be additionally supported by activities performed during the non-storm season, such as instrument maintenance and preparation, monitoring of the EWS performances, tasks planning and assignment, etc.

Figure 2.10 Photos A and B at the top demonstrate practical GCPs based on unique shapes, colours, and ability to see from a high altitude. Photos C and D, on the bottom, demonstrate error-inducing GCPs due to their height off the ground and indistinguishable shape, size, and colour in aerial images.

In order to provide more accurate qualitative outcomes further analyses should be performed. This work only presents the analysis of a small portion (Figure 2.1E) of the whole case study area (Figure 2.1D) and deeper investigations are needed to provide more robust outcomes. However, the QRP has been demonstrated to be a proper approach to quickly assess the storm effects at local level in the immediate aftermath of an event, as a combination of technologies and planning approaches. Thus, in the framework of coastal management (Figure 2.3), a proper application of the protocol can produce useful information that can be used at local, regional and national levels in order to, as example: (i) update hazard and risk maps; (ii) provide detailed information for flood-damage curves calibration (see, as example, the study of Scorzini and Frank, 2017); (iii) provide insights for the improvement of risk mitigation and management plans. Finally, as suggested in Section 2.5, the QRP can be integrated in regional protocols, improving the reliability of the regional hazard and risk assessments.

2.7 Conclusions

This study illustrates the potential of an integrated approach combining aerial drones together with on the ground RTK GPS surveys and qualitative data collection for coastal storm post-event assessments at local level. The presented protocol was applied at a pilot case study in the Emilia-Romagna coast, after the impact of an extreme coastal storm, and results were presented and discussed, for demonstration purposes, on a small portion of the pilot case study.

Limitations of the application were highlighted and recommendations for improvements of the general approach were given. As general remarks, (i) interviewing local stakeholders and people in charge of emergency response tasks can be extremely useful at supporting the organization of the field activities, as well as at detecting lacks on the alert chain, preparedness and response emergency phases; (ii) the drone approach was found to be effective for flooding and erosion assessments, being able to provide detailed, continuous and two-dimensional information, with a limited time effort on the field in comparison with the traditional GPS methodologies. The main limitation of the drone products was linked to the field implementation (i.e. manual flight, error-inducing GCPs) and lacks in the photogrammetric process. Specific suggestions for improvements were given, such as the use of automated flights, proper GCPs and the cleaning of the point cloud during the photogrammetric process.

With regard to the proposed general approach, further applications can directly support hazard and impact assessment at local and regional level, and thus addressing coastal management needs. Indeed, the outcomes of the analysis were compared with the post-event assessment performed by the regional authorities highlighting that the proposed protocol for local assessment can be easily integrated in the regional ones, improving the details and reliability of the regional assessments.

3 HIGH-ACCURACY DRONE-BASED SURVEYS: APPLICATION ON A SEDIMENTARY BEACH WITH ARTIFICIAL DUNES IN PORTO GARIBALDI (COMACCHIO, ITALY)

3.1 Introduction

The Emilia-Romagna coast is often threatened by coastal events that cause damages to its residents and economy (Armaroli and Duo, 2017). Regional coastal managers, often supported by local research groups, are active in assessing coastal risk and proposing up-to-date disaster risk reduction (DRR) solutions (e.g. Perini et al., 2016). The use of temporary artificial dunes or embankments as protection for the beach during the winter season has old, worldwide records (Bruun, 1983). Their use in Emilia-Romagna, in particular, is a long practitioners' tradition that only few years ago captured the attention of few researchers, such as Harley and Ciavola (2013) that numerically studied their cross-shore behaviour in the Ravenna area proposing design guidelines and methods. A more recent numerical investigation on the effectiveness of this particular DRR can be found in Sanuy et al. (2017), for the Ferrara area. For some local owners of beach concessions, artificial dunes are indeed the main and most effective protection for their business, being concessions located on the emerged beach, directly facing the impact of coastal storms. Local companies take care of building the artificial protections through beach scraping or sand replenishment (less frequent option), basing their work on hands-on past experience. Therefore, there is no clear control on the design of the dunes and the way that beach scraping may affect the morpho-hydrodynamics of the beach at local level. This practice indeed can have a negative effect on the inherent protective capacity of the beach, if improperly implemented (Bruun, 1983). Recently, Scarelli et al. (2017), had the opportunity to study the evolution of artificial dunes ("bulldozer dunes" in the paper) during the winter season 2014-15 in the Ravenna area, by analyzing the products of two drone-based survey (i.e. September 2014 and March 2015). Notably, these artificial protections, being built with loose sand, are also affected by meteorological forcing (i.e. rain, wind, etc.), in addition to coastal storms. These morphologic changes should be monitored through pre- and post-storm seasonally intensive monitoring programs, as seasonal surveys can only give information on the cumulative variations, making it difficult to relate morphological variations and forcing events. Moreover, the artificial protections are local features that need a level of detail that can easily be achieved with up-to-date autonomous (i.e. drones) low-cost systems.

The last decade, indeed, has seen an increase in Unmanned Aerial Vehicles (UAV or drones) applications in earth sciences due to the improvements of the hardware (i.e. the flying system, positioning and remote control) and software technology (i.e. automatic planning and security features). This trend was emphasized by the decrease in prices of industrial drone products, more often equipped with professional camera systems, that allowed for low-cost remote sensing applications. The analysis were supported by constantly improved software for photogrammetric reconstruction, mainly based on the Structure from Motion (SfM) algorithm (e.g. Westoby et al., 2012; James et al., 2017). In last few years, the use of drones for research, professional jobs and fun, pushed the governments to adopt specific rules and licenses in order to regulate their use (a brief overview of regulations is given in Turner et al., 2016). The use of UAVs for coastal monitoring is following the general trend. Several applicative works were recently published (e.g. Mancini et al., 2013; Casella et al., 2016; Scarelli et al., 2017) but only a few tried to summarize guidelines and propose protocols (e.g. Turner et al., 2016;

Trembanis et al., 2017) for their use on the coast. These systems have the ability to survey large areas in few minutes and output products (i.e. DEM, orthophoto, etc.) with high accuracy allowing to extract many type of information, such as topography, vegetation status (e.g. Berni et al., 2009), storm hazard impacts (e.g. Trembanis et al., 2017) and others.

No recent studies on the Emilia-Romagna coastal area intensively investigated the evolution of artificial protection during the winter season, that can be characterized by intense meteorological and sea conditions, with an UAV system. This study, represents a first preliminary analysis of a pilot, drone-based surveying program of the artificial dune build on the southern beach of Porto Garibaldi (Comacchio, Italy) that took place in the winter 2016-17. Five drone surveys were implemented. The evolution of the artificial dune was analyzed in terms of meteorological (i.e. wind) and sea forcing. The capacity of the UAV system to capture very subtle morphologic changes put the bases for promising future beach monitoring programs.

3.2 Study site

The Emilia-Romagna coast (Figure 3.1a) is about 130 km long and is characterized by low-lying sedimentary beaches, alternating highly touristic and natural protected areas. The human pressure is high with main infrastructures, economic and touristic activities located within few kilometeres from the shoreline. This, in combination with the morphologic characteristics of the coastal corridor (low elevated) and the hydrodynamics of the Northern Adriatic (extreme storm surges and waves), increases the level of risk for flooding and erosion. Details on the Emilia-Romagna coastal domain can be found in Armaroli and Duo (2017) (and references therein), focusing on the geomorphology, hydrodynamics and human assets. In that study, a regional coastal risk assessment is implemented and validated. Additional information on the methodology adopted at regional level to identify coastal storms can be found in Trembanis et al. (2017) while, a thorough classification of potential damaging events can be found in Armaroli et al. (2012).

The Porto Garibaldi (Comacchio, Italy; Figure 3.1b) touristic town is located in the north of the regional domain, at the north of the Lido degli Estensi. The town hosts a small canal harbour that represents the centre of the economic activities (mainly fishery and tourism) along with the touristic services (i.e. concessions) that are present on the beach (Figure 3.1a, b). As it can be seen from Figure 3.1b the town is built just on the back of the beach concessions. Erosion represents a major threat to local stakeholders and their activities as the presence of the cross-shore protection of the canal mouth interrupts the natural drift, as demonstrated by its beach width, compared to the one at Lido degli Estensi (Figure 3.1b). The presence of breakwaters (built before the 1920s; Duo and Ciavola, 2015; Garnier et al., 2017) partially counterbalances the structural erosion that characterize this location. Flooding impacts can also be intense as demonstrated by the most recent extreme coastal storm that hit the area, the February 2015 "Saint Agatha" event (Perini et al., 2015a, 2015b; Trembanis et al., 2017). During this storm, characterized by the interaction of extreme sea conditions and intense discharges in the canal, the town and the beach concessions were flooded. The study site of this work is located just north of the canal and, during that event, the artificial dunes built to protect the beach concessions were severely impacted as can be seen from Figure 3.2. The breakwaters and temporary protections were not sufficient to prevent the inundation of concessions. During the following winters, the owners of the concessions increased the level of the temporary protection by increasing their elevation, width and reducing the alongshore discontinuities (Figure 3.3).

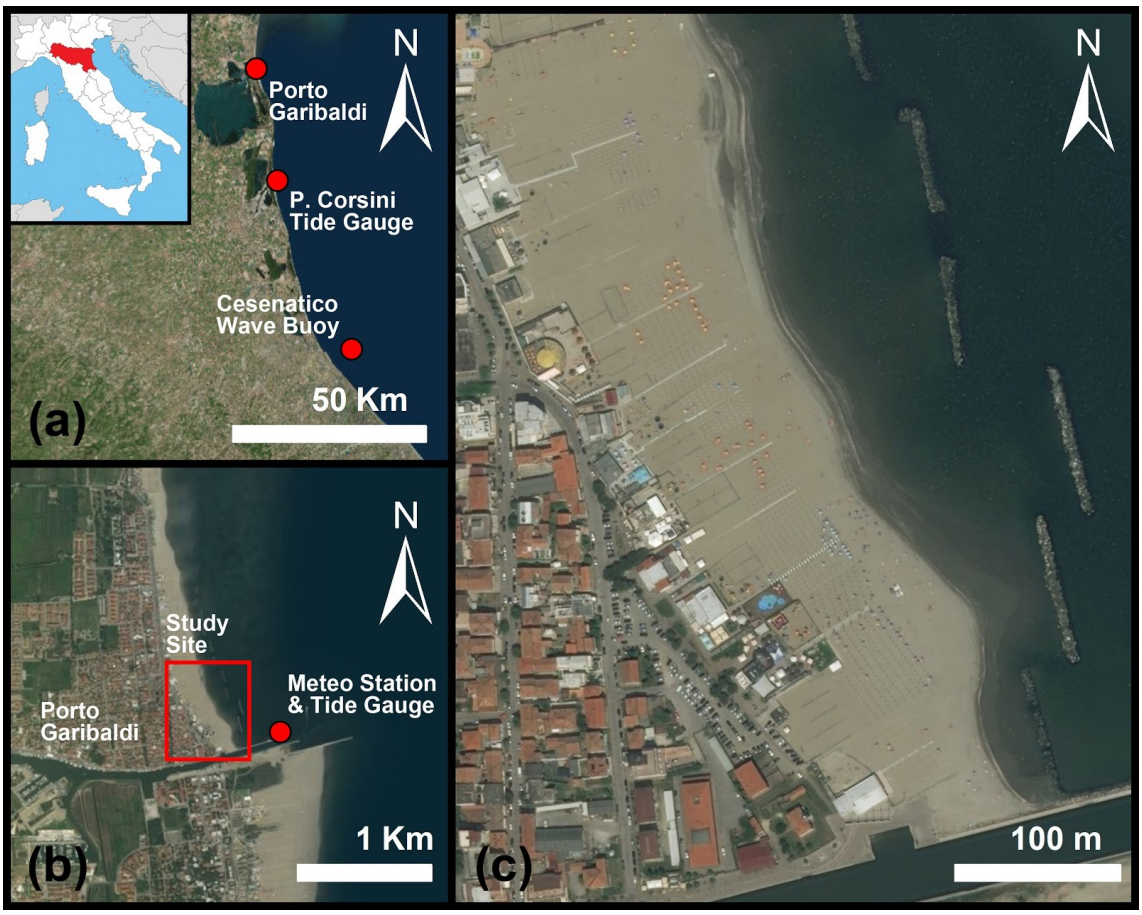

Figure 3.1 Index map of the study area: (a) the Emilia-Romagna coast in the Northern Adriatic; (b) the Porto Garibaldi (Comacchio, Italy) area; (c) the study site, just north of the canal harbour of Porto Garibaldi. The locations of measuring stations are highlighted in (a) and (b).

Figure 3.2 The impacts of the Saint Agatha event of 5-6 February 2015 on the artificial dune at the study site of Porto Garibaldi (Comacchio, Italy).

Figure 3.3 The artificial dune at the study site on the 21 December 2017.

3.3 Methodology

3.3.1 Field surveys

The field activities were performed with a quad-copter DJI Phantom 3 Professional and a RTK GPS Trimble R6. The drone missions were planned with a freeware application (i.e. Drone Deploy) setting a flight altitude of ~80 m and lateral and frontal image overlap of ~70%. Ground Control Points (GCPs) were distributed on the emerged beach (i.e. from 19 to 20 for each survey) and measured with the RTK GPS in order to be used in the photogrammetric process. Moreover, random cross-shore profiles and points along and around the artificial dune were measured with stop-and-go and kinematic techniques, respectively. These measurements were used for the error assessment of the drone-derived products (e.g. DEM). The GPS measurements were performed in geographical coordinates and elevations based on the WGS84 (ellipsoid). Then they were projected to the UTM 33N system with elevations based on the ETRF2000 (geoid), for the photogrammetric process and post-process analysis. The activities were performed when weather and daylight conditions allowed to safely flight on the study site considering also the presence of the public. In Table 3.1 an overview of the surveys performed is given. Notably, during the first field campaign (October 2016) an intensive GPS survey was performed in continuous RTK as it was not possible to flight the drone. The survey was implemented capturing all the main features of the artificial dune. The last survey (April 2017) was performed after the deconstruction of the protection that was done on the 29 March 2017.

Table 3.1 Schedule of the implemented surveys in the Porto Garibaldi study site.

Date	Local Time (GMT+01)	Notes
28 October 2016	11:00	Only GPS survey
21 December 2016	14:30	-
20 January 2017	13:05	-
14 February 2017	12:20	-
17 March 2017	12:45	-
6 April 2017	12:30	No artificial dune

3.3.2 Photogrammetric reconstruction

The drone images were processed with Agisoft Photoscan Professional (Version 1.3.2 build 4205) which is a licensed software based on the application of the Structure from Motion (SfM) algorithm for photogrammetric reconstruction. The process followed these steps:

- visual inspection of the images to detect and delete the bad quality ones and those that covered areas too far from the domain of interest;
- (S1) images were then loaded into the SfM software and pre-aligned: the GPS positions of the images, recorded with the drone's internal GPS (which positioning can have meters of errors) are not taken into account;
- (S2) a low quality mesh was built in order to take advantage of the Photoscan tool able to automatically pre-locate a GCP on all the images where it is present, once it is manually located in at least one image;
- (S3) a check and accurate manual re-positioning of the GCPs was performed and then, their coordinates and accuracies were input;
- (S4) images were re-aligned (without GPS information) with a high quality process during which the camera distortion parameters were calibrated a first time;
- (S5) the optimisation of the camera parameter was then performed including all the GCPs input;
- (S6) a high quality dense point cloud was built;
- (S7) a high quality mesh was built
- (S8) a texture model was built;
- (S9) a DEM was built using the dense point cloud as source;
- (S10) an orthomosaic was built using the texturized mesh.

The DEM and orthomosaic were built in WGS84 UTM zone 33N. Additional information on specific steps are summarized in Table 3.2. The DEM and orthomosaic were then exported with 0.1 m resolution, in tiff format, for further assessments. In comparison with the process described in Chapter 2 (Section 2.3.5) of this thesis, the main differences are related to the different software used, which can slightly vary in terms of processing flows and options. Several comparative reviews were made by privates or scientific teams and are available online (e.g. blogs, commercial websites, etc.) and in scientific journals (e.g. Aicardi et al., 2016; Niederheiser et al., 2016). However, none of them seems to indicate that one is better than the other as both can produce very accurate results, if properly applied. Nowadays both software present very similar processing options, mutually affecting each other during the developments applied during the last few years.

Table 3.2 Details on the steps of the implemented photogrammetric reconstruction process of the drone images.

Step	Settings	Products
S1	Accuracy: Medium; Generic preselection: Yes; Reference preselection: No; Key and Tie point: Default; Adaptive camera model: Yes.	Medium quality sparse point cloud.
S2	Surface type: Height field; Face count: 200'000.	Low quality mesh.
S4	Accuracy: High; Generic preselection: Yes; Reference preselection: No; Key and Tie point: Default; Adaptive camera model: Yes;	High quality sparse point cloud; Calibrated camera model.
S5	Parameters: f, b1, b2, cx, cy, k1, k2, p1, p2; Fit rolling shutter: Yes.	Optimized camera model.
S6	Quality: High; Depth filtering: Disabled.	High quality dense point cloud.

S7	Surface type: Height field; Face count: 10’000’000;	High quality mesh
S8	Mapping mode: Orthophoto; Blending mode: Mosaic Enable color correction: No Enable hole filling: Yes	Textured model
S9	Source data: Dense cloud; Interpolation: Enabled; Resolution: default (highest).	High resolution DEM
S10	Blending mode: Mosaic; Surface: Mesh; Enable color correction: No; Enable hole filling: Yes; Resolution: default (highest).	High resolution orthomosaic

3.3.3 Error analysis

The error analysis of the DEM was performed by comparing it with the observed GPS point elevations. In particular the error on the single point was calculated as the difference between the drone-derived DEM elevation and the GPS observed one. A positive value of the error means that the DEM overestimates the GPS observed elevation, and vice versa. The mean and standard deviation of the error were calculated considering all the observed points. As synthetic error indicator, the Root Mean Squared Error (RMSE) was also computed for each survey. Moreover, an R^2 linear fitting indicator was also calculated between the DEM and GPS elevations.

3.3.4 Morphological variations and interpretation

The advantage of repeated surveys is that is possible to calculate a DEM of Difference (DoD) as difference between two consecutive DEMs. This is regularly done in order to detect morphological changes in natural and/or semi-artificial environments by subtracting the older DEM from the newest one. However, a simple subtraction does not allow for a proper detection of significant changes, which cannot exclude considerations on the accuracy of the input DEMs and their propagation (Wheaton et al., 2010). In this study, a DoD between the surveys of December 2016 and January 2017 was calculated and filtered with a threshold for change detection (TCD). This, translated in practice, means that the DoD values are considered in the analysis only if their absolute value is equal or higher than the TCD. Generally, a TCD is defined considering the propagation of the errors, given by the root of the sum of the square of the errors of the two analyzed DEMs. In this study, different values of TCD were tested to analyze the sensitivity of the significance of the morphological variations to the TCD. The applied values were 0.05, 0.10, 0.15, 0.20 and 0.25 m and results were compared with the unfiltered DoD.

The calculations were implemented through the Geomorphic Change Detection (GCD) tool for ArcGIS (Wheaton et al., 2010) which, besides the calculation of vertical variations, also allows for volume change assessment including the uncertainty evaluation. In this case, the propagation of the uncertainty calculated through the GCD tool is based on the linear theory of error propagation, under the assumption that the calculated DoD has a spatially constant error equal to the selected TCD (Wheaton et al., 2010). Thus, the uncertainties of the average vertical variation and volume change can be assessed *a priori* being, respectively, equal to the selected TCD and proportional to it of a factor given by the ratio of the calculated volume change and the average vertical variation. The average vertical variations, volume changes and related uncertainties were calculated for the TCD 0.10, 0.15 and 0.20 m.

The morphological interpretation of the detected significant changes was done including in the analysis the main drivers (i.e. forcing) of the sediment dynamics. These drivers were previously identified as the wind (i.e. wind intensity and direction) and sea conditions (i.e. waves and total water levels). The wind and water level data for the monitored period were retrieved from the meteorological station and the tide gauge of Porto Garibaldi (Figure 3.1b), respectively. The wave data were obtained by the Cesenatico wave buoy (Figure 3.1a). Coastal storms were detected considering the storm definition described in Harley (2017). The adopted thresholds referred to Armaroli et al. (2012): minimum significant wave height of 1.5 m, minimum duration of 6 hrs, meteorological independence criterion of 3 hrs and minimum total water level of 0.45 m. An overview of the forcing conditions is given in Figure 3.4. In the figure, the wind observations highlighted in red represent the extremes which were identified through a peak-over-threshold (POT) analysis defining a 95% threshold calculated for the wind velocity in the period 2009-2017. The red triangles on the wave and water level time-series represent the beginning of an identified coastal storm. The green vertical lines represent the date of the surveys.

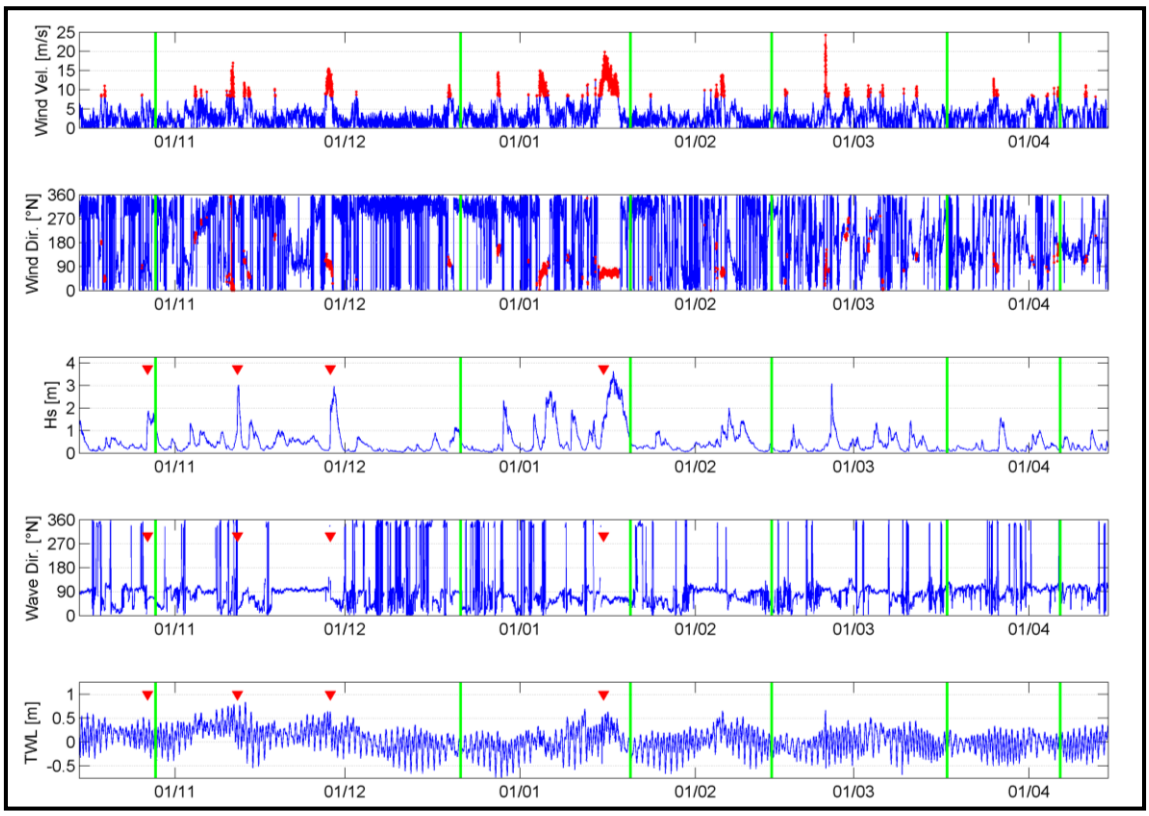

Figure 3.4 Wind velocity and direction (Porto Garibaldi meteorological station), significant wave height, wave direction (Cesenatico buoy) and water level (Porto Garibaldi tide gauge) data of the period 15 October 2016 - 15 April 2017. Extreme wind events are highlighted in red in the first two plots (wind velocity and direction); red triangles indicate the occurrence of coastal storms (waves and water levels); green lines represent the day of the performed surveys.

3.4 Preliminary results

3.4.1 Analysis of the DEM error

An overview of the assessed errors is shown in Figure 3.5, for all performed surveys. Moreover, two example monographs are presented for the drone surveys of the 21 December 2016 (in Figure 3.6) and the 20 January 2017 (in Figure 3.7). Each monograph includes: (i) a synthetic table with information on the planned drone mission (e.g. flight altitude, image overlap, etc.) and on the photogrammetric assessment (e.g. processed area, flight altitude, number of GCP, etc.); (ii) synthetic graphical and quantitative information on the assessed error of the DEM product (e.g. error distribution, RMSE, etc.); (iii) the orthophoto product (resolution: 10cm) with the spatial distribution of the GCP, the GPS observed points and their calculated error and (iv) the DEM product (resolution: 10 cm). A comparison between some representative GPS observed profiles and the values extracted from the DEM (UAV-derived) is given in Figure 3.8 for the surveys performed in December 2016 (a, b and c) and January 2017 (d and e). The profiles are represented with associated uncertainty bands (i.e. defined *a priori*: ±15 cm for drone derived data and ±5 cm for GPS data). For each profile, the error assessment is given (i.e. RMSE; *a posteriori*). A map shows the position of the profiles.

The preliminary error analysis (Figure 3.5) showed a reasonably good agreement between the DEMs, produced through the photogrammetric process of the drone

images, and the observed GPS points. All surveys, but the last one (i.e. April 2017), showed that 95% of the calculated errors are contained within -0.1 and 0.1 m and RMSE is lower than 0.05 m. The first survey (December 2016) showed a larger confidence range if compared with the following three (January, February and March 2017). On the other hand, the last survey (April 2017) showed the largest confidence interval and the highest mean error (~0.08 m) and RMSE (~0.09 m). The results for the surveys of December 2016 and January 2017 (monographs in Figure 3.6 and Figure 3.7; examples of profile comparisons in Figure 3.8) showed more details on the distribution of the errors. The UAV survey performed in December 2016 produced a DEM that presented larger errors when compared with the one derived from the survey of January 2017.

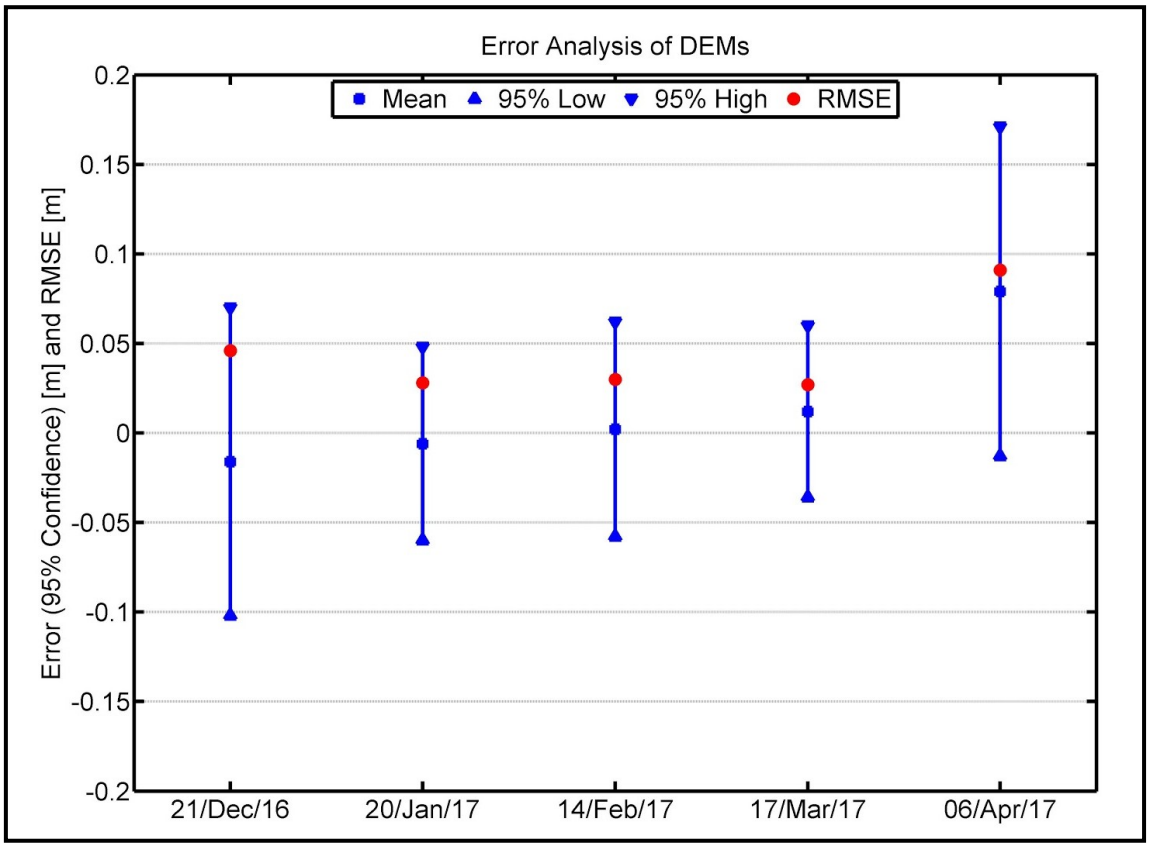

Figure 3.5 Error analysis of the UAV-derived DEM for all performed surveys. The error is calculated in comparison with the GPS measurements. The error distribution with 95% confidence is shown in blue while RMSEs are shown in red.

TECHNICAL SUMMARY

Location	Local Date and Time		Photogrammetry Assessment		
Porto Garibaldi (FE)	21/12/2016 14:30		Area	[km2]	0.188
Flight Settings			Altitude	[m]	86.1
Flight Altitude	[m]	~80	Nr. Images	[-]	198
Overlap L/F	[%]/[%]	~70/70	Camera Footprint	[cm/pix]	3.29
Camera Footprint	[cm/pix]	3.5	Nr. GCPs	[-]	21
Fligth Duration	[mm:ss]	09:15	GCP Accuracy H/V	[m]/ [m]	0.023/0.032
Nr. Images	[-]	278	DEM Min. Resol.	[m]	0.066

OUTPUT AND ACCURACY

Resolution: Orthophoto 0.1m; DEM 0.1m.

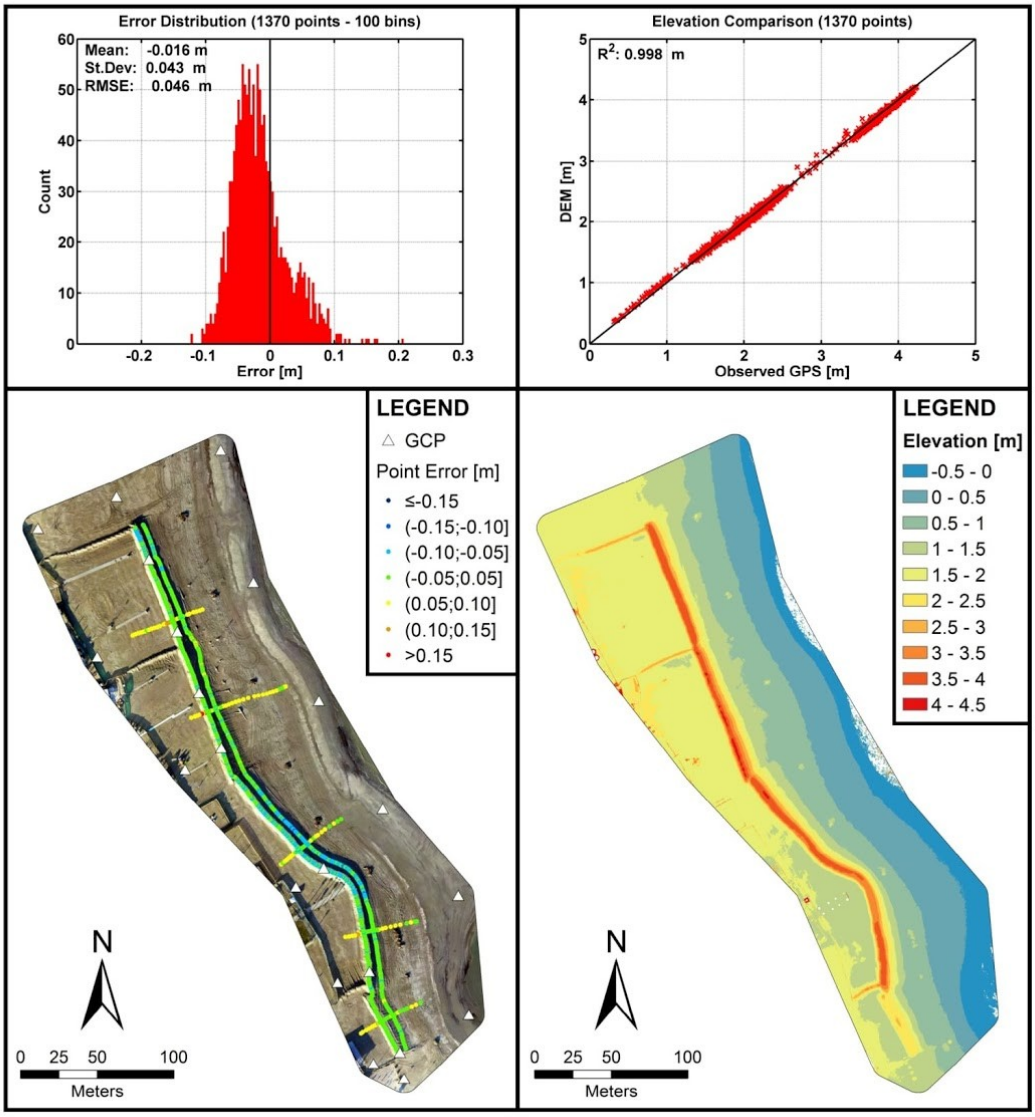

Figure 3.6 Monograph of the survey implemented on the 21 December 2016.

TECHNICAL SUMMARY

Location	Local Date and Time		Photogrammetry Assessment		
Porto Garibaldi (FE)	20/01/2017 13:05		Area	[km2]	0.228
Flight Settings			Altitude	[m]	88.1
Flight Altitude	[m]	~80	Nr. Images	[-]	285
Overlap L/F	[%]/[%]	~70/70	Camera Footprint	[cm/pix]	3.27
Camera Footprint	[cm/pix]	3.5	Nr. GCPs	[-]	21
Fligth Duration	[mm:ss]	09:30	GCP Accuracy H/V	[m]/ [m]	0.021/0.034
Nr. Images	[-]	285	DEM Min. Resol.	[m]	0.066

OUTPUT AND ACCURACY

Resolution: Orthophoto 0.1m; DEM 0.1m.

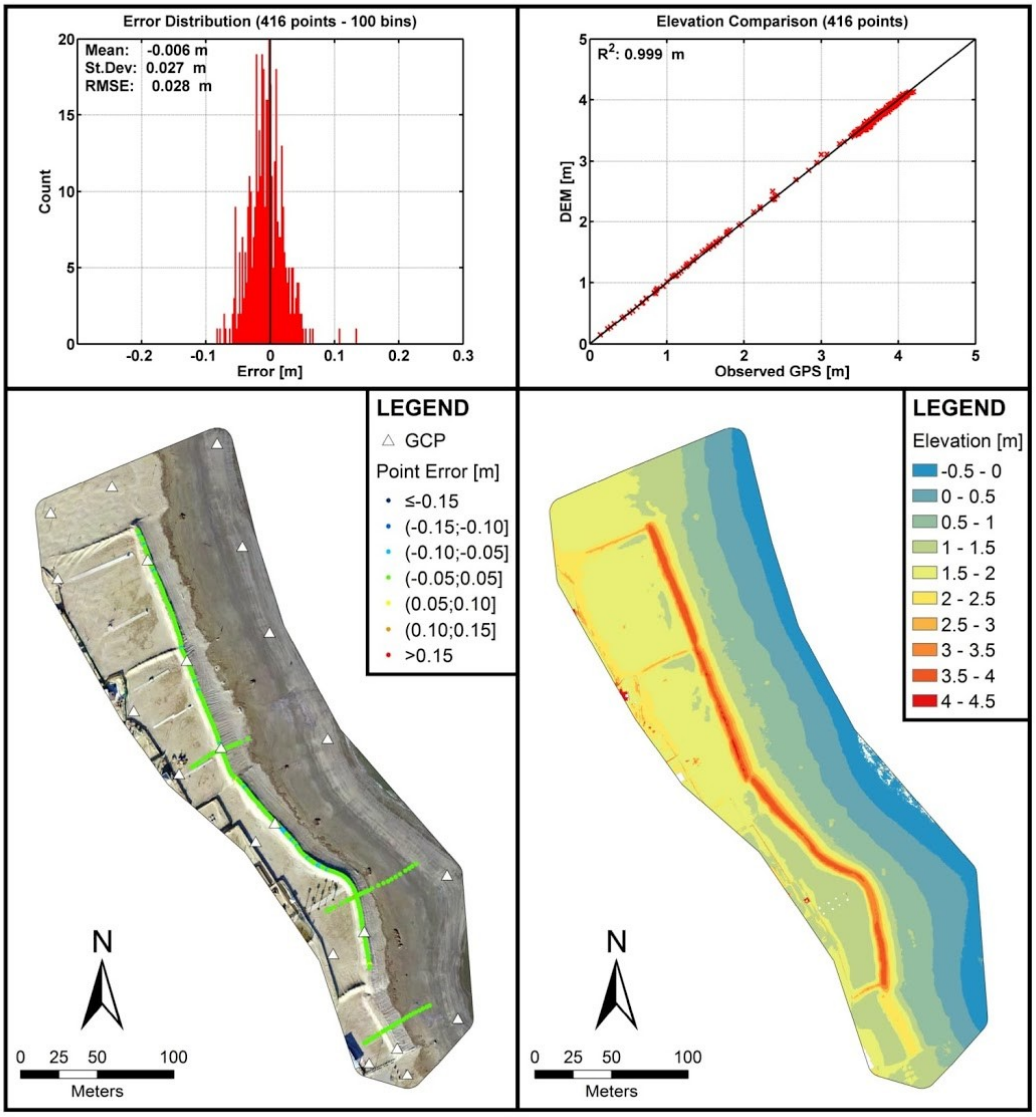

Figure 3.7 Monograph of the survey implemented on the 20 January 2017.

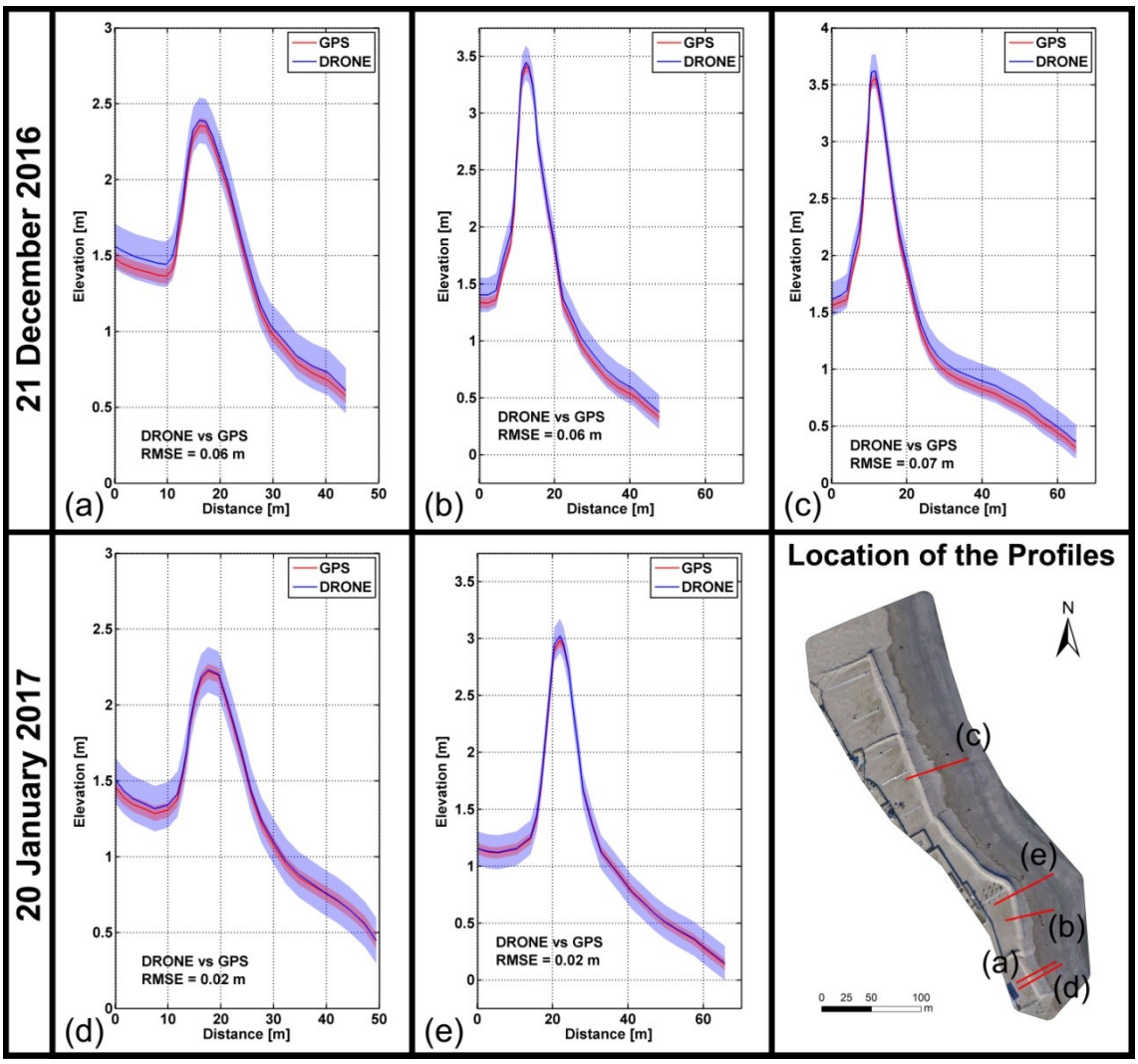

Figure 3.8 Examples of profile comparison (UAV-derived DEM vs GPS measurements) for the surveys of December 2016 (a, b and c) and January 2017 (d and e). The profiles are represented with uncertainty bands defined *a priori* (±15 cm for the UAV-derived DEM and ±5 cm for GPS) for visualization purposes. The RMSE, calculated *a posteriori* comparing the UAV-derived DEM and the GPS measurements, is reported for each profile. A map shows the position of the profiles.

3.4.2 Morphological variations

The morphological variations occurred between the surveys of December 2016 and January 2017 are shown in Figure 3.9. The analysis of the DoD was performed by applying different TCD (i.e. none; 0.05 m; 0.10 m; 0.15 m; 0.20 m and 0.25 m). The erosion patterns are shown with colours from light orange to red, while deposit from dark yellow to green. Notably the map in Figure 3.9a (not filtered DoD) show a general erosive trend on the shoreline, the artificial dune front and top, the areas at the back of the dune. Deposit of sediment can be found on the back slope of the protection, on the inland limit of the domain and in front of the southern portion of the protection. As expected, by increasing the threshold of detection, the area showing morphological variations decreases. As example, the 0.10, 0.15 and 0.20 m selected TCD highlighted changes on the 28%, 11.8% and 5.4% of the total area, respectively. The average vertical variations and volume changes calculated for the same TCD are shown in

Figure 3.10 along with a visual representation of their uncertainties. As expected, the average vertical change (Figure 3.10, left panel) increases for both erosion and deposition while increasing the TCD, which also represent its uncertainty. On the other hand, the volume change and its uncertainty range (Figure 3.10, right panel) decrease by increasing the TCD. The significance of the thresholds is discussed in the following section.

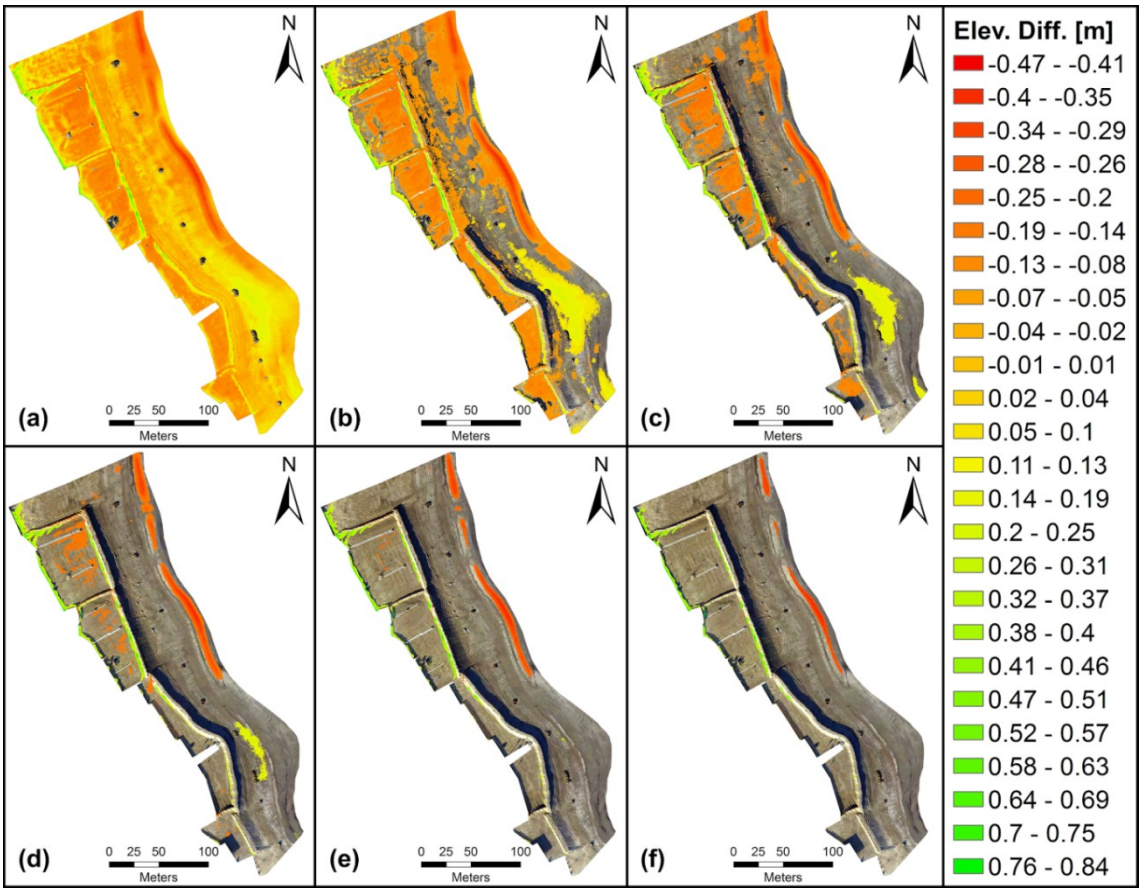

Figure 3.9 Morphological variations between the survey of 21 December 2016 and 20 January 2017 calculated through the minimum threshold for change detection. The thresholds for change detection are as follows: (a) None; (b) 0.05 m; (c) 0.10 m; (d) 0.15 m; (e) 0.20 m; and (f) 0.25 m. The legend on the left indicates the magnitudes of the variations which is negative for erosion and positive for deposition.

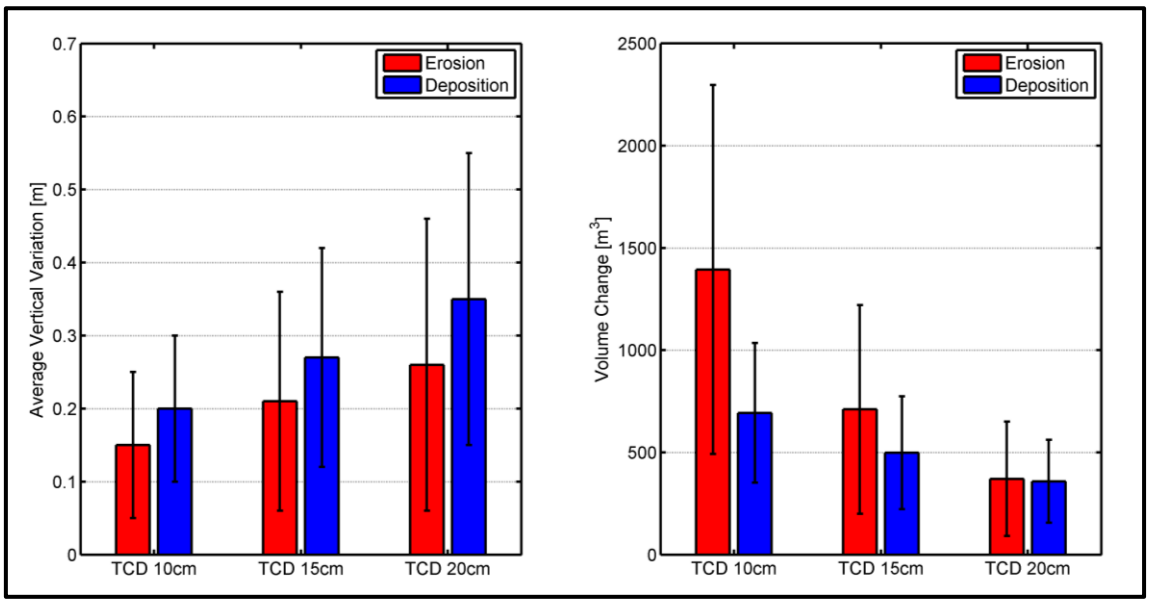

Figure 3.10 Comparisons of significant erosion and deposition (a) average vertical variations and (b) volume changes for the 0.10, 0.15 and 0.20 m threshold for change detection. The uncertainties related to the assessed variables are also shown.

3.5 Preliminary discussion and interpretation

The error assessment (i.e. UAV-derived DEM vs GPS measurements) showed, for the surveys implemented between December 2016 and March 2017, lower errors (i.e. RMSE; Figure 3.5) than those presented in Mancini et al. (2013), Casella et al. (2016) and Scarelli et al. (2017). Moreover, the error distributions show smaller standard deviations than those presented in Turner et al. (2016). The large overestimation of the DEM derived from the last survey (April 2017; Figure 3.5) is most probably explained as a systematic error introduced during the survey. This hypothesis is supported by Figure 3.11 where all errors calculated for that survey are positive and the whole distribution is shifted on the right side of the graph. Besides, the survey performed in December 2016 produced a DEM that presented a tendency to overestimate (5-10 cm) the elevation of the cross-shore profiles (Figure 3.6 and Figure 3.8a, b and c). The same DEM underestimated the elevation of a specific area on the artificial dune (Figure 3.6). This, however, could be due to some inaccuracies due to the GPS kinematic technique adopted to measure the points, whereas cross-shore profiles were measured with the stop-and-go technique (see Section 3.3.1). Indeed, in comparison with the stop-and-go approach, the kinematic one forces the surveyor to hold the instrument slightly higher (in order to facilitate the gait, especially on slopes or in the presence of debris) and thus heading to an illusory underestimation for the UAV-derived DEM. Vice versa, if not properly implemented, the stop-and-go survey can lead to the opposite when the tip of the instrument considerably penetrates the sand. This probably explain the large (if compared with the other errors summarized in Figure 3.5) overestimation highlighted for the April 2017 survey. In that case, indeed, only cross-shore profiles where measured as demonstrated by Figure 3.12. Finally, all error calculations are affected by limitations related to the spatial coverage of the GPS survey. As can be seen for example in Figure 3.6 and Figure 3.7, the distribution of the GPS points does not cover the whole domain. During some surveys, indeed, weather conditions or delays caused this limitation that can actually affect the error assessment.

Focusing on the morphological variations, as anticipated, the TCD affects the extension of the area that show significant changes (Figure 3.9). Considering the assessed errors of the two analyzed DEMs (RMSE ~5 cm and ~3 cm, for December and January, respectively) the minimum threshold to detect the significant morphological variations can be assumed to be higher than their propagation (~6 cm), thus TCD equal to 0.1 m (Figure 3.9c). However, it can be noted that increasing the threshold to 0.15 m still produces a significant decrease of the affected area (Figure 3.9d). The distributions of the morphological variations shown in maps (d), (e) and (f) in Figure 3.9 suggest that a more appropriate TCD is between 0.15 and 0.2 m (Figure 3.9d and e, respectively) as the area that show significant changes can be considered stable by increasing the threshold, if compared with previous maps (Figure 3.9b and c). Focusing on the maps at the bottom of Figure 3.9 (d, e and f), significant morphological variations can be highlighted (i) close to the shoreline in the north of the surveyed domain, where erosion occurred, and (ii) on the back of the artificial dune, where deposition of sediments was detected. Notably, more robust methodologies exist to derive reliable DoDs on the basis of probabilistic spatially varying thresholds. Wheaton et al. (2010) provided an overview of this methodologies, comparing them with the approach here adopted. Those advanced approaches will be applied in the future to this dataset for further investigations. In this piece of work, given the heterogeneous and partial coverage of the domain of the GPS measurements used to derive the accuracy assessment, the TCD approach was preferred. The analysis was supported by a sensitivity analysis of the thresholds.

The significant morphological variations highlighted in Figure 3.9 (e) and (f) were limited to an eroded area in the north of the surveyed domain, close to the shoreline, and a deposit of sediment that characterized the back of the northern part of the dune. These variations can be explained by considering the wind and sea conditions measured between the two analyzed surveys. The wind velocity and direction, the significant wave height, wave direction and the total water level time-series are shown in Figure 3.13 for the considered period, along with wind extremes and identified coastal storms. The sea conditions were characterized by non-extreme TWLs (< 0.7 m), the occurrence of some minor wave events (H_s < 2.5 m) and a coastal storm with H_s ~3.6 m, main direction ENE and duration longer than 90 hrs. This long energetic event however, did not exceeded the combined critical thresholds defined by Armaroli et al. (2012) as TWL was lower than 0.7 m. Indeed there is no recorded evidence of damages at regional or local level for this event. Moreover, as can be seen from the orthophoto in Figure 3.7, product of the survey of January 2017 that was implemented few hours after the end of the event, the sea did not reach the foot of the artificial dune. Thus, the coastal wave storm can only explain the eroded area as the result of the berm erosion during this event. Notably, the berm area in the south of the domain did not show any significant change for TCD equal to 20 cm. This area, indeed, is well protected by breakwaters (Figure 3.1c) for minor-medium events and actually showed some deposit for lower detection thresholds (Figure 3.9a, b, c and d). Considering the direction of the event (ENE), it is reasonable to assume that part of the sediment eroded from the northern berm deposited there.

The wind conditions showed a slightly different picture, with three main detected extreme events (Figure 3.13). The first two reached force 6-7 of the Beaufort Scale (strong breeze-near gale) while, the last one, force 7-8 (near gale-gale) with a maximum velocity of ~19.8 m/s. This event in particular was characterized by directions between 60 and 70 °N. It is therefore reasonable to assume that the major morphological changes (i.e. the significant deposition detected) occurred on the back slope of the artificial dune are linked to the wind conditions and in particular to this last event, as suggested by the

typical eolian-driven features shown in Figure 3.14b, in comparison with the morphology presented in Figure 3.14a which still shows the tracks of the bulldozers used to build the protection. This morphological feature, as first assessment, can be considered consistent with the main direction of the extreme wind event. Thus, eolian transport can affect this kind of artificial features which mimic the natural coastal dunes that are created and transformed by winds and coastal storms. The magnitude of this interaction, however, is still under investigation at this site. It is also difficult to explain whether the deposited sediment comes from the top of the artificial dune or somewhere else, as the map in Figure 3.9e did not show significant erosion of the top of the dune. This phenomena however, is significant for the map in Figure 3.9d suggesting that part of the deposited sediment could come from the dune top. Notably, the back slope of the dune in the southern part only shows minor significant deposit. This is probably due to the different orientation and geometry (i.e. front slope and height) of the artificial protection.

The analysis of average vertical variations and volume changes (Figure 3.10) demonstrated that the uncertainties on the assessment are strictly dependant on the selected TCD, while applying a non-probabilistic uniform threshold. The TCD also affects the loss of information as the larger is the TCD, the smaller is the area with significant changes. This also affects the assessed volumes.

Notably, for TCD > 0.15 m the analysis of the assessed eroded and deposited volumes show that the larger is the TCD, the more comparable are the magnitude of the volumes. Given the previous preliminary interpretation, it is reasonable to assume that the eroded (from the northern berm) and deposited (on the back of the artificial dune) volumes are driven by the action of waves and winds, respectively. This implies that, in this location and for the assessed period, the volume of sediment mobilized (at different locations and time scales) by extreme winds can be comparable to the variations due to low-medium wave events and non-extreme total water levels. It must be stressed that the deposited and eroded volumes are not connected in terms of drivers and pathways (i.e. supply/delivery) and no considerations can be done on the submerged area or the volume of sediment that get in or out the monitored domain.

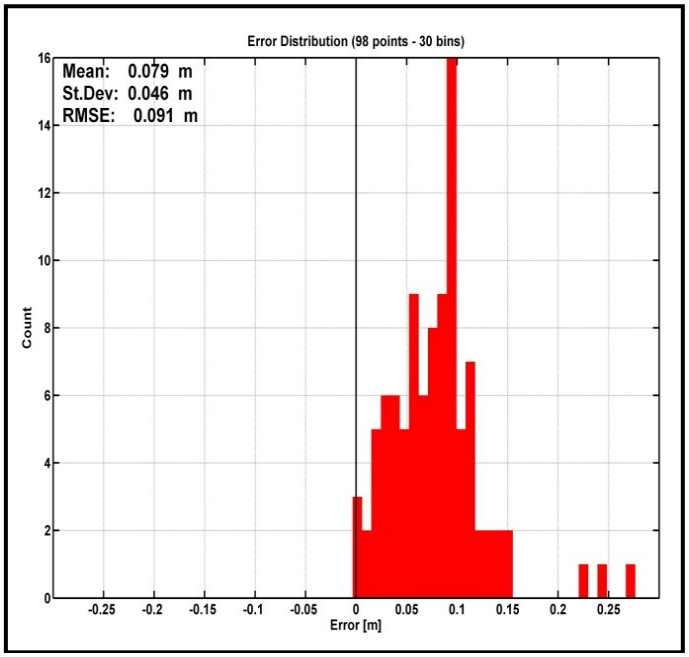

Figure 3.11 Error distribution, calculated in comparison with the GPS measurements, of the DEM derived from the survey of the 6 of April 2017.

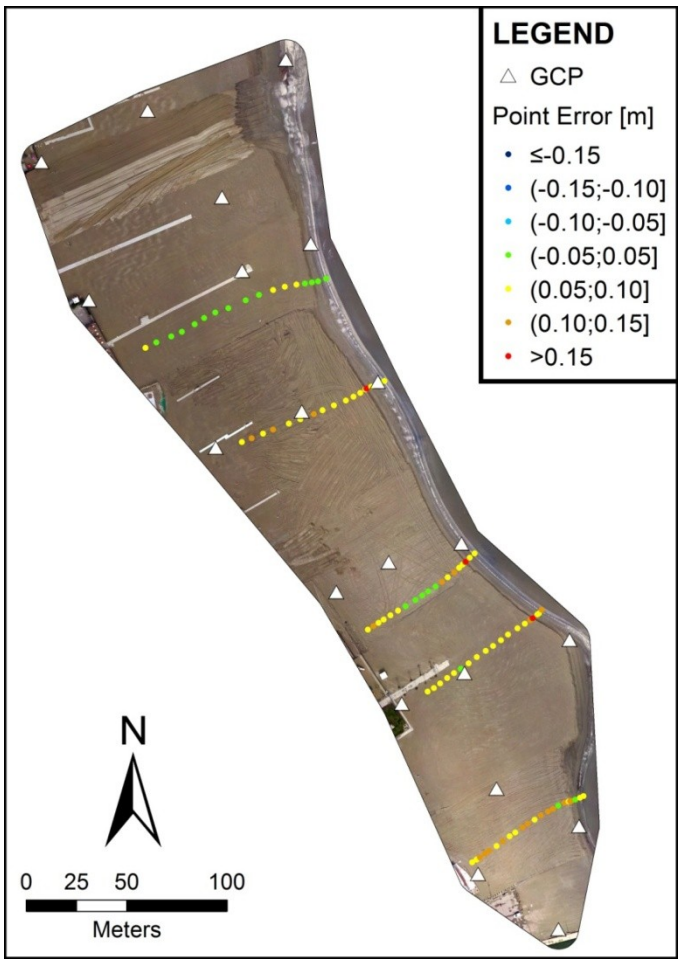

Figure 3.12 The orthophoto produced from the survey of 6 April 2017 (resolution: 10cm) with the spatial distribution of the GCPs, the GPS observed cross-sections and their calculated error (UAV-derived DEM vs GPS measurements).

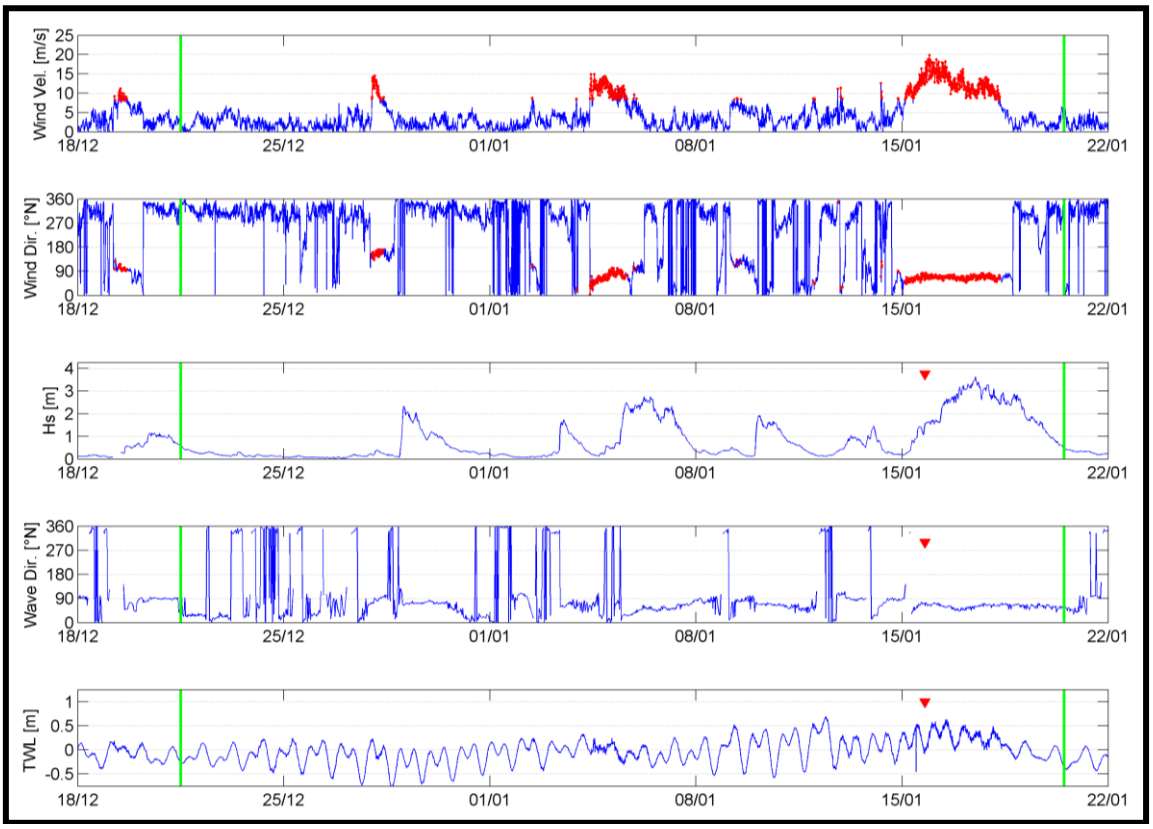

Figure 3.13 Wind velocity and direction (Porto Garibaldi meteorological station), significant wave height, wave direction (Cesenatico buoy) and water level (Porto Garibaldi tide gauge) data of the period 18 October 2016 - 23 January 2017. Extreme wind events (POT 95%) are highlighted in red in the first two plots (wind velocity and direction); red triangles indicate the occurrence of coastal storms (waves and water levels); green lines represent the day of the performed surveys.

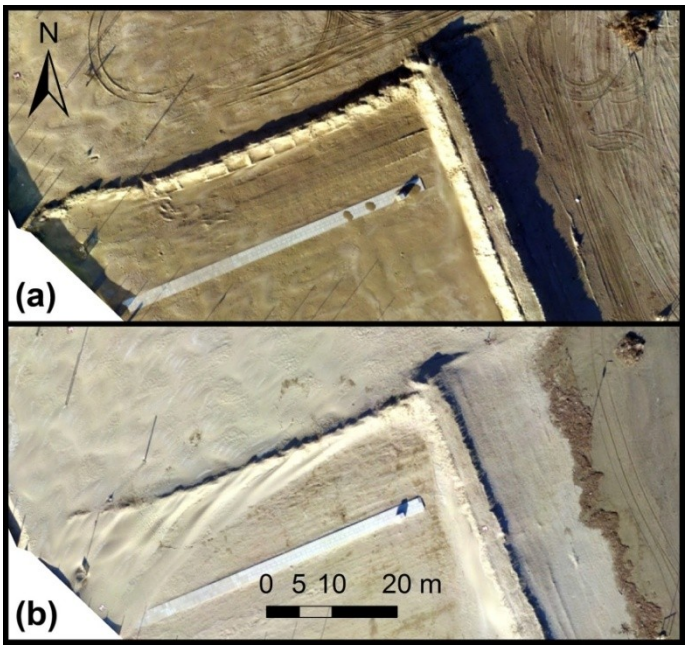

Figure 3.14 Eolian morphological features: orthophotos from (a) 21 December 2016 and (b) 20 January 2017. The signature of the bulldozer used to build the protection are still visible in (a). The morphological features visible in (b) at the back of the protection have an eolian origin.

3.6 Preliminary conclusions and future developments

This work focused on a preliminary analysis of a high-resolution (in time and space) drone-based surveying program held in the winter 2016/17 at the southern beach of Porto Garibaldi (Comacchio, Italy), in the Northern Adriatic. The target of the program was to test and assess the accuracy of beach drone surveys and to analyze the evolution of the artificial dune that is regularly built at the study site as protection for beach concessions. Five drone surveys were implemented from December 2016 and April 2017.

The majority of the drone-derived DEMs, compared with GPS observations, resulted in high accuracies (RMSE < 0.05 m) with 95% of the absolute errors lower than 0.1 m. The higher errors were linked to inaccuracies related to the GPS survey techniques adopted to measure the cross-shore profiles (i.e. stop-and-go) and the points (i.e. kinematic).

A sensitivity analysis of the significant morphological variations was implemented using the approach based on the threshold for change detection. The most reliable threshold was found to be higher than 0.15 m and lower than 0.20 m.

During the monitored period, no significant coastal storms hit the coast. However, strong winds occurred. In agreement with the analyzed forcing, the main morphological variations of the artificial dunes were identified as eolian-driven, as waves and sea water levels only affected the berm area in front of the protection. The volume of sediment mobilized by the extreme winds were found to be comparable to the volume moved by the low-medium intensity coastal storm.

This work demonstrated the capability of drones for coastal beach surveying, in agreement with most of recent UAV's published studies. Moreover, it was demonstrated that subtle morphological variations can be efficiently captured with UAV-based surveys, but their significance must be interpreted considering the error propagation of the original DEMs.

Therefore, future analysis of the presented dataset will focus on the interaction between the artificial dune and the wind forcing. Meanwhile, the drone-based survey approach will be intensively implemented for beach monitoring in future winter seasons at the study site in order to capture extreme events that will help to understand the effectiveness of the temporary protection in lowering the impacts of coastal storms.

4 SYNTHETIC STORMS: UNCERTAINTIES AND LIMITATIONS OF THEIR APPLICATION IN COASTAL HAZARD MODELLING

4.1 Introduction

The reliability of the hazard component is crucial for coastal risk assessments. Coastal inundation and erosion hazards need to be properly evaluated, especially when dealing with local assessments on sandy beaches. As example, the magnitudes of the maximum inundated area or the shoreline retreat are important in order to properly evaluate the associated consequences for exposed elements. Moreover, local managers could be interested in quantitative information in order to design DRR measures, such as dikes or nourishments, and prepare management plans.

Nowadays, hazard assessments largely rely on numerical model simulations. Models are indeed capable to reproduce a large amount of processes that affect the interaction between the morphology of the beach and the storm event that hits the coast, in order to provide multi-hazard results (Roelvink and Reniers, 2012). Models can be setup, calibrated and validated with real events, when data is available. Generally, the degree of robustness of a numerical model is related to the data availability: the more reliable information is available for model calibration and validation, the more robust is the model. This is valid for the information on the morphology of the beach, the characteristics of the sediment, and the hydrodynamics. The storm event needs to be properly described and included in numerical models as forcing. Continuous, observed or hindcasted, storm time-series of waves and water levels are extremely important in order to capture the evolution of the event and, thus, its dynamic interaction with the emerged beach. Notably, this aspect become of crucial importance when dealing with operational systems that need proper forecasts (Harley et al., 2016).

When continuous forcing time-series are unavailable, the event is generally described through observed or assessed bulk information, such as maximum significant wave height (H_s), peak wave period (T_p), maximum total water level (TWL), duration (Dur) and main direction (Dir) (Harley, 2017). The lack of continuous data leads to the introduction of simplifications and assumptions in order to proceed with the analysis of storm impacts. The most simplified approaches calculate impacts directly with statistical bulk information (see Ranasinghe and Callaghan, 2017). However, taking into account wave and water level variations during the storm is necessary to improve quantitative impact assessments. In these cases, the evolution of the storm has to be represented by parametric approaches, assuming a synthetic shape of the event, hereafter called Synthetic Storm (SS), as generic synthetic representation of the Real Storm (RS). SSs are regularly used when probabilistic parametric events (i.e. representative of a given return period) have to be tested. A first attempt to standardize a procedure for SS applications can be found in Carley and Cox (2003), which proposed a Synthetic Design Storm (SDS) approach for erosion assessments based on empirical probabilistic curves of H_s (for different return periods) exceeded for various durations that define the evolution of the storm. A typical SDS has a symmetrical evolution around the peak (defined by the Hs exceeded for 1 hr duration) with exponential-like growth and decay phases. On the other hand, the Triangular Synthetic Storm (TSS) approach is widely applied for coastal studies (e.g. McCall et al., 2010; Corbella and Stretch, 2012). Moreover, as the innovative probabilistic approaches for hazard and risk assessments are increasing the need of simulating large number of realistic storm

conditions, TSSs are often used to cover all the possible combinations of forcing (e.g. Poelhekke et al., 2016; Plomaritis et al., 2017; Sanuy et al., 2017).

Thus, the SS represents an useful approach for coastal hazard assessments and its use is recommended for planning purposes by Nielsen and Adamantidis (2007). However, SSs show some inherent limitations related to, as example, the assumptions on the probabilistic relations between storm characteristics and the inability to take into account beach recovery processes (Callaghan et al., 2009). As a matter of fact, SSs represent an additional source of uncertainty to the analyses. Sánchez-Arcilla et al. (2009) compared computed erosion impacts from RS and SS in the Spanish Mediterranean. In particular, the study showed overestimation of eroded volumes and shoreline retreat while adopting schematized, linearly varying H_s and T_p. On the other hand, the erosion impacts were found to be underestimated while adopting real H_s and schematized T_p (linearly varying). Callaghan et al. (2009) assessed the reliability of SDS (Carley and Cox, 2003) for erosion assessments at Narrabeen Beach (Sydney, Australia) by comparing erosion impacts computed adopting statistic events (i.e. representative of given return periods and simulated with SDS) and statistics of measured impacts. This study found a tendency to underestimate the computed eroded volumes with return periods between 3 and 10 years. No study has never assessed the role of SSs in the propagation of uncertainties through a model chain (coupling of models) able to assess both coastal inundation and erosion impacts.

This study focused on comparing the use of Symmetric TSS (STSS) against their real evolution, for flooding and erosion numerical assessment. The adopted model chain was based on a coupling between XBeach (1D) (Roelvink et al., 2009) and LISFLOOD-FP (2DH) (Bates and De Roo, 2000). This model train was used in the RISCKIT project in order to efficiently simulate a large number of storms for hotspot detection and comparison (Viavattene et al., 2017; Christie et al., 2017). The simulation results were integrated in a Bayesian Network (BN), linking forcing and comparative results through conditional probabilities.

Assessments involving STSS simulations as input for model chains such as the one adopted in this study, are usually applied in coastal areas which are sensitive to the impact of inundation and erosion. In this work, the approach was implemented in two Mediterranean locations representative of this type of coasts: one in Spain (North-Western Mediterranean) and the second in Italy (Northern Adriatic). The two cases represent low-lying highly touristic locations, predominantly dissipative in Italy and reflective in Spain. At the Spanish case, the analyzed storm time-series covered more than 40 years while, in the Italian one, waves and water levels, which play an important role in that micro-tidal low energetic environment, only covered 8 years. This work aims at investigating how the synthetic representation of real coastal storms can influence the coastal multi-hazard assessments and which are the characteristics of the real storm that need to be captured by a synthetic event in order to properly reproduce the hazard component. The results presented the main focus and significance in Tordera Delta, where a longer data record is available and therefore the comparison is statistically more robust. Then, the Italian case is used to confirm and/or complement observed tendencies in a different case study.

4.2 Case studies

The two selected study sites have an extension in the order of ~4-6 km and are representative of the regional characteristics at the NW Mediterranean and northern Adriatic coasts. The Tordera Delta (TD; Figure 4.1c) is part of the 280 km of sandy

shoreline at the Catalan coast (Figure 4.1a), whereas Lido degli Estensi-Spina (ES; Figure 4.1d) belongs to the 130 km long coast of the Emilia-Romagna (Figure 4.1b).

Both locations are characterized by low-lying sedimentary beaches, prone to be impacted by coastal flooding and erosion (Perini and Calabrese, 2010; Sardá et al., 2013). These impacts have been emphasized due to the lack of river sediment supply (Jiménez et al., 2011; Preciso et al., 2012), subsidence at ES (Taramelli et al., 2015) and strong structural erosion due to net littoral drift at TD (Jiménez et al., 2011; Sardá et al., 2013). In addition, tourism is one of the main drivers of the local economy at both ES and TD. Therefore, both sites have experienced urbanisation and infrastructural growth close to the shoreline (limiting natural beach accommodation processes), and economic activities (e.g. beach facilities, campsites, restaurants) are directly located on the beach or in the immediate first part of the hinterland. These led to a situation where the coast keeps offering its recreational function, but lacks part or all of its protective function against storms (Sanuy et al., 2017). Hence, the two case studies already experienced the impact of severe events and are well-known as coastal critical sectors (so called hotspots) at the regional level (Armaroli and Duo, 2017; Jiménez et al., 2017c).The coastal hydrodynamics are well-known at both study sites (see for ES: IDROSER, 1996; Ciavola et al., 2007; Masina and Ciavola, 2011; Masina et al., 2015; and for TD: Trigo et al., 2002; Lionello et al., 2006; Mendoza et al., 2011). Thus, in both case studies risk assessment tools and methods are usually applied. Methodologies based on numerical modelling, where a large number of storms are simulated, including synthetic events, are likely to be applied in coastal sectors such as the two presented here.

Although all presented similarities, the selected study sites have some significant differences making them complementary for the present work. Regarding the morphology, ES is characterized for being mainly dissipative, with fine sediment (D50 ~0.23 mm), whereas the beachfront in TD is mainly reflective, with coarse sediment (D50 ~1 mm). Thus, each study site responds differently to the impact of storm events. Regarding the hydrodynamics, both sites are micro-tidal environments but the tidal range at ES (neap tidal range: 0.3-0.4 m; spring tidal range: 0.8-0.9 m) is higher than in TD (neap tidal range: 0.2-0.25 m; spring tidal range: 0.3-0.4 m). In addition, ES is characterized by a low-energetic wave climate (mean H_s ~0.4 m; 60% of waves below 1 m, max recorded H_s = 4.6 m at the buoy in Figure 4.1b), and surge events can be extreme and play an important role (1-in-2 years storm surge: 0.61 m). These lead to high impacts even during low energetic storms (Armaroli et al., 2009, 2012; Harley and Ciavola, 2013; Perini et al., 2015b; Harley et al., 2016). Differently, TD has a more energetic wave climate (average H_s from 2.8 to 6.6 m for the different storm classes in Mendoza et al., 2011), where surge is observed to be independent and with little contribution to the total water level at the shoreline, when compared to the wave component (Mendoza and Jiménez, 2008).

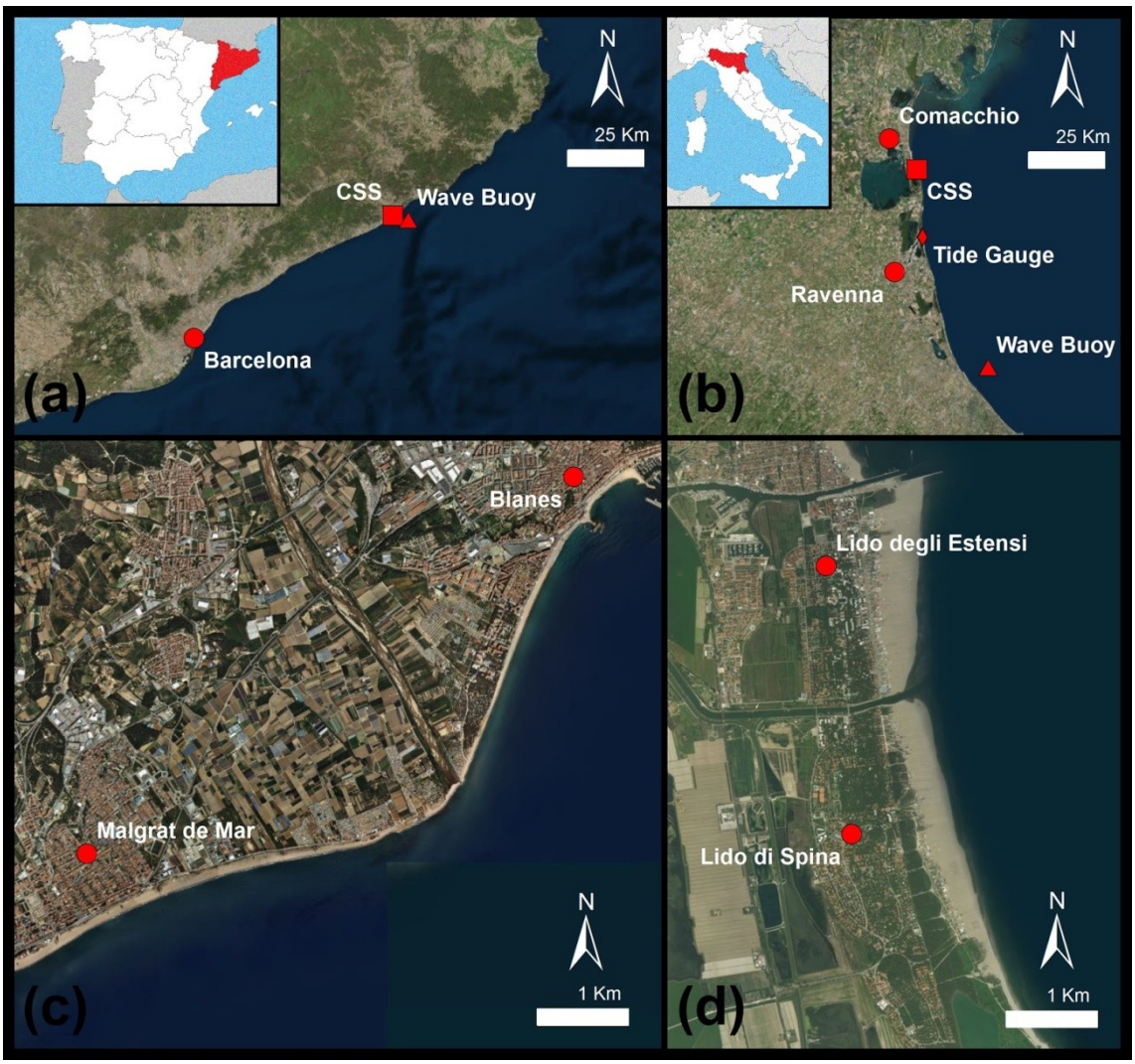

Figure 4.1 Regional and local contexts: (a) the central-northern Catalan coast; (b) Emilia-Romagna coast; (c) the study site of Tordera Delta; (d) the study site of Lido degli Estensi-Spina. The main locations are highlighted with red dots.

4.3 Methods

In general, the approach began isolating the storm events from the available time-series at the case studies. For each event, the main bulk information were retrieved and the design time-series were calculated. Both real and design storms were simulated using a process-based multi-hazard model chain. Only the events observed to produce a significant inundation (> 1 ha) were then included in the final comparison analysis. Representative retreat, overtopping water volume and flooded area were compared and results integrated in a BN. The BN was used to investigate the relations between forcing characteristics and comparative results. In the following sections, details on the steps of the methodology are given.

4.3.1 Storm data and identification

Hindcast wave time-series were used to derive the storms at the Tordera Delta. The dataset was composed by SIMAR time-series (covering the period from 1958 to 2001) and WANA time-series (covering the period from 2004 to 2013), both obtained from Puertos del Estado. The storm were isolated following the storm definition by Harley

(2017) and applying the threshold and parameters listed in Table 4.1. The total amount of identified real storms was 93. Finally, only storms with a minimum simulated inundation over 1ha (43 storms) are included in the BN-based assessment, to avoid noise in the comparison variables.

For the Italian case study, the water level data was retrieved from the tide gauge located in the Ravenna harbour (Porto Corsini), while the wave data from the Cesenatico buoy. The overlap between the time-series allowed analyzing the period between the beginning of 2007 and the summer 2015. However, the wave time-series was characterized by periods with missing data, in particular: January - May 2009, November - December 2010, October 2011 - March 2012 and February - June 2014. Notably, as the aim of the study was to compare the modelling outcomes of design and real time-series, this limitation only affected the number of storms that were isolated for Lido degli Estensi-Spina. Storm events were identified considering the general storm definition described in Harley (2017) and applying the thresholds adopted by Armaroli et al. (2012), reported in Table 4.1. The isolated storms were 80 but when only significant inundation events were considered (> 1 ha), the number reduced to 11 for the Italian site. Although this number of events is low to perform a proper robust statistical analysis, it is enough to complement results obtained in the Spanish study site in order to confirm tendencies and common outcomes.

Table 4.1 Thresholds and parameters for storm identification and isolation following Harley (2017). (*) Armaroli et al. (2012); (**) High Spring Tide.

Case Study	Significant Wave Height Threshold	Minimum Storm Duration	Meteorological Independence Criterion	Total Water Level Threshold
Lido Estensi-Spina	1.5 m(*)	6 hrs(*)	3 hrs(*)	0.45 m(**)
Tordera Delta	2 m $H_{s,max}$ > 2.75 m	6 hrs	72 hrs	None

4.3.2 Real and triangular storms

An isolated storm is generally well represented by the time evolution of offshore waves and total water levels (tide + surge). The data can be analyzed to retrieve bulk information. The main bulk parameters necessary to describe the storm in a compact manner are: max significant wave height ($H_{s,max}$), peak period at peak (T_p), main direction (Dir), max total water level (TWL_{max}) and duration (Dur). Then, synthetic storms can be calculated assuming different time evolution of the storm. As anticipated, this work focused on Symmetric Triangular Synthetic Storms (STSSs). A STSS wave time-serie is defined, for H_s, as shown in Figure 4.2. The STSS can be similarly applied to represent the T_p and the surge component of the TWL. In this work, the STSS was applied to H_s.

Depending on the evolution of the real storm, the STSS can lead to: (i) an anticipation or delay of the storm peak and (ii) the under- or overestimation of the energy content (E; [$m^2 \cdot s$]), which is defined as follows (Equation 4.1):

$$E = \int H^2 dt \quad (4.1)$$

Notably, these perturbations are propagated through the model chain to the final results. These effects are taken into account by considering the Peak Delay (PD; see Figure 4.2) and the energy content ratio (ER; Equation 4.2) between the synthetic and the real storm:

$$ER = E_s / E_r \quad (4.2)$$

where E_r and E_s are the energy content of the real and synthetic storm, respectively.

Additionally, it was defined the Peak Persistency (PP) of a storm as the percentage of the storm duration during which the H_s exceed the 90% of the $H_{s,max}$ of the storm. It was therefore possible to calculate the PP for the real (PP_r) and synthetic (PP_s) event. The Peak Persistency Ratio (PPR) was defined as follows (Equation 4.3):

$$PPR = PP_s / PP_r \quad (4.3)$$

Notably, the use of these indicators may not be exhaustive enough to capture in detail the goodness of the storm representations. However, they can still give reliable information for the purposes of this study.

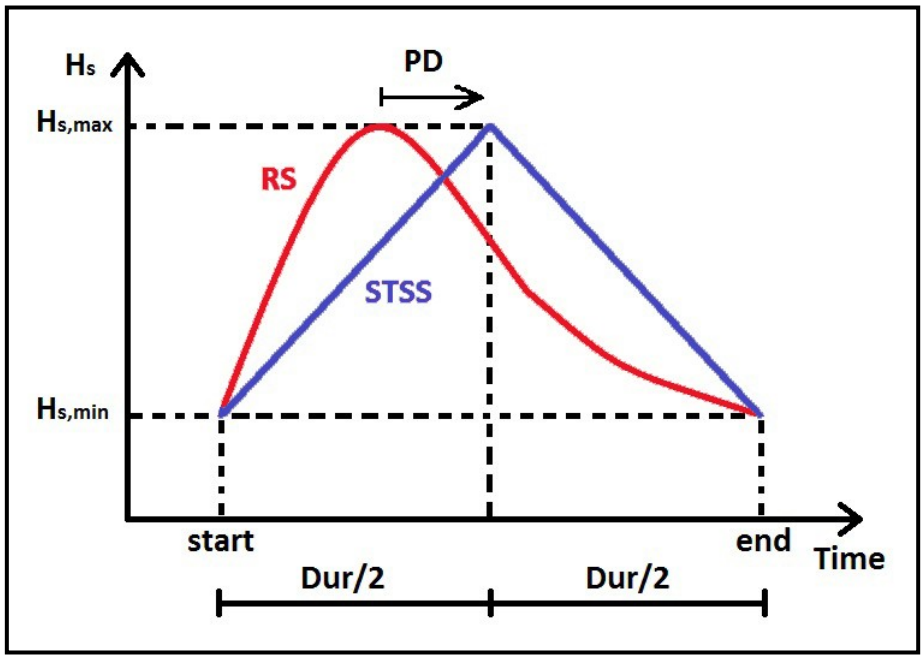

Figure 4.2 Schema of the real storm (RS; in red) and its representation with the symmetric triangular synthetic storm (STSS; in blue). The peak delay (PD) is graphically defined.

4.3.3 Model chains

Conceptually, the model chain aims at reproducing the flooding and erosion hazards in a sandy coastal environment under different storm conditions, real and synthetic (i.e. RS and STSS, respectively). Therefore, it has to be capable to reproduce the processes that affect the hazards in an integrated manner (i.e. process-based models). The model chain used in this study consisted of a coupling between 1D cross-shore XBeach (Roelvink et al., 2009) profiles and a 2D LISFLOOD-FP (Bates and De Roo, 2000) model of the hinterland. This approach was successfully adopted in the RISKIT project in order to compare regional hotspots (Viavattene et al., 2017; Christie et al., 2017).

The main focus of this study was on storm wave intensity, TWL and duration, and therefore the effect of storm direction was neglected by forcing waves to be orthogonal to the shoreline. Using XBeach in 1D mode allowed this simplification, not applicable to a single 2D model (even more expensive in terms of computational effort).

When the depth of the recorded data is greater than the XBeach offshore boundary one, a propagation function must be applied in order to transfer the storm characteristics from the location of the data source (hindcast grid point or wave buoy) to the process-based module offshore boundary. When propagation is included, it may lead to an additional source of uncertainty which needs to be assessed.

The 1D XBeach model propagates the storm forcing through the nearshore domain towards the beach. This was implemented through a number of profiles which have to represent the morphological/elevation characteristics of the whole stretch of coast of the case study and should be carefully selected depending on (i) the submerged and emerged morphology of the beach and, most important for inundation assessment, (ii) the barrier and back-barrier morphology. Therefore, profiles should be representative of homogeneous sectors of varying lengths, depending on the characteristics of the beach.

The XBeach computed results were then processed (i) to assess the erosion impacts of the storm on the profile - thus, on the represented sector - and (ii) to retrieve the time-serie of the profile discharge to be input into the LISFLOOD-FP model. This model represented the second step of the process-based module of the chain and computed the inundation assessment. Notably, the position where the computed discharge was retrieved was defined by a dynamic approach taking into account the morphological response of the profile during the storm. The position was defined as a point 10 m inland from where erosion stops. Therefore, the overtopping discharge time-serie was always located on a non-eroded position. This approach allowed taking into account the contribution of the cross-shore bed level changes to the discharge output. Notably, as the discharge was computed on the profile (i.e. unitary discharge), it had to be multiplied for the length of the beach sector represented by the profile. The discharge was then poured in the LISFLOOD-FP model domain by distributing it in several discharge points along the represented sector, in order to avoid massive localized volumes of water entering the domain. The simulated water depths were then processed to calculate the inundation extension.

At the Tordera Delta, wave linear propagation (shoaling and refraction) was applied to the storm time-series, since data were available at deep waters, at a location far away from the offshore boundary of the XBeach model. Hazard estimation with XBeach (i.e. beach retreat and overtopping discharges) was performed by representing the study area with 67 1D cross-shore profiles starting at 20 m depth at the offshore boundary. The bathymetric information used to interpolate the profiles consisted of detailed bathymetry measured in 2010 provided by the Ministry of Agriculture, Food and Environment. The XBeach parameter set-up used in this work is the same as in Sanuy and Jiménez (submitted). XBeach discharge results were used to feed the LISFLOOD-FP model, which in the Tordera Delta consists of a 3x3 m DSM grid interpolated from LIDAR data from 2010 provided by the Institut Cartogràfic de Catalunya.

At Lido Estensi-Spina, 90 profiles were identified to properly capture the beach morphology and were extracted from a merged topo-bathymetry (emerged: Lidar, October 2014; nearshore bathy, down to 3 m depth: Lidar, 2012; offshore bathy: Multibeam 2013). The profiles were input in the XBeach model (facua = 0.1; D50 = 0.00023 m; morfac = 5; default elsewhere) as computational grids (resolution: 20 m deep water; 1 m surf zone). The LISFLOOD-FP model (infiltration = 0.00003; default

elsewhere) was built on the basis of the Lidar of October 2014 by setting a regular grid resolution of 3 m.

4.3.4 Comparative analysis

Retreat

The erosive effect of a storm was quantified by calculating for each profile a representative retreat (R; [m]) of the shoreline. The eroded area of the profile was detected and there the horizontal displacements of the profile at different elevations were retrieved. R was defined as the average of the horizontal displacements. The comparison between the representative retreats calculated for the real (R_r) and synthetic (R_s) storms was based on the relative difference between the two, defined as (Equation 4.4):

$$\Delta R = (R_s - R_r)/R_r \qquad (4.4)$$

The comparative variable ΔR gives quantitative relative information on the differences between the computed retreats.

Water volumes

The discharge time-series were retrieved from the XBeach output for each profile of the domain, for a given storm. For each profile was therefore possible to know the volume of overtopping water (WV; [m^3]) of a storm, calculated considering the length of the sector represented by the profile. Consequently, the total water volume (TWV; [m^3]) expected to inundate the inland was given by the sum of the WV for all the profiles.

The comparisons between profile WV_r (of the real storm) and WV_s (of the synthetic storm) was based on the logaritmic loss, defined as follows (Equation 4.5):

$$\Delta WV = log_{10}(WV_s) - log_{10}(WV_r) \qquad (4.5)$$

The comparative variable ΔWV gives an indication on the order of magnitude of the differences. The same approach was adopted to quantify the differences between the computed TWV (ΔTWV) expected to inundate the inland, for a given storm.

Flooded area

The flooded area (A; [ha]) was computed by post-processing the water depth results of the LISFLOOD-FP model simulations. A cell of the domain was considered flooded when the maximum water depth during the simulation exceeded 0.1 m. The comparisons between the A_r (from the real storm) and A_s (from the synthetic storm) was implemented following Bates et al. (2005) through the performance measure (Equation 4.6):

$$F = \frac{A_r \cap A_s}{A_r \cup A_s} \qquad (4.6)$$

The comparative variable F is equal to 1 when A_r and A_s coincide, and 0 when the flooded areas do not overlap.

4.3.5 Bayesian Network

Bayesian Networks are statistical graphical tools describing relationships between variables by means of probability theory (Lauritzen and Spiegelhalter, 1988; Pearl, 1988; Jensen, 1996). In particular, they are based on Bayes' rule given by (Equation 4.7):

$$P[O_i|P_i] = P[P_i|O_i] \cdot P[P_i] \qquad (4.7)$$

In Equation 4.7, P_i represents the parent characteristics variables linked through the BN to any given output O_i. In this application, results between real and synthetic storms were compared. The storm characteristics (H_s, Duration, TWL) were used as parents for the variables representing the difference between real and synthetic time-series (ER, PD and PPR) and for the output comparative variables (ΔR, ΔWV, ΔTWV and F). ER, PD and PPR were also linked to ΔTWV and F. The BN scheme adopted for the two case study sites is represented in Figure 4.3.

In this way, the BN allows a comparative assessment conditioned to different combinations of parent variables, and thus, allows locating those conditions with lower/higher differences and, at the same time, assessing the interdependencies between morphological characteristics and final observed differences. The BN produces probability distributions that are empirically calculated through conditional probability tables for each variable, and updates them as new conditions are specified. Two separate BNs were graphically built for each case study with the Netica software and fed with the performed simulations.

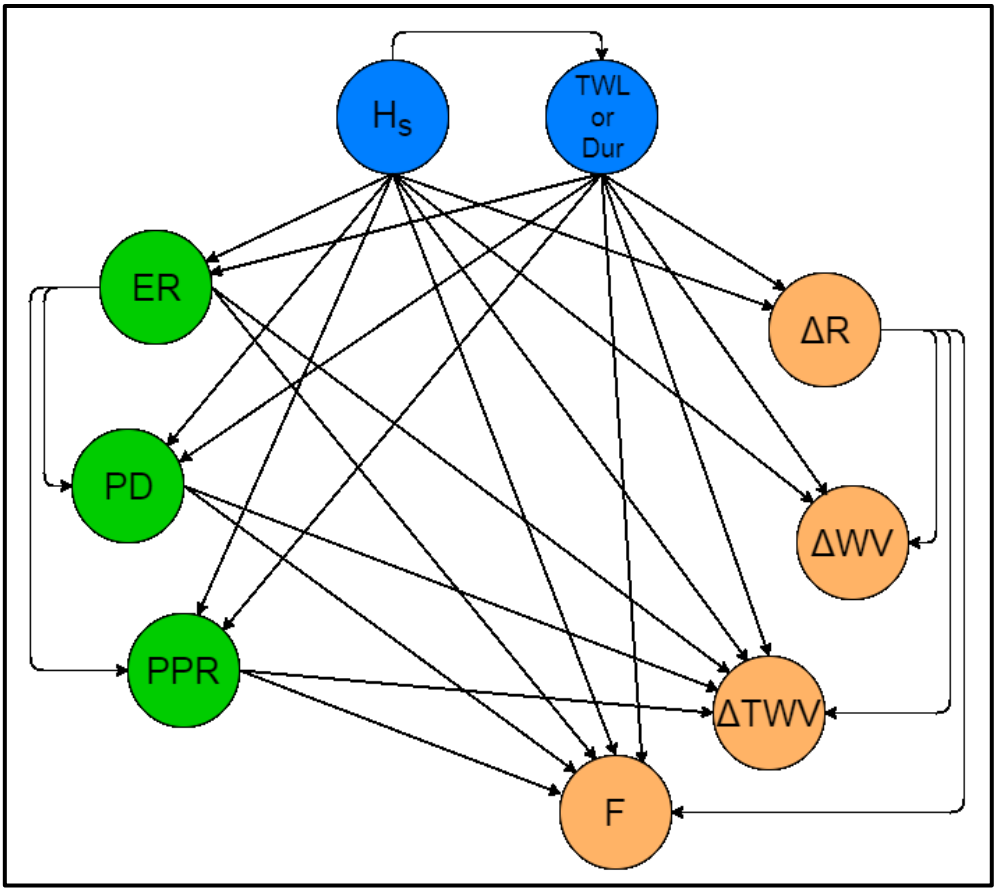

Figure 4.3 Bayesian Network scheme adopted for the two case study sites. Variables are represented by circles while arrows represent the mutual influence between two variables. The storm characteristics (Hs, Dur or TWL) are coloured in blue, the variables representing the differences between real and synthetic time-series of waves (ER, PD and PPR) in green while, the comparative output variables are in orange.

4.4 Results

In the following, obtained uncertainties and differences on hazard estimation when using Symmetric Triangular Synthetic Storm (STSS) instead of Real Storm (RS) wave time-series are presented. First, one specific and well-documented storm at each study site is introduced, analysed and used as an example to illustrate the comparative analysis later performed integrating multiple storms (Section 4.4.1). Then, an overview of the dataset is given (Section 4.4.2). Later, aggregated statistical results from all simulated storms are used to assess the difference for the representative storm characteristics at each study site, using a Bayesian Network approach (Section 4.4.3). In the following, the case study site names were abbreviated as follows: TD for Tordera Delta (Spain) and ES for Lido degli Estensi and Spina (Italy). Integrated results at TD were statistically more robust given the length of the dataset and therefore the total number of analysed storms. Therefore the ES case will be used here to complement TD in terms of determining similarities and common trends or responses.

4.4.1 Storm examples at the case studies

At TD, the "St. Esteve Storm" hit the coast on the 26 December 2008 (Figure 4.4b). The storm was an event with a $H_{s,max}$ of 4.5 m in deep waters that, after propagation to the 20 m depth, evolved to a 17 hrs event with an $H_{s,max}$ of 3.95 m. The storm showed a characteristic shape for NW Mediterranean conditions: the peak was closer to the beginning of the storm than to the middle of the event duration. Results showed a good capacity of the STSS to capture to total energy content (ER ~1). However, it failed in capturing the energy contained at the peak (PPR = 0.75) and the timing of the peak (PD = 12 hrs).

The storm event of 31 October 2012 at ES ("Halloween storm"; Harley et al., 2016; Figure 4.4a) was characterized by low waves ($H_{s,max}$ = 2.43 m) and high total water level (TWL = 1.16 m). The storm lasted for almost 18 hrs. Its temporal evolution was characterized by an instantaneous initial increase in significant wave height followed by a long peak persistency. The exceptionality of this storm (Harley et al., 2016) was mainly driven by the extreme TWL, rather than the low observed waves. The corresponding STSS is shown in Figure 4.4a. In this study site both real and design events were simulated using the real TWL data. Thus, the analysis focuses only on differences due to STSS considering waves, and not the composition of synthetic waves and synthetic surge. The comparison between the real and synthetic time-series resulted in ER = 0.95, PD = 0.75 hrs and PPR = 0.71, meaning that the STSS was capable to capture the energy content and the peak of the storm but failed at reproducing the energy at the peak of the storm.

In terms of obtained hazards, the comparison between STSS and RS storm showed that the first one underestimated the representative retreat (R) at both case studies (Figure 4.5a and b, left panels). At TD, the STSS underestimated the overwash deposit and berm erosion at the top of the beach (Figure 4.5b, left panel). In the case of ES, the STSS underestimated the erosion of the bar (Figure 4.5a, left panel). The TWV entering the domain was also underestimated at both study sites (ΔTWV equal to -0.46 at TD and -0.17 at ES). Consequently, the comparison between the flooded areas (A) showed an underestimation of the synthetic event (Figure 4.5a and b, blue area) in comparison with the real one (Figure 4.5a and b, red area). The fitness factor (F) was 0.15 in TD and 0.558 in ES. Differences are higher in TD given the higher differences in TWV entering the hinterland which are also related to the underestimation of berm lowering during the storm. Notably, the inundated surface can be enhanced or damped with respect to differences in TWV as a function of the local topography.

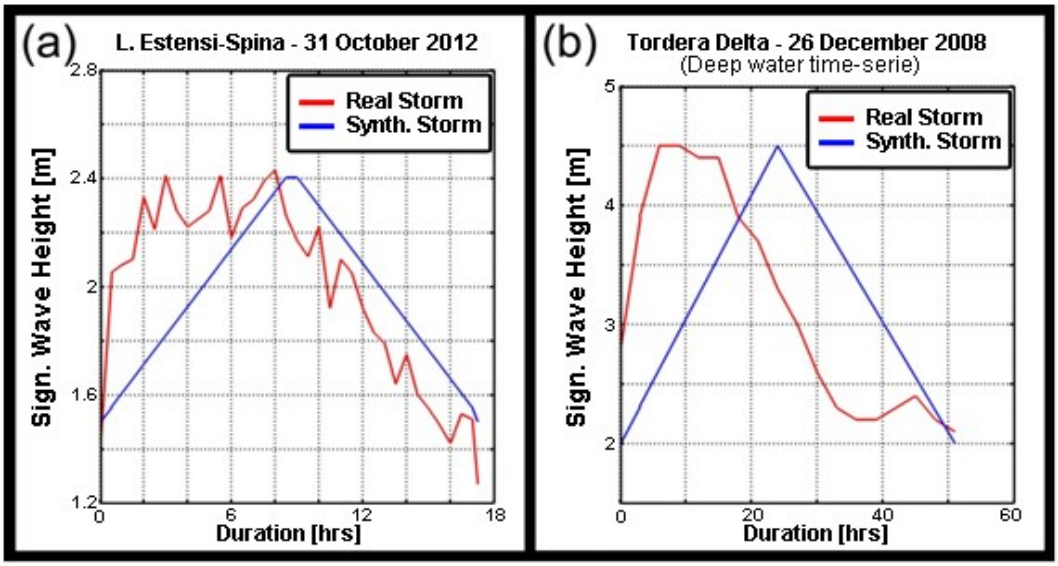

Figure 4.4 Comparisons between real storm (RS; in red) and symmetric tringular synthetic storm (STSS; in blue) wave input: the events of (a) 31 October 2012 at Lido degli Estensi-Spina and of (b) 26 December 2008 at Tordera Delta.

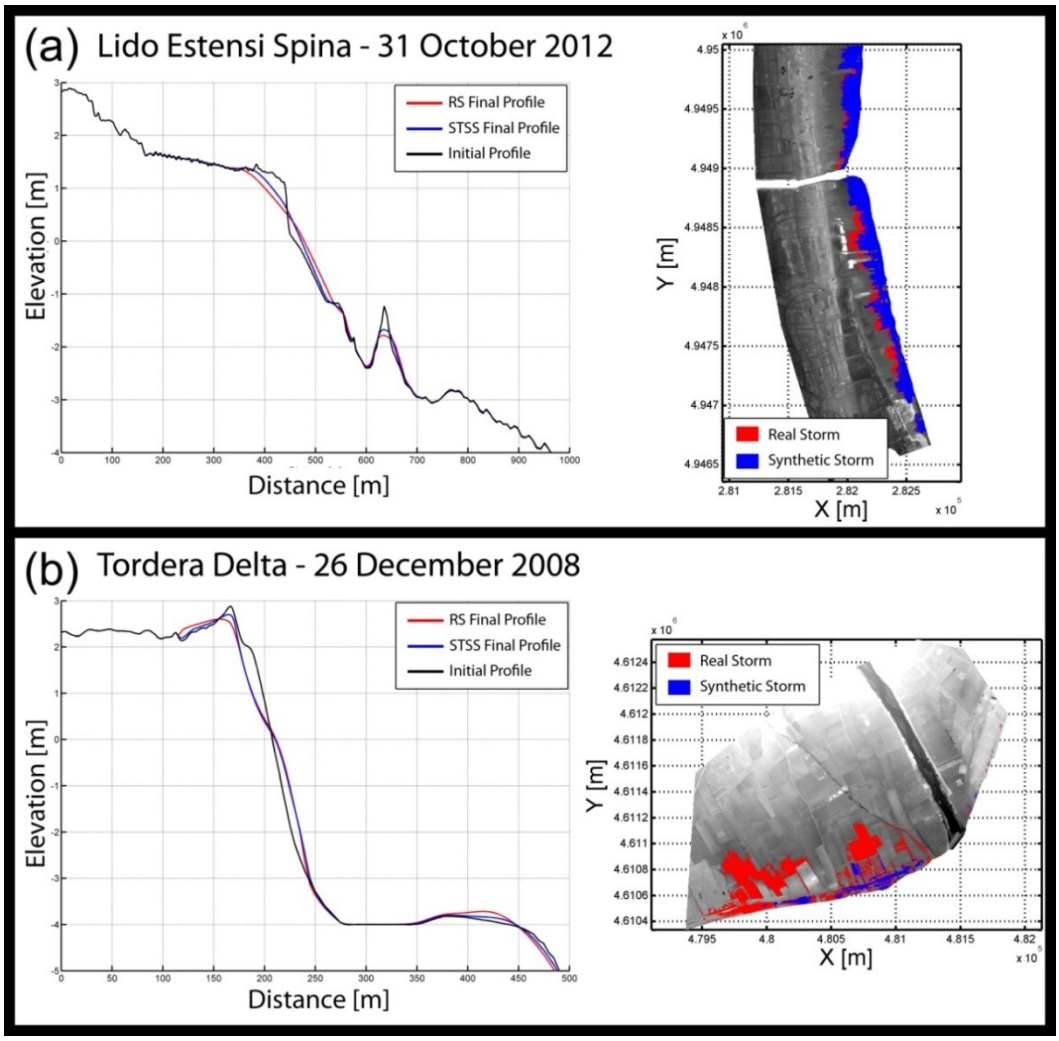

Figure 4.5 Comparisons between real storm (RS; in red) and symmetric tringular synthetic storm (STSS; in blue) output (post-storm profiles on the left and inundation on the right): the events of (a) 31 October 2012 at Lido degli Estensi-Spina and of (b) 26 December 2008 at Tordera Delta.

4.4.2 Direct comparisons

A first overview of the dataset is given through direct comparisons (i.e. scatter plots) between the RS and STSS variables. The energy (E) and peak persistency (PP) comparisons are shown in Figure 4.6 while, the retreat (R) and inundated surface (A) can be found in Figure 4.7. The computed profile (WV) and total water volume (TWV) discharges are shown in Figure 4.8.

The visual analysis of the scatter plots revealed that the STSS is able to capture the storm energy (E) of the majority of the events at both case studies. However, it has shown a tendency to overestimate the energy for some events at TD (Figure 4.6a). The peak persistency (PP) showed a more scattered picture with a slight tendency to underestimate the highest PP values of the real storm at TD while using STSS (Figure 4.6b). Differently, at ES high PP values seemed to be overestimated, but this observation is based only on two events and should be confirmed with a larger dataset.

The computed results showed a good reproduction of the retreat (R) at TD, while STSS tended to underestimate R at ES (Figure 4.7a). The RS inundated surface (A) seemed well captured by the STSS at ES. At TD some events of intermediate-large inundations (20 to 75 ha) showed a clear underestimation (Figure 4.7b). Regarding WV and TWV water discharge volumes, the scatter plots of the whole dataset (Figure 4.8a and b, respectively) showed for TD an overestimation of profile WV for the storm with higher simulated TWV. Profile discharges were generally underestimated for the remaining medium to large WV (Figure 4.8c and d, respectively), leading to the corresponding underestimation of TWV. Finally, for low WV, both over- and underestimation was observed, with a tendency towards underestimation. At ES the main tendency is the underestimation of RS water volume discharges but of lower magnitude than in TD (Figure 4.8c and d).

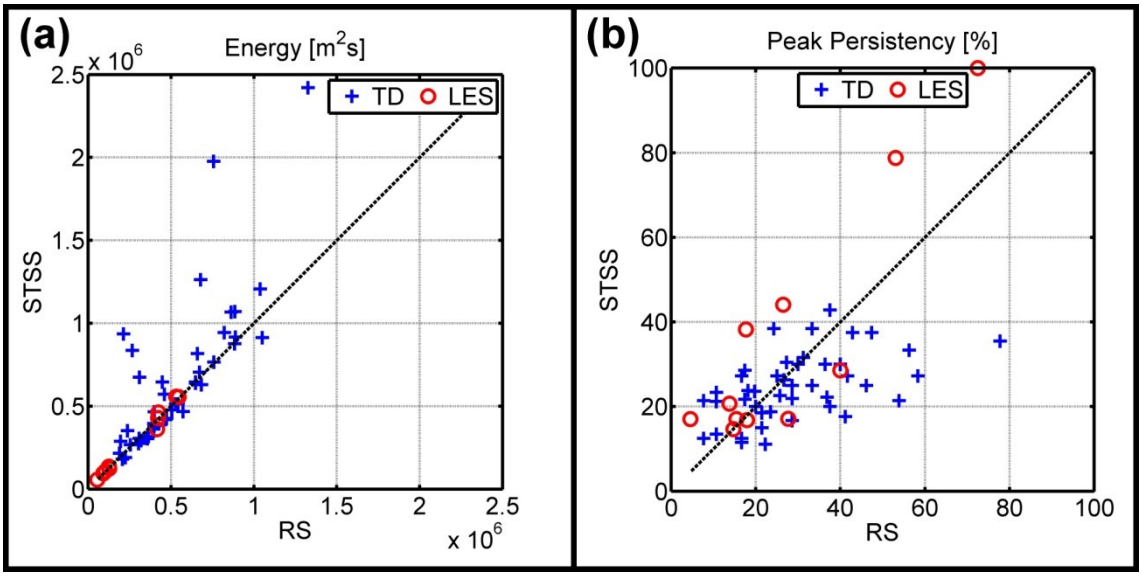

Figure 4.6 Direct comparisons of (a) storm energy (E) and (b) peak persistency (PP) of the analyzed real storms (RSs) and the symmetric tringular synthetic storms (STSSs) for both case study sites (Tordera Delta in blue and Lido degli Estensi-Spina in red).

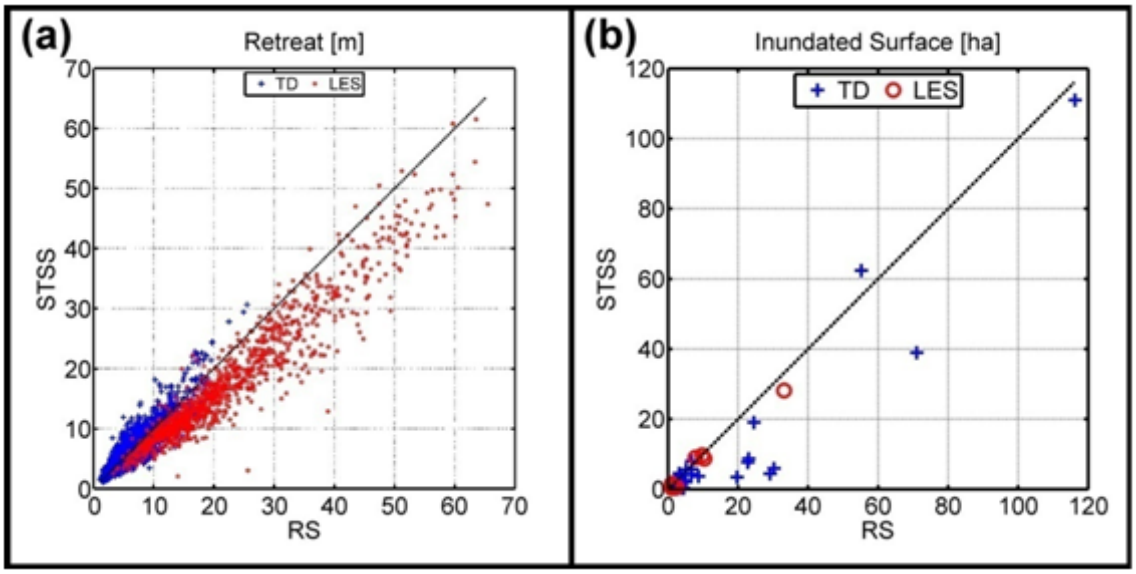

Figure 4.7 Direct comparisons of computed (a) retreats (R) and (b) inundated surfaces (A) of the analyzed real storms (RSs) and the symmetric tringular synthetic storms (STSSs) for both case study sites (Tordera Delta in blue and Lido degli Estensi-Spina in red).

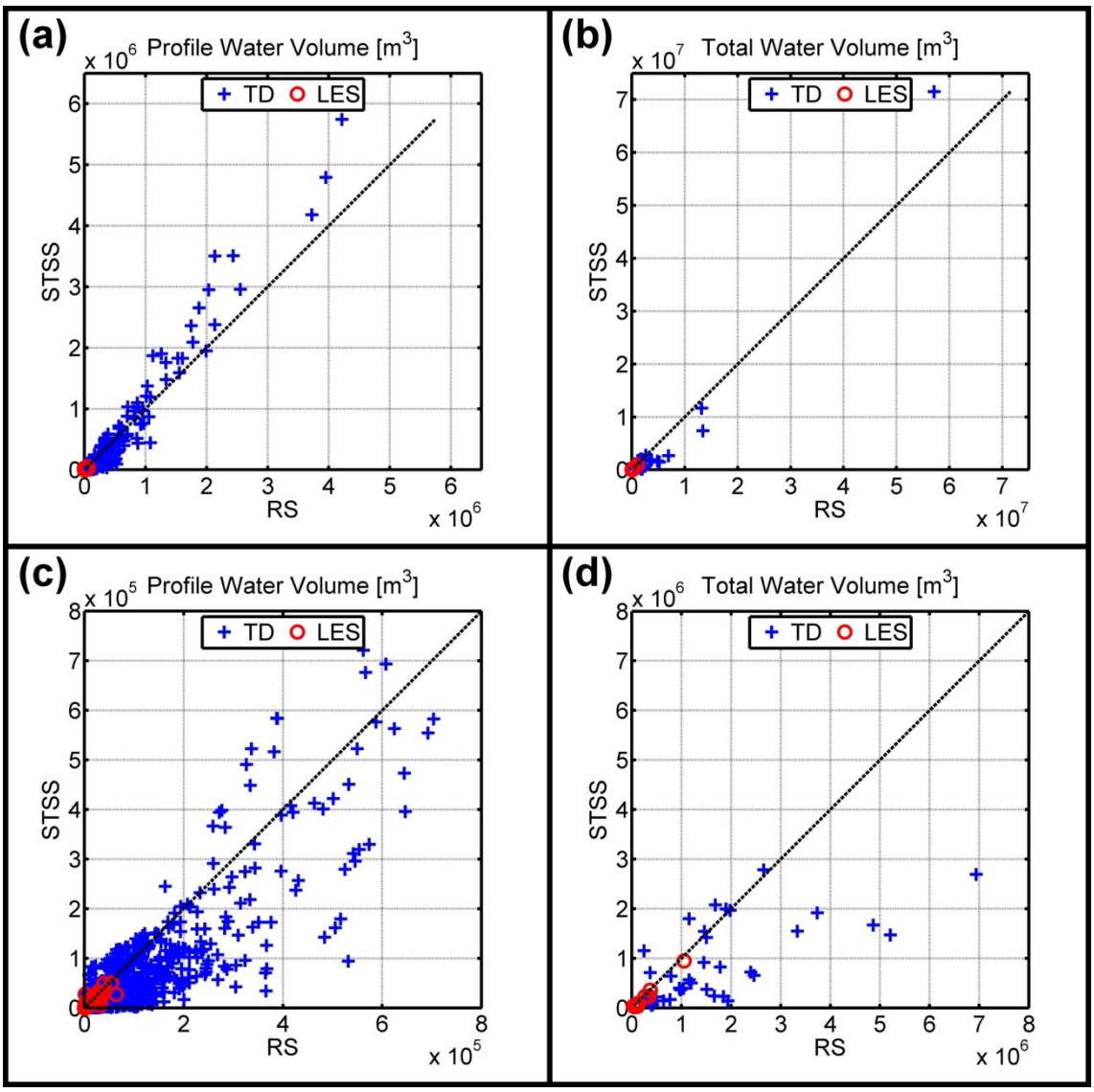

Figure 4.8 Direct comparisons of computed (a) profile water volume (WV) discharge and (b) total water volume (TWV) discharge of the analyzed real storms (RSs) and the symmetric tringular synthetic storms (STSSs) for both case study sites (Tordera Delta in blue and Lido degli Estensi-Spina in red). In (c) and (d) the focus of the bottom left areas of the (a) and (b) plots are shown, respectively.

4.4.3 Bayesian Network integrated outcomes

In order to show the comparative results for the whole range of available storm characteristics, all simulated storms were included in a BN, for each case study. The combinations of storm characteristics analyzed in this study are summarized in Table 4.2. The aggregated hazard results of the forcing combinations were assessed (Figure 4.9 and Figure 4.10), and later, the relations between ΔTWV and storm shape characteristics (ER, PD and PPR) and morphological output (ΔR) were explored (Figure 4.11 and Figure 4.12). In the figures, the horizontal black solid lines represent the interval defined by the 12.5%-87.5% quartiles of the samples while, the black boxes indicate the 25-75% ones. The red vertical line is the median of the sampled variable. It must be noted that cases ES-A and ES-F only contain one storm, and thus, results given by these categories show the resolution of the variables discretization and have to be carefully considered. This will be stressed throughout this section.

Table 4.2 Simulated combinations at the study cases.

Lido Estensi-Spina (ES)	**H_s [m]**	**TWL [m]**	**Nr. Events (Tot. 11)**
ES-A	1.6-2.5	0.45-0.8	1
ES-B		0.8-1.1	2
ES-C		1.1-1.3	2
ES-D	2.5-4.2	0.45-0.8	2
ES-E		0.8-1.1	3
ES-F	4.2-4.6	1.1-1.3	1
Tordera Delta (TD)	**H_s [m]**	**Duration [hrs]**	**Nr. Events (Tot. 43)**
TD-A	3.4-3.7	16-32	5
TD-B		32-64	7
TD-C		64-105	3
TD-D	3.7-4.4	16-32	3
TD-E		32-64	6
TD-F		64-105	5
TD-G	4.4-7.5	16-32	3
TD-H		32-64	5
TD-I		64-105	6

The analysis of water volumes showed similar results at both study sites. As expected, a remarkable correlation (i.e. comparable patterns) between the profile ΔWV and the ΔTWV is observed (Figure 4.9a and b; Figure 4.10a and b). Notably, ΔWV results are out of the displayed graph limits since, at the profile scale, differences of multiple orders of magnitude can be locally observed. The ΔTWV is calculated as sum of the contributions of the profiles, reasonably leading to a balancing of the under/overestimations. Thus, the distributions of ΔTWV showed narrower confidence intervals. In both case study sites, the discharges were generally underestimated when using STSS (Figure 4.9a and b; Figure 4.10a and b) with the exception of the combination ES-A, at the Italian case study, which only contains one storm. In particular, ΔWV and ΔTWV showed a better agreement (lower absolute values) between STSS and RS, as H_s increases. Thus, STSS gave good discharge predictions for events with high H_s. This is clear looking at TD results and seems to be confirmed in ES, with the case ES-F containing only one storm.

The inundation fitness factor F results (Figure 4.9d and Figure 4.10d) showed a similar trend: better inundation results are obtained for storms with higher H_s, at both study sites. At TD, medium and higher durations (TD-A and TD-B) showed a significantly higher variability than lower durations (TD-C) for low peak H_s storms (Figure 4.9d). In general, low H_s storms with any duration gave bad inundation results (median of $F < 0.3$) when modelled with a STSS. Extreme storms with H_s higher than 4.4 meters in propagated conditions gave the best F parameter (TD-G, TD-H and TD-I with median of $F > 0.6$; Figure 4.9d). Differently, at ES combinations with low waves (ES-A, ES-B, ES-C and ES-D in Figure 4.10d), showed a decrease in fitness by increasing the TWL. On the contrary, for medium wave events (ES-E and ES-F in Figure 4.10d), the increase in TWL led to an increase in F.

Regarding the simulated representative retreat (R) at TD, ΔR distributions are well centred and contained within the 25% in almost all cases in Figure 4.9. This means that all storm characteristics produce an equal amount of over- and underestimation of the erosion, with most of |ΔR| within the 10% and not exceeding the 25 %. The exceptional case is TD-D where a significant overestimation of erosion is observed. On the other hand, at ES (Figure 10c) general underestimation ($\Delta R < 0$) for all combinations can be observed. However, the underestimation is contained (median of $\Delta R > -0.25$) for the majority of the combinations. An exception is represented by the combination with high TWL and low H_s (TWL>1.1m and H_s<0.25m; ES-C in Figure 4.10c) which showed the worst behaviour on retreat simulation ($\Delta R<-0.25$).

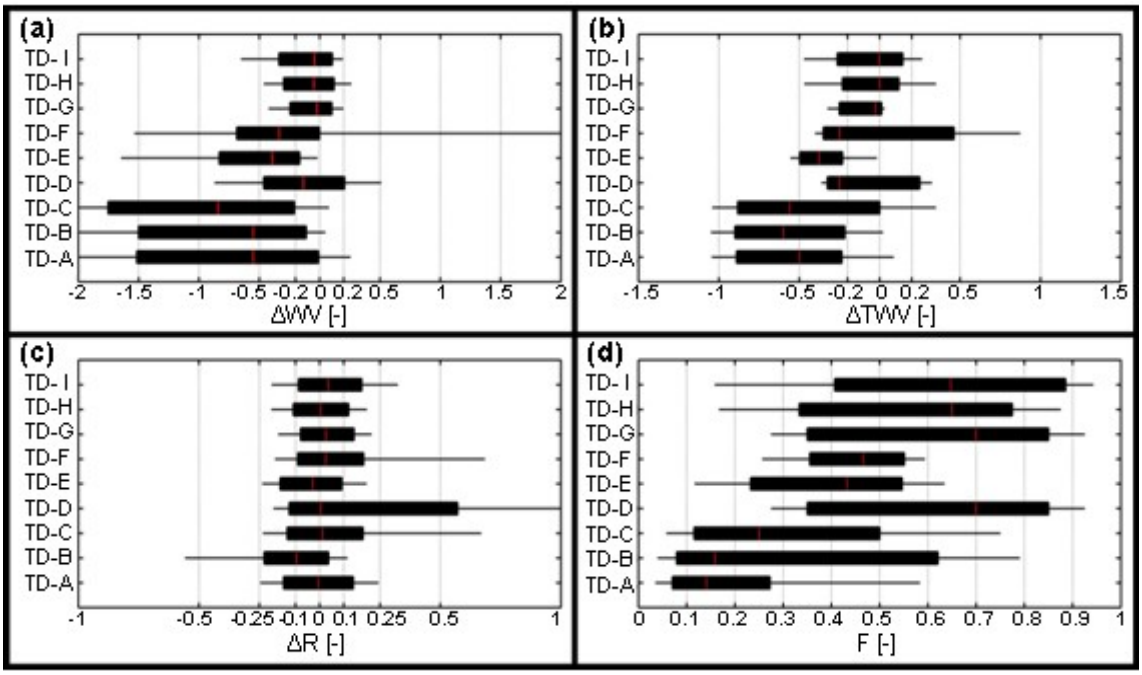

Figure 4.9 The comparative results in profile water volume (ΔWV), total water volume (ΔTWV), relative difference in representative retreat (ΔR) and inundation fitness factor (F) for the forcing combinations at the Tordera Delta case study.

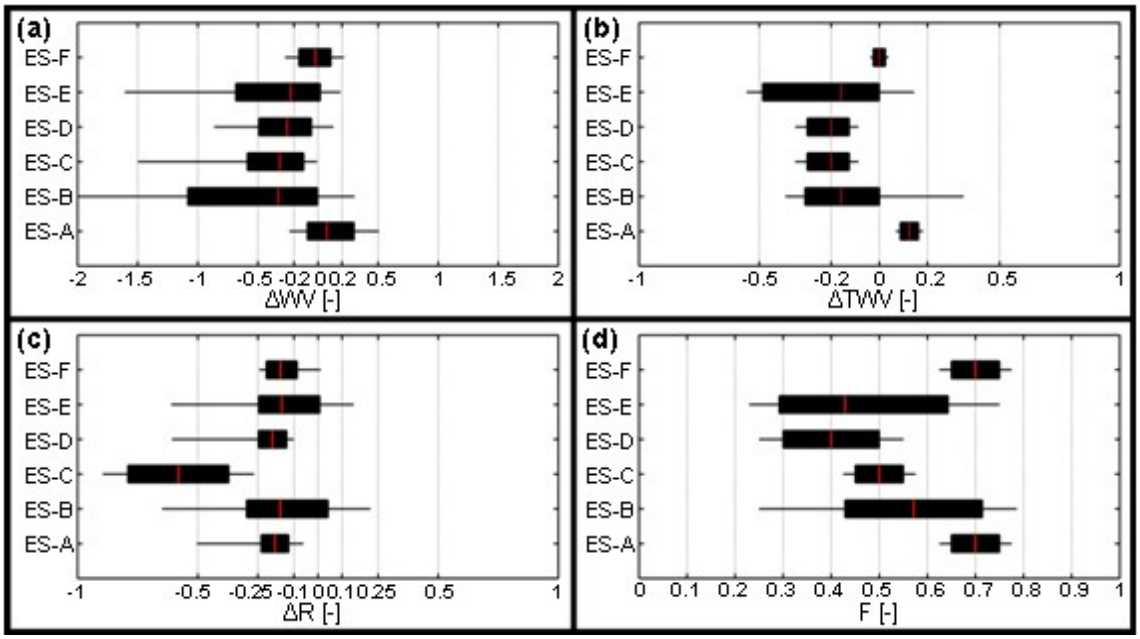

Figure 4.10 The comparative results in profile water volume (ΔWV), total water volume (ΔTWV), relative difference in representative retreat (ΔR) and inundation fitness factor (F) for the forcing combinations at the Lido degli Estensi-Spina case study.

To better understand the role of the storm shape comparative parameters (ER, PD and PPR) on errors on predicted discharges, the variables are plotted against ΔTWV (Figure 4.11a, b and c; Figure 4.12a, b and c). The role of ΔR is also included in the assessment (Figure 4.11d and Figure 4.12d). The analysis of the storm shape variables highlights the peak persistency (PP) as the most important factor controlling good predictions of the TWV. Indeed, the PPR variable has the closest median to the unity (best of fitness) and with less associated variability for the case ΔTWV = -0.05 ÷ 0.05 (Figure 4.11c and Figure 4.12c), in comparison to the other categories shown in the graphs. Therefore, a good reproduction of the PP of the RS is necessary, to properly reproduce TWV at both TD and ES. It must be noted that in ES only one storm has ΔTWV = -0.05 ÷ 0.05.

It is observed that good representations of PPR, can lead to good results even with overestimation of ER and postponed (at TD) or anticipated (at ES) storm peaks (Figure 4.11a and b; Figure 4.12a and b). However, the opposite is not observed, and good representations of energy and peak position can lead to bad results when the PPR variable is not well reproduced. Neither capturing the energy content (ER~1), nor correctly getting the position in time of the storm peak (PD ~0 hrs) showed a clear significant correlation with good predictions of TWV (Figure 4.11a and b; Figure 4.12a and b). Nevertheless, good PPR is not sufficient and the other two variables play a secondary role in combination with PPR.

At TD some correlation was observed between ER and ΔTWV (Figure 4.11a) and between ΔR and ΔTWV. This suggests that ER and ΔR might be correlated as well, which is in agreement with the fact that energy content and erosion are strictly related. In addition, large overestimations in TWV (ΔTWV > 0.2) were linked to significant overestimations of R (Figure 4.11d) and large delay of the storm peak (>50% of the PD distribution between 3 and 48 hrs; Figure 4.11b).

Overall, results at ES (Figure 4.12), led to a more difficult interpretation and identification of trends due to the scarce data. However, they confirmed the importance of the PPR variable with respect to the other two. They also confirmed the observed relation between ΔR and ΔTWV.

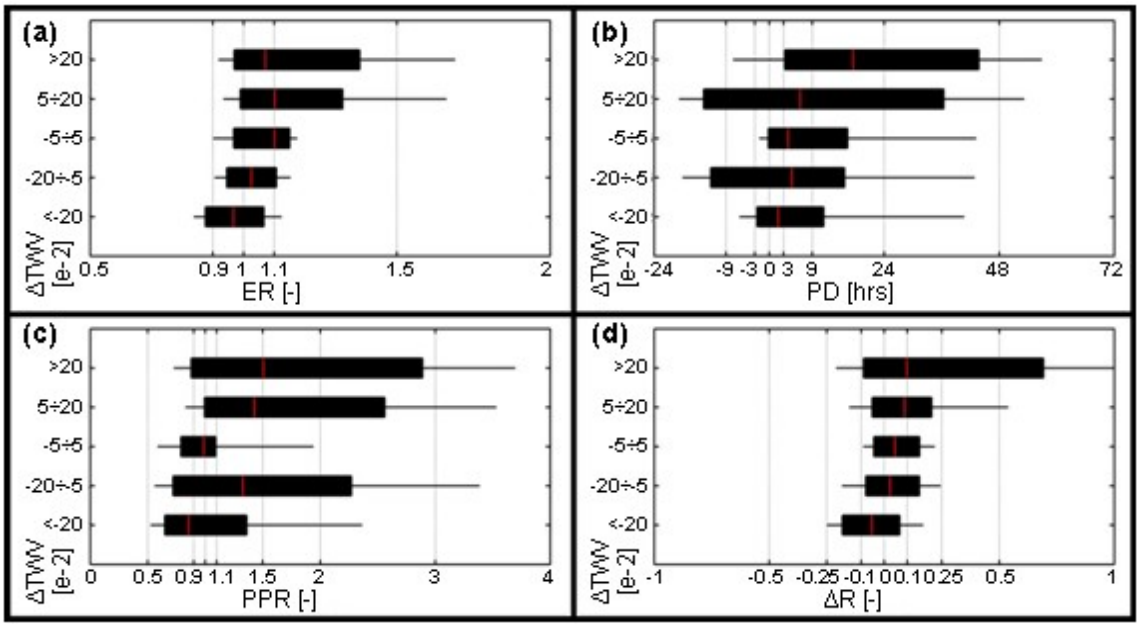

Figure 4.11 Relations between comparisons in total water volume (ΔTWV), energy ratio (ER), peak delay (PD), peak persistency ratio (PPR) and relative difference in representative retreat (ΔR) at the Tordera Delta case study.

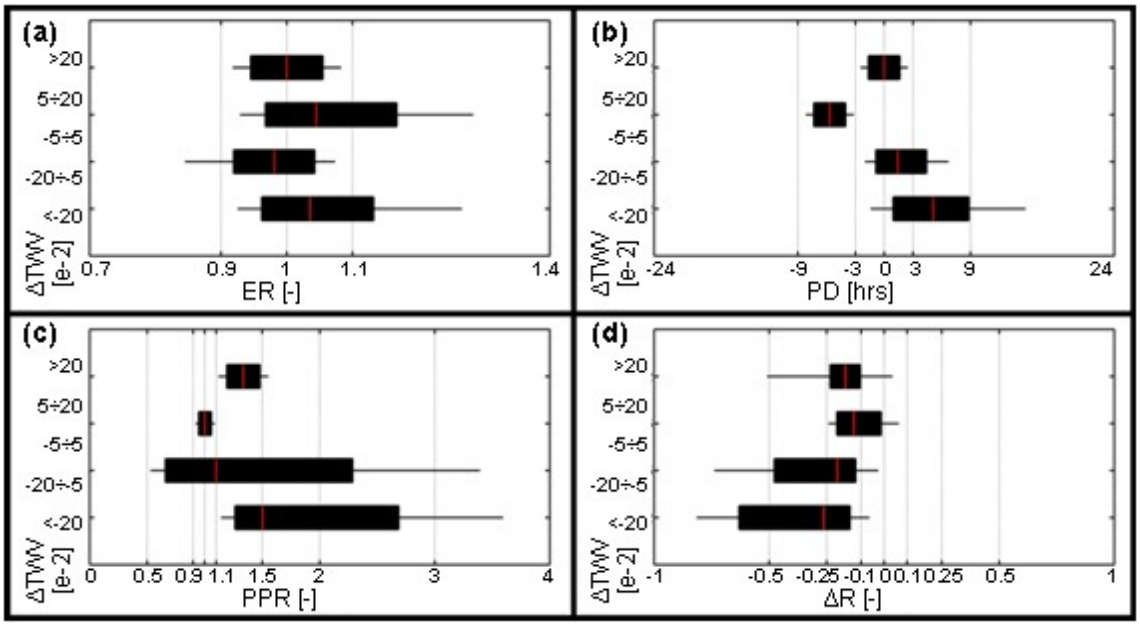

Figure 4.12 Relations between comparisons in total water volume (ΔTWV), energy ratio (ER), peak delay (PD), peak persistency ratio (PPR) and relative difference in representative retreat (ΔR) at the Lido degli Estensi-Spina case study.

4.5 Discussion

This study focused on comparing computed hazard results (erosion and flooding) of Real Storm (RS) and Symmetric Triangular Synthetic Storm (STSS). Simplifications and numerical assumptions were homogeneously applied to both RS and STSS implementations. Two study sites, pre-identified as hotspots and sensitive to erosion and inundation from coastal storms (Armaroli and Duo, 2017; Jiménez et al., 2017c), were chosen to apply the analysis. Data availability posed methodological limitations in terms of number of storms analyzed at the case study sites. In particular, while for TD the number of analyzed storms was 43, at ES it was 11. It follows that, considering the possible combinations of forcing characteristics at each case study, at TD, the analyzed storms were able to cover most of them (and thus statistics are more robust) while, at ES, the storms were only sufficient to complement the TD results in terms of common and complementary trends.

The presented scatter plots (Section 4.4.2) highlighted that the output variables at TD showed larger ranges (and thus, variability) in comparison to ES. Storm energy is slightly overestimated at both study sites. At TD this overestimation was significant in some particular events that can be linked to multi-peak storms, whereas the overestimation at ES was little and storm energy was considered to be well-captured by the STSS (Figure 4.6). Peak persistency presented a larger scatter (Figure 4.7), and significant overestimation for high energetic events at TD. This can be associated with the bad total water volume and inundation fitness results obtained generally with the STSS since PPR has been highlighted as a key variable in order to obtain good results. In addition, differences in profile water volume, total water volume and inundation surface were observed to be greater in TD than in ES (Figure 4.7 and Figure 4.8). This can be associated to a combination of factors: storms in TD are more energetic and at the same time energy estimates with STSS are generally worse at TD; TD is predominantly reflective, responds faster, and therefore is more sensitive to differences in energy and peak energy; and finally the topography of the hinterland plays an

important role when spreading the inundation. In TD the southern domain from the river is a low-lying large floodplain protected by a relatively short beach (less than 50 meters). This means that small differences in TWV are enough to cause large differences in inundation and thus low fitness factor values.

Notably, the result analyses showed consistent assessments at the case studies. It has been shown, at both study sites, that inundation impacts (i.e. discharges and flooded areas) of storms with high H_s values at the peak tended to be better reproduced with STSS, although with still high uncertainties, meaning that, even in that case, large errors can be observed. In addition, the peak persistency, proxy of the energy content at the peak, has been highlighted as one of the key storm shape comparative variable in relation with good discharge predictions.

At TD, STSS with best PPR scores were mainly observed for storms with high H_s at peak and medium (12 to 21 hrs) durations. Worst PPR score were obtained for storms with low H_s at the peak (Figure 4.13a). At ES, excluding ES-A and ES-F which only contain one storm event, it was also observed that high H_s values at the peak in combination with moderate durations led to good PPR reproductions.(Figure 4.14a and b). On the other hand, ER and PD were observed to have less influence than PPR. However, there is some relation between those and ΔTWV. A linear-like trend was observed at TD between ER and ΔTWV, and similarly between ΔR and ΔTWV. This is due to the correlation between energy and erosion which was confirmed in Figure 4.15. In addition, Figure 4.13 showed how an increase in variability in ER (case TD-D) along with a high variability in PPR led to an increase in variability in ΔTVW, F and ΔR (Figure 4.11). Regarding PD, it was observed that all ΔTWV results between -0.05 and 0.05 were frequently obtained for STSS with positive PD values, but close to zero and with low variability. This means that obtaining values of PD close to zero helps to have better results, but does not guarantee them and/or is not always necessary when other variables are well reproduced.

Focusing on morphological impact assessments, the results of this study can be also compared with previous studies on synthetic storm representations, bearing in mind the remarkable differences between the approaches. Sánchez-Arcilla et al. (2009) compared the computed erosive impacts of real storms and their schematic evolution. The schematization was applied by simplifying the H_s and T_p time-series with polylines. Thus, the representation was able to follow the main evolution of the storm by linearly interpolating the local minimums and maximums of the time-series. This led to an average overestimation of the energy content of 15% (with a maximum of 60%). On the other hand, the way the synthetic storms were built ensured that storm peaks (absolute and local ones) were well captured. The study highlighted an overestimation of eroded volumes and shoreline erosion, possibly due to the overestimation of the energy content. The present study showed a different tendency at ES. The synthetic-derived representative retreat, indeed, was generally lower than the real-derived one, despite the fact that the energy of the real storms was well captured (see Figure 4.6a and Figure 4.11a). On the other hand, this result is in line with erosion impact underestimation highlighted by Callaghan et al. (2009), which, however, focused on a different type of storm representation (i.e. Synthetic Design Storms; Carley and Cox, 2003) in comparison with statistics of measured beach erosion. This is assumed to be caused by the interaction of waves with surge, and indeed, at ES, extreme values of TWL, combined with low waves, were found to increase the magnitude of the retreat underestimation using synthetic storms. At TD, the tendency showed a fairly good reproduction of the shoreline retreat, with limited errors ($|\Delta R|<0.25$). Additionally, in agreement with Sánchez-Arcilla et al. (2009), overestimation of the energy content was linked with overestimation of the erosive impacts at TD (Figure 4.15b). Notably, at this

case study, the overestimation of the retreat was linked with an overestimation of TWV (see Section 4.4.3) and, therefore, a strong relation between ΔR and PPR was also observed (Figure 4.15a).

In the current work STSSs were applied only on waves time-series. A step forward for this study would require a comprehensive analysis of the propagation of the uncertainty while adopting synthetic surge time-series.

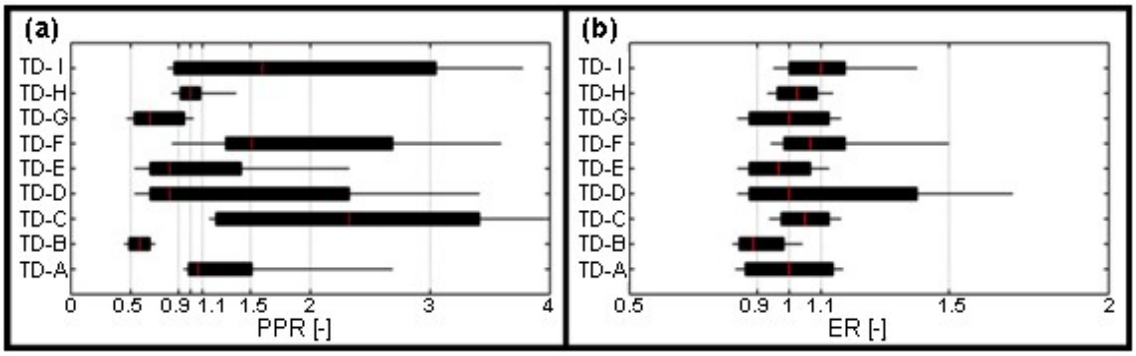

Figure 4.13 Results of peak persistency ratio (PPR) and peak delay (PD) for the forcing combinations at the Tordera Delta case study.

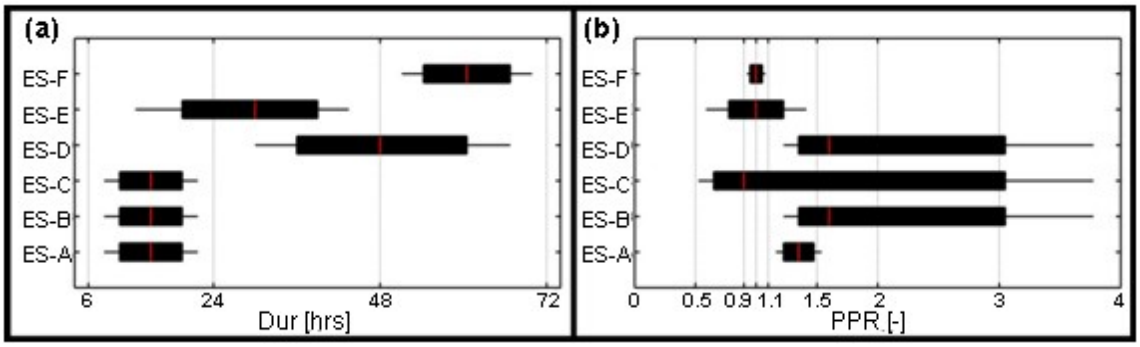

Figure 4.14 Results of duration (Dur) and peak persistency ratio (PPR) for the forcing combinations at the Lido degli Estensi and Spina case study.

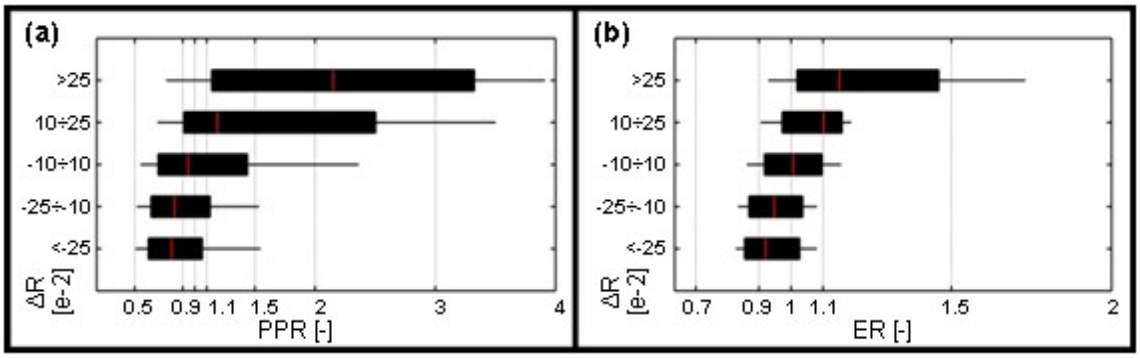

Figure 4.15 Relations between (a) peak persistency ratio (PPR) and relative difference in representative retreat (ΔR) and (b) energy ratio (ER) and relative difference in representative retreat (ΔR) at the Tordera Delta case study.

4.6 Conclusions

This study represents a first step in the attempt to fill a gap of knowledge on the uncertainty related to the use of synthetic forcing time-series for integrated coastal multi-hazard (i.e. flooding and erosion) assessments. The investigation was implemented by simulating real storms, and their synthetic reproduction through symmetric triangular shaped time-series of waves, with a chain of models (i.e. XBeach and LISFLOOD-FP). Comparative variables were used to assess the differences between the real- and synthetic-derived flooding and erosion hazards (i.e. discharges, inundated areas and shoreline retreat). A Bayesian Network was used to link forcing input and comparative variables in order to analyse the overall behaviour of the dataset. The approach was applied at two case study sites: Lido degli Estensi and Spina (Comacchio, Italy) on the Emilia-Romagna coast (Northern Adriatic) and Tordera Delta (Blanes-Maresme, Spain) on the Catalan coast (North-Western Mediterranean).

The work evidenced that representing real storms through triangular symmetric synthetic ones led to generally poor results when modelling inundation. Reasonable results can be achieved as example for high Hs storms with moderate durations (12 to 40 hr) which showed better predictions. However uncertainties were high in all cases. Moreover, errors due to the use of synthetic events can be large, leading to wrong inundation maps or significant noise when used in combination with other data for integrated assessments. Larger errors were observed for low to medium Hs storms. Erosion predictions were observed to be more accurate with relative errors limited to 25%. However when large surges were simulated in a dissipative environment (Lido degli Estensi-Spina case study), general underestimation of retreats was observed.

Peak persistency of the storm (duration over the 90% of the Hs at the peak) was detected as key variable for better synthetic storm performance. Therefore, synthetic storm designs should focus on accurately predicting that variable and secondly on total storm energy and peak timing (or alternatively, having a similar effect, the storm growth and decay rates).

Future works should include the effect of designing synthetic surge time-series along with the wave ones, while adopting larger amount of data. Future steps of this study, should aim at providing guidelines for storm shape design for given coast and sea conditions. The synthetic storms should minimize errors and uncertainty, while the current common practices were proved to produce large uncertainty when compared with the application of real forcing.

5 VALIDATION OF THE COASTAL STORM RISK ASSESSMENT FRAMEWORK ALONG THE EMILIA-ROMAGNA COAST

5.1 Introduction

The Italian peninsula has almost 8 000 km of coastlines, of which more than 60% are low shores. The 34% of the Italian territory located in a corridor of 300 m from the shoreline is urbanised, with higher percentages in the regions facing the Adriatic sea (ISPRA, 2013). The effect of marine processes on the coastal area has therefore a great importance, as erosion and inundation hazards are increasingly threatening large portions of the coastline, human structures and the population. In fact, coastal inundation caused by storm events represents a major issue, especially in low-lying areas such as alluvial plains.

National and regional governments urge a comprehensive evaluation of coastal risk, to better manage coastal areas in terms of allocation of funds for coastal protection and definition of effective land-use plans (Viavattene et al., 2017, and references therein).

The Emilia-Romagna coastline (Figure 5.1) is particularly exposed to erosion and inundation hazards (Armaroli et al., 2012; Perini et al., 2016) because of its low-lying nature and high coastal urbanization. Consequently, there is an increasing demand for effective methodologies to properly evaluate coastal risk, which in the RISC-KIT project was defined as the probability of a hazard and its impacts (consequences) (Viavattene et al., 2015).

The RISC-KIT project (Van Dongeren et al., 2017) provided a tool for coastal hotspot assessment and selection at the regional level: the Coastal Risk Assessment Framework (CRAF) (Viavattene et al., 2017). The Phase 1 of the tool provides a conceptual framework to implement a screening process able to identify areas that can be classified as hotspots, through the integration of hazard and socio-economic components. Then, the Phase 2 of the CRAF is applied to rank the identified hotspots to select the most critical ones. The CRAF method is described in the paper by Viavattene et al. (2017), together with a comprehensive review of different methodologies adopted to evaluate coastal risk and the main differences between the CRAF and previous methods.

In this work the outcomes of the application of the CRAF Phase 1 along the Emilia-Romagna coast are presented. The results were validated with historical data provided by the end-users involved in the project. Regional managers, land-use planners and decision-makers were indeed involved in all the phases of CRAF Phase 1 implementation, because of their awareness and knowledge of coastal characteristics and issues that are important and valuable. Furthermore, they made a lot of data available for the analysis and followed the key steps of the assessment, providing suggestions and comments. Finally it is important to point out that, although CRAF phase 1 was applied at the regional level, the application of CRAF phase 2 and other tools implemented in the RISC-KIT project was carried out in the area of Porto Garibaldi - Bellocchio (Ferrara province, Figure 5.1), that was selected as the case study site (CSS hereafter) along the Emilia-Romagna coastline.

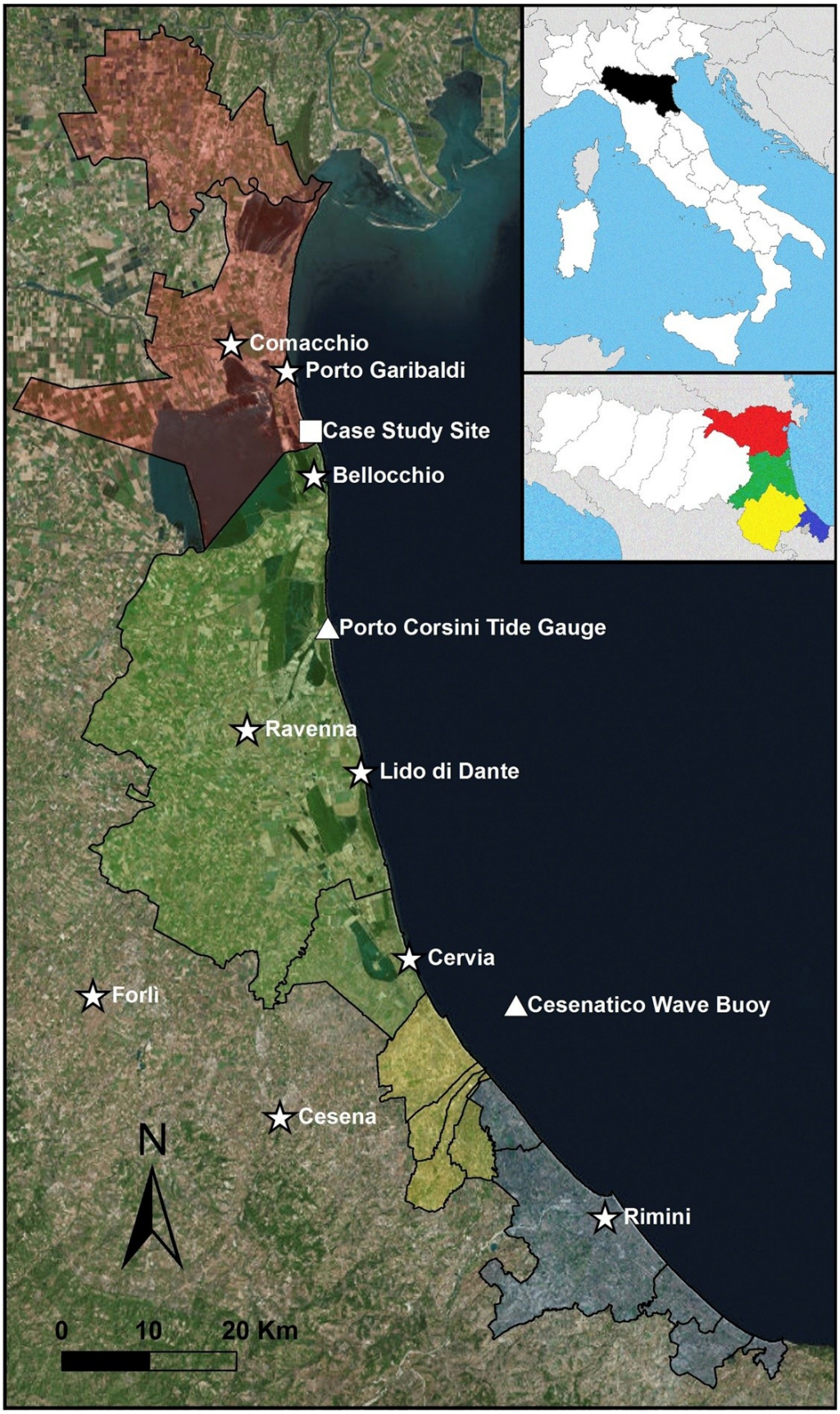

Figure 5.1 The coast of the Emilia-Romagna Region: coastal municipalities belonging to the provinces of Ferrara (red), Ravenna (green), Forlì-Cesena (yellow) and Rimini (blue) and the location of localities presented in the text is highlighted.

5.2 Study area

The coast of the Emilia-Romagna Region (RER hereafter) is located in northern Italy, facing the Adriatic Sea (Figure 5.1). It is composed of almost 130 km-long sandy beaches characterized by mild slopes and a dissipative nature (Perini et al., 2010b). The northern part of the coastline comprises the Ferrara and Ravenna provinces. The coastal corridor, defined as a strip of ~2 km cross-shore width, is composed of wide and low-lying coastal plains, generally below MSL (minimum values of -2/-3 m; Perini et al., 2010a; Figure 5.1). Furthermore it includes the last dune fields of the region that occupy almost 40% of this sector. The southern part includes the Forlì-Cesena and Rimini provinces (Figure 5.1). The coastal corridor is characterized by 2–3 m elevations above MSL and the dunes have disappeared because of tourist pressure in the last 50 years (Sytnik and Stecchi, 2015). Over 60% of the coastline is protected by hard defence structures such as groins, breakwaters, submerged barriers, artificial embankments, dikes and rubble mound slopes.

The human pressure is significant (Lorito et al., 2010). The territory facing the sea is occupied by coastal villages and towns that, in the southern provinces, represent a continuous urbanization. The natural subsidence of the coastal area (composed of alluvial sediments) is dramatically increased up to 2 cm/year (Ravenna area, Figure 5.1) by groundwater extraction for agriculture, human consumption, especially in the summer season, and gas extraction (Teatini et al., 2005; Taramelli et al., 2015). The marine flooding hazard significantly augmented over the last century due to the massive urbanization and exploitation of the coast for tourism. Besides, beach erosion is worsened by the negligible sediment supply from rivers (Ciavola et al., 2005), due to a strong human control and exploitation of water courses (Preciso et al., 2012) and the reforestation of the Apennines (Billi and Rinaldi, 1997).

The area is micro-tidal with a range between 80-90 cm (spring tides) and 30–40 cm (neap tides). The wave climate is of low Energy (60% of H_s below 1.0 m; IDROSER, 1996; Ciavola et al., 2007). Storm directions are from E–NE (Bora wind) and SE (Scirocco wind). Surge levels are an important element controlling total water levels measured during storms (Masina and Ciavola, 2011). The highest surge levels are generated by south-easterly winds that favour water piling in the northern Adriatic Sea, when combined with low barometric pressures caused by low-pressure weather systems. Masina and Ciavola (2011) found that the 1-in-10-year return period surge is 0.79 m and thus it can almost double the tidal range. High surge levels can cause extensive erosion and inundation when associated with storm waves (Armaroli et al., 2012). Storms can be energetic with the maximum-recorded wave height of 4.66 m, measured during the 5–6 February 2015 storm, one of the most intense ever observed on the local wave buoy of Cesenatico (Figure 5.1). Armaroli et al. (2012) identified critical storm thresholds for damages along the coast on the basis of historical data: 1) $H_s \geq 2$ m and WL (surge + tide) ≥ 0.7 m for urbanised zones; 2) $H_s \geq 3.3$ and WL (surge + tide) ≥ 0.8 m for natural areas with dunes. The most important business sector is represented by summer activities. Tourism is of the “sun-and-beach” type and the main economic asset is related to concessions. Concessions are private properties located on public beach areas that are granted to privates for commercial/tourism activities. Concessions are composed of permanent one-floor (i.e. the ground floor) buildings and other additional areas. Tourists can take advantage of a large number of services provided by concessionaires (e.g. showers, changing rooms, toilets, access paths to the sea, bar, restaurant, playgrounds and babysitting, volley/basket/mini soccer fields, gym, etc). Furthermore, concessionaires rent sun-chairs/beds and umbrellas to holidaymakers. Beaches in the summer season are occupied by a large number of sun-umbrellas, that

are placed from the concession to the shoreline, to form a cross-shore and alongshore continuum. Concessions are present along almost 76% of the coastline.

5.3 End-users know-how and expertise

The regional authorities have been collecting information on the coastline since the half of the last century. The first Coastal Regional Plan dates back to the early 1980s (IDROSER, 1981) and includes physical information of the coastal area (evolution, sediment characteristics, topo-bathymetric data, type and location of coastal defences and their effectiveness, subsidence rates, etc) together with data on wave and wind climate, tide and surge analysis, a list and description of management practices and, finally, the relevant issues in terms of coastal protection. The most important hazards, such as coastal flooding and erosion, are also highlighted. The plan was compiled to list the interventions carried out along the coast, to propose new solutions and to provide a reference database for coastal managers and decision makers. Another Coastal Regional Plan was issued in 1996 (IDROSER, 1996). Several other reports describing the state of the coastline (main problems, interventions, etc) were issued since then.

The amount of data and information collected over the last 60 years is very large and is available also online (http://ambiente.regione.emilia-romagna.it/geologia/temi/costa), since the early 2000s, through a web-based platform (Coastal Information System, SIC). The regional Servizio Geologico Sismico e dei Suoli (SGSS hereafter) is responsible for data collection, validation, elaboration and online publication, and analyses remote sensing data (aerial photographs, Lidar, etc), as well as any other source of information, from desktop research to direct surveys and digitalization of archived records. Data collected are presented through a web-GIS tool, therefore it is possible to access a large number of geospatial datasets, e.g. land use information (derived from photo-interpretation), medium-term shoreline variability, land subsidence rates, location of offshore sand deposits and a collection of storm events that caused damages along the coast, among many others. Data collection and validation is continuously carried out in order to update the web-GIS platform. Furthermore, data related to storms and their impacts are compiled in cooperation with the Civil Protection and local authorities to create a comprehensive database that includes detailed information on impacts, costs, extension of inundation, degree of erosion and type of emergency interventions performed during the event and in the aftermath. The first step towards the current practice of collecting detailed data on storm events is represented by the work carried out in the MICORE project (Ciavola et al., 2011b; www.micore.eu) that led to the publication of a regional storm catalogue which includes the most significant and damaging events from 1946 to 2010 (Perini et al., 2011).

For what concerns coastal hazards, the RER runs an operational Early Warning System (EWS), also based on the critical storm thresholds defined above, that is used by the Civil Protection to evaluate wave and water level forecasts and their morphological impact along representative profiles located along the whole coastline. The EWS was developed in the framework of the MICORE project. More details can be found in Harley et al. (2016).

5.4 Methodology

The methodology adopted to apply CRAF Phase 1 is presented hereafter. The method to compute the extension and magnitude of the hazard component will be briefly described. The implementation of the exposure indicators will be described shortly. However, the key steps and definitions will be presented.

The CRAF Phase 1 methodology is based on the calculation of a Coastal Index (CI) along a regional coastline (~100 km) that is divided into sectors of almost 1 km alongshore length. The CI is computed for every 1 km coastal sector. The CI is a number ranging from 0 to 5 that allows the comparison between sectors to identify which sector(s) is (are) a hotspot(s). The CI is computed as Equation 5.1:

$$CI = \left(i_{hazard} \cdot i_{exposure}\right)^{1/2} \qquad (5.1)$$

where i_{hazard} is the hazard indicator and $i_{exposure}$ is the exposure index.

The first step for the computation of the CI is the hazard definition and the evaluation of its intensity. Then, the hazard indicator is represented by a number from 0 (no-hazard) to 5 (very high hazard) built through the scoring from 0 to 5 (none, very low, low, medium, high, and very high) of the hazard magnitude in each sector. If flooding and erosion are selected as main hazards, the hazard evaluation includes also the computation of the landward extension of the inundation (e.g. identification of flood-prone areas) and the shoreline retreat magnitude. Each hazard has to be considered separately.

The exposure index ranges from 1 to 5 and it is computed as Equation 5.2:

$$i_{exposure} = \sqrt[n]{i_{exp\,1} \cdot i_{exp\,2} \cdot \ldots \cdot i_{expn}} \qquad (5.2)$$

where n is the number of considered exposure indicators (i_{exp}). The exposure indicators are: utilities, transport networks, land use, business setting and the social status of the population. In general terms, the method consists in assigning to each sector a 1-to-5 score (non-existent or very low, low, medium, high, very high exposure) based on both location and importance/relevance of the indicator (the scoring has to be carried out separately for each indicator), and following ad-hoc scales implemented by the CRAF user, or already available methods or more general scales, like those proposed by Viavattene et al. (2017). For the RER coast, the proposed general scales were partly modified to consider already available datasets and methodologies, as explained in the following sections.

5.4.1 Hazards and sectors definition

The CRAF Phase 1 implementation is based on the event approach (Ferreira et al., 2017; Viavattene et al., 2017). Two main hazards are considered: inundation and erosion. The inundation hazard was taken into account on the basis of the data already available at the regional level, produced for the Floods Directive (2007/60/EC) by SGSS, and on the method described in the paper by Perini et al. (2016) that will be presented hereafter. The methodology followed to analyse the erosion hazard is along the lines of the general methods described in (Viavattene et al., 2017) and will be briefly described in the next paragraphs.

Both hazards were evaluated using two extreme events, defined according to Table 5.1 and based on the methodology adopted by regional managers (Perini et al., 2016). The total water level (TWL, Table 5.1) was computed as the sum of different variables extracted from the literature: surge levels (Masina and Ciavola, 2011), wave set up elevations (Decouttere et al., 1998) and the astronomical mean high spring tidal level (IDROSER, 1996). The methodology adopted by SGSS for the computation of TWLs does not include run-up levels and the effect of land subsidence. These elements were not considered in the analysis because the regional authorities wanted to implement a simple and quickly replicable methodology (Sekovski et al., 2015; Perini et al., 2016). Wave characteristics associated to each return period are listed in Table 5.1 and, again,

were extracted from the literature (IDROSER, 1996; Armaroli et al., 2012). The durations were selected by similarity with the most significant historical events that affected the regional coastline between 1946 and 2010, analysed in the MICORE EU Project (www.micore.eu; Perini et al., 2011).

Notably, each component (wave setup, surge and tide) taken into account to compute TWLs was statistically analysed and calculated in an independent way. Therefore, the extreme events are not the result of a combined probability analysis. Thus, they are most probably representative of less frequent events. For simplicity's sake, they are referred to as T10 and T100 hereafter.

To implement CRAF Phase 1, the RER coast was subdivided into 106 sectors almost 1 km long, according to: (i) type of coast (natural, urbanised not protected, urbanised and protected); (ii) type of protections (rubble mound slopes, groins/jetties, emerged or semi- submerged breakwaters); (iii) presence of river outlets, navigation channels, marinas and ports. Ninety-four profiles were extracted from a 2012 topo-bathymetric DTM with 5 x 5 m resolution provided by ENI (the national oil company). The number of profiles is less than the selected sectors, because a few areas have uniform characteristics alongshore (type of protection, beach characteristics, etc). Therefore, one profile was chosen to represent larger portions of the coast and the hazard indicators computed along the chosen segment were associated to more than one sector. Notably, the maximum distance between profiles is less than 2 km. Each profile is representative of the average beach morphology (slope, height, etc) of every sector it belongs to. An example of representative coastal profiles for natural and protected beaches is shown in Figure 5.2.

Table 5.1 Definition of the extreme events.

ID	Event	RP [years]	Storm Surge [m]	Tide Level [m]	Wave Setup [m]	TWL [m]	H_s [m]	T_p [s]	Duration [hrs]
T10	Freq.	10	0.79	0.4	0.3	1.49	4.7	8.9	42
T100	Low Freq.	100	1.02	0.4	0.39	1.81	5.9	9.9	55

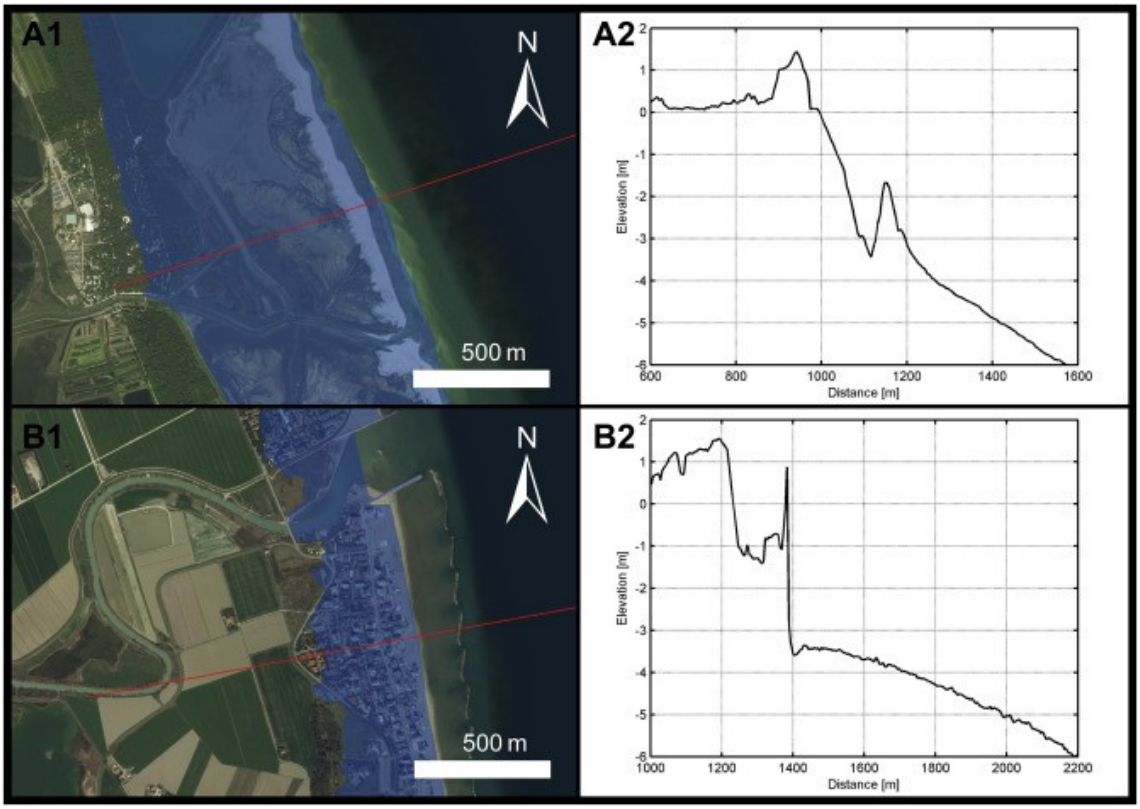

Figure 5.2 Example of two areas and corresponding beach profiles representative of natural (Bellocchio, Ferrara; A1-A2) and protected/urbanised sectors (Lido di Classe-Savio, Ravenna; B1-B2). The flood-prone areas computed by the regional authorities for the Floods Directive are also shown in blue in the left panels (T100 event) along with the tracks of the representative profiles.

5.4.2 Hazard indicators and extension

The hazard indicator (D) for flooding was built as the difference between the total water level (TWL; Table 5.1) and the elevation of the rear part of the beach (e.g. the dune crest, where present, backshore, alongshore walking paths, etc) extracted from the cross-shore profiles described in the previous section. Negative values of D showed that the backshore was higher than the TWL (representing the inundation of the beach only), therefore negative records defined a "low hazard" condition. Positive values of D, on the contrary, identified where the computed water level was higher than the rear part of the beach, thus where the coast is more exposed to flooding.

The obtained values were ranked and the corresponding scores are listed in Table 5.2. The values were classified considering both events (T10 and T100). The highest score (i.e. 5) was assigned to values above -0.10 m to take into account the vertical resolution of the DTM. The values between the minimum and -0.10 m were classified through the standard deviation of the values' distribution.

According to the methodology adopted by the regional authorities, beach inundation (i.e. negative values of the hazard indicator) is an important issue, as the beach is, along most of the coast (76 km out of 100 km analysed for the CRAF phase 1), occupied by permanent concessions. Therefore, if the analysis showed that only the beach was inundated, it meant that the concessions (e.g. beach huts, bars, etc.) were likely to be damaged, which means that the analysed extreme events were able to always generate

hazardous conditions ranging from very low to very high. Hence, there were no profiles with null hazard values.

The hazard extension, represented by the polygons that map the extension of flood-prone areas, was defined taking into account the maps produced for the Floods Directive by SGSS (Perini et al., 2016). The polygons were the result of an algorithm built through the model builder of ArcGIS. The model was based on the Cost Distance tool that was able to calculate the least path between a source (the 2010 shoreline) and landward areas. The tool calculated the distances between the shoreline and each grid cell of the DTM and assigned to each cell the lower value (i.e. least path) between all the distance values computed. The least paths were computed using the 2008 Lidar DTM (National Remote Sensing Programme) with 2 x 2 m horizontal resolution and 0.2 m of vertical precision. The method allowed the exclusion of isolated areas (i.e. areas bordered by elements with elevations above the considered TWL) and the identification of preferential paths (i.e. passages) through which the water can inundate landward areas. The tool was calibrated and the maps were validated considering historical information on past and more recent flooding events for which the inundation extension was available. More details can be found in the paper by Perini et al. (2016). The polygons provided by SGSS (Perini et al., 2016; grid 5 in their Figure 2) were used to define the domain of each sector where the exposure indicators were evaluated. The flooding hazard was calculated using the total water levels listed in Table 5.1 that are the same used by SGSS for the Floods Directive (T10 and T100).

The hazard indicator related to beach erosion was calculated in agreement with Viavattene et al. (2017). The retreat (R) of the shoreline was computed through the structural erosion function Equation 5.3 (Mendoza and Jiménez, 2006) and Equation 5.4:

$$dV = C1 \cdot JA \cdot dt + C2 \quad (5.3)$$

$$R = dV/(b + d^*) \quad (5.4)$$

where C1 and C2 are calibration parameters of the erosion structural function, JA is the erosion potential predictor, dV is the potential eroded volume, dt is the event duration, b is the elevation of the berm and d^* is the representative depth at which the erosion is null (Jiménez et al., 2015).

The general procedure was:

- identification of the type of profile (natural, urban, protected, or not protected, by breakwaters or rubble mound attached slopes);
- identification of the morphological features along the profile (submerged and emerged slopes, shoreline, berm height, dune features, etc);
- calculation of the JA erosion potential (Equation 5.3) using proper wave conditions (i.e. taking into account the presence of coastal protections);
- calculation of the representative shoreline retreat (Equation 5.4).

The procedure was applied with the following assumptions and simplifications: (i) the mean sediment diameter (D50) was assumed constant (0.23 mm) for the whole coastal region, (ii) the d^* term was set equal to a water depth of 1, (iii) the linear coefficients (C1 and C2) of the structural function were set equal to 6.1 and 29.4, respectively and, (iv) for protected beaches (breakwaters), the attenuation effect of the structures was taken into account following the method described by Armaroli et al. (2009) which is based on Van der Meer and Daemen (1994).

The D50 was chosen on the basis of the information available in the literature (e.g. Armaroli et al., 2009) and considering a sediment analysis (unpublished) implemented in winter 2014–2015 in several areas along the Ferrara and Ravenna coasts. The D50 information, although only available for some tracts along the coast, was applied uniformly to the whole coastline for consistency's sake. The C1 and C2 values were chosen on the basis of the correlation function between the calculated JA·dt and the eroded volumes computed with a morpho-hydrodynamic model (XBeach 1D) for 20 (10 natural and 10 protected) representative profiles of the regional coast, forced with the probabilistic events listed in Table 5.1. The modelling was also used to assess d^*, through the qualitative analysis of the resulting post-storm profiles. Notably, the berm height along the coast varies from 0.8 to 1.2 m. In some coastal sectors the retreat was assumed 0 m because of the presence of attached rubble mounds slopes. Notably, the total water level was not taken into account.

The hazard indicator scores were assigned according to the shoreline retreat values obtained from the analysis of both events (0-57 m for T10; 0-68 m for T100). The scores were assigned following Table 5.2. Two assumptions were applied considering the obtained shoreline retreat values: (i) erosion values below 15 m were scored 1; (ii) erosion values above 30 m were scored 5. The values were classified dividing the interval between the selected minimum and maximum into 3 classes of 5 m each to take into account the beach occupation in the summer season, when sun-umbrellas and chairs are placed on the beach in parallel rows of 3-5 m cross-shore width. Finally, the 0 score was assigned to areas protected by attached structures (i.e. rubble mounds).

The hazard extension was defined by a 10 m buffer zone landward from the limit of the maximum shoreline retreat line, sector by sector. The 10 m buffer zone identified the area where the exposure indicators were calculated. It was chosen according to the methodology adopted to define the Storm Impact Indicators (SIIs) along the coast, implemented in the MICORE project (Ferreira et al., 2009; Ciavola et al., 2011b) and that are part of the regional EWS (Harley et al., 2016).

Table 5.2 Hazard indicators scoring for flooding and erosion.

Flooding		Erosion	
D Value [m]	**Score**	**R Value [m]**	**Score**
<−2.5	0	0	0
from −2.5 to −1.6	1	<15	1
from −1.6 to −1.1	2	from 15 to 19.9	2
from −1.1 to −0.6	3	from 20 to 24.9	3
from −0.6 to −0.1	4	from 25 to 29.9	4
> −0.1	5	>30	5

5.4.3 Exposure indicators

For what concerns utilities, the location of aqueducts, wastewater treatment plants, energy distribution/supply stations was mapped along the coastal area. The same mapping was carried out for the transport network, considering roads with different importance and the railway line. The exposure indicators for utilities and transports were then built following Table 5.3 considering their location and importance. For the erosion hazard, the exposure indicators of utilities and transport were scored 1 or 2, because no one or less important utilities and roads were located into the buffer zone.

Land use data were provided by SGSS and are represented by polygons derived from the photo-interpretation of 2008 aerial images mapped at 1:5,000 scale. This, compared to the Corine Land Cover dataset (Viavattene et al., 2017), ensured a more detailed definition of specific typologies of the regional domain (e.g. concessions). The values assigned to each land use typology were chosen according to the methodology adopted by SGSS to produce flood risk maps for the Floods Directive (Perini et al., 2016). Each type of land use was valued from 1 to 4 (i.e. 1 = low, 4 = high). The regional authorities decided to consider areas occupied by human-related activities (e.g. concessions, residential areas, industrial zones, etc) as highly valuable and natural sites (e.g. areas without human occupation, beach and dunes, marshes, etc) as less valuable, according to Chapter 3, article 6, of the Floods Directive (2007/60/CE). Therefore the valuation is human-centred. The scores of each sector were assigned considering the "area x value" results of each sector, where the area is represented by the areal extension of each flood-prone typology, in every sector, according to the flood maps provided by SGSS, multiplied by its value and then summed. The resulting values were divided into 5 classes through the natural breaks method of ArcGIS and considering both return periods. The same LU data were used to implement the exposure indicator for erosion, but only the typology "concession" was affected. The affected concessions were only a few. The obtained surface values were then scored as indicated in Table 5.4.

The business settings exposure indicator was built considering the percentage of tourist arrivals in each municipality with respect to the total number of arrivals along the coast, to take into account the sun-and-beach tourist asset. Data were derived from the database of ISTAT with information from 2014. Each sector was assigned the score built as it follows: 1 = natural areas/restricted areas (e.g. military zones); 2 to 4 = dividing the obtained percentages (from 10 to 30%) into equal intervals; 5 = to the national level business figure.

It is worth mentioning that the Social Vulnerability Index was represented by an index, calculated for the whole Italian territory at the municipality level, defined by the National Institute of Statistics (ISTAT; www.ottomilacensus.istat.it). The index is named "Indice di Vulnerabilità Materiale e Sociale", that can be translated into "Social and Economic Status Vulnerability Index (ISEV)". The ISEV takes into account indicators of the social and economic status of families similarly to the UK Social Vulnerability Index (Tapsell et al., 2002). The score assigned to each sector is based on the range of ISEV values at the national level. Because the RER coastal municipalities do not show large differences with respect to ISEV values, the same score was assigned to the totality of sectors (i.e. = 3).

Table 5.3 Type of utilities and transport networks in flood-prone areas and corresponding scores.

Type of utility network in flood prone areas	Score	Type of transport network in flood prone areas	Score
None	1	Absence of transport network or dirt/local road	1
Distribution substation (electricity and water)	2	Transport road network with local importance	2
Primary substation (electricity)	3	Transport road network with regional importance	3
Grid (electricity bulk supply point) or aqueduct (water)	4	Transport road network with national importance/motorway	4
Electricity super grid OR electricity bulk supply point + aqueduct OR Wastewater treatment plant	5	Transport train networks and/or train network + national importance road network	5

Table 5.4 Land Use characteristics and corresponding scores (erosion hazard).

Score	LU area [m^2] into buffer zone
1	0 (sectors with Ports/Marinas or protected by rubble mound attached slopes)
2	0 (sectors along natural areas with dunes)
3	0 (sectors along urbanised zones with concessions or concessions among dunes)
4	≤700
5	>700

5.5 Results

A sector was defined critical when its Coastal Index (CI) was higher than 2.5. It was decided to consider CI > 2.5 to take also into account end-users' comments to the obtained CIs maps. The end-users indeed stated that the identified critical sectors were consistent with well-known critical areas for both flooding and erosion, pointing out areas with CI close or above 2.5. A hotspot is defined hereafter as one or a set of adjacent sectors with CIs above the chosen threshold. The hotspots in the regional domain were evaluated with the End-users and then two of them were further studied in the CRAF Phase 2 in order to select the most critical site (Viavattene et al., 2017).

The results of the CRAF Phase 1 coastal screening process are summarized in Table 5.5 and Table 5.6, in terms of statistics and frequency distribution of the sectors' CI, respectively. The locations of the critical areas will be shown in Section 5.6 for validation purposes.

5.5.1 Flooding

With reference to Table 5.5, the CI for flooding ranged from 1.20 to 3.78 considering both events. The average amongst the sectors increased from 2.21, for T10, to 2.61, for T100. Standard deviations were 0.61 and 0.67 for T10 and T100, respectively.

Considering Table 5.6, no sector showed null values of CI. The percentage of critical areas (CI > 2.5) with respect to the totality of sectors was 25.5% for T10 and 62.2% for T100. Amongst them, the 1.9 and the 11.3% of the 106 sectors showed CI higher than 3.5, for T10 and T100 respectively.

The LU exposure indicator, along with the hazard one, resulted the main driving factor of the final CI values for most of the sectors, as the other exposure indicators resulted lower than 3. The analysis identified six hotspots macro-areas for T10 and five for T100. Specifically, the critical areas for T10 were (from north to south, Figure 5.1): 1) the southern portion of the Ferrara province; 2) the Ravenna province where the port of

Porto Corsini is located; 3) the Lido di Dante area (a recent study on the area can be found in Harley and Ciavola, 2013); 4) part of the Cervia municipality; 5) all the municipalities of the Forlì-Cesena province and 6) the area close to the navigation channel of Rimini. As expected, the extension of the critical areas largely increased for T100, because the critical sectors for T10 located in the central part of the coast (i.e. number 4 and 5 of the previous list) merged to create a continuous hotspot (see Figure 5.3) Overall, the central area resulted very critical and included almost 20 km of urbanised coastline The northern/southernmost parts of the coast were mostly scored around 2, therefore were excluded from the list of critical zones.

5.5.2 Erosion

With reference to Table 5.5, the CI for erosion ranged from 0 to 3.27, considering both events. The average amongst the sectors increased from 2.14 for T10 to 2.29 for T100. Standard deviations were 0.77 and 0.82 for T10 and T100, respectively.

Considering Table 5.6, the 10.4% of the 106 sectors showed null CI and were the sectors with attached rubble mounds. The percentage of critical areas (CI > 2.5) was 19.8% for T10 and 37.7% for T100. No sector's CI resulted higher than 3.5 for both events.

The LU exposure and the hazard indicators were the main driving factors of the final CI values for most of the sectors, also for the erosion hazard. The analysis showed that there are several hotspots for T10 that largely increased for T100.

Table 5.5 Statistics of the CI values for flooding and erosion hazards for the 106 sectors.

Coastal Index Statistics [-]	**Flooding**		**Erosion**	
	T10	**T100**	**T10**	**T100**
Min.	1.20	1.20	0.00	0.00
Max.	3.68	3.78	3.07	3.27
Mean	2.21	2.61	2.14	2.29
St. Dev.	0.61	0.67	0.77	0.82

Table 5.6 Distribution of the CI for flooding and erosion hazards for the 106 sectors.

Coastal Index Distribution [%]	Flooding		Erosion	
	T10	T100	T10	T100
CI = 0	0.0	0.0	10.4	10.4
0 < CI = 1.5	14.2	8.5	0.0	0.0
1.5 < CI = 2.5	60.4	29.2	69.8	51.9
2.5 < CI = 3.5	23.6	50.9	19.8	37.7
3.5 < CI = 4.5	1.9	11.3	0.0	0.0
4.5 < CI = 5	0.0	0.0	0.0	0.0
Total	100	100	100	100

5.6 Validation

The maps, for both hazards and both tested events, were shown to decision makers and land use planners of SGSS, and they agreed that the critical areas identified along the coast corresponded to zones that are historically known as being prone to flooding and/or erosion impacts. Furthermore, a comparison was made between the results of the CRAF and the location of the areas affected by a huge storm that occurred in 5–6 February 2015 and that caused extensive erosion, flooding and economic damages along the coastline. Even if quantitative results based on the collected information on the impacts caused by the storm were not available, the hotspots identified with the CRAF are consistent with the zones affected by the February event (Perini et al., 2015b; Trembanis et al., 2017).

A more accurate evaluation of the validity of the CI maps derived from the comparison between the historical (1946–2010) information collected by SGSS (Perini et al., 2011) and the identified critical areas for the T100 scenario. SGSS did an evaluation of the number of inundation and erosion events that affected specific areas along the coast between 1946 and 2010. The data are available also in the web-GIS impact-oriented database of RISC-KIT (Ciavola et al., 2017). The results are shown in Figure 5.3, along with the critical areas identified with the CRAF for the T100 event, for both hazards. To note that the symbols related to the historical information (circles) are located in the proximity of places that were historically affected, not in the exact location where each impact occurred. Therefore, they should be considered as an indication of critical areas in their surroundings. Furthermore, the symbols' size represents the number of

inundation and erosion events, disregarding any other information on the magnitude of the storms. The historical information was collected taking into account the type of hazard and the impacts registered along the coast. Therefore, the comparison between the two datasets (historical data and CI maps) is appropriate.

With reference to Figure 5.3, an agreement between the identified critical areas and the historical information occurs when a circle is located inside a critical sector plus the two adjacent sectors, 1 north and 1 south, to take into account the fact that each circle identifies the impact of storms to its surroundings. Thus, each circle is compared to a stretch of coast of about 3 km (3 sectors). It follows that for both hazards, on the basis of historical records, 74 out of 106 sectors can be considered critical.

Considering the flooding hazard (Figure 5.3A), the T100 scenario highlighted 66 out of 106 critical sectors. For 71.2% of them a correspondence with historical records was found. Considering critical (47 sectors) and not critical (13 sectors) areas in the agreement evaluation, the 56.6% of the sector showed consistent results.

As an example, the Porto Garibaldi beach, located northward from the Porto Garibaldi navigation channel, is identified as critical for T100. The area was affected by huge storms in the past, also confirmed in Garnier et al. (2017). In fact, the town of Porto Garibaldi, formerly called Magnavacca, was already present in the 17th century and records of the effect of marine storms were found into historical documents. A good agreement was also found in the southern area of Lido di Spina and at the Bellocchio marsh.

The most significant discrepancy between the historical data and the critical sectors was found in the northern part of the region (the 6 northernmost sectors), Ferrara province (Figure 5.3A). Several sites showed a large number of inundation events but they were not hotspot in the CRAF. The reason for the discrepancy can be explained as it follows: the northern part of the Ferrara province historically experienced a large number of inundations that led to the decision to elongate northwards the artificial coastal defences (through the construction of wood groins, alongshore earth and geotextile dikes) that, at present, are able to protect the area from flooding. The additional protection structures were built starting from the 1990s. Therefore, as the CRAF is based on present topographic data, the areas that are protected by coastal structures resulted non critical, while, historically, they were affected by significant flooding events. The hazard maps produced by SGSS (Perini et al., 2016) with the least-path analysis show, in fact, that the area is not flood-prone, due to the presence of the protection structures. The overall agreement (critical and not critical sectors) between the CRAF outcomes and the historical records for flooding improved to 61% if the 6 northernmost sectors are removed from the comparison.

Considering the erosion hazard (Figure 5.3B), the critical areas for T100 were 40 out of 106 sectors. A correspondence with the historical records was found for 28 of them (70%). In general, the correspondence between the historical information and the CRAF results, considering the critical areas (28 sectors) and the not critical ones (20 sectors), was 45.3%.

Several sectors belonging to the RISC-KIT CSS (i.e. Porto Garibaldi - Bellocchio, Comacchio) resulted critical, especially in the area of Lido di Spina south and at the Bellocchio marsh. The results are consistent with the historical information, because the area is a well-known hotspot of erosion. The site is, in fact, the target of regular nourishment practices (Nordstrom et al., 2015). Furthermore, the beach at the Bellocchio marsh is retreating and shows large overwash fans in fast development during the last decade (Bertoni et al., 2015).

It is important to underline that the main discrepancies between registered erosion events and the identified critical sectors occurred along areas protected by rubble mounds. These areas were mostly impacted before the construction of the defences. According to the methodology adopted, they show CI = 0. Another significant inconsistency was represented by the two southernmost sectors (Figure 5.3B). In fact, two critical sectors were identified, but they do not correspond to the historically affected areas.

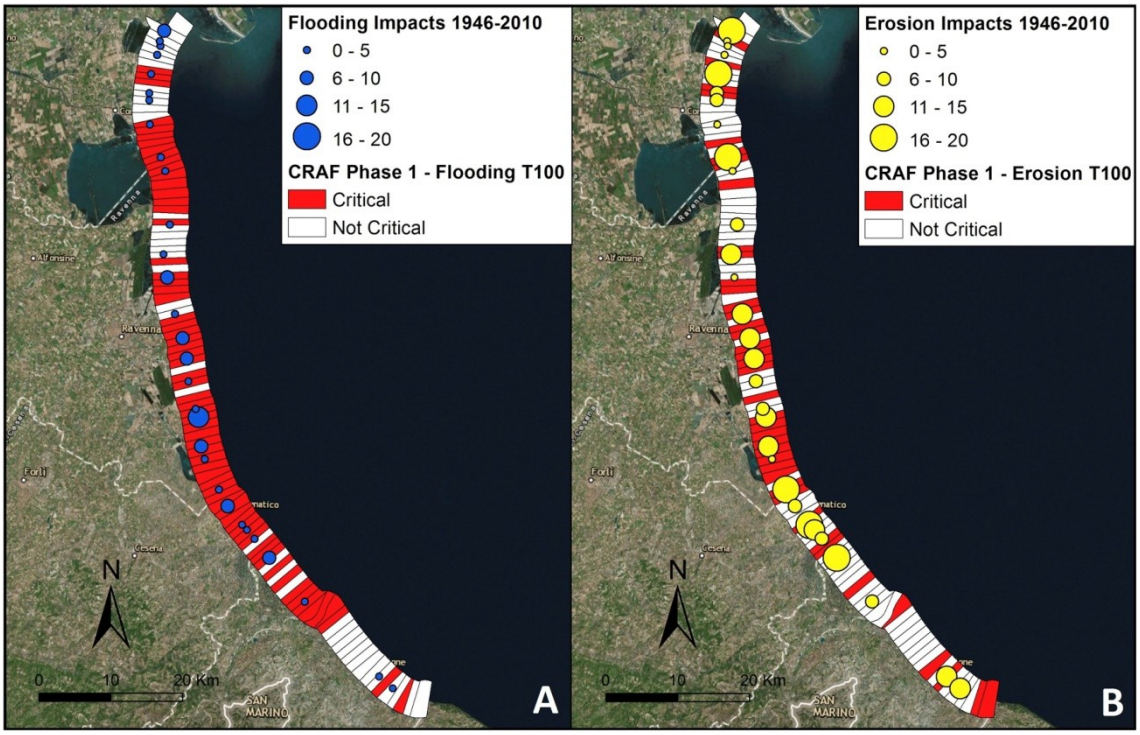

Figure 5.3 Validation of the critical sectors (CI > 2.5) obtained through the CRAF Phase 1 methodology and the historical data (1946–2010) provided by the End-Users. The comparisons are shown for both flooding (A) and erosion (B) hazards.

5.7 Conclusions

The analysis carried out to implement the CRAF Phase 1 through the event approach included a series of information, provided by the End-Users, which are significant along the coast of the Emilia-Romagna region.

It was possible to evaluate the exposure to flooding and erosion of different assets. The results showed that utilities and transports were most probably not affected by flooding and erosion, and that the social and economic status of families was an important aspect but has almost uniform values along the coast. The business sector was, on the contrary, a key element, because a large part of the regional economy is based on the coastal tourist sector. However, the land use exposure and the hazard indicators were the driving elements for the identification of critical areas. Most of the coast resulted exposed to both hazards. This is related to the large urbanization, to the low-lying nature of the territory, also affected by subsidence, although not accounted for in the present assessment, the absence of natural defences (i.e. dunes) and the reduced amount of available sand to naturally nourish the beaches. Land subsidence is a critical issue when analysing coastal risk (Aucelli et al., 2017; Perini et al., 2017) and future studies should take into account this important characteristic of the regional coast.

The methodology presented was, for the flooding hazard indicator, different from the one described in Viavattene et al. (2017), because the regional managers provided data produced for the Floods Directive (Perini et al., 2016). It was therefore possible to use flooding maps already available and derived from a different methodology than the approach proposed by Viavattene et al. (2017). Simple 1D approaches (e.g. bathtub) along profile lines could work in areas were the back barrier topography increases monotonically landwards. In low-lying areas, like the RER coastline, the bathtub approach leads to the overestimation of the flooding extension, as claimed by Gesch (2009), Murdukhayeva et al. (2013) and Perini et al. (2016). It is suggested to use bi-dimensional flood maps for CRAF Phase 1, whenever they are available. This could lead to more accurate results in terms of hotspots identification, as the presented validation points out.

The validation procedure showed that the identified critical areas were significantly consistent with the historical information on past storm events (1946–2010; Perini et al., 2011) for flooding and erosion. The Emilia-Romagna Region can be defined as a data-rich region, where information are publicly available, where all the actors dealing with coastal issues are aware of the problems, and where there are many procedures/regulations/protocols to mitigate the impact of storms. The close cooperation with the regional managers provided important suggestions to elaborate an accurate procedure, step by step. Moreover, the application of the CRAF method in a data-rich site provided the necessary information to validate the results and demonstrated that the method for the identification of hotspots is reliable. Where the End-Users' know-how is robust, the method can be improved to obtain more consistent results. It should be underlined that the End-Users were not surprised by the CRAF results, as it confirmed well-known critical areas. However, the codified methodology provided by the CRAF could help improving the already existing methods, especially for the identification, valuation and ranking of the exposure indicators, and the comparison between sectors through the coastal index approach.

6 LINKING SOURCE WITH CONSEQUENCES OF COASTAL STORM IMPACTS FOR CLIMATE CHANGE AND RISK REDUCTION SCENARIOS FOR MEDITERRANEAN SANDY BEACHES

6.1 Introduction

Increasing coastal risk due to the intensification of hazard and exposure magnitudes (IPCC, 2012, 2013), is driving the needs of coastal managers towards more innovative approaches for coastal risk assessment and management, notwithstanding the fact that the future projections are affected by large uncertainty. Highlighting these needs at the international and European levels is the impact of recent extreme events such as Hurricane Katrina in Louisiana in 2005 (Beven II et al., 2008), storm Xynthia in France in 2010 (Bertin et al., 2012; Kolen et al., 2013), Hurricane Sandy in New York in 2012 (Kunz et al., 2013; Van Verseveld et al., 2015),and the Southern North Sea storm in 2013 (Spencer et al., 2015). Similarly, in the Mediterranean, several extreme events have impacted coastal communities at the local and regional levels such as storm Klaus in 2009, as described in Bertotti et al. (2012) and cyclogenesis mechanisms in the NW Mediterranean described in Trigo et al. (2002). In this context, the coasts of Catalunya (Spain) and Emilia-Romagna (Italy) also recently experienced coastal storm impacts that caused socio-economic losses (Jiménez et al., 2012; Perini et al., 2015a; Harley et al., 2016; Trembanis et al., 2017).

Therefore, coastal managers must properly deal with coastal risk when designing plans during the prevention phase of the disaster management cycle. This is recognised in several initiatives such as the protocol of Integrated Coastal Zone Management (ICZM) for the Mediterranean, which includes a chapter on natural hazards and advises signed parties to implement vulnerability and risk assessments. In addition, the EU Floods Directive is another example dealing specifically with floods. Therefore, the need for integrated decision support systems (DSS) based on modern models and approaches for coastal risk assessment and management is increasing. Indeed, coping with storm-induced risks in coastal areas involves testing multiple disaster risk reduction (DRR) alternatives against multiple forcing conditions in current and future scenarios considering climate change.

The literature provides different approaches with which to implement these assessments. It is becoming increasingly important to consider multi-hazard approaches when assessing risk at all levels (i.e. from the regional to local scales). Therefore, the scientific community provides integrated and interdisciplinary approaches (e.g. Ciavola et al., 2011a, 2011b; Penning-Rowsell et al., 2014; Vojinovic et al., 2014; Oumeraci et al., 2015; Van Dongeren et al., 2017). Up-to-date methodologies can be used in coastal risk assessments at different scales ranging from regional approaches (up to hundreds of km) to local detailed assessments (up to 10 km). Regional methodologies aim to locate coastal sectors more prone to impacts, the so-called hotspots. Local approaches aim to achieve the highest possible level of accuracy for risk evaluation and to support decision making for previously identified hotspots. Notably, coastal risk assessments must include physical concepts to characterise physical phenomena (i.e. the source of the hazard) and socio-economic concepts to describe the impact of the physical phenomena on human assets (i.e. the consequences). A suitable conceptual flexible framework that can capture all aspects of coastal risk assessment is the Source-Pathway-Receptor-Consequence (SPRC) model (e.g. Narayan et al., 2014; Zanuttigh et al., 2014; Oumeraci et al., 2015).

When addressing the problem at the local scale, it is necessary to accurately predict the impact and reproduce in detail coastal hazards and responses. The analysis of physical impacts is regularly implemented in a deterministic way, with process-based numerical models playing a central role and providing detailed information for areas prone to multiple hazards (e.g. Roelvink et al., 2009; McCall et al., 2010; Harley et al., 2011; Roelvink and Reniers, 2012). However, this must be used with multiple forcing conditions acting at the site and under different scenarios. Bayesian Networks (BNs) have demonstrated their versatility and utility in efficiently combining multiple variables to predict system behaviour for multiple hypotheses (e.g. Plant et al., 2016). Using a BN approach, multiple multi-hazard results from process–oriented models can be integrated for joint assessment, as well as for different scenarios and alternatives (e.g. Gutierrez et al., 2011; Poelhekke et al., 2016), enabling the integration of socio-economic concepts (e.g. Van Verseveld et al., 2015).

Jäger et al. (2017) proposed the conceptual BN framework used in this work, which is based on the integration of the SPRC and was developed in the RISC-KIT EU FP7 project (Van Dongeren et al., 2017). The approach represents the Hotspot tool developed in the project to be used as DSS. Plomaritis et al. (2017) applied the framework to test its potential as an early warning system (EWS) and the response of DRRs in Ria Formosa (Portugal).

In this work, the application of the tool to select and compare strategic alternatives to reduce coastal risk in current and projected future climate scenarios is presented for two sedimentary coasts in the Mediterranean environment, namely the Tordera Delta for the Catalan coast (Spain) and the Lido degli Estensi-Spina for the Emilia-Romagna coast (Italy). In both study sites the tested DRR measures were pre-selected on the basis of stakeholders' interviews (see Martinez et al., 2017) and the outcomes of the analysis were used in a participatory process to select acceptable measures to be part of integrated DRR strategies (see Barquet and Cumiskey, 2017).

6.2 Regional contexts and case studies

The two presented case study sites (CSS; Figure 6.1) are representative of many other coastal areas in the Mediterranean consisting of sandy beaches where local economic activities are based on the tourist sector. These areas are characterised by urbanisation and infrastructural growth close to the shoreline (limiting natural beach accommodation processes) and economic activities directly on the beach and immediate first part of the hinterland (e.g. concessions, campsites, restaurants). The coast keeps offering its recreational function, but lacks part or all of its protective function against storms. Thus, depending on the morphological conditions of the hinterland and exposure to incoming storms, these coastal areas are prone to becoming sectors sensitive to the impact of extreme events.

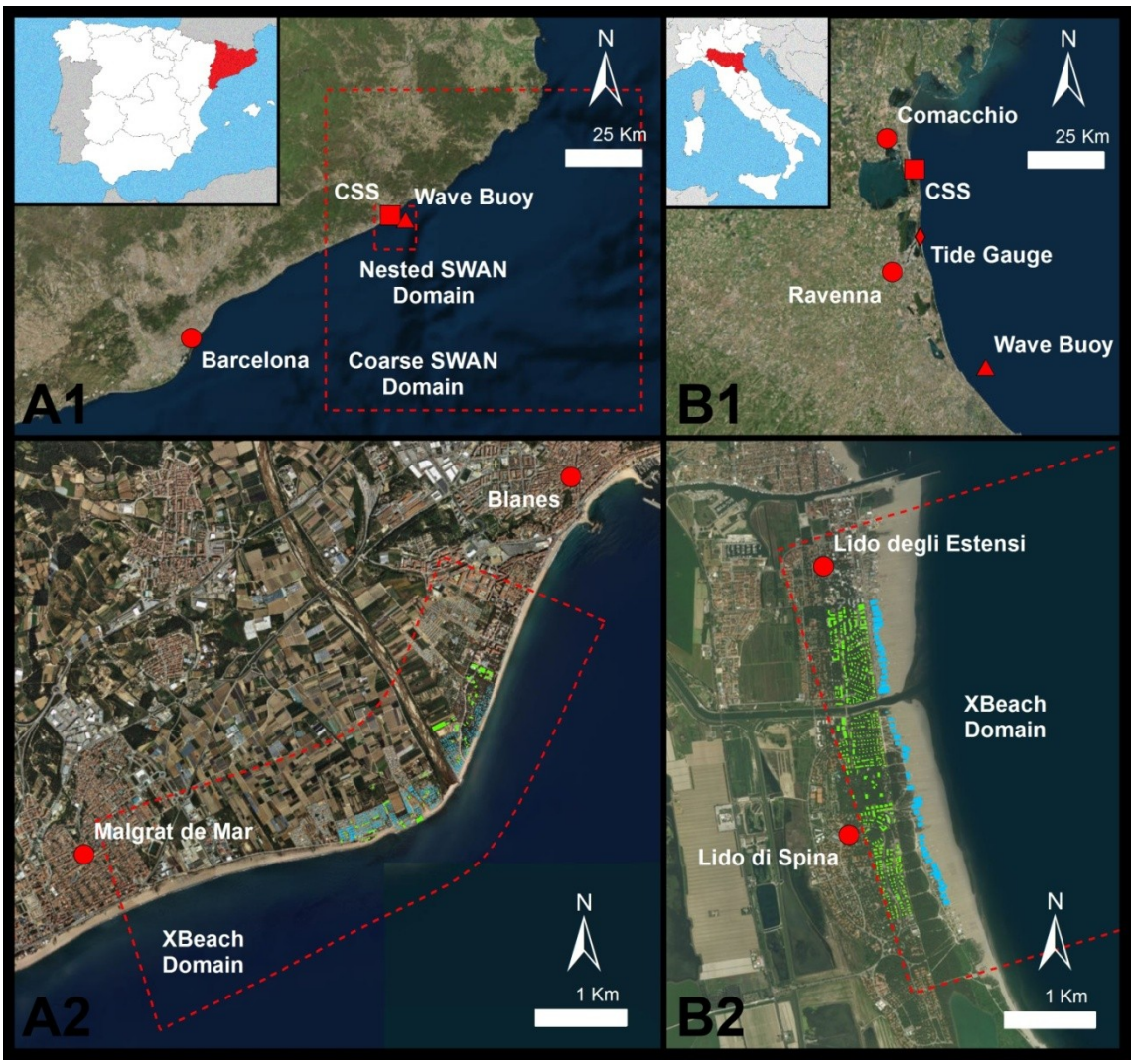

Figure 6.1 Regional and local contexts: A1) the central-northern Catalan coast; B1) Emilia-Romagna coast; A2) local hotspots of Tordera Delta; B2) local hotspots of Lido degli Estensi-Spina (2b). The main locations (red dots), wave buoys (red triangles), tide gauge (red diamond), and the CSS (red squares). The domains of the large-scale and local models (dashed red lines) are highlighted for each box.

6.2.1 Tordera Delta, Catalunya (Spain)

The Catalan coast is located in the NE Spanish Mediterranean Sea (Figure 6.1, A1). It consists of a coastline 600 km long with about 280 km of beaches. Coastal damage has increased during the last decades along regional coasts as a result of the increasing exposure along the coastal zone and progressive narrowing of existing beaches (Jiménez et al., 2012) through dominant erosive behaviour due to net littoral drift (Jiménez et al., 2011). Locations experiencing storm-induced problems are present along the entire coastline, and especially concentrated in areas experiencing the largest decadal-scale shoreline erosion rates. Among these areas, the Tordera delta, located about 50 km north of Barcelona, provides a good example (Figure 6.2).

The deltaic coast is composed of a coarse sandy coastline extending about 5 km from S'Abanell beach at the northern end and Malgrat de Mar beach in the south (see Figure 6.2). This zone is highly dynamic, and is currently in retreat as a result of net longshore sediment transport directed southwest and decrease in Tordera river sediment supplies.

Consequently, the beaches surrounding the river mouth, which were traditionally stable or accreting, are being significantly eroded (Jiménez et al., 2011; Sardá et al., 2013). As a result of the progressive narrowing of the beach in the area, the frequency of inundation episodes and damage to existing infrastructure (beach promenade, campsite installations, desalination plant infrastructure, roads) has significantly increased since the beginning of the 90s (Jiménez et al., 2011; Sardá et al., 2013) (Figure 6.2).

Subsequently, existing campsites in the most affected area have abandoned the areas closer to the shoreline, as in many cases, these areas are fully eroded or directly exposed to wave action. In other cases, owners have tried to implement local protection measures that in many cases have enhanced existing erosion (Jiménez et al., 2017c).

Coastal storms in the Catalan Sea can be defined as events during which the significant wave height (H_s) exceeds a threshold of 2 m for a minimum duration of 6 hours (Mendoza et al., 2011). Despite this, not all storms can be considered as hazardous events in terms of induced inundation and/or erosion. Mendoza et al. (2011) developed a five-category storm classification for typical conditions in the Catalan Sea based on their power content. The classification seems to well represent the behaviour of storm events in the Mediterranean, and was successfully employed in the Northern Adriatic (Armaroli et al., 2012). Furthermore, Mendoza et al. (2011) estimated the expected order of magnitude of induced coastal hazards (erosion and inundation) for each class and beach characteristics along the Catalan coast. According to their results, storms from category III (H_s = 3.5 m, duration around 50 hrs) to V (H_s = 6 m, duration longer than 100 hrs) are most likely to cause significant damage along the Catalan coast. One important aspect to consider is that wave-induced run-up is the largest contribution to the total water level (TWL) at the shoreline during storm events, because the magnitude of surges along the Catalan coast is relatively low.

6.2.2 Lido degli Estensi-Spina, Emilia-Romagna (Italy)

The Emilia-Romagna (Italy) coast is located in the northern part of the Adriatic Sea (Figure 6.1, B1). The coast is about 130 km long and characterized by low-lying, predominantly dissipative sandy beaches. The coastal corridor has low elevations, mainly ranging from -2 to 3m above MSL. The area alternates between highly urbanised touristic and natural areas with dunes, which are often threatened by flooding and erosion (Perini and Calabrese, 2010). The impact of coastal erosion was emphasised by subsidence due to water and gas extraction over the last century, especially in the Ravenna area (Taramelli et al., 2015), a decrease in riverine sediment transport, because of the strong human influence on rivers and their basins (Preciso et al., 2012), and the reforestation of the Apennines (Billi and Rinaldi, 1997). Touristic activities (accommodation, restoration, sun-and-bathe) can be considered main drivers of the coastal economy. Beach concessions, which provide sun-and-bath and restoration services, have grown exponentially in number since the second half of the last century, with negative consequences on natural areas, as in Ravenna Province (Sytnik and Stecchi, 2015). To protect the coast and its assets from the impacts of flooding and erosion, regional managers have constructed hard defences (e.g. emerged and submerged breakwaters, groins, rubble mounds; Perini and Calabrese, 2010) along the entire regional coast (over 60% of the coast is protected), and regularly implement restorative nourishment plans.

During the last decades, several EU projects such as THESEUS (www.theseusproject.eu) and MICORE (www.micore.eu) provided a good understanding of hydro-morphodynamics and risks to the coast. These projects and works published in the international literature such as Ciavola et al. (2007), Armaroli et

al. (2009, 2012), and Perini et al. (2016) were the product of strong collaboration between scientists and regional managers (Servizio Geologico Sismico e dei Suoli, SGSS). This led to the compilation and implementation of a storm database (Perini et al., 2011) and a regional EWS (Harley et al., 2016). The RISC-KIT project (www.risckit.eu) provided additional knowledge on this coastal area. The areas most exposed to coastal risk are well known, as can be seen in the works of Perini et al. (2016) and Armaroli and Duo (2017).

The hydrodynamics of the regional domain are well described in terms of storm waves and surges (IDROSER, 1996; Ciavola et al., 2007; Masina and Ciavola, 2011). These are as follows: the area is micro-tidal (neap tidal range: 0.3-0.4 m; spring tidal range: 0.8-0.9 m); the surge component plays an important role (1-in-2 years storm surge: 0.61 m) and is mainly generated from the SE (Scirocco) winds (according to the orientation of the Adriatic Sea). Furthermore, the wave climate is low energy (mean H_s ~0.4 m; 60% of waves are below 1 m). However, extreme events can be energetic, such as the storm of September 2004 ($H_{s,max}$ = 5.65 m, estimated by Ciavola et al., 2007) or the one of 5-6 February 2015 ($H_{s,max}$ = 4.66 m, measured at the Cesenatico buoy shown Figure 6.1, B1; Perini et al., 2015a; Trembanis et al., 2017).

The combination of high waves and storm surges, whose combined probability of occurrence in the area was assessed by Masina et al. (2015), can have strong impacts at the regional level, as demonstrated by Armaroli et al. (2009, 2012) and Harley and Ciavola (2013). Notably, based on historical data (Perini et al., 2011), Armaroli et al. (2012) provided a set of critical storm thresholds for natural and urbanised beaches to characterise potentially impacting storms. The thresholds included a combination of offshore H_s and TWL: 1) $H_s \geq 2$ m and TWL (surge + tide) ≥ 0.7 m for urbanised zones; 2) $H_s \geq 3.3$ m and TWL (surge + tide) ≥ 0.8 m for natural areas with dunes.

For a more local perspective, the Lido degli Estensi-Spina coastline (Comacchio municipality, Ferrara province, Italy) area represents a highly touristic stretch of coast with concessions directly facing the sea (Figure 6.1, B2). The littoral drift is northward as confirmed by the width of the sandy beaches, which increases from 20 to 50 m in the southern part of Lido di Spina to 200 to 300 m in the northern part of Lido degli Estensi. Here the sediment is trapped by the groin of the mouth of a navigation canal (Porto Canale).The beach is not protected, and regional managers implement regular nourishment in the southern part of the area (Nordstrom et al., 2015). At the back of the concessions, the villages accommodate restaurants and hotels for tourists, along with residential buildings (mainly holiday houses). South of the case study site is a natural area with dunes, which while strongly impacted by erosion, is not considered in this study. In a recent study, Bertoni et al. (2015) analysed aerial photographs of the evolution of the case study area, focusing on the stretch of coast between Porto Garibaldi and the Reno river mouth. The area was impacted by the event in February 2015 (see Figure 6.3) with limited, but not negligible, consequences for several concessions (Perini et al., 2015a; Trembanis et al., 2017).

Figure 6.2 Impacts on the Tordera Delta. Destruction of a road at Malgrat (A); overwash at campsites north of the river mouth (B); destruction of the promenade north of the river mouth (C); beach erosion, and damage to utilities and buildings at Malgrat (D and E).

Figure 6.3 Impacts of the event in February 2015 on the Lido degli Estensi-Spina case study area. Impacts of erosion and flooding on concessions at Lido di Spina south (A, B) and Lido degli Estensi (C); sandy scarp due to the erosion of the dune in the south of Lido di Spina (D); eroded Winter Dune in Porto Garibaldi (E); damages to the Porto Canale front at the Lido degli Estensi (F).

6.3 Methodology

6.3.1 General approach: from source to consequences

The analysis framework employed in this study follows Jäger et al. (2017) and is based on the use of the SPRC model (Samuels et al., 2008; Oumeraci et al., 2015), as shown in Figure 6.4. This model is mostly used in coastal risk management (e.g. Narayan et al., 2014) and permits a clear representation of all risk components and their links from source to consequence.

Source (S) includes the forces determining coastal response to the impact of extreme events, which are essentially a set of storms representative of the storm climates of the study sites over the entire intensity range (from moderate to extreme storms). These sources propagate to the coast and lead to different hazard pathways (P) such as erosion and inundation, the focus of the analysis. The pathways are solved through a process-oriented model to propagate storms and quantify induced processes. They are assessed for the entire coastal domain where receptors (R) are characterised according to their location on the coastal plain and typology, which define their exposure, and vulnerability to each hazard type. Finally, consequences (C) are evaluated by combining the vulnerability and exposure of each receptor with the magnitude of the hazards.

Since the main objective of the analysis is to test DRR strategies to help decision makers in future planning, the framework is applied under current conditions (hereafter current scenario, CUS) to define the baseline scenario and climate change conditions (hereafter climate change scenarios, CCS) to define a plausible future scenario. Finally, the analysis is repeated considering different DRR measures.

The general approach uses the ability of a BN to assess dependency relations between variables to reproduce the steps of the SPRC model. This conditions the application of the steps of the SPRC model, as explained in the following sections. At the same time, its data assimilation capabilities allows to integrate large amounts of data. As such, the BN can consider all dependency relations between the analysed variables, enabling the assessment of multi-hazards and the consequences on receptors for all tested incoming conditions, scenarios, and DRR alternatives in a condensed, graphic, probabilistic, and single tool.

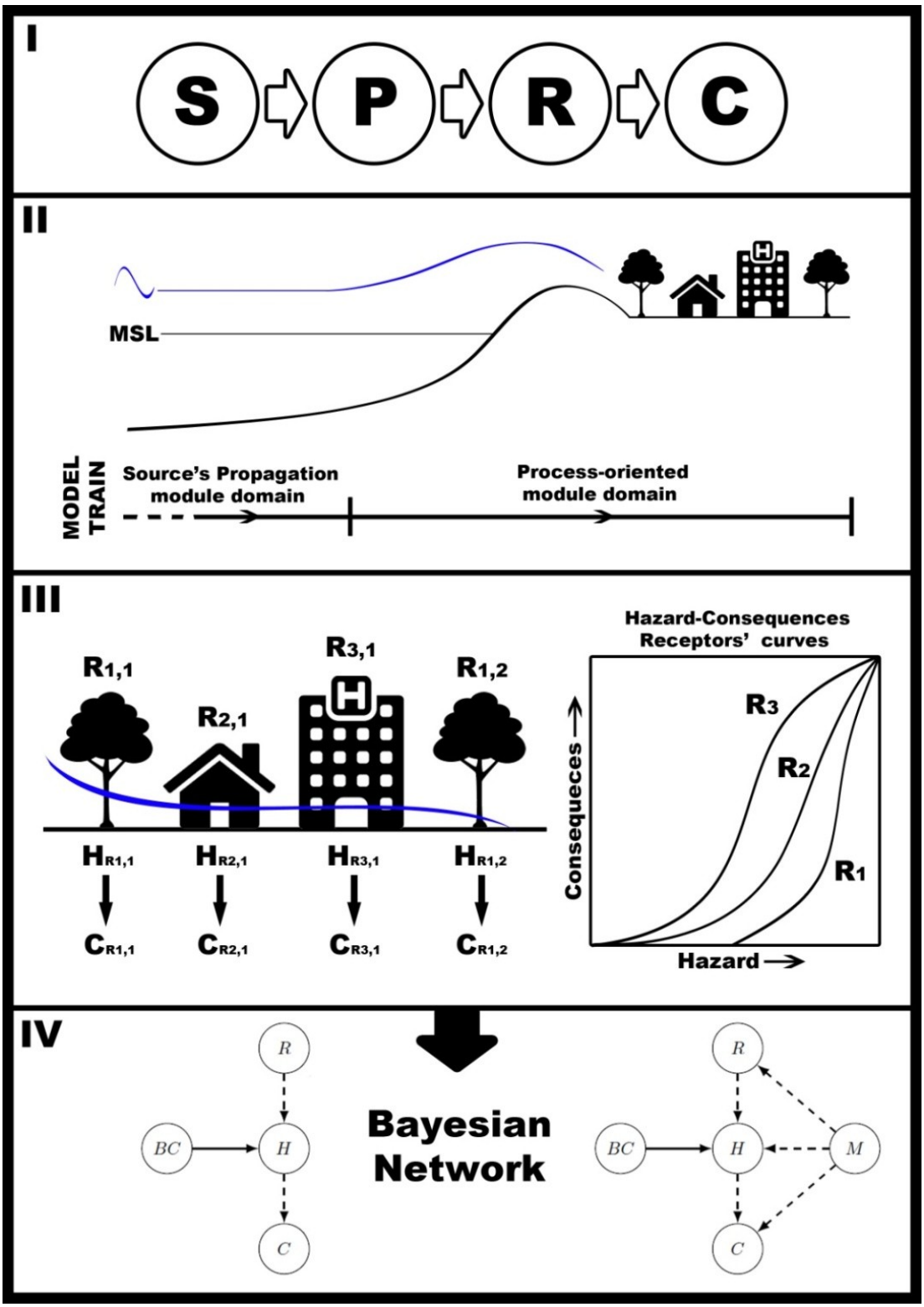

Figure 6.4 General methodology. (I) The SPRC conceptual framework is implemented through (II) a model chain, which consists of a propagation module of the source (S) and a process-oriented module for the coastal area reproducing the pathway (P). Then, (III) the consequences (C) are calculated based on the computed hazards (H) at the receptor (R) scale by using vulnerability relations (i.e. hazard-consequences functions). In the last step (IV), all variables including source boundary conditions (BC) are fitted in a BN, adding impacts after the implementation of measures (M).

6.3.2 Source: identification and design

Since the objective of this work was to test DRR measures for risks induced by coastal storms, these are the source considered. To properly characterise storms, all relevant variables controlling the magnitude of induced hazards (erosion and inundation) must be considered, in other words, significant wave height (H_s), wave period (T_p), wave direction, storm duration, and water level. In this approach, storm characteristics are defined in terms of a set of representative storms or storm scenarios that cover the typical conditions at each study site. This information is obtained from existing wave time series or bulk data of the events (recorded or modelled), usually in deep waters, propagated towards the coast to characterise storm conditions at the nearshore area of the study cases. Probable combinations that cannot be covered using existing records are represented by synthetic designed storms (e.g. Poelhekke et al., 2016; Jäger et al., 2017; Plomaritis et al., 2017). The storm events were selected based on the information available for each study site through the RISC-KIT WEB-GIS impact-oriented database (Ciavola et al. 2017; http://risckit.cloudapp.net/risckit/#/), which provided synthetic information on the physical parameters (measured or assessed at the regional level) and socio-economic impacts of the events. In addition, time series of waves and water levels were used to characterise all events, when available.

For the Tordera Delta case, the selected variables to define storm scenarios were H_s at the peak of the storm, total storm duration, and incoming storm direction. T_p does not significantly vary during storms in the study area (see Mendoza et al., 2011) and was not included to reduce the number of variable combinations. The coastline configuration and wave climate characteristics necessitated considering the main wave directions in terms of dominant (E) and secondary (S) directions. Finally, TWL (tide + surge) during the event was included to reproduce hypothetical future projections of MSL due to climate change. The selected discrete bins are shown in Table 6.1. These led to 12 combinations defining the source that were tested in the current MSL and another 12 in the future MSL scenario (see Section 6.3.5). Each combination was simulated twice slightly varying the storm conditions to account for variability. Thus, 24 storms in the current MSL and 24 in the future projected one were simulated. Of the 24 source storms in the current situation, 16 corresponded to historic (recorded) events including the two largest that occurred in November 2001 and December 2008. These were classified as extreme storms (category V) according to the Mendoza et al. (2011) classification. The remaining eight storms were created using combinations of Hs-duration-direction ever recorded. These events were modelled assuming a triangular-shaped time-evolution with the peak intensity at the half of their duration (e.g. McCall et al. 2010; Poelhekke et al., 2016) Data used to reproduce the historic events include the time series of hindcast wind fields and 2D wave spectra time series in deep waters for the NW Mediterranean (Guedes Soares et al., 2002; Ratsimandresy et al., 2008). Wave conditions must propagate towards the coast to properly define storm events at the study site. At the Catalan coast, the storm surge contribution to the sea surface level is one magnitude lower than the wave-induced component, and the two variables are uncorrelated (Mendoza and Jiménez, 2008). All historical events with recorded associated water levels were simulated with the real storm surge, while the synthetic storms were simulated with a storm surge of a 0.25 m constant throughout the event, as representative of the site (Mendoza and Jiménez, 2008).

For the Lido degli Estensi-Spina case study, the source variables, identified as drivers of the impacts of flooding and erosion, were the maximum Hs and maximum TWL of the storm event. The literature for the area recognizes these as main important variables with TWL having more importance (Armaroli et al 2009, 2012). In addition, the relative

sea level rise (RSLR) was considered as a Boolean variable to represent the CCS. The direction of the storms was not considered as a source characteristic variable since storms are either ENE or SE, and each Hs-TWL combination is simulated twice accounting for variability inside this directional range. The source combinations were classified into the variable ranges shown in Table 6.1. Seven historically based events were selected from the RISC-KIT Database, and to cover all possible combinations, 5 additional synthetic events were considered for a total of 12 events in the CUS. Notably, for several historic events, neither reliable nor continuous time series for waves and water levels were available from local measuring stations. To ensure consistency, source events were represented based on the following methodology. Starting with the list of bulk synthetic information for each event (maximum H_s, T_p, main direction of the storm, maximum TWL or duration when available), triangular symmetric storm distributions (e.g. Carley and Cox, 2003; Corbella and Stretch, 2012) for H_s, T_p, and surge were created for both historical and synthetic events. This approach is common for coastal modelling application (e.g. McCall et al. 2010; Poelhekke et al., 2016) The peak of the waves was assumed to occur at the same time as the maximum surge (calculated as the difference between the TWL and maximum astronomical predicted tide). When bulk parameters were missing, the following "worst case" assumptions were introduced: T_p at peak of 10 s, wave direction of 90 ºN, and duration based on similarity with other storms.

Table 6.1 Source characterization. Variable discretization applied at the study sites.

Case Study Site	H_s ranges [m]	Storm Duration [hrs]	Incoming direction [ºN]	Water Level [m]
Tordera Delta	2 to 3	6 to 30	30 to 135 (E)	0 to 0.6 m
	3 to 4	30 to 65	135 to 220 (S)	Current + SLR
	4 to 5			
Lido Degli Estensi-Spina	2 to 3	6 to 68	60 to 90	0.65 to 1.05
	3 to 4			1.05 to 1.45
	4 to 5			1.45 to 1.85
	5 to 6			Current + SLR

6.3.3 Pathways: modelling multi-hazard impacts

To reproduce the pathway from source (storm) to impact (hazards), a model chain was designed and adapted for each site (Figure 6.4, II). The chain must be able to reproduce all hazards to be assessed (i.e. erosion and inundation). To do this, a detailed 2D process-oriented model simulating inundation and erosion in an integrated way was employed (the obtained inundation includes the morphodynamic feedback associated with coastal erosion during the storm). The XBeach model was used for this purpose in both study cases (see Roelvink et al., 2009, for model details).

The model chain for the Tordera Delta study case consists of two blocks, one "external" and one "internal". The external module comprises three models (HAMSOM,

HIRLAM, and WAM models) that supply the forcing conditions (time series of water levels, wind fields, and waves) and are run by Puertos del Estado (Spanish Ministry of Public Works). The output of these models is taken directly as an input for the internal module, which comprises the SWAN (Booij et al., 1997) and XBeach (Roelvink et al., 2009) models. SWAN was used to propagate wave conditions provided by the external models (regional scale) to the offshore boundary of the XBeach model (20 m depth), while XBeach was employed to assess the extension and magnitude of inundation and erosion hazards at the study site (local scale). The model chain was validated through the St Esteve event in 2008 (Sanuy and Jiménez, submitted).

The model chain for the Lido degli Estensi-Spina case study only included the XBeach model. This simple approach was possible based on the assumption that the information derived from the RISC-KIT Database can be considered representative of the storm in the regional domain, as collected from different sources (e.g. offshore buoys, harbours' tide gauges, newspapers, etc.) along the Emilia-Romagna coast (Perini et al., 2011; Ciavola et al., 2017). The model was qualitatively validated with the February 2015 event (Perini et al., 2015a; Trembanis et al., 2017).

6.3.4 Receptors and consequences

The methodology applied in this work individually identified receptors located at the study sites (Figure 6.4, III) (Jäger et al., 2017). First, receptors with homogeneous vulnerability characteristics were defined and separately considered. Then, for each group of receptors, polygons were drawn using a GIS-based tool to account for their exact location and size. Finally, the polygons were intersected with the cells of the 2D detailed model grid (XBeach) to assign to each receptor the nodes of the model that will affect them.

For the inundation hazard, the value of the maximum water depth inside each receptor was used as the impact variable. Then, by using flood-damage curves for the corresponding receptor typology, inundation water depth was translated to relative damage. Thus, flood-damage curves are the vulnerability relations used to quantitatively assess inundation risk. This was then translated into four levels of impact - none, low, medium, and high - which are case and receptor dependent (see the following sections). The chosen damage curves do not include uncertainties. They were adopted on the basis of the available information at both study sites. Damage ranges and damage-hazard relations are different at each study site and therefore the final impact levels (from none to high) are also site-specific, since they are calculated from the definition of the corresponding damage curves. This assumption aimed at better communicate results to local stakeholders (see Section 6.5 and Barquet and Cumiskey, 2017).

The magnitude of the risk associated with erosion depends on the combination of vertical erosion and distance of erosion to the receptors. This was implemented by building multiple buffers (increasing in distance) around each receptor and intersecting them with the information of maximum vertical erosion output from XBeach. The definition of risk categories related to erosion thresholds and distances is site dependent.

Exposure and vulnerability in the Tordera Delta case study

The distribution of receptors for the Tordera Delta case study was derived from cartographic information from the Catalan Cartographic Institute (ICC) and completed manually through an orthophoto analysis. The study site was divided into eight areas, of which four are located at the south of the river mouth, corresponding to the Malgrat de Mar municipality, and the other four to the north, corresponding to the Blanes municipality. These two sets of four areas were selected to enable an analysis of the

impact at different bands regarding the limit of the public domain (which separates the public beach from the hinterland). The first band corresponds to the first 20 m of hinterland. The second band is 30 m wide and located just after the first one 20 to 50 m from the boundary of the public domain. The third covers the range from 50 to 75 m, while the fourth band covers all the hinterland omitted between the end of the third band and inland simulation domain boundary. This enables an assessment of the distribution of the impacts of the different scenarios in terms of distance to the coastline. Thus, the effectiveness of removing receptors from each of the bands considered could be assessed, which corresponds to different setbacks as DRR measures. Three groups of receptors were considered to have homogeneous vulnerabilities, namely houses (concrete buildings), campsite elements (soft buildings and caravans), and infrastructure (promenade and road at the back of the beach). Table 6.2 shows the distribution of campsite elements and houses in the different areas. The infrastructural receptors (promenade at the north and road at the south) are only located in the first 20 m band (Areas 1 and 5).

The consequences of flooding were assessed through flood damage curves used to characterise the relative damage based only on water depth. Data (see details in Table 6.3) was obtained from the Agència Catalana de l'Aigua (2015), which derived it from FEMA (2001).

The relative damage values to buildings and campsite elements were converted into the level of risk as follows: (i) No impact for 0% relative damage to buildings and campsite elements, (ii) Low impact for damages below 26% to buildings and 50% for campsite elements, (iii) Medium impact when damages to buildings range from 26 to 45% and damages to campsite elements range between 50 to 70%, and (iv) High impact for relative damages higher than those formerly exposed for both receptors.

The buffers defined to assess the erosion hazard at the Tordera Delta are as follows: (i) The 20-m distance corresponds to the average beach retreat at the site for a storm with a return period of 38 years. This was used as a threshold ranging from 'none' to 'low' risk of direct impact due to erosion. The return period is commonly used for infrastructural receptors similar to those in the Tordera Delta (low economic importance for a lifetime of about 25 years). (ii) The 12-m buffer (average retreat for the 10-year return period) was used as the threshold from low to 'medium' impact. For a medium impact, receptors are in the post-monitoring situation and begin to be exposed to the direct impact of relatively frequent storms. (iii) Finally, the 3-m buffer was used as the threshold for the 'high' impact risk, meaning that the receptor is directly affected by erosion at the toe or impacted by a direct wave in the analysed scenario. A buffer was considered to have been affected when a vertical erosion threshold of 50 cm was imposed.

Table 6.2 Distribution of receptors at the Tordera Delta study site.

Area	No. of Houses	No. of Campsite Elements
Area 1 (0 to 20 m *Malgrat de Mar*)	16	45
Area 2 (20 to 50 m *Malgrat de Mar*)	10	71
Area 3 (50 to 75 m *Malgrat de Mar*)	8	169
Area 4 (> 75 m *Malgrat de Mar*)	46	509
Area 5 (0 to 20 m *Blanes*)	1	95
Area 6 (20 to 50 m *Blanes*)	4	156
Area 7 (50 to 75 m *Blanes*)	7	72
Area 8 (> 75 m *Blanes*)	51	189
Total	143	1306

Table 6.3 Vulnerability relations for houses and campsite elements at the Tordera Delta study site with and without DRR measures (FRM).

Water depth at the receptor [m]	Relative Damage [%]			
	Houses	Campsites	Houses - FRM	Campsites - FRM
0	0	0	0	0
0-0.3	18.3	50	0	0
0.3-0.6	26.5	71	18.3	50
0.6-0.9	33.2	82	18.3	50
0.9-1.5	44.7	89	26.5	71
1.5-2.1	54.1	91	33.2	82
2.1-3.0	64.5	100	44.7	89
3.0-4.0	71.2	100	54.1	91
4.0-5.0	75	100	64.5	100

Exposure and vulnerability in the Lido degli Estensi-Spina case study

The analysed receptors belong to the central area of the model domain at approximately 600 m from the lateral boundaries (Figure 6.1, B2). Two main types of receptors were selected: (i) the residential and commercial buildings mainly present in the towns of L. Estensi and L. Spina, and (ii) beach concessions on the beach directly facing the sea. In this study, only receptors belonging to the seafront of Lido degli Estensi and Lido di Spina were considered, as they are mainly impacted by sea storms. Receptors were extracted from a recent Regional Topographic Map (Carta Topografica Regionale, scala 1:25,000, anno 2013), and the polygons were drawn in ArcGIS. Table 6.4 summarises the identified receptors. Following this, the grid cells affecting each receptor were defined.

The vulnerability relation for inundation hazards was defined considering a flood-damage curve from a recent study on Italian territory by c. This work was based on a micro and macro-scale study of the impacts of the 2010 river flood in Veneto (Italy) on residential houses. In the current work, it was adapted and applied to the receptors of the area (see details in column A of Table 6.5), and relates the flood relative damage factor (FRDF; values: 0-1) to flood depth. In particular, the worst case curve was used, which represents flood-related damages to single-family detached buildings with a basement. Although this curve is for residential buildings, it is assumed the same for commercial buildings and beach concessions, as no additional and specific information was available. The curve was modified considering the DRR implementation described in Section 6.3.5. The level of flood risk was defined as follows: none, when the FRDF is null; low, when the FRDF is higher than zero but lower than 0.1; medium, for an FRDF between 0.1 and 0.2; and high, for an FRDF higher than 0.2.

The vulnerability relation for erosion was defined for concessions only. The impacts due to the erosion hazard were defined based on a two-buffer approach for each receptor. The buffers were defined as follows: (i) the first buffer was the footprint of the receptor, and (ii) the second included a corridor of 10 m around the receptor.

Erosion was considered significant (and thus, present) when >0.05m. The erosion risk categories for each receptor were set as follows: (i) Safe: no erosion in any buffer, (ii) Potential Damage: when erosion is present in the 10-m buffer and/or is present with values less than 0.5 m in the footprint buffer, and (iii) Damage: when the erosion limit of 0.5 m is exceeded for the footprint buffer. Notably, the threshold of 0.5 m was set considering the uncertainty of the model grid topography (± 0.15 m) and assuming that the foundations of the concessions are a minimum of 0.2 m thick.

Table 6.4 Distribution of receptors at Lido degli Estensi and Lido di Spina.

Area	Residential and Commercial Buildings	Concessions
Lido degli Estensi Seafront	26	16
Lido di Spina Seafront	47	28

Table 6.5 Vulnerability relation for flooding adopted for the receptors at Lido degli Estensi-Spina without (A) and with DRR measures (B).

Flood Depth [m]	Flood Relative Damage Factor [-]	
	A - adapted from Scorzini and Frank (2017)	B - modified considering the FRM
0	0	0
<0.3	<0.1	<0.1
0.3-0.7	0.1-0.2	<0.1
0.7-1.1	0.2-0.3	0.2-0.3
>1.1	>0.3	>0.3

6.3.5 Testing scenarios and DRR alternatives

To compute the analysis under CCS and under the implementation of DRRs, it was necessary to identify the variables and settings affected by each scenario, either a future projection or implementation of a risk reduction measure. Therefore, an appropriate approach was selected to consider these modifications in the SPRC chain.

The CCS mainly affect the hazard and therefore, are applied in the modelling chain. The DRRs can affect both hazard and vulnerability/exposure variables. In the following, the implementation of the CCS and DRRs is described for each case study, emphasising the affected variables and steps of the methodology. The DRR measures were pre-selected on the basis of the analysis of stakeholders' interviews (see Martinez et al., 2017). All assessed DRRs were considered fully implemented and completely effective (DRR uptake and effectiveness: 100%) in all cases.

Climate change scenarios in the case studies

Future projections of MSL were based on the AR5 RCP8.5 (Church et al., 2013). Other factors such as changes in storminess, winds, or waves were not expected to change significantly in the NW Mediterranean (Lionello et al., 2008; Conte and Lionello, 2013), and are characterised by high uncertainty in the Northern Adriatic (IPCC, 2013). Data to include the sea level rise (SLR) in the assessment of future scenarios was provided by the EC Joint Research Centre database (for further detail, see Vousdoukas et al., 2016). For the Tordera Delta study case, the time horizon of 2100 was chosen, while the 2050 projection was used for Lido degli Estensi-Spina, because the SLR projections in the Adriatic are more uncertain than in the NW Mediterranean. Therefore, the 2100 horizon could yield highly unreliable results.

At the Tordera Delta, the RCP8.5 estimates an increase of 0.73 m by 2100. Therefore, all 24 simulations described in Section 6.3.2 were repeated with the projected future MSL. Moreover the potential beach accommodation to SLR was modelled following Bosom (2014) and Jiménez et al. (2017a). This was accomplished assuming an equilibrium coastal profile response following the Bruun rule (Bruun, 1962), resulting in landward and upward displacement of the beach profile. The estimated shoreline retreat due to the SLR in the area is 22 m. Thus, morphological coastal adaptation to SLR is included in the assessment. Finally, Casas-Prat and Sierra (2012) predicted a directional change in mean sea conditions from the current dominant (E) to the secondary direction (S). This effect was qualitatively explored by assessing eastern incoming storms in the CUS and imposing an equal likelihood of eastern and southern incoming storms in the CCS. Therefore, three different CCS were explored: (i) CUS + SLR with the corresponding estimated beach accommodation (CCS1), (ii) CUS + effect of direction switch in incoming storms (CCS2), and (iii) assessing the contribution of both components if occurring at the same time, i.e. SLR + switch in storm incoming direction (CCS3).

In Lido degli Estensi-Spina, the combined contribution of the predicted SLR with the subsidence component (not negligible in the area, e.g. Taramelli et al., 2015) was implemented. The resulting value of RSLR by 2050 used in the analysis is 0.30 m. The forcing events' water level time-series were modified, including the predicted RSLR by 2050 in the CCS. The morphological accommodation to the SLR was not implemented in the numerical analysis; however, its effect is discussed in Section 6.5.2. In total, 24 additional simulations were run for the CCS.

DRR alternatives in the case studies

Three DRR measures were tested for the Tordera Delta zone (see Figure 6.5): (i) Receptors Setback (RSB), (ii) Flood Resilience (set of) Measures (FRM), and (iii) Nourishment + Dune (N+D).

The RSB measure affects the exposure of the receptors. It entails removing all receptors inside a defined band measured from the public domain coastal limit (the limit between the back of the beach and hinterland). Three scenarios of the setback were simulated: 20 m, 50 m, and 75 m.

The FRM affects the vulnerability of receptors so that for a given water depth, the expected impact on campsites and houses during an inundation event decreases from the current situation when the DRR measure is implemented. It is assumed that resilience measures such as raised electricity outlets and utilities, adapted flooring, resilient plaster, and waterproof doors and windows were installed in all houses and campsite elements.

Finally, the N+D affects the inundation/erosion hazard. It includes beach nourishment at the south of the river mouth to increase the beach width by 50 m over 1 km at the south of the river mouth, where the highest erosion occurs. In addition, the level at the top of the beach was increased on both sides of the river mouth, with non-erodible sandbags at the northern side, where the campsites are closer to the coastline, and a sandy dune at the southern side. At both sides, the final height of the protective measure was 4.8 m above MSL. Since this measure affects the pathway, 24 extra simulations, this measure was implemented in the XBeach grid, were needed, and another 24 to combine the implemented measure with the CCS.

The selected DRR measures tested for the Lido degli Estensi-Spina case study were: (i) a Winter Dune (WD) system, affecting both flooding and erosion impacts, and therefore the hazards modelling process; and (ii) a set of FRM, influencing the flood vulnerability relations of receptors.

The WD (see Figure 6.6) is a common DRR practice along the Emilia-Romagna coast, especially in the Ravenna province (Harley and Ciavola, 2013), and regularly implemented by local concessionaires without a scientifically based design criterion. It consists of a set of embankments built with loose sand on the beach in front of concessions through beach scraping or sand replenishment (less frequent option). This DRR measure was implemented in the process-oriented module (XBeach). The WD was designed as a continuous dune that protects more than one concession, introducing breaks in the continuity of the feature where natural/human obstacles or passages were located. The top of the WD was fixed at 3 m above the MSL and the width (at the top) at 10 m. The WD was integrated in the model modifying the bed levels through the Dune Maker 2.0 tool (Harley, 2014). Both the CUS and CCS were tested with the DRR WD adding 48 additional simulations.

The FRM decreases the receptor's physical vulnerability to floods. It was assumed that the effective application of these measures would decrease the damages (FRDF > 0.1) for water levels lower than a certain threshold, assumed here as 0.7 m (e.g. all electrics have to be placed above the threshold). This assumption was integrated in the analysis by modifying the selected depth-damage curve, as defined in column B of Table 6.5, and included in the BN. Considering the adopted definition of flood risk levels (see Section 6.3.4), the FRM results in a complete obliteration of receptors for the medium flood risk, therefore increasing the receptors at the low level and not affecting receptors at high risk.

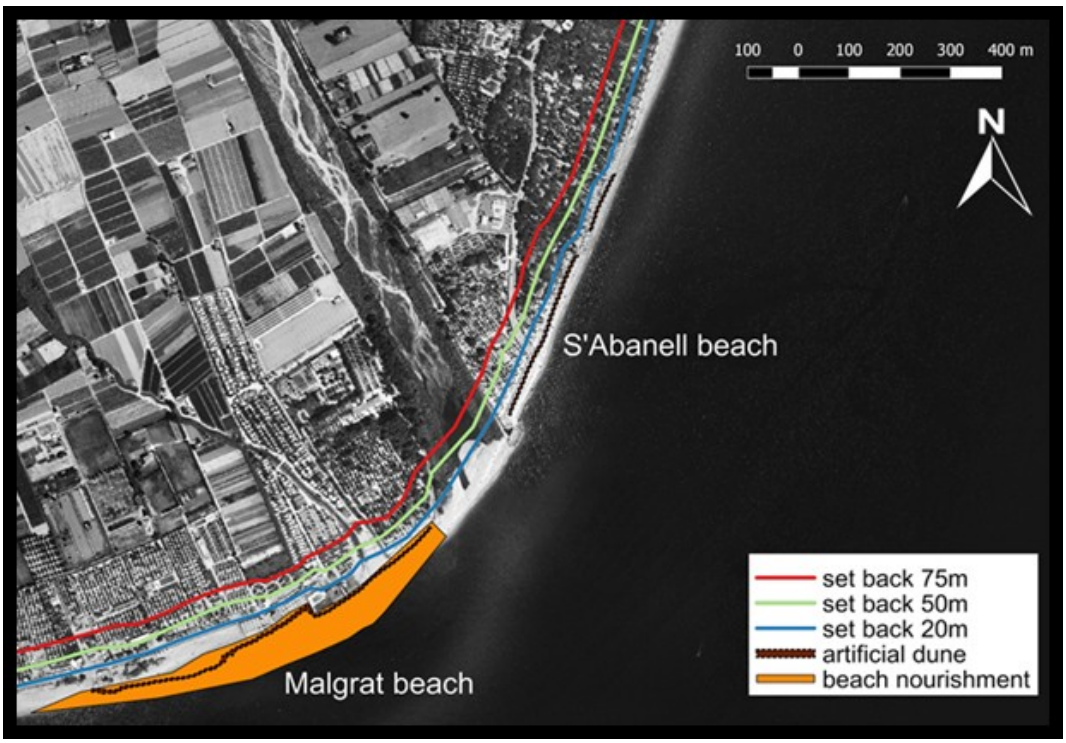

Figure 6.5 DRR measures at Tordera Delta. Coastal setbacks (20, 50, and 75 m) and Infrastructural Defence (beach nourishment at Malgrat beach + artificial dune at S'Abanell and Malgrat beaches).

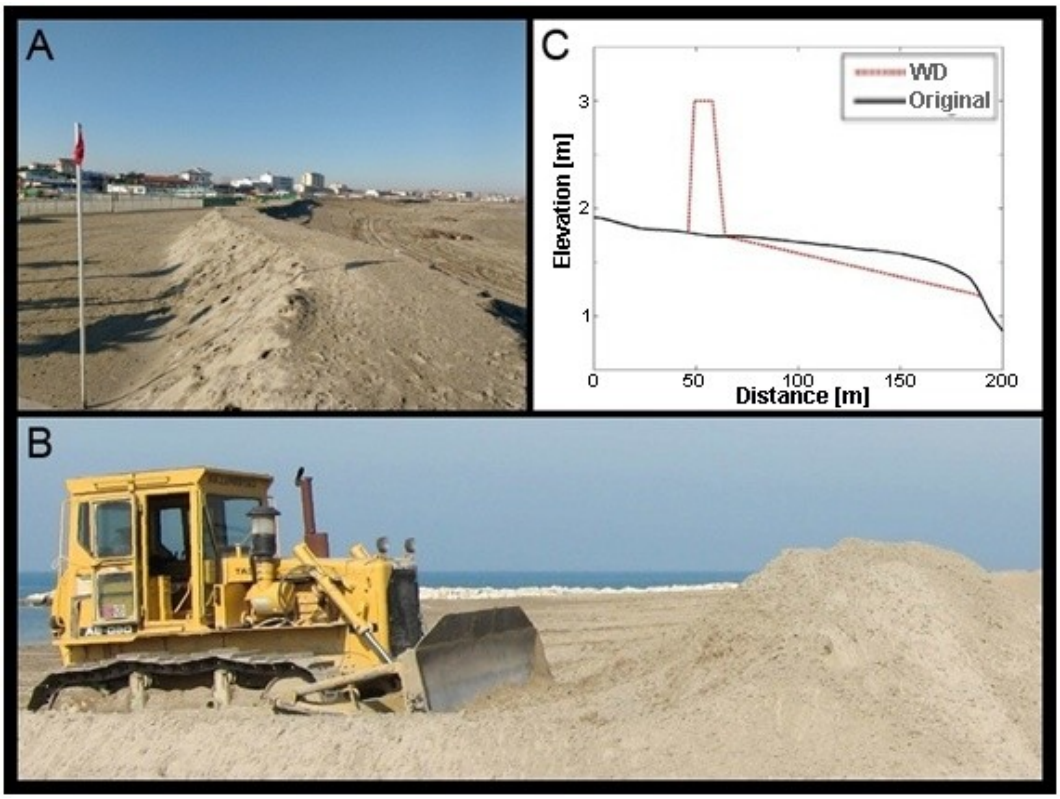

Figure 6.6 Artificial winter dunes in Emilia-Romagna: A) Winter dune in Porto Garibaldi (Comacchio, Italy); B) Building of a winter dune by beach scraping at Lido di Dante (Ravenna, Italy) (Harley, 2014); C) Representative model profiles at Lido di Spina north (original: black solid line; with winter dune DRR: red dashed line).

6.3.6 Bayesian Network DSS

BNs use probability theory to describe the relationships between many variables, and can evaluate how the evidence of some variables influence other unobserved variables. For example, evidence could be a forecast of the source variables characterising an impending storm. On the other hand, local hazards and damages in the coastal area have not yet been observed, but can be predicted with the BN. The model can also be updated with artificial evidence to explore extreme event scenarios or investigate the potential of disaster risk reduction plans. A BN is based on a graph (Figure 6.7). It consists of nodes connected by arcs that represent random variables and the potential influences between them. The direction of the arcs is crucial for the probabilistic reasoning algorithm of the BN, but does not necessarily indicate causality. For any two variables connected by an arc, the influencing one is called a parent, while the one influenced is referred to as the child. Thus, in Figure 6.7, X_1, X_2, and X_3 are the parents of X_4. A simple way to parameterise a BN is to discretise continuous variables after defining their data range, and to specify conditional probability tables for each node. This approach was adopted for this work. The conditional probability tables indicated how much a variable could be influenced by others. Mathematically, the graph structure and conditional probability tables define the joint distribution of all variables in the network, X_1, ..., X_n, based on the factorisation of conditional probability distributions (Equation 6.1):

$$p(X_1, \dots, X_n) = \prod_{i=1}^{n} p\big(X_i | \, pa(X_i)\big) \qquad (6.1)$$

where $pa(X_i)$ are the parents of node X_i (Pearl, 1988; Jensen, 1996). Once the joint distribution has been defined, the effects of any evidence can be propagated with efficient algorithms throughout the network (Lauritzen and Spiegelhalter, 1988).

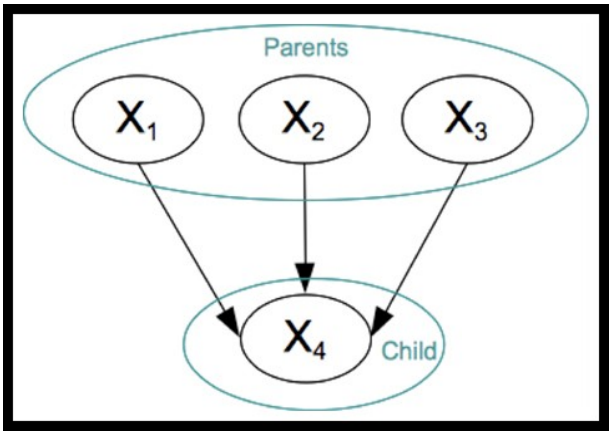

Figure 6.7 BN graph with four nodes.

In the RISC-KIT project, a generic structure for a BN that can support decision-making in coastal risk management was proposed. This structure is based on the SPRC and has five components: source boundary condition (BC), hazard (H), receptor (R), impact/consequence (C), and DRR measure (M). Typically, each component includes several variables. Panel (IV) in Figure 6.4 shows their influence on each other. In general, all boundary conditions influence all hazards, as indicated by the solid arc in Figure 6.4. Differently, each type of receptor (e.g. people, buildings, infrastructure, and ecosystems) has a sub-module in the BN consisting of an R node (representing the locations of receptors on the site), H nodes (representing the hazards given the locations of the receptors), and C nodes (representing the consequences given - some of - the hazards for the receptors). The dashed arcs in Figure 6.4 represent the fact that the sub-

modules are not directly interconnected. Nevertheless, dependencies arise from the common parents, which are boundary conditions and possibly DRR measures.

Alongside the generic structure, a c++ programme that automatically creates the BN (https://github.com/openearth/coastal-dss) is also provided. As input, the programme requires variable definitions and land use data, vulnerability relationships, and a 2D gridded simulation output of numerical physical process-based models of hindcast or synthetic extreme event scenarios. Essentially, the programme extracts the values of hazard variables from the simulation output at the locations of every individual receptor so that it was possible to obtain hazard distributions for each receptor type. Because each simulation contains the coastal response to one storm scenario under a set of DRR measures, the distributions are conditional and can be stored directly as entries of the conditional probability tables associated with each hazard node. Being parents of the hazard nodes, boundary conditions and DRR measures define the dimensions of the conditional probability tables. By simulating those storm scenarios that correspond to all possible value combinations, the tables are completely filled. In the final step, the conditional hazard distributions were transformed to conditional impact distributions with vulnerability steps.

BN implementation at the case study sites

The schemes of the BNs implemented for the Tordera Delta and Lido degli Estensi-Spina case study sites are shown in Figure 6.8 and Figure 6.9 respectively. The nodes (circles) define the variables of the network, while arcs (arrows) show the relations between the variables. The BCs are the blue nodes, and the location and distributions (R) of the receptors are the grey nodes. These nodes affect those in dark orange, which refer to the receptors' hazards (H). The hazard was then transformed through the vulnerability relations into consequences (C), which are represented by the light orange circles. The measures' nodes (M) are indicated in green and can affect the H, C, or R nodes.

The structure is very flexible and can be applied at different coastal settings. As anticipated, the scheme can be adapted with different BC, H, R, C and M depending on the needs driven by research and/or coastal management objectives. It follows that, for very similar coasts, or even for the same case study, the scheme can differ. Additional hazards can be included for the same (or additional) receptors taking into account the proper boundary conditions and vulnerability curves. More measures can be tested, also including efficiency analysis (Cumiskey et al., 2017). Other examples can be found in Jäger et al. (2017), Plomaritis et al. (2017) and other scientific works related to the EU RISC-KIT project.

Whit regard to the present work, the BC variables were divided in equidistant ranges (see Table 6.1) that were defined in order to minimize the simulations needed, while limiting the loss in accuracy. As first application of the methodology, this was considered a good compromise, although more combinations (and thus, more computational effort) would capture in better details the variability of the source. For each combination of BC, the selected storm was repeated twice (see Section 6.3.2). Then, all simulations were repeated for the scenarios that affected the hazard component of the assessment (i.e. CCS and DRR; see details in Section 6.3.5) A total of 96 simulations were included in the BNs for both case studies. The H and C variables were divided accordingly to the definitions and assumptions adopted to calculate the impacts (see Section 6.3.4). The trained BN was used to explore and compare scenarios, focusing on the variation of the impacts (consequences). In particular, uniform

distributions of BC (forcing, source) were considered, disregarding the real distribution of the forcing. The discussion of this aspect can be found in Section 6.5.

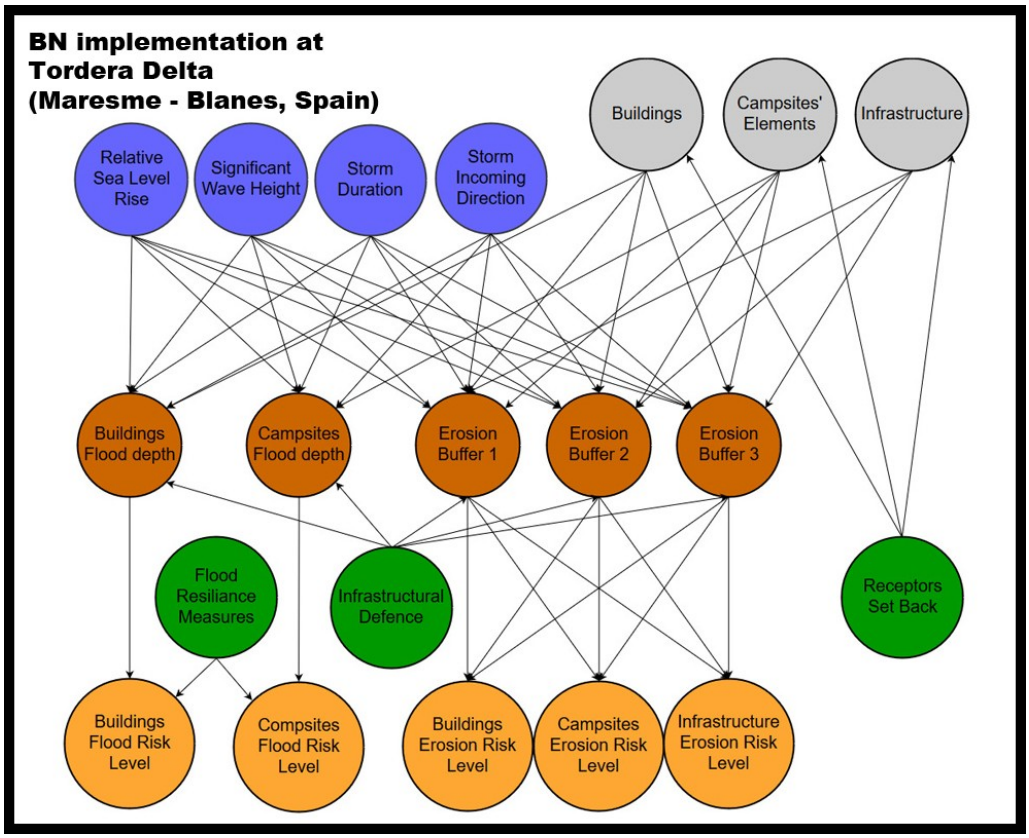

Figure 6.8 Bayesian Network scheme for the Tordera Delta site.

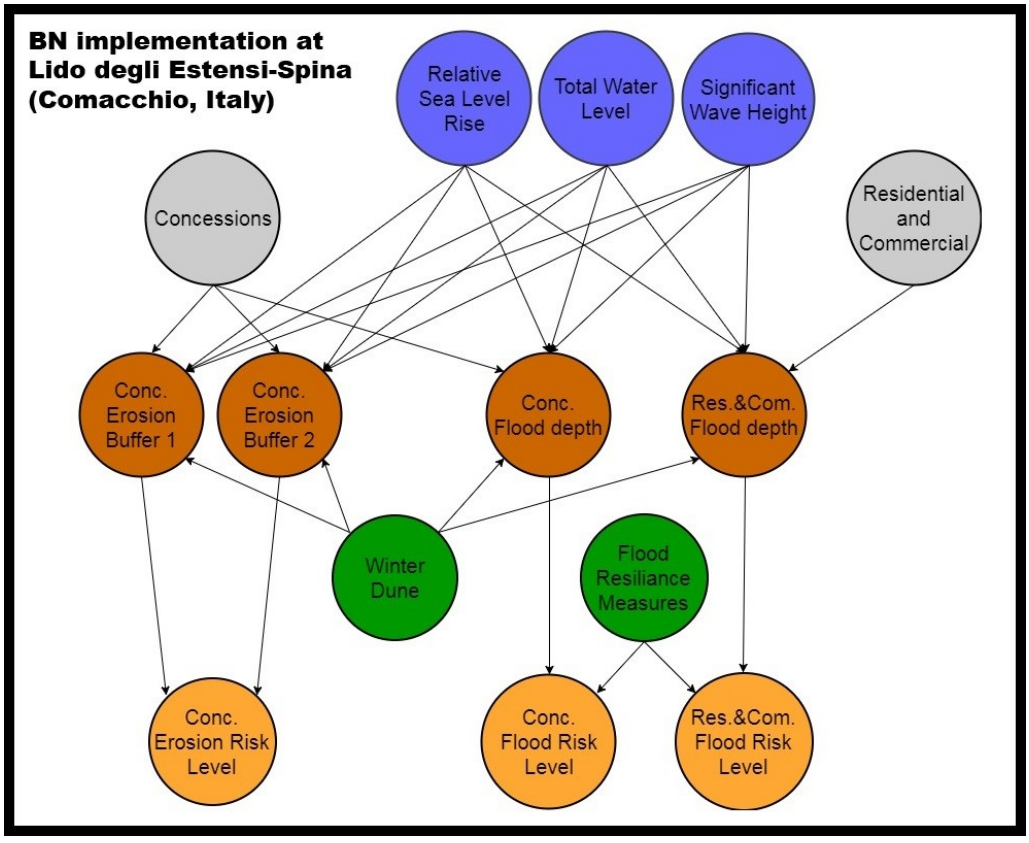

Figure 6.9 Bayesian Network scheme for the Lido degli Estensi-Spina site.

6.4 Results

In this section, the results of scenario testing are provided for each case study through an integrated comparison of computed risk levels in terms of percentages of receptors at each level of risk for flooding and erosion for each type of receptor and relevant location in the CUS and CCS. The DRR impacts are shown by comparing the risk levels in the CUS and CCS with those computed in each scenario with the implemented DRR.

The results are generated through the BN by setting uniform distributions of forcing combinations, assuming that no prior knowledge of the forcing input is available but their possible ranges. This is shown to be sufficient for the purpose of exploring scenarios.

6.4.1 Tordera Delta

The results assessment was performed separately for both sides of the river at s'Abanell beach at the north and Malgrat beach at the south. The inundation impact assessment considered all receptors at the study site whereas the erosion analysis focussed only on the first 20-m band of hinterland because the only receptors exposed to an erosion hazard are located in that area.

The results of the flooding impacts on campsite elements and houses (Figure 6.10 to Figure 6.13) indicate that in the CUS (E incoming storms with current MSL), campsite elements at both sides of the river mouth are expected to suffer the same magnitude of damages: 80-83% of elements will be safe, while only 2-3% of the elements are under high-impact risk (Figure 6.10). The situation differs slightly when assessing houses (Figure 6.12), since more damages are expected to occur south of the river mouth (20% of elements are at low risk and 2% at medium risk), rather than in the northern domain (2% at low risk and 1% at medium risk).

When assessing the CCS, results demonstrate a different behaviour at each side of the river mouth. In S'Abanell, the SLR significantly increases the impacts of flooding (CCS1, Figure 6.10), whereas the directional shift of storm direction (equal frequency of E and S incoming storms) does not increase any of the receptors at risk (CCS2 and CCS3, Figure 6.11). In the CCS1, the impact on campsite elements increases from 17% to 37% of affected receptors. Campsite elements expected to suffer high impacts increase from 2% to 14%. However, expected impacts under CCS2 are similar and even lower than those observed under the CUS, and the results obtained for CCS3 are comparable to CCS1 for the northern domain.

On the other hand, south of the river mouth, the response to CCS is equally sensitive to changes in storm incoming direction than to SLR. In fact, 50% of houses and 56% of campsite elements are affected by some level of impact under CCS1 (Figure 6.10 and Figure 6.11), while 38% of houses and 40% of campsite elements are affected under CCS2 (Figure 6.11 and Figure 6.13). Therefore, when CCS3 conditions are tested south of the river mouth, the outcome obtained from the BN shows that 63% of houses (34% at medium risk) and 69% of campsite elements (41% at high risk) are affected.

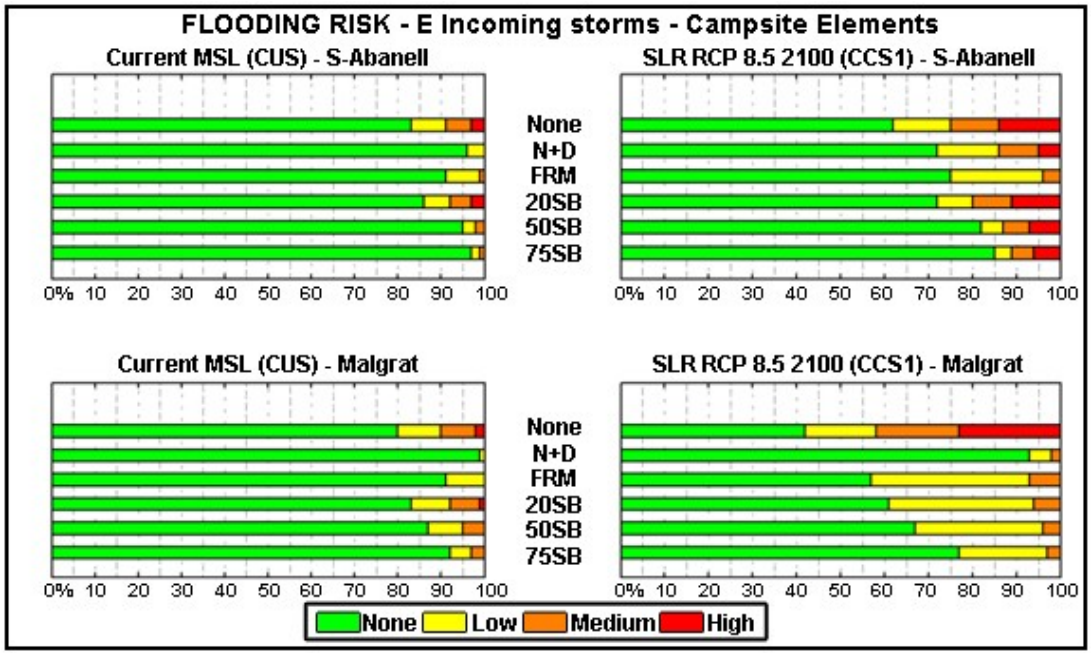

Figure 6.10 Distribution of campsite elements at every level of flooding risk. Top-left: current scenario at S'Abanell; Top-right: climate change scenario 1 (SLR) at S'Abanell; Bottom-left: current scenario at Malgrat; Bottom-right: climate change scenario 1 (SLR) at Malgrat. Each bar in a panel represents a DRR configuration ("None": no DRR implemented; "N+D": Nourishment and Dune; "FRM": Flood Resilience Measures; "20SB", "50SB", and "75SB": 20, 50, and 75 m setbacks, respectively).

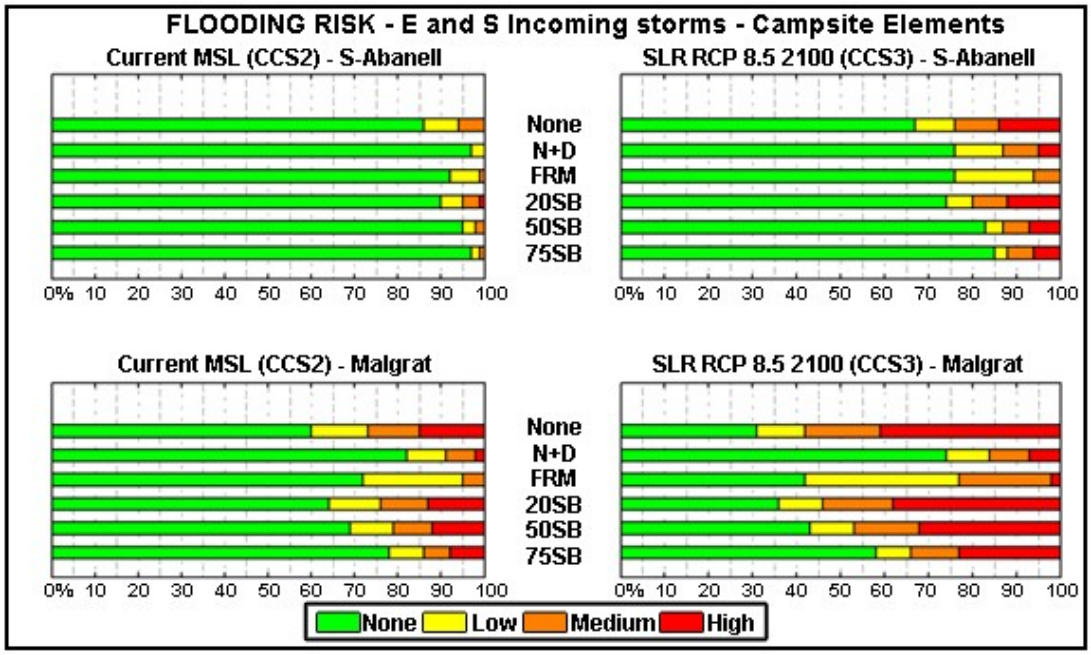

Figure 6.11 Distribution of campsite elements at every level of flooding risk. Top-left: climate change scenario 2 (50-50% east-south storms) at S'Abanell; Top-right: climate change scenario 3 (50-50% of east-south storms + SLR) at S'Abanell; Bottom-left: climate change scenario 2 (50-50% east-south storms) at Malgrat; Bottom-right: climate change scenario 3 (50-50% of east-south storms + SLR) at Malgrat. Each bar in a panel represents a DRR configuration ("None": no DRR implemented; "N+D": Nourishment and Dune; "FRM": Flood Resilience Measures; "20SB", "50SB", and "75SB": 20, 50, and 75 m setbacks, respectively).

Comparing the effectiveness of the DRR highlights N+D as the most effective measure against flooding for the CUS and all tested CCS. As expected, the effectiveness is higher in Malgrat than in S'Abanell, as beach nourishment is located only south of the river mouth and the dune is present on both sides. It was observed that all significant impacts (medium and high) to receptors under the CUS were removed for both sides of the river. Moreover, at the Malgrat domain, the number of affected receptors was reduced by 19%-22% for the CUS, CCS1, and CCS2 scenarios, and 40-46% under CCS3.

The implementation of the FRM was effective in terms of preventing high impacts on any receptor, but did not significantly reduce the total number of receptors affected by some level of risk. The magnitude of reduction of receptors at risk was ~9%. It should be mentioned that this is a theoretical measure, as it was assumed that the FRM were properly designed and 100% effective for site conditions.

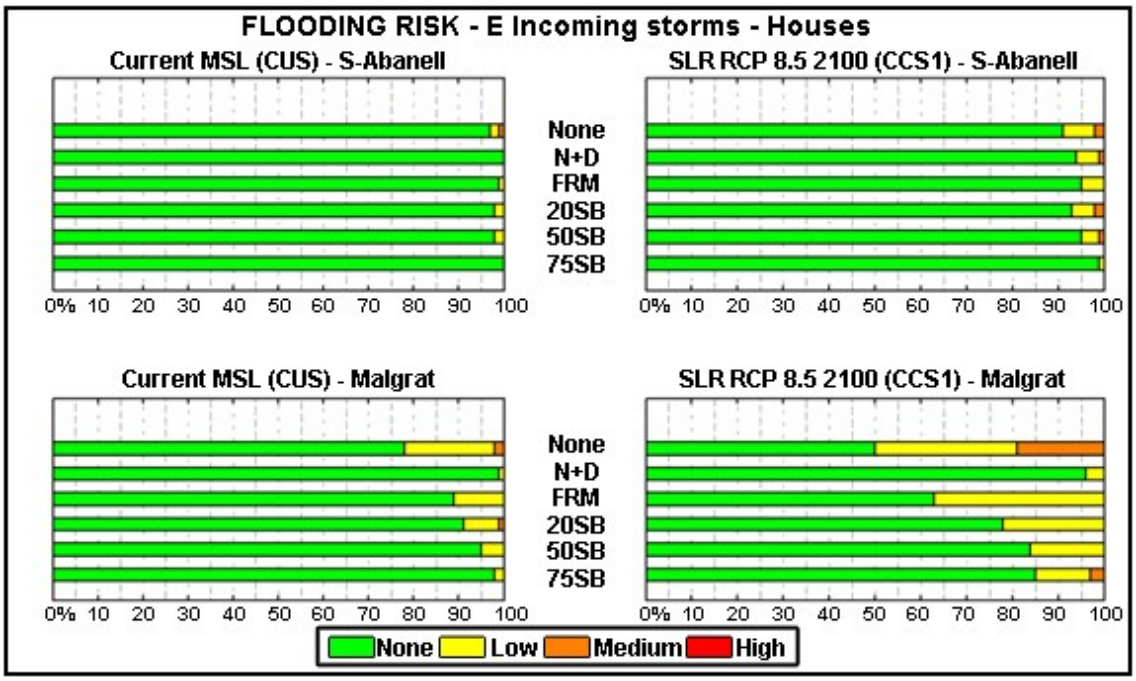

Figure 6.12 Distribution of houses at every level of flooding risk. Top-left: current scenario at S'Abanell; Top-right: climate change scenario 1 (SLR) at S'Abanell; Bottom-left: current scenario at Malgrat; Bottom-right: climate change scenario 1 (SLR) at Malgrat. Each bar in a panel represents a DRR configuration ("None": no DRR implemented; "N+D": Nourishment and Dune; "FRM": Flood Resilience Measures; "20SB", "50SB", and "75SB": 20, 50, and 75 m setbacks, respectively).

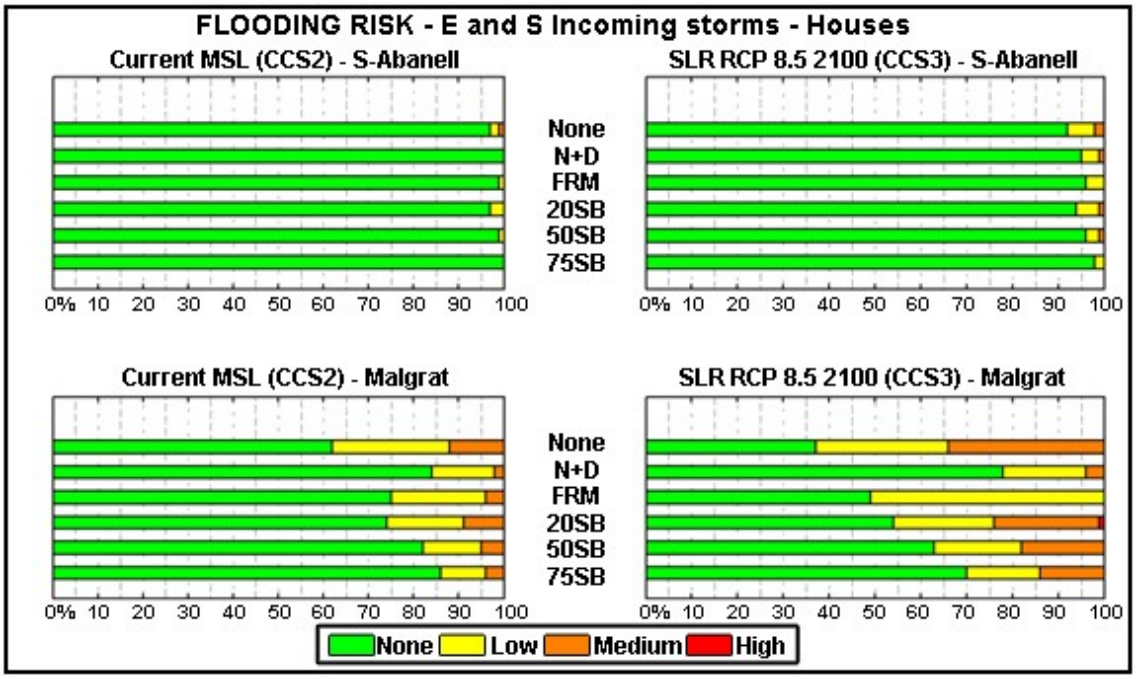

Figure 6.13 Distribution of houses at every level of flooding risk. Top-left: climate change scenario 2 (50-50% east-south storms) at S'Abanell; Top-right: climate change scenario 3 (50-50% of east-south storms + SLR) at S'Abanell; Bottom-left: climate change scenario 2 (50-50% east-south storms) at Malgrat; Bottom-right: climate change scenario 3 (50-50% of east-south storms + SLR) at Malgrat. Each bar in a panel represents a DRR configuration ("None": no DRR implemented; "N+D": Nourishment and Dune; "FRM": Flood Resilience Measures; "20SB", "50SB", and "75SB": 20, 50, and 75 m setbacks, respectively).

Finally, three RSB were tested: 20 m (20SB), 50 m (50SB), and 75 m (75SB). The results indicate that only the 75 m setback demonstrated a risk reduction magnitude comparable to infrastructural defence; however, in most cases, the efficiency of the N+D was higher than the managed retreat. Only in S'Abanell, with higher topography and where the measure consists of only dune without nourishment, a greater risk reduction was achieved through the 75SB.

Results for the erosion impact risk assessment showed similar results for the three analysed receptor categories and no significant differences between CUS-CCS1 and CCS2-CCS3. For simplicity, results related to Campsites (Figure 6.14) and Infrastructure (Figure 6.15), for the CUS and CCS1 scenarios are provided in the following.

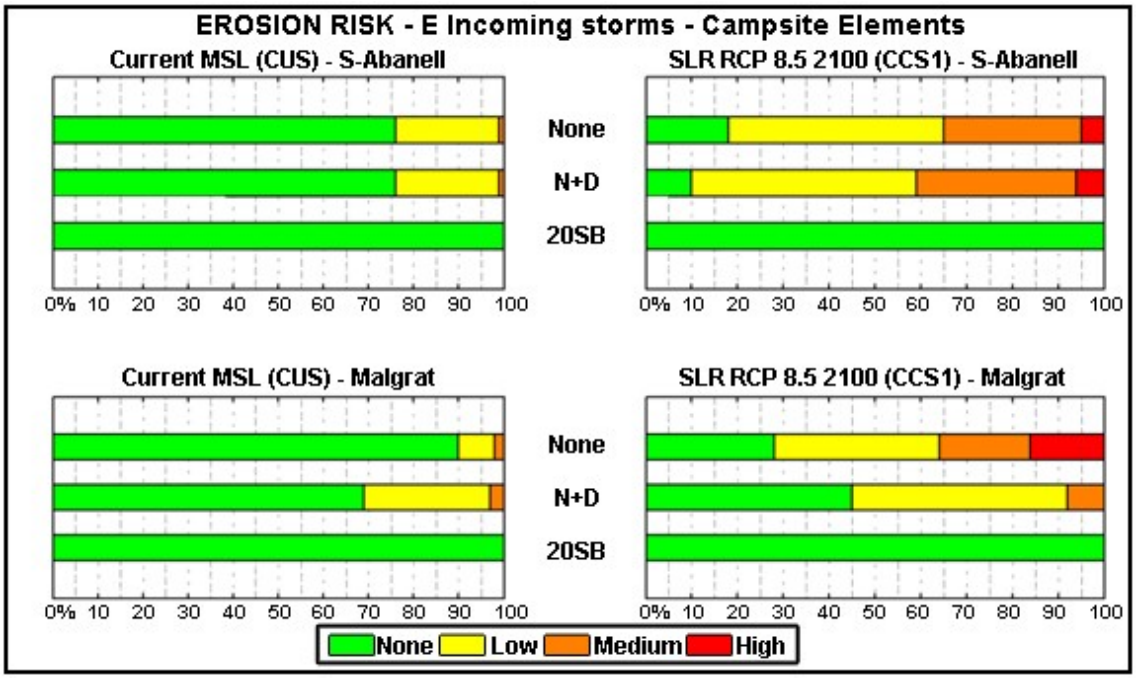

Figure 6.14 Distribution of campsite elements at every level erosion risk. Top-left: current scenario at S'Abanell; Top-right: climate change scenario 1 (SLR) at S'Abanell; Bottom-left: current scenario at Malgrat; Bottom-right: climate change scenario 1 (SLR) at Malgrat. Each bar in a panel represents a DRR configuration ("None": no DRR implemented; "N+D": Nourishment and Dune; "FRM2: Flood Resilience Measures; "20SB", "50SB", and "75SB": 20, 50, and 75 m setbacks, respectively).

Under the CUS, 23% of campsite receptors (Figure 6.14) in s'Abanell and 8% in Malgrat are at low risk, whereas only 1-2% demonstrate a medium risk in both areas. The CCS indicated that the level of erosion risk increases much more when the SLR increases than for the directional switch of incoming storms on both sides of the river mouth. In the CCS1 scenario, receptors located in s'Abanell at medium risk increase to 30%, while 5% are at high risk. In Malgrat, the same scenario results in 20% of campsite elements being at medium risk and 14% at high risk. On the other hand, the CCS2 scenario does not imply a significant difference for the CUS and similarly, the impacts in CCS3 are comparable and lower than those obtained for CCS1.

Focusing on the infrastructural receptors (Figure 6.15), the promenade at the north of the river mouth is currently at significant risk (70% at medium risk and 13% at high risk), whereas the road in Malgrat is potentially safe. In the CCS1 scenario, the assessment highlights that because of the increase of MSL and corresponding morphological accommodation, the percentage of promenade under high risk and therefore direct erosion at the toe increases up to 33%,with some impact on the road in Malgrat.

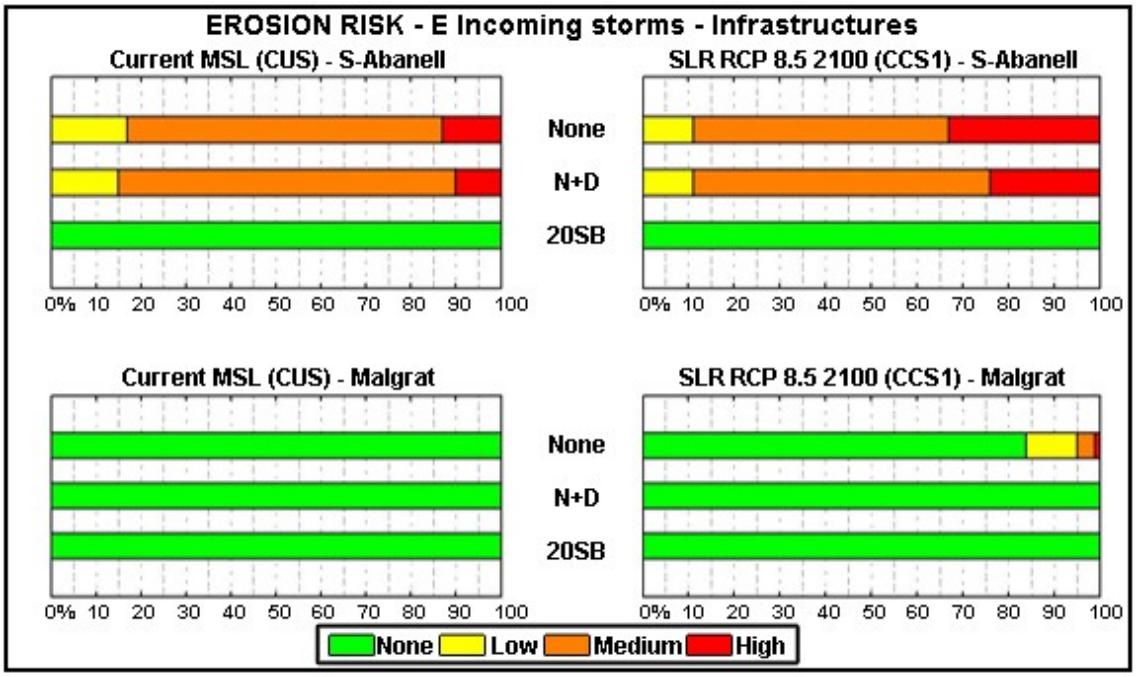

Figure 6.15 Distribution of Infrastructures at every level erosion risk. Top-left: current scenario at S'Abanell; Top-right: climate change scenario 1 (SLR) at S'Abanell; Bottom-left: current scenario at Malgrat; Bottom-right: climate change scenario 1 (SLR) at Malgrat. Each bar in a panel represents a DRR configuration ("None": no DRR implemented; "N+D": Nourishment and Dune; "FRM": Flood Resilience Measures; "20SB", "50SB", and "75SB": 20 , 50, and 75 m setbacks, respectively).

The assessment of the efficiency of the DRR regarding erosion indicates that the N+D does not have any significant impact on reducing risk. In fact, in some scenarios, the number of affected receptors at low risk seems to increase, because of the indirect effect of alongshore change in erosion/accretion patterns caused by the measure. In addition, the beach nourishment is regularly washed out in severe storm conditions. In the case of the road in Malgrat, the nourishment is placed in a position with higher local erosion rates; thus, the measure prevents the impact in CCS1. On the other hand, RSB is 100% effective in dealing with the impact of erosion, and the 20SB is enough to cope with risk under the present situation and for all future projected conditions.

6.4.2 Lido degli Estensi-Spina

The overall results for the risk of flooding for residential and commercial buildings located in the towns of Lido degli Estensi and Lido di Spina are provided in Figure 6.16. The overall results for concessions are shown in Figure 6.17 and Figure 6.18, for flooding and erosion risks respectively.

The CUS for residential and commercial buildings (Figure 6.16) evidenced that most receptors in Lido degli Estensi-Spina are safe from flooding impacts, with the exception of the 2% at low risk in Lido degli Estensi. In the CCS, the receptors at low risk increased in Lido degli Estensi to 10%, while 1% were at medium risk. The increase in receptors at low risk is more limited in Lido di Spina (–5%). The WD demonstrated a positive effect on receptors' level of risk. In particular, under the CCS, it decreased the receptors at low risk by almost 10% of the total. The effect of FRM is limited to the CCS at Lido degli Estensi, where the receptors at medium risk were reclassified at a low level.

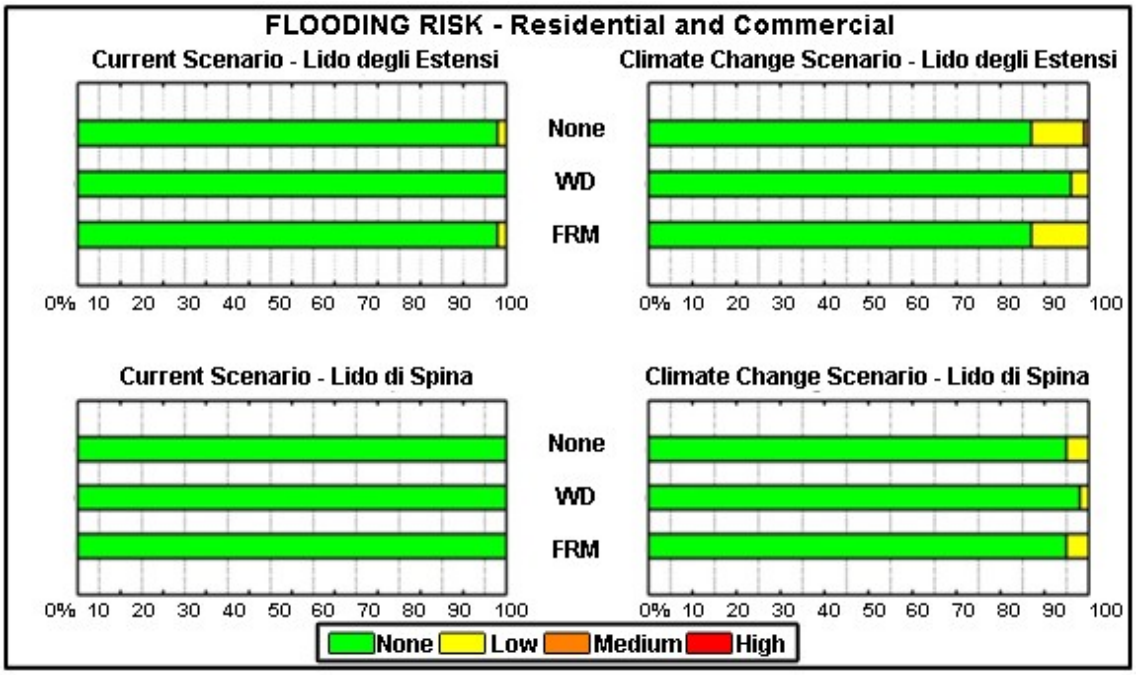

Figure 6.16 Distribution of residential and commercial buildings for every level of flooding risk. Top left: current scenario at Lido degli Estensi; Top right: climate change scenario at Lido degli Estensi; Bottom left: current scenario at Lido di Spina; Bottom right:climate change scenario at Lido di Spina. Each bar in a panel represents a DRR configuration ("None": no DRR implemented; "WD": Winter Dune; "FRM": Flood Resilience Measures).

Focusing on the flooding risk for concessions (Figure 6.17), the CUS evidenced noticeable impacts. At Lido degli Estensi, almost 30% of receptors were categorised at low risk and 15% at medium risk. In comparison, at Lido di Spina, the receptors at risk increased in number and intensity. The results showed that 27% were at low risk, 25% at medium risk, and 6% at high risk of flood. The CCS exacerbated the impacts for both locations. At Lido degli Estensi, the concessions at low risk increased to 50%, those at medium risk remained stable, but 8% of receptors were at high flooding risk. Similarly, at Lido di Spina, the percentages of concessions categorised at risk increased to 34% at low risk, 33% at medium risk, and 20% at high risk.

The WD system had a positive impact in all cases for both the CUS and CCS. At Lido degli Estensi, the concessions at risk decreased from 44% (29% at low and 15% at medium risk) to 10% (only low risk) of the total for the CUS. The same scenario for Lido di Spina demonstrated limited impacts (13% at low and 3% at medium risk) for concessions when the WD was implemented, while the total receptors at risk without DRR was 58%. The impacts on the CCS also decreased with the WD compared to the scenario without DRR. For Lido degli Estensi, where previously more than 60% of concessions were at risk, 8% of the receptors were at low risk and 14% at medium risk. At Lido di Spina, the positive effects of the WD system increased the percentage of safe receptors from 13% to 59%, thus decreasing the concessions at risk (26% at low, 6% at medium, and 9% at high flooding risk).

The FRM had positive effects on impacts by moving all receptors at medium risk to the low risk category. In particular, under the CUS, the concessions at low risk increased from 29% to 44% and from 27% to 52% at Lido degli Estensi-Spina respectively. For the CCS, the same results increased from 50% to 65% at Lido degli Estensi, and from 34% to 67% at Lido di Spina.

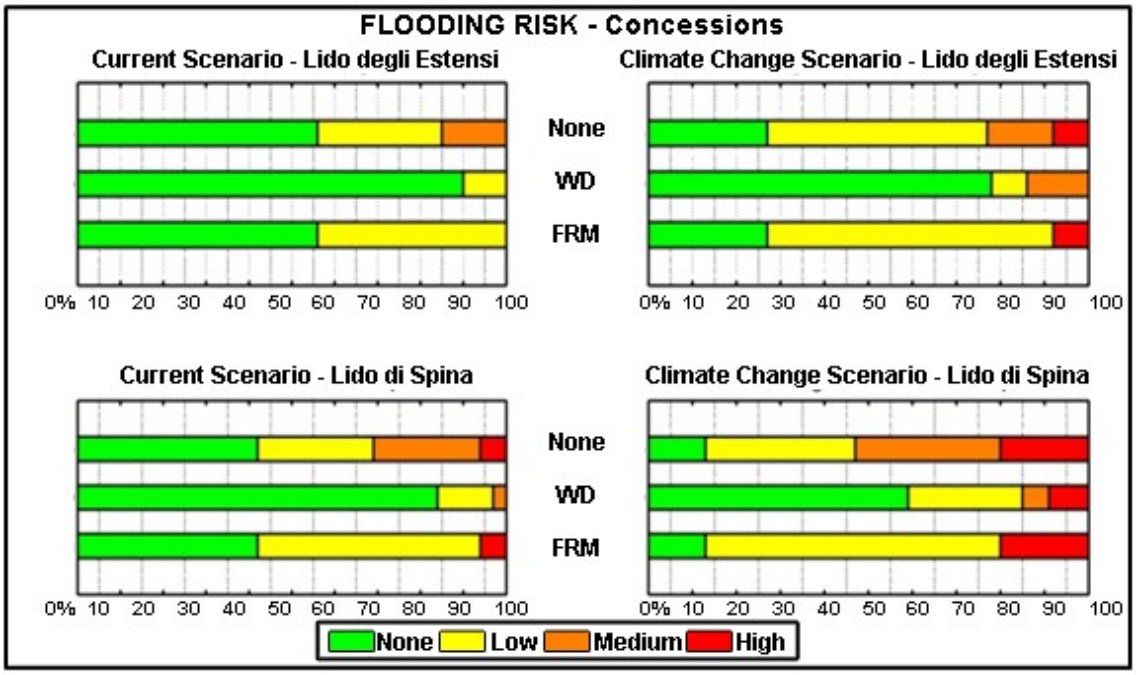

Figure 6.17 Distribution of concessions for every level of flooding risk. Top left: current scenario at Lido degli Estensi; Top right: climate change scenario at Lido degli Estensi; Bottom left: current scenario at Lido di Spina; Bottom right: climate change scenario at Lido di Spina. Each bar in a panel represents a DRR configuration ("None": no DRR implemented; "WD": Winter Dune; "FRM": Flood Resilience Measures).

The risk assessment results related to coastal erosion (Figure 6.18) showed the potential level of damage of risk under the CUS: 8% and 14% of concessions at Lido degli Estensi-Spina respectively. In the CCS, the previous results increased to 11% and 30% respectively. Notably, 1% of the concessions in Lido degli Estensi were indicated as being possibly damaged.

The WD system demonstrated positive effects on the potentially damaged concessions at Lido di Spina under the CUS by decreasing the receptors at potential risk from 14% to 5%. In contrast, at Lido degli Estensi, the potentially damaged receptors increased from 8% to 13% when implementing the WD DRR. This negative effect also occurred in the CCS. At Lido degli Estensi, the receptors at potential risk increased to 17%, while damaged receptors remained stable. At Lido di Spina, the WD had a contradictory effect. It decreased potentially damaged receptors to 14% and increased damaged concessions to 2%.

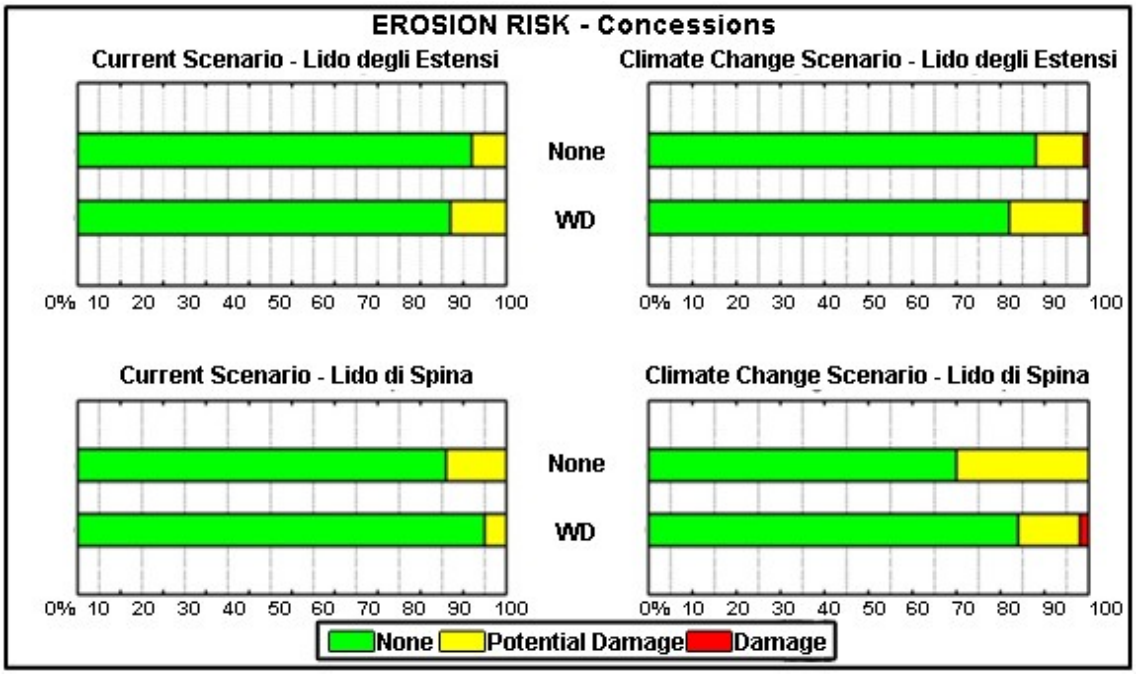

Figure 6.18 Distribution of concessions for every level of erosion risk. Top left: current scenario at Lido degli Estensi; Top right: climate change scenario at Lido degli Estensi; Bottom left: current scenario at Lido di Spina; Bottom right:climate change scenario at Lido di Spina. Each bar in a panel represents a DRR configuration ("None": no DRR implemented; "WD": Winter Dune; "FRM": Flood Resilience Measures).

A further step in the analysis of risk scenarios was undertaken using the BN to show the distribution of the boundary conditions that generate flood damage to concessions at Lido degli Estensi-Spina in the configuration without and with the WD DRR. The BN enables assessing the distribution of boundary conditions related to an impact scenario where all receptors suffer consequences uniformly for all risk levels (i.e. all receptors are affected by flooding at least at a low level of risk). The results of this analysis are shown in Figure 6.19 for the CUS, with (green bars) and without the WD DRR (red bars). The graph on the left shows the distribution of the TWL and the H_s on the right.

Notably, under the CUS without DRR, the H_s is distributed more uniformly (values ranging from 15% to 31%) compared to the TWL, which demonstrated a strong tendency to increase (values ranging from 10% to 58%). This indicates that compared to wave conditions, the water level is the main driver for flood impacts.

The results for the WD DRR scenario showed that the most probable conditions leading to flood damages to concessions are TWL > 1.45 m (93%) and H_s > 4 m (4 < H_s < 5 m: 47%; 5 < H_s < 6 m: 43%). These results indicated that the WD DRR in the CUS can minimise the consequences of coastal storms with TWL < 1.45 m and H_s < 4 m.

The same analysis was performed for the CCS, as shown in Figure 6.20. In this case, the scenario without DRR (green bars) demonstrated a less dominant influence of TWL (ranging from 24% to 40%) on flood consequences to concessions, even if still stronger than the H_s, and an almost uniform distribution (all bins around 25%). As expected, the RSLR (+0.3 m; RCP8.5 by 2050) increased the risk of lower intensity storms. Thus, in general, under the CCS, all storm combinations generated flood consequences to concessions.

The results for the WD (red bars) in the CCS showed that the most probable condition leading to flood damages to concessions is when TWL > 1.45 m (75%) in combination with H_s > 4m (4 < H_s < 5 m: 35%; 5 < H_s < 6 m: 33%). Thus, under the CCS, the influence of the WD system is less effective than the CUS. Indeed, lower intensity storms can still lead to flood damages to concessions (TWL < 1.45 m: 25%; H_s < 4 m: 32%).

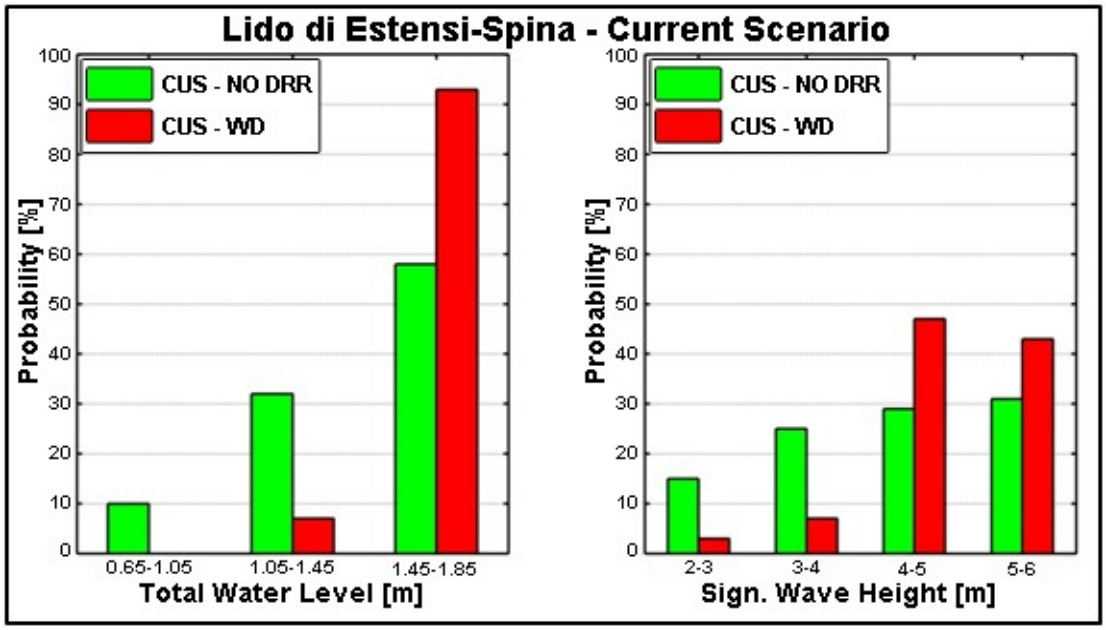

Figure 6.19 Distribution of boundary conditions (TWL on the left and H_s on the right) that generate flood damages in the current scenario for Lido degli Estensi-Spina. The configuration without DRR (green bars) and for the implementation of the WD DRR (red bars) were compared.

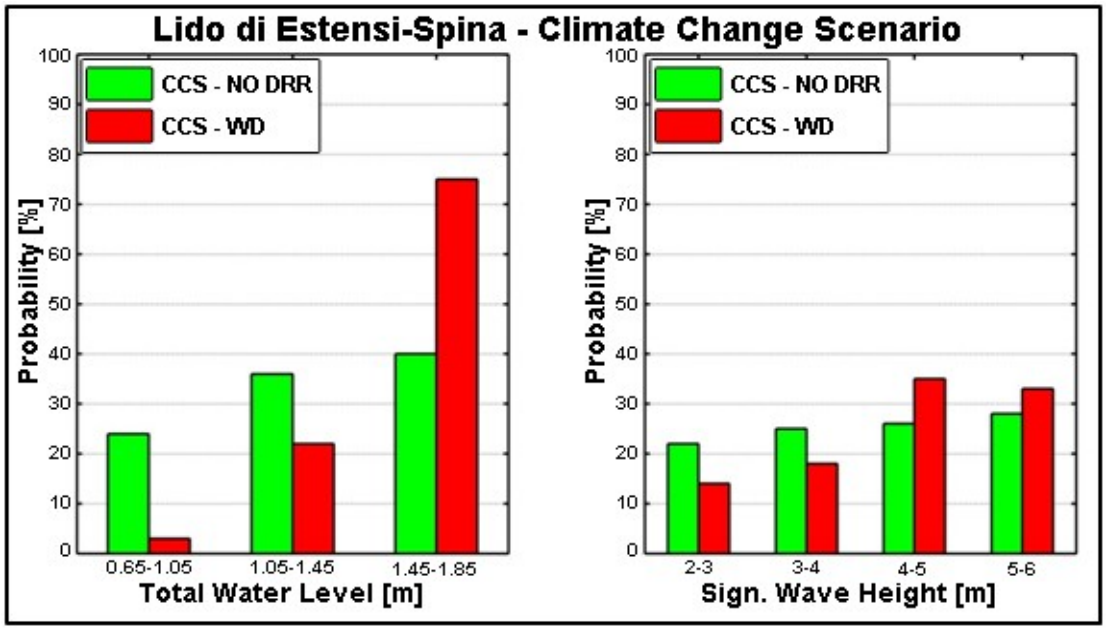

Figure 6.20 Distribution of boundary conditions (TWL on the left and H_s on the right) that generate flood damages in the climate change scenario for Lido degli Estensi-Spina. The configuration without DRR (green bars) and under the implementation of the WD DRR (red bars) were compared.

6.5 Discussion

The aim of the present work was to demonstrate the application of the RISC-KIT Hotspot tool (Jäger et al., 2017) at two Mediterranean sandy beaches (Tordera Delta, Spain and Lido degli Estensi-Spina, Italy). The tool acts at the level of the prevention phase of the disaster management cycle. It was designed (and it was here applied) as a DSS for coastal management and therefore used for comparison purposes to support the assessment of DRR strategic alternatives. The approach was thought to follow an investigatory process (see Martinez et al., 2017) where stakeholders and end-users were interviewed to select possible DRR measures for critical coastal areas (i.e. local scale). The involvement of local people and managers should guarantee the acceptability of the pre-selected measures. Finally, the aim of the tool was to provide rather simple information on the (combination of) measures to be used in a participatory process (see Barquet and Cumiskey, 2017) aiming at selecting acceptable measures to be applied as part of an integrated local strategy for risk reduction.

With regard to this specific work, the application of the tool as DSS allowed the analysis of a large set of simulations, covering many (current and future) conditions and multiple hazards. Following the approach, results were integrated in a BN including the assessment of consequences (impacts) for the receptors and the effect of DRR measures that were preselected on the basis of stakeholders' interviews. Certainly, the analysis has some inherent uncertainties associated with the implementation of the steps of the SPRC concept. However, the approach has demonstrated flexibility. As such, its application to other types of risks (i.e. rock falls, landslides, etc.) is currently under investigation. In addition to the use as DSS, the tool has the potential to be applied as an EWS (Plomaritis et al., 2017) once it is properly validated. However, for that purpose, more focus on the validation of the model chain is needed.

Some general aspects related to the use of a BN-based approach are worth to mention. The BN indeed can produce different kinds of outcomes, such as the impacts of real distributions of inputs or specific events, either equal to known historical ones or related to given return periods. This probabilistic approach, in particular, requires prior analyses of forcing, not always available at local level because of lack of data. On the other hand, coastal managers could be interested in assessing measures in terms of impact reduction disregarding the real distribution of possible events. This work demonstrated that this can be successfully done considering all the possible (but still realistic) occurrences of forcing combinations. Indeed, the results were produced considering uniform distribution of storm combinations being able, however, to provide useful information on the tested measures. Moreover, once the BN is properly trained, it can be used to provide the results for a given distribution of forcing or a single event (probabilistic or deterministic). In this work, the balance between computational expense and accuracy was pursued. Therefore, the chosen forcing combinations (i.e. source) were limited to those defining most important storm features driving coastal impacts and variable discretization was performed with equal intervals covering the whole range of so far observed values. Nonetheless, the BNs integrated 96 simulations at each site. Uncertainties related to individual process-oriented models or vulnerability curves were not included in this application. However, the methodology can easily integrate them when simulations from multiple models are used to feed the BN and uncertainties related to damage curves are known.

In the following sections, specific uncertainties and limitations of the application of the approach at both study sites are presented and discussed alongside the obtained results. Then, an overview is given, integrating the results from both sites.

6.5.1 Tordera Delta

The source characterization and the variables' categorization affect the accuracy of the output of the BN. Some input parameters have a wide range (30 hrs steps in duration and only 2 main wave directions) and more simulations are desirable for a better representation of the variability of the results inside each bin. Alternatively, a higher bin resolution could be tested at the expense of a significant increase in computational efforts. The tested combinations provide a representative picture of the coastal response of the site and effectively describe the input-output relations meant to be captured in the BN. Larger amounts of forcing time series would better represent the schematisation for all combinations of storms, reducing those represented through synthetic events.

Later, a model chain to obtain the hazards' pathway was set and implemented. The validation of both models in the model chain (SWAN and XBeach) was performed using the St. Esteve 2008 event (Sanuy and Jiménez, submitted). Better validations of the model chain could be achieved using more storms to cover a representative range of characteristics for the site.

Regarding receptors and consequences, the locations of receptors have little associated uncertainty. Houses and promenades were derived from accurate land use data available for the site, and the campsite elements were manually located and delimited from available GIS-based tools and raster imagery. Some uncertainty remains, associated with the natural mobility of some campsite elements between seasons. Identification of receptors was static in time and based on assuming the worst case (i.e. campsite elements present at any campsite space allocated to them). A future projection of distribution and number of receptors was not performed.

The damage curves used in the analysis for houses and campsite elements (Table 6.3) were derived from the recommendations by Agència Catalana de l'Aigua (2015) and the FEMA (2001) guidelines; therefore, no specific depth-damage curve derived and calibrated for this specific site was used, which may introduce additional uncertainty to the performed analysis on induced damages. Erosion buffers were selected according to the experience from the side, and aimed to represent the impact on the protective function of the coast. Additional assessments could include the impact on the recreational function related to the loss of beach width.

The CCS based on RCP8.5 SLR had the inherent uncertainties of said projections. The effect of directional changes of incoming storms represents a hypothetical scenario for comparison purposes. Casas-Prat and Sierra (2012) predicted directional changes related to mean sea conditions, but whether these changes will also affect storms is uncertain.

Regarding the DRR measures, it was assumed that protective strategies are completely and efficiently implemented when the storm event occurs. This means that for the FRM, it was assumed that all elements in the area (campsites and houses) implemented flood-proofing measures. However, social and economic conditions influence the percentage of campsite or house owners in the area that take flood-proofing measures, likely reducing this value to below 100%. Further research is needed at the case study site for accurate estimations.

In terms of the setback analysis, the background erosion of the area (Jiménez et al., 2017c) was not considered. The measure is valid to cope with storm-induced hazards, but to be efficient in time, setback distances must be increased to include the expected magnitude of decadal shoreline retreat. This also applies to infrastructural measures, as the N+D was assumed to be in place every time a storm reaches the coast. This means that beach nourishment would have to be rebuilt each time after being eroded during a storm event to maintain the 50 m increase in beach width. Moreover, it was assumed

that the position and level of the barriers are adapted to the new position of the shoreline along with the predicted SLR.

Despite the limitations, the results obtained mimic the system behaviour under present conditions. For instance, the temporary capability of beach nourishment to protect the site against erosion is well known in the Tordera Delta, where several nourishments have been implemented over the last decade at both sides of the river mouth with the same outcome. The measure was completely washed out after the first incoming storm event. However, this measure should be considered in the DRR comparison, since one of the main needs of the economic activity of the area (campsites) is having a sandy beach available in front.

North of the river mouth (S'Abanell), erosion and overwash problems are the main issue for campsites and the promenade (Jiménez et al., 2011). This is well captured by the tool, which shows a notable increase of these impacts under the SLR. This is similar to the observed increase in damages due to the decadal background erosion of the site, where campsites located in unprotected areas are forced to lose the first line of elements progressively impacted by storms. The coastal promenade has also experienced increased damages over the last decades (Jiménez et al., 2011).

Thus, the primary results summarised in the following and observed as in accordance with known reality, are useful in providing coastal managers with an integrated global picture of the impacts at the site and the best measures to counter them.

The overall results indicate that both sites of the river mouth are likely to double expected flooding impacts after the SLR (CCS1). South of the river, impacts are also likely to double because of a switch in the direction of incoming storms, even without an increase in the MSL (CCS2). Therefore, at that side of the river, the combination of these two factors (CCS3) is likely to triple the expected flooding risk. This is not the case at the north of the Tordera, where the orientation of the coast means that the directional switch does not imply any significant increase on the extension and magnitude of flooding. The erosion hazard is likely to increase under CCS1, and no significant increase is expected for the other two climate change scenarios (CCS2 and CCS3). The expected increase in erosion impacts is larger than for flooding, since the beach accommodation and future MSL mean that receptors are likely to be affected by erosion. Furthermore, the magnitude of the hazard itself is expected to worsen one magnitude in the present situation.

The most efficient DRR against flooding is beach nourishment and dunes, and the best option against erosion is managed retreat. However, each measure has drawbacks from the socio-economic standpoint, which must be assessed in a further step, since the aim of the BN tool is to objectively assess the efficiency of reducing impacts.

6.5.2 Lido degli Estensi-Spina

Regarding storm characterisation, all the events were designed using triangular design storms. Although this practice is common for numerical investigations, especially for erosion issues (e.g. Carley and Cox, 2003; McCall et al., 2010; Corbella and Stretch, 2012; Poelhekke et al., 2016), the listed assumptions may have introduced a degree of uncertainty in the modelling. This may lead to uncertainties in the simulation of the coastal flood extension and intensity, as well as on the erosion patterns and magnitude. Regarding overall representativeness, it must be highlighted that the forcing events (historical and synthetic) were selected to cover all possible (and realistic) combinations that can affect the area.

The XBeach model setup was affected by simplifications and assumptions as well as the uncertainty related to the input data (i.e. topo-bathymetry merged from different years). A proper calibration was not implemented, but the model was validated against the event in February 2015, evidencing a reasonable fit with observed flood inundation. However, a slight overestimation of the inundated area for the southern part of the Lido di Spina beach was demonstrated. Proper calibration and validation of the model is needed to improve the reliability of the results.

The location of receptors was estimated by cadastral maps from 2013. As an important aspect of risk assessment is the updating of exposed elements, more recent information can improve the results. For the CCS, no increase in exposure was considered, which may lead to underestimating the impacts. For coastal areas, an increase in exposed elements was forecast (IPCC, 2012). This aspect can exacerbate coastal risk at the regional level when compared to increases in local hazard conditions driven by climate change (Sekovski et al., 2015).

Uncertainties related to consequences are linked to the choice of vulnerability functions. The selected flood-damage curve (Scorzini and Frank, 2017) was the most recently developed for river floods in Italy. Although it was developed based on data of damage to residential buildings, it was applied here for coastal floods impacting all types of receptors. This increases the degree of uncertainty of the results, as the expected damages to a concession are likely to be lower than for a residential building for a given water depth. The methodology applied to link erosion patterns and potential damages was set a priori using homogeneous thresholds of 0.5 m and a 10 m buffer.

The uncertainties of the CCS definition are related to the reliability of the SLR future projections. Indeed, the RMSE of the predicted RSLR (including subsidence) was 28 cm in the northern Adriatic (the average RMSE for the central Mediterranean was 14 cm) (Vousdoukas et al., 2016). Thus, more detailed and consistent data may lead to more reliable impact projections. Moreover, the CCS was implemented without considering implicitly in the modelling the long-term morphological adaptation of the beach to SLR. However, this aspect can be assessed *a posteriori* through a profile response equilibrium model (Bruun, 1962).

The WD system was implemented modifying the topography in front of beach concessions using the Dune Maker 2.0 tool (Harley, 2014). The accuracy of the representation of this feature strongly depends on the alongshore resolution of the model, as the WD develops in that direction. Moreover, only one type of WD was tested, while more configurations should be investigated in which the geometry of the system is varied. It is important to underline that the efficiency of artificial dunes strictly depends on the beach width. Therefore, as observed by Harley and Ciavola (2013), the dune height and crest width (i.e. the sand volume of the dune) should be designed differently for different coastal stretches, such as the case of Lido degli Estensi-Spina, where the beach characteristics are not uniform. The location of the sand dune with respect to the MSL is another important component that can affect the final results.

The FRM measure was assumed a priori as completely effective. However, as its implementation depends on physical and socio-economic factors (e.g. education, economic status, etc.), which can decrease the efficiency of the measure, the assumption leads to overestimating its effect.

Despite the highlighted limitations, the comparative analysis of scenarios is robust and valid. Impacts related to the CUS are reliable in terms of magnitude and comparable with the knowledge of the area (Perini et al., 2016; Trembanis et al., 2017). Moreover,

the dominance of water level characteristics of storms on the impacts of flooding compared to wave characteristics is highlighted in previous works (e.g. Armaroli et al., 2012).

The impacts in the CCS increased compared to the CUS for all tested cases. In addition, when beach accommodation to the SLR was assessed *a posteriori*, the obtained shoreline retreat (Bruun, 1962) is 60-100 m, leading to a significant loss of the protective function of the beach. Thus, including beach accommodation would probably lead to higher erosion and flooding impacts than those previously presented.

As expected, the WD measure is effective in decreasing the impacts of flooding, as previously demonstrated by Harley and Ciavola (2013). Their research focused on two case studies in the Ravenna province, and tested different dune geometries against the impacts of the February 2012 event. That work and others (Wells and McNinch, 1991; Bruun, 1983) highlights the need for appropriate guidelines for dune implementation to limit beach manipulation due to scraping activities. Beach manipulation can lead to undesired changes in slopes (Wells and McNinch, 1991), and consequently in morphodynamics, which can locally increase the impacts of storms. In the case of Lido degli Estensi-Spina, the increase in erosion impacts on a few receptors can be attributed to the relative position between the receptors and discontinuities of the dune, which was designed as a non-continuous morphology. The induced alongshore variability increased localised erosive impacts. This was in contrast to the general decrease of erosion consequences for the majority of receptors, as demonstrated for the WD scenario compared to the configuration without DRR. The effect of the WD on adjacent beaches was not analysed. However, the scraping depths were in the range proposed by Bruun (1983) to avoid effects on adjacent beaches. The interest in FRM was related to the opportunity to merge the measure with the WD system. Indeed, the combination of measures can effectively reduce damage caused by floods.

6.5.3 Overview of the application at the study sites

At both study sites, the approach demonstrated impact responses in the current situation in accordance with existing knowledge on the sites. Tordera Delta, which is characterised by quick and intense erosive responses to storms, showed greater impacts to erosion than Lido degli Estensi-Spina. Inundation and erosion impacts are likely to increase in all assessed future projections at both study sites. As expected, the flooding impact in the current situation and projected increase in future scenarios is higher for receptors located closest to the shoreline or at the most low-lying areas of the hinterland (i.e. concessions at Lido di Spina and campsites at Malgrat). Regarding the impacts of future projected erosion, the obtained increase at the Tordera Delta was significantly higher than in the Lido degli Estensi-Spina, because of the morphological accommodation response to the projected MSL. This highlights the importance of including morphological adaptation to the SLR in impact and risk assessment studies.

The DRR assessment highlighted as effective the construction of artificial dunes as protection against inundation at both study sites, even when compared to other measures such as managed retreats or flood resilience measures applied to all receptors. However, the dune was less effective and sometimes ineffective against erosion at both study sites. As expected, and derived from results for the Tordera Delta, dune performance against flooding improved when tested along with beach nourishment. However, beach nourishment did not improve dune performance against erosion. Managed retreat seems to be the best option to tackle the impacts of erosion.

6.6 Conclusions

In this work, a methodological framework for storm-induced coastal risk management purposes developed within the framework of the RISC-KIT EU project, the so-called Hotspot tool, was presented and applied in two coastal study sites in the North Western Mediterranean and Northern Adriatic. The aim of the study was to test DRR measures in current and climate change scenarios. The measures were pre-selected through the analysis of stakeholders' interviews and the results of the testing, properly simplified, were then used as input for a participatory process to design local-scale DRR integrated strategies.

The study was based on the integration of the SPRC concept in a BN. This was fed with a large number of numerical simulations obtained through a model-chain composed of process-oriented models able to reproduce multiple storm-induced hazards at the receptor scale. The BN integrates impact results that account for all receptors in the hinterland. The tool can be regularly updated with additional simulations and extended with new scenarios.

The choice and discretisation of storm variables to perform the analysis covered all possible and realistic combinations at both study sites. The entire range of characteristics of forcing events was appropriately represented.

At both study sites, the implemented model chains successfully predicted the coastal response to storm events. Target hazards were suitably captured through the process-based models, which simultaneously assessed erosion and inundation.

A BN was used to integrated impact results, calculated at the receptor scale, from a large number of simulations to produce a robust comparative assessment. It was successful in detecting significant changes on expected impacts. Therefore, even with the inherent uncertainties and limitations, the BN approach allows realistic scenario testing and comparisons between DRRs.

Many types of results can be extracted from the BN tool once fed with data that are easy to interpret and quantitative (and therefore comparable). As expected, this work confirmed the potential of the BN as a data assimilation approach.

The work highlighted that the approach was able to quantify and compare current and future impacts for the receptors at both case studies. Most important for the coastal management point of view, DRR solutions were tested and compared. The comparison between sites evidenced that artificial dunes and managed retreat were the most effective measure against flooding and erosion impacts, respectively.

The approach can be further improved by addressing the limitations discussed in Section 6.5, including data and methodological improvements that, however, may increase computational efforts.

In conclusion, coastal management can be significantly improved by methodologies based on the integration of large amounts of data, stochastically condensed so that multiple scenarios can be easily compared. Uncertainties due to data quality, numerical approximation, simplifications, and assumptions will always be present. However, the assimilation of results though a BN provides robust comparison across different conditions. Therefore, the observed variations of impacts, when significant, will help decision-makers select between strategic alternatives of measures or, provide simplified information as input for participatory processes aiming at designing integrated local-scale DRR strategies.

7 CONCLUSIVE SUMMARY

Innovative approaches (i.e. drones, up-to-date numerical and statistical techniques, new conceptual frameworks for risk assessment) were applied for field monitoring, numerical modelling and coastal management. The applications on the Emilia-Romagna coast and some of its critical areas were paired, for some aspects, with implementations at the Tordera Delta (Catalunya, Spain). In each chapter, specific conclusions and further developments can be found whereas general integrated conclusions, key messages and opportunities for further studies are given in the following.

7.1 Key messages

7.1.1 Post-storm assessment protocols

The regional protocols for coastal storm post-event assessments in Emilia-Romagna showed some limitations in terms of acquired information and coastal domain coverage (Chapter 2). A local standardized, drone-based post-storm protocol, applied in February 2015 at Lido degli Estensi, demonstrated its effectiveness in collecting high-quality data to be successfully integrated, along with qualitative information, in regional response protocols.

> *Key message 1.1. Regional post-storm assessments protocols should be implemented by regional authorities after every major event. It is possible to support and integrate them with standardized local assessment protocols, that can help to collect qualitative and quantitative detailed data that can be used for multi-scale risk assessments. Furthermore, it is important to include local people perceptions in the post-storm assessments and use up-to-date technologies for data collection and process.*

7.1.2 Drones for coastal surveys and monitoring

Unmanned Aerial Vehicles (UAV) systems demonstrated to be very useful instruments for coastal field surveying. They were applied at the beaches of Lido degli Estensi (Chapter 2) and Porto Garibaldi (Chapter 3), on the Emilia-Romagna coast. Their capability to capture continuous, two-dimensional and high-resolution information was effective in determining the extension of the inundation of an extreme event (Chapter 2) and in the assessment of the morphodynamic beach response, under short term (Chapter 2) and seasonal forcing (Chapter 3). The ease with which UAVs can be used and the speed of the drone-based surveys, however, do not automatically imply an easy and precise result. In Chapter 3 it was demonstrated that very accurate results can be achieved by capturing images using automatic planned flights and adopting recognizable and precisely measured ground control points (GCPs). On the other hand, manual flights and the selection of inappropriate GCPs led to higher errors (Chapter 2). Besides, the photogrammetric process has to be applied iteratively, testing different setups to obtain the best accuracies of the final products, especially when dealing with subtle morphological features, such as those analyzed in Chapter 3.

> *Key message 2.1. UAVs have a great potential for the purposes of coastal research and risk assessments providing high-quality, high-resolution data. Considering their limitations, it is suggested to use*

them for local scale beach surveying, rather than extensive, large scale assessments. Besides, it is recommended to precisely organize and implement the field activities, as well as, to properly process the data with photogrammetric approaches, in order to provide reliable outcomes.

7.1.3 Numerical applications

Sophisticated numerical applications confirmed to provide unique contributions for accurate hazard and risk assessments. However, simplifications and assumptions propagate uncertainties into the final outcomes. The traditional approach of simulating storms with triangular synthetic time-series of forcing was found to produce considerable errors in the analysis of flooding and erosion hazard impacts, when applied, in Chapter 4, at two Mediterranean case studies (i.e. Lido degli Estensi and Spina, Emilia-Romagna, Italy and Tordera Delta, Catalunya, Spain). Notably, computing large number of simulations and statistically analyzing their outcomes in comparative terms can increase the reliability of the assessments, as demonstrated in Chapter 6.

Key message 3.1. Numerical-based studies are invaluable contributions for coastal research and hazard assessments, but are also affected by large uncertainties and errors that can influence further risk assessments. It is therefore important that every numerical-based assessment should be considered on the basis of its limitations and supported by uncertainty analysis.

Key message 3.2. Synthetic time-series of forcing are widely applied for coastal numerical studies but propagate uncertainties along the model chains. It is recommended, as future research topics, to analyze the propagation of uncertainties related to their use at different locations and applying diverse synthetic approaches.

Key message 3.3. Deterministic approaches for numerical analysis showed limitations that can be solved by simulating a large number of conditions in diverse scenarios. The analysis of these datasets should be performed with full or semi-probabilistic approaches.

7.1.4 Integrated coastal risk assessments

The RISC-KIT tools for coastal risk assessment were found to be an important contribution in support to coastal management. The CRAF tool for regional assessment was properly adapted and applied at the Emilia-Romagna coast and validated with historical information in Chapter 5. Socio-economic concepts were applied to evaluate the exposure of human assets. The Emilia-Romagna coastal managers (i.e. Servizio Geologico Sismico e dei Suoli) contributed to the application with valuable input. This confirms the importance of stakeholder involvements in the assessment process. The Hotspot tool was applied for testing risk reduction measure in the current and future scenarios, at two case studies, Lido degli Estensi and Spina and Tordera Delta, respectively on the coasts of Emilia-Romagna (Italy) and Catalunya (Spain) (Chapter 6). The tested measures were previously selected on the basis of stakeholder interviews, ant the outcomes of this study were used as a basis for a participatory process, where

stakeholders had to evaluate effective and acceptable risk reduction strategies. At the local level, socio-economic concepts for vulnerability and exposure characterization, applied with the support of experts and input from coastal managers, were found to be crucial to properly derive risk assessments. Bayesian Networks were found to be very effective tools for this study, especially for the analysis of the interconnections between variables and for scenario comparisons. Notably, the multi-disciplinary approach was invaluable in properly providing robust and effective frameworks for coastal assessment, at regional (Chapter 5) and local level (Chapter 6).

> *Key message 4.1. The RISC-KIT approach is a valuable methodology in support of coastal management that can hence rely on effective and flexible tools for risk evaluation and reduction. It is suggested to apply it order to provide multi-hazard, multi-disciplinary integrated risk assessments at different scales and to propose risk reduction strategies that can be easily accepted by the local communities.*
>
> *Key message 4.2. The participatory involvement of local stakeholders in the risk evaluation processes is very valuable. It is indeed effective in providing a comprehensive knowledge of the local socio-economic context and risk perception, in order to propose adequate risk reduction plans.*
>
> *Key message 4.3. Multi-disciplinarity is the key to properly address coastal risk issues. It is therefore suggested to adopt multi-disciplinary methodologies and approaches for risk evaluation and the preparation of reduction strategies.*

7.2 Research opportunities

In this section the main aspects that can be further investigated are summarized while more details can be found in the discussions and conclusive sections of each chapter.

Several limitations were discussed regarding the implementation of UAV for coastal surveying and photogrammetric reconstruction. More effort should be spent on addressing them, improving the quality and accuracy of the collected data, while focusing on new technological advancements of the hardware and software components. More applications on the coasts are needed in order to investigate limits and new exploitations of the UAVs. These applications should not only focus on the physical aspects but, also, on ecological and social ones.

Numerical models were demonstrated to be affected by large uncertainties. Limitations can arise at different steps of the modelling. These can actually be reduced with further investigations, however, will be always present. Further researches should focus on reducing complexity, increasing the control of the numerical tools and improving reliability. Pure numerical applications should be avoided in favour of approaches based on a good balance between field measurements, local knowledge and modelling.

The field of coastal management is evolving towards the adoption of more scientific, multi-disciplinary approaches for risk assessments and reduction. Future researches should focus on improving these aspects, widening the communication between managers, scientists and local stakeholders. The tools presented in this thesis are the

state-of-the-art. However, examples of application are limited and the tools should be applied at a larger number of coastal settings, including more aspects related to coastal risk, such as cost-benefit analysis, ecological and social considerations, uncertainty of the input and others. Besides, other fields related to coastal management are in need of improvements, such as the preparedness and response to the impact of coastal events. In this sense, researchers should focus on improving the reliability of forecasts and warning systems, while simplifying and strengthening the communication with, and between, the end-users, the coastal communities and the responders.

The PhD candidate is actually involved, through the COSTUF team (Dep. of Physics and Earth Sciences, University of Ferrara), in developing new approaches or improving the analysis reported in this thesis. Other field applications based on autonomous platforms and new technologies are under discussion and will be implemented in collaboration with Prof. Arthur C. Trembanis and the CSHEL team of the School of Marine Science and Policy of the University of Delaware (Newark, DE, US). Besides, the COSTUF team, in collaboration with Dr. Andrea Ninfo (Dep. of Physics and Earth Sciences, University of Ferrara), is implementing intensive UAV-based surveys and photogrammetric reconstruction analysis for coastal monitoring. More improvements in numerical modelling applications are actually under development in collaboration with Marc Sanuy and Prof. José A. Jiménez (Laboratori d'Enginyeria Marítima, Universitat Politècnica de Catalunya, Barcelona, Spain). Advancements of the regional Early Warning System and further investigations related to coastal risk assessments are in discussion and will be implemented in collaboration with the Servizio Geologico Sismico e dei Suoli of the Regione Emilia-Romagna.

7.3 Conclusive remarks

The innovations applied during this PhD work are valuable for further developments in coastal risk research. The thesis provides up-to-date methodologies for field, numerical and coastal risk management applications, while highlighting limitations and providing suggestions for improvements. The tools and methods developed for this thesis have the potential to be applied anywhere coastal risk is present. Clearly, applications at different case study sites, or scales (e.g. European scale), would imply specific adaptations, simplifications or schematizations of the approaches, according to the level of detailed information available.

As final general consideration, simplifications and assumptions were applied at all levels of coastal risk evaluations: on the field, using numerical models and for the coastal management applications. It follows that, coastal managers have to take into account that every decision they make, even when supported by scientific results, it is susceptible of error, and thus critical. For this reason, they should be aware of all aspects that characterize coastal risk assessments and, nowadays more important, they have to include local stakeholders in the decision process and adopt multi-disciplinary approaches. This is necessary to increase the cooperation between local people, scientists and decision-makers and to adopt risk reduction measures that are acceptable, sustainable and feasible. This will also help in reducing the distance between the population and the experts of the field. This will make easier to talk and explain to the public the challenges that the future will pose to us, designing adaptation strategies. This is mandatory if we consider that climate change is threatening the future of human beings. We do not have time anymore.

REFERENCES

Agència Catalana de l'Aigua: Pla especial d'emergències per inundacions de Catalunya (INUNCAT), Barcelona, Spain, available at: http://interior.gencat.cat/web/.content/home/030_arees_dactuacio/proteccio_civil/plans_de_proteccio_civil/plans_de_proteccio_civil_a_catalunya/documents/inuncat.pdf, 2015.

Aicardi, I., Chiabrando, F., Grasso, N., Lingua, A. M., Noardo, F. and Spanò, A.: UAV Photogrammetry with Oblique Images: First Analysis on Data Acquisition and Processing, Int. Arch. Photogramm. Remote Sens. Spat. Inf. Sci., 41, 835–842, doi:10.5194/isprs-archives-XLI-B1-835-2016, 2016.

Alexander, D. E.: The L'Aquila Earthquake of 6 April 2009 and Italian Government Policy on Disaster Response, J. Nat. Resour. Policy Res., 2(4), 325–342, doi:10.1080/19390459.2010.511450, 2010.

Anderson, K. and Gaston, K. J.: Lightweight unmanned aerial vehicles will revolutionize spatial ecology, Front. Ecol. Environ., 11(3), 138–146, doi:10.1890/120150, 2013.

Armaroli, C. and Duo, E.: Validation of the coastal storm risk assessment framework along the Emilia-Romagna coast, Coast. Eng., in press, doi:10.1016/j.coastaleng.2017.08.014, 2017.

Armaroli, C., Ciavola, P., Masina, M. and Perini, L.: Run-up computation behind emerged breakwaters for marine storm risk assessment, J. Coast. Res., SI 56 (Proceedings of the 10th International Coastal Symposium, Lisbon, Portugal), 1612–1616, available at: http://www.jstor.org/stable/25738062, 2009.

Armaroli, C., Ciavola, P., Perini, L., Calabrese, L., Lorito, S., Valentini, A. and Masina, M.: Critical storm thresholds for significant morphological changes and damage along the Emilia-Romagna coastline, Italy, Geomorphology, 143–144, 34–51, doi:10.1016/j.geomorph.2011.09.006, 2012.

ARPA E-R SIMC: Rapporto dell'evento meteorologico del 5 e 6 febbraio 2015, Bologna, available at: http://www.arpa.emr.it/cms3/documenti/_cerca_doc/meteo/radar/rapporti/Rapporto_meteo_20150205-06.pdf, 2015.

Aucelli, P. P. C., Di Paola, G., Incontri, P., Rizzo, A., Vilardo, G., Benassai, G., Buonocore, B. and Pappone, G.: Coastal inundation risk assessment due to subsidence and sea level rise in a Mediterranean alluvial plain (Volturno coastal plain - southern Italy), Estuar. Coast. Shelf Sci., 198, 597–609, doi:10.1016/j.ecss.2016.06.017, 2017.

Baart, F., Bakker, M. A. J., Van Dongeren, A., Den Heijer, C., Van Heteren, S., Smit, M. W. J., Van Koningsveld, M. and Pool, A.: Using 18th century storm-surge data from the Dutch Coast to improve the confidence in flood-risk estimates, Nat. Hazards Earth Syst. Sci., 11(10), 2791–2801, doi:10.5194/nhess-11-2791-2011, 2011.

Barquet, K. and Cumiskey, L.: Using participatory Multi-Criteria Assessments for assessing disaster risk reduction measures, Coast. Eng., in press, doi:10.1016/j.coastaleng.2017.08.006, 2017.

Bason, C., Jacobs, A., Howard, A. and Tymes, M.: White Paper on the Status of Sudden Wetland Dieback in Saltmarshes of the Delaware Inland Bays, Delaware Department of Natural Resources and Environmental Control, available at: http://www.dnrec.delaware.gov/Admin/DelawareWetlands/Documents/swdwhitepaper07final.pdf, 2007.

Bates, P. D. and De Roo, A. P. J.: A simple raster-based model for flood inundation simulation, J. Hydrol., 236(1–2), 54–77, doi:10.1016/S0022-1694(00)00278-X, 2000.

Bates, P. D., Dawson, R. J., Hall, J. W., Horritt, M. S., Nicholls, R. J., Wicks, J. and Hassan, M. A. A. M.: Simplified two-dimensional numerical modelling of coastal flooding and example applications, Coast. Eng., 52(9), 793–810, doi:10.1016/j.coastaleng.2005.06.001, 2005.

Becu, N., Amalric, M., Anselme, B., Beck, E., Bertin, X., Delay, E., Long, N., Marilleau, N., Pignon-Mussaud, C. and Rousseaux, F.: Participatory simulation to foster social learning on coastal flooding prevention, Environ. Model. Softw., 98, 1–11, doi:10.1016/j.envsoft.2017.09.003, 2017.

Benedet, L., Finkl, C. W. and Hartog, W. M.: Processes Controlling Development of Erosional Hot Spots on a Beach Nourishment Project, J. Coast. Res., 23(1), 33–48, doi:10.2112/06-0706.1, 2007.

Berni, J. A. J., Zarco-Tejada, P. J., Suárez, L. and Fereres, E.: Thermal and Narrowband Multispectral Remote Sensing for Vegetation Monitoring From an Unmanned Aerial Vehicle, IEEE Trans. Geosci. Remote Sens., 47(3), 722–738, doi:10.1109/TGRS.2008.2010457, 2009.

Bernstein, D. J., Freeman, C., Forte, M. F., Park, J.-Y., Gayes, P. T. and Mitasova, H.: Survey design analysis for three-dimensional mapping of beach and nearshore morphology, in: Proceedings of the International Conference on Coastal Sediments 2003, Clearwater Beach, Florida, USA (18–23 May 2003), edited by R. A. Davis, A. Sallenger, and P. Howd, World Scientific, 2003.

Bertin, X., Bruneau, N., Breilh, J.-F., Fortunato, A. B. and Karpytchev, M.: Importance of wave age and resonance in storm surges: The case Xynthia, Bay of Biscay, Ocean Model., 42, 16–30, doi:10.1016/j.ocemod.2011.11.001, 2012.

Bertoni, D., Armaroli, C. and Ciavola, P.: Fast retreat of a barrier system due to reduced sediment supply (Bellocchio, Northern Adriatic Sea, Italy), in: Coastal and Maritime Mediterranean Conference, Edition 3, Ferrara, Italy, 25-27 November 2015, edited by D. Levacher, M. Sanchez, P. Ciavola, and E. Raymond, pp. 7–10, Editions Paralia, doi: 10.5150/cmcm.2015.002, 2015.

Bertotti, L., Bidlot, J.-R., Bunney, C., Cavaleri, L., Delli Passeri, L., Gomez, M., Lefèvre, J.-M., Paccagnella, T., Torrisi, L., Valentini, A. and Vocino, A.: Performance of different forecast systems in an exceptional storm in the Western Mediterranean Sea, Q. J. R. Meteorol. Soc., 138(662), 34–55, doi:10.1002/qj.892, 2012.

Beven II, J. L., Avila, L. A., Blake, E. S., Brown, D. P., Franklin, J. L., Knabb, R. D., Pasch, R. J., Rhome, J. R. and Stewart, R. S.: Atlantic Hurricane Season of 2005, Mon. Weather Rev., 136(3), 1109–1173, doi:10.1175/2007MWR2074.1, 2008.

Billi, P. and Rinaldi, M.: Human impact on sediment yield and channel dynamics in the Arno River basin (central Italy), in: Human Impacts on Erosion and

Sedimentation: Proceedings of Rabat Symposium S6, Rabat, Morocco, 23 April - 3 May 1997, edited by D. E. Walling and J.-L. Probst, pp. 301–311, International Association of Hydrological Sciences, 1997.

Booij, N., Holthuijsen, L. H. and Ris, R. C.: The "Swan" Wave Model for Shallow Water, in: Coastal Engineering 1996 Proceedings of the 25th International Conference on Coastal Engineering, Orlando, Florida, September 2-6, 1996, edited by B. L. Edge, pp. 668–676, American Society of Civil Engineers, doi:10.1061/9780784402429.053, 1997.

Bosom, E.: Coastal Vulnerability to Storms at Different Time Scales. Application to the Catalan Coast, PhD Thesis, Universitat Politècnica de Catalunya, 2014.

Brown, S., Nicholls, R. J., Woodroffe, C. D., Hanson, S., Hinkel, J., Kebede, A. S., Neumann, B. and Vafeidis, A. T.: Sea-Level Rise Impacts and Responses: A Global Perspective, in: Coastal Hazards, edited by C. W. Finkl, pp. 117–149, Springer, Dordrecht, The Netherlands, 2013.

Bruun, P.: Beach scraping - Is it damaging to beach stability?, Coast. Eng., 7(2), 167–173, doi:10.1016/0378-3839(83)90011-X, 1983.

Bruun, P.: Sea-Level rise as a cause of shore evolution, J. Waterw. Harbours Div., 88(1), 117–132, 1962.

Burton, I., Kates, R. W. and White, G. F.: The Environment as Hazard, Oxford University Press, Oxford, 1978.

Bush, D. M., Neal, W. J., Young, R. S. and Pilkey, O. H.: Utilization of geoindicators for rapid assessment of coastal-hazard risk and mitigation, Ocean Coast. Manag., 42(8), 647–670, doi:10.1016/S0964-5691(99)00027-7, 1999.

Callaghan, D. P., Roshanka, R. and Andrew, S.: Quantifying the storm erosion hazard for coastal planning, Coast. Eng., 56(1), 90–93, doi:10.1016/j.coastaleng.2008.10.003, 2009.

Carapuço, M. M., Taborda, R., Silveira, T. M., Psuty, N. P., Andrade, C. and Freitas, M. C.: Coastal geoindicators: Towards the establishment of a common framework for sandy coastal environments, Earth-Science Rev., 154, 183–190, doi:10.1016/j.earscirev.2016.01.002, 2016.

Carley, J. T. and Cox, R. J.: A methodology for utilising time-dependent beach erosion models for design events, in: Coasts & Ports 2003 Australasian Conference: Proceedings of the 16th Australasian Coastal and Ocean Engineering Conference, the 9th Australasian Port and Harbour Conference and the Annual New Zealand Coastal Society Conference, Auckland, New Zealand, 9-1, edited by P. S. Kench and T. M. Hume, pp. 587–595, Institution of Engineers, Australia, 2003.

Casas-Prat, M. and Sierra, J. P.: Trend analysis of wave direction and associated impacts on the Catalan coast, Clim. Change, 115(3–4), 667–691, doi:10.1007/s10584-012-0466-9, 2012.

Casella, E., Rovere, A., Pedroncini, A., Mucerino, L., Casella, M., Cusati, L. A., Vacchi, M., Ferrari, M. and Firpo, M.: Study of wave runup using numerical models and low-altitude aerial photogrammetry: A tool for coastal management, Estuar. Coast. Shelf Sci., 149, 160–167, doi:10.1016/j.ecss.2014.08.012, 2014.

Casella, E., Rovere, A., Pedroncini, A., Stark, C. P., Casella, M., Ferrari, M. and Firpo, M.: Drones as tools for monitoring beach topography changes in the Ligurian

Sea (NW Mediterranean), Geo-Marine Lett., 36(2), 151–163, doi:10.1007/s00367-016-0435-9, 2016.

Chaumillon, E., Bertin, X., Fortunato, A. B., Bajo, M., Schneider, J. L., Dezileau, L., Walsh, J. P., Michelot, A., Chauveau, E., Créach, A., Hénaff, A., Sauzeau, T., Waeles, B., Gervais, B., Jan, G., Baumann, J., Breilh, J. F. and Pedreros, R.: Storm-induced marine flooding: Lessons from a multidisciplinary approach, Earth-Science Rev., 165, 151–184, doi:10.1016/j.earscirev.2016.12.005, 2017.

Christie, E. K., Spencer, T., Owen, D., McIvor, A. L., Möller, I. and Viavattene, C.: Regional coastal flood risk assessment for a tidally dominant, natural coastal setting: North Norfolk, southern North Sea, Coast. Eng., in press, doi:10.1016/j.coastaleng.2017.05.003, 2017.

Church, J., Clark, P., Cazenave, A., Gregory, J., Jevrejeva, S., Levermann, A., Merrifield, M., Milne, G., Nerem, R., Nunn, P., Payne, A., Pfeffer, W., Stammer, D. and Unnikrishnan, A.: Sea level change, in: Climate Change 2013: The Physical Science Basis. Contribution of Working Group I to the Fifth Assessment Report of the Intergovernmental Panel on Climate Change, edited by T. F. Stocker, D. Qin, G.-K. Plattner, M. Tignor, S. K. Allen, J. Boschung, A. Nauels, Y. Xia, V. Bex, and P. M. Midgley, p. 1535, Cambridge University Press, Cambridge, United Kingdom and New York, NY, USA, 2013.

Ciavola, P. and Coco, G. (Eds.): Coastal storms: processes and impacts, First Edit., John Wiley & Sons Ltd., 2017.

Ciavola, P., Armaroli, C., Chiggiato, J., Valentini, A., Deserti, M., Perini, L. and Luciani, P.: Impact of storms along the coastline of Emilia-Romagna: the morphological signature on the Ravenna coastline (Italy), J. Coast. Res., SI 50 (Proceedings of the 9th International Coastal Symposium, Gold Coast, Australia), 540–544, 2007.

Ciavola, P., Billi, P., Armaroli, C., Preciso, E., Salemi, E. and Balouin, Y.: Morphodynamics of the Bevano Stream outlet: the role of bedload yield, Geol. Tec. Ambient., 1, 41–57, 2005.

Ciavola, P., Ferreira, O., Haerens, P., Van Koningsveld, M., Armaroli, C. and Lequeux, Q.: Storm impacts along European coastlines. Part 1: The joint effort of the MICORE and ConHaz Projects, Environ. Sci. Policy, 14(7), 912–923, doi:10.1016/j.envsci.2011.05.011, 2011a.

Ciavola, P., Ferreira, O., Haerens, P., Van Koningsveld, M. and Armaroli, C.: Storm impacts along European coastlines. Part 2: Lessons learned from the MICORE project, Environ. Sci. Policy, 14(7), 924–933, doi:10.1016/j.envsci.2011.05.009, 2011b.

Ciavola, P., Harley, M. D. and Den Heijer, C.: The RISC-KIT storm impact database: A new tool in support of DRR, Coast. Eng., in press, doi:10.1016/j.coastaleng.2017.08.016, 2017.

Conte, D. and Lionello, P.: Characteristics of large positive and negative surges in the Mediterranean Sea and their attenuation in future climate scenarios, Glob. Planet. Change, 111, 159–173, doi:10.1016/j.gloplacha.2013.09.006, 2013.

Corbella, S. and Stretch, D. D.: Multivariate return periods of sea storms for coastal erosion risk assessment, Nat. Hazards Earth Syst. Sci., 12(8), 2699–2708, doi:10.5194/nhess-12-2699-2012, 2012.

Cumiskey, L., Priest, S., Valchev, N., Viavattene, C., Costas, S. and Clarke, J.: A framework to include the (inter)dependencies of Disaster Risk Reduction measures in coastal risk assessment, Coast. Eng., in press, doi:10.1016/j.coastaleng.2017.08.009, 2017.

Cutter, S. L., Emrich, C. T., Mitchell, J. T., Boruff, B. J., Gall, M., Schmidtlein, M. C., Burton, C. G. and Melton, G.: The Long Road Home: Race, Class, and Recovery from Hurricane Katrina, Environ. Sci. Policy Sustain. Dev., 48(2), 8–20, doi:10.3200/ENVT.48.2.8-20, 2006.

Davidson, M., Van Koningsveld, M., De Kruif, A., Rawson, J., Holman, R., Lamberti, A., Medina, R., Kroon, A. and Aarninkhof, S.: The CoastView project: Developing video-derived Coastal State Indicators in support of coastal zone management, Coast. Eng., 54(6–7), 463–475, doi:10.1016/j.coastaleng.2007.01.007, 2007.

Decouttere, C., De Backer, K., Monbaliu, J. and Berlamont, J.: Storm Wave Simulation in the Adriatic Sea, in: CENAS Coastline Evolution of the Upper Adriatic Sea due to Sea Level Rise and Natural and Anthropogenic Land Subsidence, pp. 185–205, Springer Netherlands, Dordrecht, NL, doi:10.1007/978-94-011-5147-4_9, 1998.

Dohner, S. M., Trembanis, A. C. and Miller, D. C.: A tale of three storms: Morphologic response of Broadkill Beach, Delaware, following Superstorm Sandy, Hurricane Joaquin, and Winter Storm Jonas, Shore & Beach, 84(4), 2016.

Duo, E. and Ciavola, P. (Eds.): RISC-KIT D.1.1 - Review report of key challenges and lessons learned from historical extreme hydro-meteorological events, available at: http://www.risckit.eu/np4/file/23/RISC_KIT_Deliverable_D.1.1_V3.pdf, 2015.

FEMA: Understanding your risks. Identifying hazards and estimating losses, Federal Emergency Management Agency, USA, 2001.

Fernández-Montblanc, T., Del Río, L., Izquierdo, A., Gracia, F. J., Bethencourt, M. and Benavente, J.: Shipwrecks and man-made coastal structures as indicators of historical shoreline position. An interdisciplinary study in the Sancti Petri sand spit (Bay of Cádiz, SW Spain), Mar. Geol., 395, 152–167, doi:10.1016/j.margeo.2017.10.005, 2018.

Ferreira, Ó., Ciavola, P., Armaroli, C., Balouin, Y., Benavente, J., Río, L. Del, Deserti, M. and Esteves, L. S.: Coastal Storm Risk Assessment in Europe: Examples from 9 study sites, J. Coast. Res., SI 56 (Proceedings of the 10th International Coastal Symposium, Lisbon, Portugal), 1632–1636, available at: http://www.jstor.org/stable/25738066, 2009.

Ferreira, Ó., Plomaritis, T. A. and Costas, S.: Process-based indicators to assess storm induced coastal hazards, Earth-Science Rev., 173, 159–167, doi:10.1016/j.earscirev.2017.07.010, 2017.

Figueiredo, R. and Martina, M.: Using open building data in the development of exposure data sets for catastrophe risk modelling, Nat. Hazards Earth Syst. Sci., 16(2), 417–429, doi:10.5194/nhess-16-417-2016, 2016.

Gaillard, J. C. and Texier, P.: Religions, natural hazards, and disasters: An introduction, Religion, 40(2), 81–84, doi:10.1016/j.religion.2009.12.001, 2010.

Garnier, E., Ciavola, P., Spencer, T., Ferreira, O., Armaroli, C. and McIvor, A.: Historical analysis of storm events: Case studies in France, England, Portugal and Italy, Coast. Eng., in press, doi:10.1016/j.coastaleng.2017.06.014, 2017.

Gesch, D. B.: Analysis of Lidar Elevation Data for Improved Identification and Delineation of Lands Vulnerable to Sea-Level Rise, J. Coast. Res., SI(53), 49–58, doi:10.2112/SI53-006.1, 2009.

Gray, J. D. E., O'Neill, K. and Qiu, Z.: Coastal residents' perceptions of the function of and relationship between engineered and natural infrastructure for coastal hazard mitigation, Ocean Coast. Manag., 146, 144–156, doi:10.1016/j.ocecoaman.2017.07.005, 2017.

Guedes Soares, C., Weisse, R., Carretero, J. C. and Alvarez, E.: A 40 years hindcast of wind, sea level and waves in European waters, in: Proceedings of OMAE'02 21st International Conference on Offshore Mechanics and Arctic Engineering, Oslo, Norway, June 23–28, 2002, pp. 669–675, ASME, 2002.

Gutierrez, B. T., Plant, N. G. and Thieler, E. R.: A Bayesian network to predict coastal vulnerability to sea level rise, J. Geophys. Res. Earth Surf., 116(F02009), doi:10.1029/2010JF001891, 2011.

Hampson, R., MacMahan, J. and Kirby, J. T.: A Low-Cost Hydrographic Kayak Surveying System, J. Coast. Res., 27(3), 600–603, doi:10.2112/JCOASTRES-D-09-00108.1, 2011.

Hansen, J. E. and Barnard, P. L.: Sub-weekly to interannual variability of a high-energy shoreline, Coast. Eng., 57(11–12), 959–972, doi:10.1016/j.coastaleng.2010.05.011, 2010.

Harley, M. D. and Ciavola, P.: Managing local coastal inundation risk using real-time forecasts and artificial dune placements, Coast. Eng., 77, 77–90, doi:10.1016/j.coastaleng.2013.02.006, 2013.

Harley, M. D., Valentini, A., Armaroli, C., Perini, L., Calabrese, L. and Ciavola, P.: Can an early-warning system help minimize the impacts of coastal storms? A case study of the 2012 Halloween storm, northern Italy, Nat. Hazards Earth Syst. Sci., 16(1), 209–222, doi:10.5194/nhess-16-209-2016, 2016.

Harley, M. D.: DuneMaker 2.0: A MATLAB tool to simulate artificial dunes using XBeach, doi:10.13140/2.1.3941.7120, 2014.

Harley, M., Armaroli, C. and Ciavola, P.: Evaluation of XBeach predictions for a real-time warning system in Emilia-Romagna, Northern Italy, J. Coast. Res., SI 64 (Proceedings of the 11th International Coastal Symposium, Szczecin, Poland), 1861–1865, 2011.

Harley, M., Valentini, A., Armaroli, C., Ciavola, P., Perini, L., Calabrese, L. and Marucci, F.: An early warning system for the on-line prediction of coastal storm risk on the Italian coastline, in: Coastal Engineering 2012 Proceedings of 33rd Conference on Coastal Engineering, Santander, Spain, 1-6 July 2012, edited by P. Lynett and J. M. Smith, Coastal Engineering Research Council, doi:10.9753/icce.v33.management.77, 2012.

Harley, M.: Coastal Storm Definition, in: Coastal Storms: Processes and Impacts, edited by P. Ciavola and G. Coco, pp. 1–21, John Wiley & Sons Ltd., 2017.

Hewitt, K.: Reviewed Work: The Environment as Hazard by Ian Burton, Robert W. Kates and Gilbert F. White, Ann. Assoc. Am. Geogr., 70(2), 306–311 [online] Available from: http://www.jstor.org/stable/2562965, 1980.

IDROSER: Piano progettuale per la difesa della costa adriatica Emiliano-Romagnola, Regione Emilia-Romagna, Bologna, Italy, 1981.

IDROSER: Progetto di Piano per la difesa del mare e la riqualificazione ambientale del litorale della Regione Emilia-Romagna, Regione Emilia-Romagna, Bologna, Italy, 1996.

IPCC: Climate Change 2013: The Physical Science Basis. Contribution of Working Group I to the Fifth Assessment Report of the Intergovernmental Panel on Climate Change, edited by T. F. Stocker, D. Qin, G.-K. Plattner, M. Tignor, S. K. Allen, J. Boschung, A. Nauels, Y. Xia, V. Bex, and P. M. Midgley, Cambridge University Press, Cambridge, UK and New York, NY, USA, doi:10.1029/2000JD000115, 2013.

IPCC: Managing the Risks of Extreme Events and Disasters to Advance Climate Change Adaptation. A Special Report of Working Groups I and II of the Intergovernmental Panel on Climate Change, edited by C. B. Field, V. Barros, T. F. Stocker, D. Qin, D. J. Dokken, K. L. Ebi, M. D. Mastrandrea, K. J. Mach, G.-K. Plattner, S. K. Allen, M. Tignor, and P. M. Midgley, Cambridge University Press, Cambridge, UK and New York, NY, USA, 2012.

ISPRA: Annuario Dei Dati Ambientali 2012, Istituto Superiore per la Protezione e la Ricerca Ambientale, Rome, Italy, available at: http://www.isprambiente.gov.it/files/pubblicazioni/statoambiente/tematiche2011, 2013.

Jäger, W. S., Christie, E. K., Hanea, A. M., den Heijer, C. and Spencer, T.: A Bayesian network approach for coastal risk analysis and decision making, Coast. Eng., in press, doi:10.1016/j.coastaleng.2017.05.004, 2017.

James, M. R., Robson, S. and Smith, M. W.: 3-D uncertainty-based topographic change detection with structure-from-motion photogrammetry: precision maps for ground control and directly georeferenced surveys, Earth Surf. Process. Landforms, 42(12), 1769–1788, doi:10.1002/esp.4125, 2017.

Jensen, F. B.: An introduction to Bayesian networks, UCL Press, London, UK, 1996.

Jiménez, J. A., Armaroli, C., Berenguer, M., Bosom, E., Ciavola, P., Ferreira, O., Plomaritis, H., Roelvink, D., Sanuy, M. and Sempere, D.: RISC-KIT D.2.1 - Coastal Hazard Assessment Module, available at: http://www.risckit.eu/np4/file/23/RISCKIT_D.2.1_Coastal_Hazard_Asssessment.pdf, 2015.

Jiménez, J. A., Gracia, V., Valdemoro, H. I., Mendoza, E. T. and Sánchez-Arcilla, A.: Managing erosion-induced problems in NW Mediterranean urban beaches, Ocean Coast. Manag., 54(12), 907–918, doi:10.1016/j.ocecoaman.2011.05.003, 2011.

Jiménez, J. A., Sancho-García, A., Bosom, E., Valdemoro, H. I. and Guillén, J.: Storm-induced damages along the Catalan coast (NW Mediterranean) during the period 1958-2008, Geomorphology, 143–144, 24–33, doi:10.1016/j.geomorph.2011.07.034, 2012.

Jiménez, J. A., Valdemoro, H. I., Bosom, E., Sánchez-Arcilla, A. and Nicholls, R. J.: Impacts of sea-level rise-induced erosion on the Catalan coast, Reg. Environ. Chang., 17(2), 593–603, doi:10.1007/s10113-016-1052-x, 2017a.

Jiménez, J. A., Armaroli, C. and Bosom, E.: Preparing for the Impact of Coastal Storms: A Coastal Manager-Oriented Approach, in: Coastal Storms: Processes and Impacts, edited by P. Ciavola and G. Coco, pp. 217–239, John Wiley & Sons Ltd., 2017b.

Jiménez, J. A., Sanuy, M., Ballesteros, C. and Valdemoro, H. I.: The Tordera Delta, a hotspot to storm impacts in the coast northwards of Barcelona (NW Mediterranean), Coast. Eng., in press, doi:10.1016/j.coastaleng.2017.08.012, 2017c.

Kolen, B., Slomp, R. and Jonkman, S. N.: The impacts of storm Xynthia February 27-28, 2010 in France: Lessons for flood risk management, J. Flood Risk Manag., 6(3), 261–278, doi:10.1111/jfr3.12011, 2013.

Kreibich, H., van den Bergh, J. C. J. M., Bouwer, L. M., Bubeck, P., Ciavola, P., Green, C., Hallegatte, S., Logar, I., Meyer, V., Schwarze, R. and Thieken, A. H.: Costing natural hazards, Nat. Clim. Chang., 4(5), 303–306, doi:10.1038/nclimate2182, 2014.

Kunz, M., Mühr, B., Kunz-Plapp, T., Daniell, J. E., Khazai, B., Wenzel, F., Vannieuwenhuyse, M., Comes, T., Elmer, F., Schröter, K., Fohringer, J., Münzberg, T., Lucas, C. and Zschau, J.: Investigation of superstorm Sandy 2012 in a multi-disciplinary approach, Nat. Hazards Earth Syst. Sci., 13(10), 2579–2598, doi:10.5194/nhess-13-2579-2013, 2013.

Larson, M. and Kraus, N. C.: Temporal and spatial scales of beach profile change, Duck, North Carolina, Mar. Geol., 117(1–4), 75–94, doi:10.1016/0025-3227(94)90007-8, 1994.

Lauritzen, S. L. and Spiegelhalter, D. J.: Local Computations with Probabilities on Graphical Structures and Their Application to Expert Systems, J. R. Stat. Soc. Ser. B, 50(2), 157–224, available at: http://www.jstor.org/stable/2345762, 1988.

Lee, G.-H., Nicholls, R. J. and Birkemeier, W. A.: Storm-driven variability of the beach-nearshore profile at Duck, North Carolina, USA, 1981-1991, Mar. Geol., 148(3–4), 163–177, doi:10.1016/S0025-3227(98)00010-3, 1998.

Lee, J.-M., Park, J.-Y. and Choi, J.-Y.: Evaluation of Sub-aerial Topographic Surveying Techniques Using Total Station and RTK-GPS for Applications in Macrotidal Sand Beach Environment, J. Coast. Res., SI 65 (Proceedings 12th International Coastal Symposium, Plymouth, England), 535–540, doi:10.2112/SI65-091.1, 2013.

Ligorio, C., Primerano, S., Strocchi, M. and Beghelli, E. (Eds.): Il sistema regionale di allertamento per il rischio idrogeologico-idraulico, Regione Emilia-Romagna and Agenzia Regionale di Protezione Civile, Bologna, Italy, 2012.

Lionello, P., Bhend, J., Buzzi, A., Della-Marta, P. M., Krichak, S. O., Jansà, A., Maheras, P., Sanna, A., Trigo, I. F. and Trigo, R.: Cyclones in the Mediterranean Region: Climatology and Effects on the Environment, in: Developments in Earth and Environmental Sciences, IV: Mediterranean Climate Variability, edited by P. Lionello, P. Malanotte-Rizzoli, and R. Boscolo, pp. 325–372, Elsevier, 2006.

Lionello, P., Boldrin, U. and Giorgi, F.: Future changes in cyclone climatology over Europe as inferred from a regional climate simulation, Clim. Dyn., 30(6), 657–671, doi:10.1007/s00382-007-0315-0, 2008.

Lorito, S., Calabrese, L., Perini, L. and Cibin, U.: Uso del suolo della costa, in: Il sistema mare-costa dell'Emilia-Romagna, edited by L. Perini and L. Calabrese, pp. 109–118, Regione Emilia-Romagna, Bologna, Italy, 2010.

Mancini, F., Dubbini, M., Gattelli, M., Stecchi, F., Fabbri, S. and Gabbianelli, G.: Using Unmanned Aerial Vehicles (UAV) for High-Resolution Reconstruction of Topography: The Structure from Motion Approach on Coastal Environments, Remote Sens., 5(12), 6880–6898, doi:10.3390/rs5126880, 2013.

Martinez, G., Armaroli, C., Costas, S., Harley, M. D. and Paolisso, M.: Experiences and results from interdisciplinary collaboration: Utilizing qualitative information to formulate disaster risk reduction measures for coastal regions, Coast. Eng., in press, doi:10.1016/j.coastaleng.2017.09.010, 2017.

Masina, M. and Ciavola, P.: Analisi dei livelli marini estremi e delle acque alte lungo il litorale ravennate, Studi Costieri, 18, 87–101, available at: http://www.gnrac.unifi.it/rivista/Numero18/Articolo6.pdf, 2011.

Masina, M., Lamberti, A. and Archetti, R.: Coastal flooding: A copula based approach for estimating the joint probability of water levels and waves, Coast. Eng., 97, 37–52, doi:10.1016/j.coastaleng.2014.12.010, 2015.

McCall, R. T., Van Thiel de Vries, J. S. M., Plant, N. G., Van Dongeren, A. R., Roelvink, J. A., Thompson, D. M. and Reniers, A. J. H. M.: Two-dimensional time dependent hurricane overwash and erosion modeling at Santa Rosa Island, Coast. Eng., 57(7), 668–683, doi:10.1016/j.coastaleng.2010.02.006, 2010.

Mendoza, E. T. and Jiménez, J. A.: Clasificación de tormentas costeras para el litoral catalán (Mediterráneo NO), Ing. hidráulica en México, XXIII(2), 23–34, 2008.

Mendoza, E. T. and Jiménez, J. A.: Storm-Induced Beach Erosion Potential on the Catalonian Coast, J. Coast. Res., SI 48 (Proceedings of the 3rd Spanish Conference on Coastal Geomorphology, Las Palmas de Gran Canaria, Spain), 81–88, available at: http://www.jstor.org/stable/25737386, 2006.

Mendoza, E. T., Jiménez, J. A. and Mateo, J.: A coastal storms intensity scale for the Catalan sea (NW Mediterranean), Nat. Hazards Earth Syst. Sci., 11(9), 2453–2462, doi:10.5194/nhess-11-2453-2011, 2011.

Morton, R. A., Leach, M. P., Paine, J. G. and Cardoza, M. A.: Monitoring Beach Changes Using GPS Surveying Techniques, J. Coast. Res., 9(3), 702–720, doi:10.2307/4298124, 1993.

Morton, R. A.: Factors Controlling Storm Impacts on Coastal Barriers and Beaches-A Preliminary Basis for for near Real-Time Forecasting, J. Coast. Res., 18(3), 486–501, available at: http://www.jstor.org/stable/4299096, 2002.

Murdukhayeva, A., August, P., Bradley, M., LaBash, C. and Shaw, N.: Assessment of Inundation Risk from Sea Level Rise and Storm Surge in Northeastern Coastal National Parks, J. Coast. Res., 29(6A), 1–16, doi:10.2112/JCOASTRES-D-12-00196.1, 2013.

Narayan, S., Nicholls, R. J., Clarke, D., Hanson, S., Reeve, D., Horrillo-Caraballo, J., le Cozannet, G., Hissel, F., Kowalska, B., Parda, R., Willems, P., Ohle, N., Zanuttigh, B., Losada, I., Ge, J., Trifonova, E., Penning-Rowsell, E. and

Vanderlinden, J. P.: The SPR systems model as a conceptual foundation for rapid integrated risk appraisals: Lessons from Europe, Coast. Eng., 87, 15–31, doi:10.1016/j.coastaleng.2013.10.021, 2014.

Neumann, B., Vafeidis, A. T., Zimmermann, J. and Nicholls, R. J.: Future Coastal Population Growth and Exposure to Sea-Level Rise and Coastal Flooding - A Global Assessment, PLoS One, 10(3), doi:10.1371/journal.pone.0118571, 2015.

Nguyen, T. T. X., Bonetti, J., Rogers, K. and Woodroffe, C. D.: Indicator-based assessment of climate-change impacts on coasts: A review of concepts, methodological approaches and vulnerability indices, Ocean Coast. Manag., 123, 18–43, doi:10.1016/j.ocecoaman.2015.11.022, 2016.

Nicholls, R. J., Wong, P. P., Burketts, J. O., Codignotto, J. E., McLean, R. F., Ragoonaden, S. and Woodroffe, C. D.: Coastal systems and low-lying areas, in: Climate Change 2007: Impacts, Adaptation and Vulnerability. Contribution of Working Group II to the Fourth Assessment Report of the Intergovernmental Panel on Climate Change, edited by M. L. Parry, O. F. Canziani, J. P. Palutikof, P. J. Van Der Linden, and C. E. Hanson, pp. 315–356, Cambridge University Press, Cambridge, UK, 2007.

Niederheiser, R., Mokroš, M., Lange, J., Petschko, H., Prasicek, G. and Elberink, S. O.: Deriving 3d point clouds from terrestrial photographs comparison of different sensors and software, Int. Arch. Photogramm. Remote Sens. Spat. Inf. Sci., 41, 685–692, doi:10.5194/isprsarchives-XLI-B5-685-2016, 2016.

Nielsen, A. F. and Adamantidis, C. A.: Defining the Storm Erosion Hazard for Beaches, Aust. J. Civ. Eng., 3(1), 39–50, doi:10.1080/14488353.2007.11463920, 2007.

Nordstrom, K. F., Armaroli, C., Jackson, N. L. and Ciavola, P.: Opportunities and constraints for managed retreat on exposed sandy shores: Examples from Emilia-Romagna, Italy, Ocean Coast. Manag., 104, 11–21, doi:10.1016/j.ocecoaman.2014.11.010, 2015.

Odigie, K. O. and Warrick, J. A.: Coherence Between Coastal and River Flooding along the California Coast, J. Coast. Res., in press, doi:10.2112/JCOASTRES-D-16-00226.1, 2017.

Oumeraci, H., Kortenhaus, A., Burzel, A., Naulin, M., Dassanayake, D. R., Jensen, J., Wahl, T., Mudersbach, C., Gönnert, G., Gerkensmeier, B., Fröhle, P. and Ujeyl, G.: XtremRisK — Integrated Flood Risk Analysis for Extreme Storm Surges at Open Coasts and in Estuaries: Methodology, Key Results and Lessons Learned, Coast. Eng. J., 57(1), doi:10.1142/S057856341540001X, 2015.

Passarella, M., Goldstein, E. B., Muro, S. De and Coco, G.: The use of genetic programming to develop a predictor of swash excursion on sandy beaches, Nat. Hazards Earth Syst. Sci. Discuss., in review, doi:10.5194/nhess-2017-232, 2017.

Pawlowicz, R., Beardsley, B. and Lentz, S.: Classical tidal harmonic analysis including error estimates in MATLAB using T_TIDE, Comput. Geosci., 28(8), 929–937, doi:10.1016/S0098-3004(02)00013-4, 2002.

Pearl, J.: Probabilistic Reasoning in Intelligent Systems: Networks of Plausible Inference, Morgan Kaufmann, San Francisco, California, USA, 1988.

Penning-Rowsell, E. C., De Vries, W. S., Parker, D. J., Zanuttigh, B., Simmonds, D., Trifonova, E., Hissel, F., Monbaliu, J., Lendzion, J., Ohle, N., Diaz, P. and Bouma, T.: Innovation in coastal risk management: An exploratory analysis of

risk governance issues at eight THESEUS study sites, Coast. Eng., 87, 210–217, doi:10.1016/j.coastaleng.2013.12.005, 2014.

Perini, L. and Calabrese, L. (Eds.): Il sistema mare-costa dell'Emilia-Romagna, Pendragon, Bologna, Italy, 2010.

Perini, L., Calabrese, L., Deserti, M., Valentini, A., Ciavola, P. and Armaroli, C.: Le mareggiate e gli impatti sulla costa in Emilia-Romagna 1946-2010, ARPA Emilia-Romagna, Bologna, Italy, 2011.

Perini, L., Calabrese, L., Lorito, S. and Luciani, P.: Costal flood risk in Emilia-Romagna (Italy): the sea storm of February 2015, in: Coastal and Maritime Mediterranean Conference, Edition 3, Ferrara, Italy, 25-27 November 2015, edited by D. Levacher, M. Sanchez, P. Ciavola, and E. Raymond, pp. 225–230, Editions Paralia, doi:10.5150/cmcm.2015.044, 2015a.

Perini, L., Calabrese, L., Lorito, S. and Luciani, P.: Il rischio da mareggiata in Emilia-Romagna: l'evento del 5-6 Febbraio 2015, il Geologo, 53, 8–17, available at: http://www.geologiemiliaromagna.it/il-geologo-anno-xv-2015-n-53/, 2015b.

Perini, L., Calabrese, L., Luciani, P., Olivieri, M., Galassi, G. and Spada, G.: Sea-level rise along the Emilia-Romagna coast (Northern Italy) at 2100: scenarios and impacts, Nat. Hazards Earth Syst. Sci. Discuss., in review, doi:10.5194/nhess-2017-82, 2017.

Perini, L., Calabrese, L., Salerno, G., Ciavola, P. and Armaroli, C.: Evaluation of coastal vulnerability to flooding: Comparison of two different methodologies adopted by the Emilia-Romagna region (Italy), Nat. Hazards Earth Syst. Sci., 16(1), 181–194, doi:10.5194/nhess-16-181-2016, 2016.

Perini, L., Luciani, P. and Calabrese, L.: Altimetria della fascia costiera, in: Il sistema mare-costa dell'Emilia-Romagna, edited by L. Perini and L. Calabrese, pp. 57–66, Regione Emilia-Romagna, Bologna, Italy, 2010a.

Perini, L., Carrara, G., Luciani, P., Lorito, S. and Calabrese, L.: Batimetrie e modelli digitali dei fondali, in: Il sistema mare-costa dell'Emilia-Romagna, edited by L. Perini and L. Calabrese, pp. 67–86, Regione Emilia-Romagna, Bologna, Italy, 2010b.

Pescaroli, G. and Magni, M.: Flood warnings in coastal areas: How do experience and information influence responses to alert services?, Nat. Hazards Earth Syst. Sci., 15(4), 703–714, doi:10.5194/nhess-15-703-2015, 2015.

Phillips, M. S., Blenkinsopp, C. E., Splinter, K. D., Harley, M. D., Turner, I. L. and Cox, R. J.: High-frequency observations of berm recovery using a continuous scanning Lidar, in Australasian Coasts & Ports 2017: Working with Nature, pp. 872–878, Barton ACT: Engineers Australia, PIANC Australia and Institute of Professional Engineers New Zealand, 2017.

Pietro, L. S., O'Neal, M. A. and Puleo, J. A.: Developing Terrestrial-LIDAR-Based Digital Elevation Models for Monitoring Beach Nourishment Performance, J. Coast. Res., 24(6), 1555–1564, doi:10.2112/07-0904.1, 2008.

Plant, N. G., Robert Thieler, E. and Passeri, D. L.: Coupling centennial-scale shoreline change to sea-level rise and coastal morphology in the Gulf of Mexico using a Bayesian network, Earth's Future, 4(5), 143–158, doi:10.1002/2015EF000331, 2016.

Plomaritis, T. A., Costas, S. and Ferreira, Ó.: Use of a Bayesian Network for coastal hazards, impact and disaster risk reduction assessment at a coastal barrier (Ria Formosa, Portugal), Coast. Eng., in press, doi:10.1016/j.coastaleng.2017.07.003, 2017.

Poelhekke, L., Jäger, W. S., van Dongeren, A., Plomaritis, T. A., McCall, R. and Ferreira, Ó.: Predicting coastal hazards for sandy coasts with a Bayesian Network, Coast. Eng., 118, 21–34, doi:10.1016/j.coastaleng.2016.08.011, 2016.

Poljanšek, K., De Groeve, T., Marín Ferrer, M. and Clark, I. (Eds.): Science for disaster risk management 2017: knowing better and losing less, Publications Office of the European Union, Luxembourg, doi:10.2788/688605, 2017.

Preciso, E., Salemi, E. and Billi, P.: Land use changes, torrent control works and sediment mining: Effects on channel morphology and sediment flux, case study of the Reno River (Northern Italy), Hydrol. Process., 26(8), 1134–1148, doi:10.1002/hyp.8202, 2012.

Ranasinghe, R. and Callaghan, D.: Assessing Storm Erosion Hazards, in: Coastal Storms: Processes and Impacts, edited by P. Ciavola and G. Coco, pp. 241–256, John Wiley & Sons Ltd., 2017.

Ranasinghe, R.: Assessing climate change impacts on open sandy coasts: A review, Earth-Science Rev., 160, 320–332, doi:10.1016/j.earscirev.2016.07.011, 2016.

Ratsimandresy, A. W., Sotillo, M. G., Carretero Albiach, J. C., Álvarez Fanjul, E. and Hajji, H.: A 44-year high-resolution ocean and atmospheric hindcast for the Mediterranean Basin developed within the HIPOCAS Project, Coast. Eng., 55(11), 827–842, doi:10.1016/j.coastaleng.2008.02.025, 2008.

Roelvink, D. and Reniers, A.: A guide to modeling coastal morphology, World Scientific Publishing Co. Pte. Ltd., 2012.

Roelvink, D., Reniers, A., van Dongeren, A., van Thiel de Vries, J., McCall, R. and Lescinski, J.: Modelling storm impacts on beaches, dunes and barrier islands, Coast. Eng., 56(11–12), 1133–1152, doi:10.1016/j.coastaleng.2009.08.006, 2009.

Samuels, P. G., Morris, M. W., Sayers, P., Creutin, J., Kortenhaus, A., Klijn, F., Mosselman, E., Os, A. Van and Schanze, J.: Advances in flood risk management from the FLOODsite project, in: Flood risk management: research and practice, edited by P. Samuels, S. Huntington, W. Allsop, and J. Harrop, pp. 433–443, Taylor & Francis Group, London, 2008.

Sánchez-Arcilla, A., Mendoza, E. T., Jiménez, J. A., Peña, C., Galofré, J. and Novoa, M.: Beach Erosion and Storm Parameters: Uncertainties for the Spanish Mediterranean., in: Coastal Engineering 2008 Proceedings of the 31st International Conference Hamburg, Germany, 31 August – 5 September 2008, edited by J. McKee Smith, pp. 2352–2362, World Scientific, doi: 10.1142/9789814277426_0194, 2009.

Sanuy, M. and Jiménez, J. A.: Sensitivity to incoming storm direction of a deltaic curve coast (NW Mediterranean), Coast. Eng., Submitted, n.a.

Sanuy, M., Duo, E., Jäger, W. S., Ciavola, P. and Jiménez, J. A.: Linking source with consequences of coastal storm impacts for climate change and DRR scenarios' testing in sandy beaches on the Mediterranean sea, Nat. Hazards Earth Syst. Sci. Discuss., accepted with major revision and further review, doi:10.5194/nhess-2017-345, 2017.

Sardá, R., Conde, R., Casadesús, M., Sánchez, A. and Pablo, J.: Erosión en las playas y gestión desintegrada: la problemática actual de la playa de S'Abanell, in: Hacia un nuevo modelo integral de gestión de playas, edited by R. Sardá, J. Pintó, and J. F. Valls, pp. 51–71, Documenta Universitaria, Girona, 2013.

Saye, S. E., Van der Wal, D., Pye, K. and Blott, S. J.: Beach-dune morphological relationships and erosion/accretion: An investigation at five sites in England and Wales using LIDAR data, Geomorphology, 72(1–4), 128–155, doi:10.1016/j.geomorph.2005.05.007, 2005.

Scarelli, F. M., Sistilli, F., Fabbri, S., Cantelli, L., Barboza, E. G. and Gabbianelli, G.: Seasonal dune and beach monitoring using photogrammetry from UAV surveys to apply in the ICZM on the Ravenna coast (Emilia-Romagna, Italy), Remote Sens. Appl. Soc. Environ., 7, 27–39, doi:10.1016/j.rsase.2017.06.003, 2017.

Scorzini, A. R. and Frank, E.: Flood damage curves: new insights from the 2010 flood in Veneto, Italy, J. Flood Risk Manag., 10(3), 381–392, doi:10.1111/jfr3.12163, 2017.

Sekovski, I., Armaroli, C., Calabrese, L., Mancini, F., Stecchi, F. and Perini, L.: Coupling scenarios of urban growth and flood hazards along the Emilia-Romagna coast (Italy), Nat. Hazards Earth Syst. Sci., 15(10), 2331–2346, doi:10.5194/nhess-15-2331-2015, 2015.

Spencer, T., Brooks, S. M., Evans, B. R., Tempest, J. A. and Möller, I.: Southern North Sea storm surge event of 5 December 2013: Water levels, waves and coastal impacts, Earth-Science Rev., 146, 120–145, doi:10.1016/j.earscirev.2015.04.002, 2015.

Steinberg, T.: Acts of God: The Unnatural History of Natural Disaster in America, Oxford University Press, Oxford, 2006.

Stelljes, N., Martinez, G. and McGlade, K.: Introduction to the RISC-KIT web based management guide for DRR in European coastal zones, Coast. Eng., in press, doi:10.1016/j.coastaleng.2017.09.012, 2017.

Stockdon, H. F., Sallenger Jr., A. H., List, J. H. and Holman, R. A.: Estimation of Shoreline Position and Change Using Airborne Topographic Lidar Data, J. Coast. Res., 18(3), 502–513, doi:10.2307/4299097, 2002.

Stone, G. W., Liu, B., Pepper, D. A. and Wang, P.: The importance of extratropical and tropical cyclones on the short-term evolution of barrier islands along the northern Gulf of Mexico, USA, Mar. Geol., 210(1–4), 63–78, doi:10.1016/j.margeo.2004.05.021, 2004.

Swales, A.: Geostatistical estimation of short-term changes in beach morphology and sand budget, J. Coast. Res., 18(2), 338–351, available at: http://www.jstor.org/stable/4299079, 2002.

Sytnik, O. and Stecchi, F.: Disappearing coastal dunes: tourism development and future challenges, a case-study from Ravenna, Italy, J. Coast. Conserv., 19(5), 715–727, doi:10.1007/s11852-014-0353-9, 2015.

Tapsell, S. M., Penning-Rowsell, E. C., Tunstall, S. M. and Wilson, T. L.: Vulnerability to flooding: health and social dimensions, Philos. Trans. R. Soc., 360(1796), 1511–1525, doi:10.1098/rsta.2002.1013, 2002.

Taramelli, A., Di Matteo, L., Ciavola, P., Guadagnano, F. and Tolomei, C.: Temporal evolution of patterns and processes related to subsidence of the coastal area

surrounding the Bevano River mouth (Northern Adriatic) - Italy, Ocean Coast. Manag., 108, 74–88, doi:10.1016/j.ocecoaman.2014.06.021, 2015.

Tatham, P., Spens, K. and Oloruntoba, R.: Cyclones in Bangladesh - A Case Study of a Whole Country Response to Rapid Onset Disasters, in: POMS 20th Annual Conference, Orlando, Florida, USA, 2009.

Teatini, P., Ferronato, M., Gambolati, G., Bertoni, W. and Gonella, M.: A century of land subsidence in Ravenna, Italy, Environ. Geol., 47(6), 831–846, doi:10.1007/s00254-004-1215-9, 2005.

Theuerkauf, E. J. and Rodriguez, A. B.: Impacts of Transect Location and Variations in Along-Beach Morphology on Measuring Volume Change, J. Coast. Res., 28(3), 707–718, doi:10.2112/JCOASTRES-D-11-00112.1, 2012.

Trembanis, A. C., Duo, E., Dohner, S., Grottoli, E. and Ciavola, P.: Quick Response Assessment of the Impact of an Extreme Storm Combining Aerial Drone and RTK GPS, Nat. Hazards Earth Syst. Sci. Discuss., in review, doi:10.5194/nhess-2017-337, 2017.

Trembanis, A., Duval, C., Beaudoin, J., Schmidt, V., Miller, D. and Mayer, L.: A detailed seabed signature from Hurricane Sandy revealed in bedforms and scour, Geochemistry, Geophys. Geosystems, 14(10), 4334–4340, doi:10.1002/ggge.20260, 2013.

Trigo, I. F., Bigg, G. R. and Davies, T. D.: Climatology of Cyclogenesis Mechanisms in the Mediterranean, Mon. Weather Rev., 130(3), 549–569, doi:10.1175/1520-0493(2002)130<0549:COCMIT>2.0.CO;2, 2002.

Turner, I. L., Harley, M. D. and Drummond, C. D.: UAVs for coastal surveying, Coast. Eng., 114, 19–24, doi:10.1016/j.coastaleng.2016.03.011, 2016.

Van der Meer, J. W. and Daemen, I. F. R.: Stability and Wave Transmission at Low-Crested Rubble-Mound Structures, J. Waterw. Port, Coastal, Ocean Eng., 120(1), 1–19, doi:10.1061/(ASCE)0733-950X(1994)120:1(1), 1994.

Van Dongeren, A., Ciavola, P., Martinez, G., Viavattene, C., Bogaard, T., Ferreira, Ó., Higgins, R. and McCall, R.: Introduction to RISC-KIT: Resilience-increasing strategies for coasts, Coast. Eng., in press, doi:10.1016/j.coastaleng.2017.10.007, 2017.

Van Koningsveld, M., Davidson, M. A. and Huntley, D. A.: Matching Science with Coastal Management Needs: The Search for Appropriate Coastal State Indicators, J. Coast. Res., 21(3), 399–411, doi:10.2112/03-0076.1, 2005.

Van Verseveld, H. C. W., Van Dongeren, A. R., Plant, N. G., Jäger, W. S. and Den Heijer, C.: Modelling multi-hazard hurricane damages on an urbanized coast with a Bayesian Network approach, Coast. Eng., 103, 1–14, doi:10.1016/j.coastaleng.2015.05.006, 2015.

Viavattene, C., Jiménez, J. A., Ferreira, O., Priest, S., Owen, D. and McCall, R.: Selecting coastal hotspots to storm impacts at the regional scale: A Coastal Risk Assessment Framework, Coast. Eng., in press, doi:10.1016/j.coastaleng.2017.09.002, 2017.

Viavattene, C., Micou, A. P., Owen, D., Priest, S. J. and Parker, D. J.: RISC-KIT D.2.2 - Library of Coastal Vulnerability Indicators. Guidance Document, available at: http://www.risckit.eu/np4/file/23/RISC_KIT_D.2.2_CVIL_Guidance_Document.pdf, 2015.

Vojinovic, Z., Abebe, Y., Sanchez-Torres, A., Medina, N., Nikolic, I., Manojlovic, N., Makropoulos, C., Pelling, M. and Abbott, M.: Holistic Flood Risk Assessment In Coastal Areas - The PEARL Approach, in: Proceedings of the 11th International Conference on Hydroinformatics (HIC 2014), New York City, NY, USA, 17 – 21 August 2014, pp. 1497–1504, International Conference on Hydroinformatics 2014, New York City, NY, USA, available at: https://academicworks.cuny.edu/cc_conf_hic/396/, 2014.

Vousdoukas, M. I., Voukouvalas, E., Annunziato, A., Giardino, A. and Feyen, L.: Projections of extreme storm surge levels along Europe, Clim. Dyn., 47(9–10), 3171–3190, doi:10.1007/s00382-016-3019-5, 2016.

Waverley, J. A.: Report of the departmental committee on coastal flooding, 1954.

Wells, J. T. and McNinch, J.: Beach scraping in North Carolina with special reference to its effectiveness during Hurricane Hugo, J. Coast. Res., SI8, 249–261, available at: http://www.jstor.org/stable/25735419, 1991.

Westoby, M. J., Brasington, J., Glasser, N. F., Hambrey, M. J. and Reynolds, J. M.: "Structure-from-Motion" photogrammetry: A low-cost, effective tool for geoscience applications, Geomorphology, 179, 300–314, doi:10.1016/j.geomorph.2012.08.021, 2012.

Wheaton, J. M., Brasington, J., Darby, S. E. and Sear, D. A.: Accounting for uncertainty in DEMs from repeat topographic surveys: Improved sediment budgets, Earth Surf. Process. Landforms, 35(2), 136–156, doi:10.1002/esp.1886, 2010.

Young, A. P. and Ashford, S. A.: Performance Evaluation of Seacliff Erosion Control Methods, Shore & Beach, 74(4), 16–24, 2006.

Zanuttigh, B., Simcic, D., Bagli, S., Bozzeda, F., Pietrantoni, L., Zagonari, F., Hoggart, S. and Nicholls, R. J.: THESEUS decision support system for coastal risk management, Coast. Eng., 87, 218–239, doi:10.1016/j.coastaleng.2013.11.013, 2014.

Zanuttigh, B.: Editorial, Coast. Eng., 87, 1–3, doi:10.1016/j.coastaleng.2014.01.003, 2014.

APPENDIX A: Summary of scientific contributions

Contribution to scientific conferences and workshops

Ciavola, P., Uddin, M. M., Duo, E., Lee, B. and Fakhruddin, S. H. M.: Vulnerability of the Bangladesh coastline to inundation under cyclone activity: past records and DRR strategies at Sandwip Island, in: E-proceedings of the 36th IAHR World Congress 28 June – 3 July, 2015, The Hague, the Netherlands, edited by A. Mynett, IAHR, 2015. *(Oral presentation)*

Duo, E., Casari, A. and Ciavola, P.: Feasibility long-term numerical study of a mega-nourishment in the Northern Adriatic, in: Coastal and Maritime Mediterranean Conference, Edition 3, Ferrara, Italy, 25-27 November 2015, edited by D. Levacher, M. Sanchez, P. Ciavola, and E. Raymond, pp. 37–42, Editions Paralia, doi:10.5150/cmcm.2015.008, 2015. *(Oral presentation and proceedings)*

Duo, E. and Armaroli, C.: Assessing coastal risk impacts at regional level - Application to the Emilia-Romagna (Italy) coast, in: Workshop on Hazards And Risks In Natural And Urban Environments, Riederalp, Switzerland (21-25 March, 2017), 2017. *(Oral presentation, as speaker)*

Duo, E. and Armaroli, C.: Testing coastal DRR in current and climate change scenarios – Artificial winter dune system in a highly touristic beach in the Northern Adriatic, in: EGU General Assembly 2017, 23–28 April 2017 Wien, Austria, 2017. *(Poster presentation)*

Armaroli, C., Duo, E. and Ciavola, P.: Evaluation of marine flooding impacts along the coast of Emilia-Romagna (Italy): new methods and comparison with user-driven assessments, in: 3rd European Climate Change Adaptation Conference, 5-9 June 2017, Glasgow, Scotland, 2017. *(Oral presentation, as speaker)*

Duo, E. and Armaroli, C.: Approcci innovativi per la gestione costiera: gli strumenti sviluppati nel progetto RISC-KIT, in: RemTech Expo 2017 20-22 September 2017, Ferrara, Italy, 2017. *(Oral presentation, as speaker)*

Sanuy, M., Duo, E., Jäger, W. S., Ciavola, P. and Jiménez, J. A.: Bayesian Network Approach for Climate Change and DRR Scenarios' Testing - Pilot Cases from Italy and Spain, in: XBeachX Conference, 1-3 November 2017, Delft, The Netherlands, 2017. *(Oral presentation, as speaker)*

Contribution to scientific journals

Armaroli, C. and Duo, E.: Validation of the coastal storm risk assessment framework along the Emilia-Romagna coast, Coast. Eng., in press, doi:10.1016/j.coastaleng.2017.08.014, 2017. *(In press)*

De Angeli, S., D'Andrea, M., Cazzola, G., Duo, E. and Rebora, N.: Coastal Risk Assessment Framework: Comparison of modelled fluvial and marine inundation impacts, Bocca di Magra, Ligurian coast, Italy, Coast. Eng., in press, doi:10.1016/j.coastaleng.2017.09.011, 2017. *(In press)*

Sanuy, M., Duo, E., Jäger, W. S., Ciavola, P. and Jiménez, J. A.: Linking source with consequences of coastal storm impacts for climate change and DRR scenarios' testing in sandy beaches on the Mediterranean sea, Nat. Hazards Earth Syst. Sci. Discuss., in review, doi:10.5194/nhess-2017-345, 2017. *(Accepted with Major Revision and further review)*

Trembanis, A. C., Duo, E., Dohner, S., Grottoli, E. and Ciavola, P.: Quick Response Assessment of the Impact of an Extreme Storm Combining Aerial Drone and RTK GPS, Nat. Hazards Earth Syst. Sci. Discuss., in review, doi:10.5194/nhess-2017-337, 2017. *(In review)*

Papers in preparation

Duo, E., Sanuy, M., Jiménez, J. A., and Ciavola, P.: Synthetic Storms: Uncertainties and Limitations of their Application Coastal Hazard Modelling. *(In preparation for the Elsevier journal Coastal Engineering)*

Duo, E., et al.: High-Accuracy Drone-Based Surveys: Application on a Sedimentary Beach with Artificial Dunes in Porto Garibaldi (Comacchio, Italy). *(In preparation)*

Other publications

Duo, E. and Ciavola, P. (Eds.): RISC-KIT D.1.1 - Review report of key challenges and lessons learned from historical extreme hydro-meteorological events, available at: http://www.risckit.eu/np4/file/23/RISC_KIT_Deliverable_D.1.1_V3.pdf, 2015.

Contribution to European projects

The PhD candidate participated to the EU FP7 project Resilience-Increasing Strategies for Coast - toolKIT (RISC-KIT; GA 603458; www.risckit.eu) by contributing to the Work Packages (WPs) 1, 2, 5 and 6. In particular, the following activities were implemented:

- WP1: review of the national and supra-national polices for emergency and disaster risk reduction; support to the historical review at the case study site of Porto Garibaldi - Bellocchio (Comacchio, Italy); contribution to and editing of the RISC-KIT Deliverable D.1.1;
- WP2: building of the CRAF Phase 2 Hazard module (Matlab code) for erosion and flooding, in collaboration with M. Sanuy , PhD student at the Laboratori d'Enginyeria Marítima (LIM) of the Universitat Politècnica de Catalunya (Barcelona, Spain);
- WP5: application of the RISC-KIT tools to the Porto Garibaldi - Bellocchio (Comacchio, Italy) case study site and contribution to deliverables;
- WP6: contribution (2 papers) to the RISC-KIT Special Issue in Coastal Engineering; organization and teaching support during the RISC-KIT Summer School held in Ferrara (Italy), 12-16 September 2016.

The author of this PhD thesis is currently involved in the EU H2020 project Enhancing Emergency Management and Response to Extreme Weather and Climate Events (ANYWHERE; GA 700099; www.anywhere-h2020.eu), contributing to the WP2 and WP6.

Abroad research stays

The PhD candidate worked at the Laboratori d'Enginyeria Marítima (LIM) of the Universitat Politècnica de Catalunya (Barcelona, Spain) under the supervision of Prof. J. A. Jiménez, for a period of 3 months (non-continuous) between 12 April 2016 and 30

July 2016. The aim of the abroad stay was to develop the numerical study that is reported in Chapter 4 of this thesis. The work was done in collaboration with M. Sanuy, PhD student at LIM-UPC. The stay was funded with the contribution "5 per mille assegnato all'Università di Ferrara - dichiarazione dei redditi dell'anno 2013".

The author of this thesis visited, between the 5 and 19 of November 2016, the Coastal Sediments, Hydrodynamics And Engineering Lab (CSHEL) of the School of Marine Science and Policy of the University of Delaware (Newark, DE, US), under the supervision of Prof. A. C. Trembanis. The aim of the visit was to learn to use different autonomous platform for coastal monitoring, also contributing to fieldwork in Lewes (DE, US). During the period, the PhD candidate worked with S. Dohner, PhD student at the University of Delaware, and Prof. A. C. Trembanis, on the very first draft of the paper that is included in this thesis as Chapter 2 and is currently under review in Natural Hazard and Earth System Sciences.